

**DEVELOPMENT OF INSTRUMENTED INSOLE
USING FORCE SENSING RESISTORS**

LENG YEN RAN

**A project report submitted in partial fulfilment of the
requirements for the award of the degree of
Bachelor (Hons.) of Biomedical Engineering**

**Faculty of Engineering and Science
Universiti Tunku Abdul Rahman**

April 2011

DECLARATION

I hereby declare that this project report is based on my original work except for citations and quotations which have been duly acknowledged. I also declare that it has not been previously and concurrently submitted for any other degree or award at UTAR or other institutions.

Signature : _____

Name : _____

ID No. : _____

Date : _____

APPROVAL FOR SUBMISSION

I certify that this project report entitled “**DEVELOPMENT OF INSTRUMENTED INSOLE USING FORCE SENSING RESISTORS**” was prepared by **LENG YEN RAN** has met the required standard for submission in partial fulfilment of the requirements for the award of Bachelor of Engineering (Hons.) Biomedical Engineering at Universiti Tunku Abdul Rahman.

Approved by,

Signature : _____

Supervisor: Mr. Chong Yu Zheng

Date : _____

The copyright of this report belongs to the author under the terms of the copyright Act 1987 as qualified by Intellectual Property Policy of University Tunku Abdul Rahman. Due acknowledgement shall always be made of the use of any material contained in, or derived from, this report.

© 2011, Leng Yen Ran. All right reserved.

Specially dedicated to
my beloved family.

ACKNOWLEDGEMENTS

First and foremost, I would like to express my utmost gratitude to the Universiti Tunku Abdul Rahman (UTAR) for giving me the opportunity to pursue this project as a partial fulfilment of the requirement for the degree. The laboratories and library available in UTAR indeed contributed the major parts of this project by providing all the necessary equipments and apparatus for this project.

Throughout this project, I am very fortunate to be blessed with the guidance and encouragement from my project supervisor, Mr. Chong Yu Zheng for his invaluable advice, guidance and his enormous patience throughout the development of the research.

In addition, I would also like to express my sincere gratitude to my friends and research team-mates, Chan Meng Nen who had contributed to the successful completion of this project. Great experience, co-operation, communication, and problem-solving skills are being gained and learned in completing this project.

Last but not least, I would like to express my utmost appreciation to my loving family for their fully fledged support and understanding. Furthermore, I would like to thank to my friends and course mates who have showed their motivational support and believed in me always.

DEVELOPMENT OF INSTRUMENTED INSOLE USING FORCE SENSING RESISTORS

ABSTRACT

This research involves the development of an instrumented insole system which can be used for continuous and real-time monitoring gait. This project presents the design of an instrumented insole system for the direct kinetic measurement during human's walking activity. In this project, a general introduction, aims, and objectives are being discussed clearly to state the purposes of this project evidently. Furthermore, literature review is necessary for research on the aspects such as history, force distribution, and type of walking patterns to have a clearer understanding about this project. The related diseases and disabilities are being discussed too as one of the applications of this instrumented insole system in improving patients' walking orientation. Besides, current methods and technologies need to be revised up to date as they are very useful for conceptual design. Next, a conceptual design has been proposed where it consists of its own design with the usage of electronic components in order to achieve the aims and objectives of this project. Each of the components used in this project is being introduced and the methodology on how the designed system being constructed is being discussed thoroughly. After constructing the designed system, gait simulation is being carried out to test for the system. Subject testing is being conducted as well for comparison and benchmarking with other studies. Further improvements and optimizations are suggested by referring to each problems and difficulties. Last but not least, an overall conclusion and future work are discussed by summarizing the important facts and points of this project.

TABLE OF CONTENTS

DECLARATION	ii
APPROVAL FOR SUBMISSION	iii
ACKNOWLEDGEMENTS	vi
ABSTRACT	vii
TABLE OF CONTENTS	viii
LIST OF TABLES	xii
LIST OF FIGURES	xiii
LIST OF SYMBOLS / ABBREVIATIONS	xxvi
LIST OF APPENDICES	xxix

CHAPTER

1	INTRODUCTION	1
	1.1 Background	1
	1.2 Aims and Objectives	3
	1.2.1 Aim	3
	1.2.2 Group Objectives	3
	1.2.3 Individual Objectives	4
	1.3 Progress Report Outline	4
2	LITERATURE REVIEW	6
	2.1 History of Gait Analysis	6
	2.2 Diseases and Disabilities	12
	2.3 Gait Cycle	16
	2.4 Force Distributions	20

2.5	Current Method/Technology	25
2.5.1	Force Platform	25
2.5.2	Instrumented Insole	28
3	METHODOLOGY	34
3.1	Introduction	34
3.2	Preferred Design	35
3.2.1	Sensors	35
3.2.2	Position of Sensors	36
3.2.3	Power Supply	36
3.2.4	Signal Conditioning	37
3.2.5	Data Logging	38
3.2.6	Data Transmission	38
3.2.7	Data Storage	39
3.2.8	Data Display	39
3.2.9	Data Analysis	40
3.2.10	Summary of Preferred Design	41
3.3	Process Flow	42
3.4	Hardware	44
3.4.1	Components and Tools	44
3.4.2	Hardware Assembly	66
3.5	Software	80
3.5.1	Microchip PIC Programming	80
3.5.2	XBee Module (SKXBee) Communication	90
3.5.3	HyperTerminal Testing	97
3.5.4	National Instruments LabVIEW Interactions	101
3.6	PIC Coding and LabVIEW Graphical Programming	105
3.6.1	PIC Microcontroller Programming	105
3.6.2	LabVIEW Graphical Programming	111
3.7	Gait Simulation and Subject Testing	135
3.7.1	Gait Simulation	135
3.7.2	Subject Testing	142

4	RESULTS AND DISCUSSIONS	147
4.1	Result Interface and Format	147
4.2	Analysis Tool	151
4.2.1	Adjustment Filter	151
4.2.2	Read From Text File	153
4.3	Gait Simulation	157
4.3.1	Initial Testing	157
4.3.2	Static Device with No Inputs	162
4.3.3	Static Device with Static Forces Inputs	163
4.3.4	Standing	165
4.3.5	Sitting	166
4.3.6	Walking	167
4.3.7	Running	168
4.3.8	Summary of Results and Discussion	169
4.4	Subject Testing	171
4.4.1	Subject Information	171
4.4.2	Summary of Results	176
4.4.3	Benchmarking of Results	180
4.5	Readings from Multimeter	195
4.6	Problems and Difficulties	196
4.6.1	Force Sensing Resistors Interface	196
4.6.2	XBee Module Interface	197
4.6.3	PIC Coding and Programming	198
4.6.4	LabVIEW Discovery	199
4.6.5	Hardware Assembly	200
4.6.6	Noise Disturbance	201
4.6.7	Time Delay	202
4.6.8	Text File Saving	203
4.6.9	Data Analysis Format	204
4.7	Further Improvements and Optimizations	205
4.7.1	Force Sensing Resistors Interface	205
4.7.2	XBee Module Interface	207
4.7.3	PIC Coding and Programming Enhancement	208
4.7.4	LabVIEW Enhancement	209

4.7.5	Advanced Hardware Assembly	210
4.7.6	Noise Reduction	211
4.7.7	Rechargeable Power Supply	212
4.7.8	Amounts and Positions of Sensors	213
4.7.9	Data Analysis Enhancement	215
5	CONCLUSION AND RECOMMENDATIONS	217
5.1	Conclusion and Future Work	217
5.2	Cost and Expenses	219
5.3	Gantt Chart	219
	REFERENCES	223
	APPENDICES	239

LIST OF TABLES

TABLE	TITLE	PAGE
2.1	Time-line of major contributors to the history of gait analysis (Baker, 2007)	7
2.2	Comparison of values reported in other studies (Martinez-Nova, Cuevas-Garcia, Pascual-Huerta, and Sanchez-Rodriguez, 2007)	24
3.1	Microchip PIC16F877A microcontroller device features	57
3.2	Functions of each labelled components in SK40C enhanced 40 pins PIC start-up kit	60
3.3	Functions of each labelled components in SKXBee XBee starter kit	63
3.4	Product specification of SKXBee XBee starter kit	64
3.5	Type of simulation and parameters based on human locomotion activity (Gait cycle)	137
4.1	Demographic Information and analysed parameters of previous gait analysis for normal gait	187
4.2	Demographic Information and analysed parameters of previous gait analysis for abnormal gait	190
4.3	Specifications of XBee module	197
4.4	Comparison between XBee module and XBee-PRO module	208

LIST OF FIGURES

FIGURE	TITLE	PAGE
2.1	Illustration from Descartes textbook of physiology De Homine (1662) (Baker, 2007)	8
2.2	The alignment of the trunk and lower limbs at 14 instants during the gait cycle (Baker, 2007)	9
2.3	The characteristic shape of the vertical component of the ground reaction force as first recorded by Carlet (Baker, 2007)	9
2.4	Braune and Fischer's subject wearing the experimental suit (Baker, 2007)	10
2.5	Amar's "Trottoire Dynamographique" (Baker, 2007)	11
2.6	Characteristic pattern of the vertical ground reaction force during a gait cycle for a slow (patient) and the normal speed (Drerup, Szczepaniak, and Wetz, 2008)	12
2.7	Left foot insole sensor location and sample output by sensor for the (a) normal child and (b) child with planovalgus foot deformity (Abu-Faraj, Harris, Anbler, Wertsch, and Smith, 1996)	13
2.8	Three-dimensional and a flat display of plantar foot pressures for a normal subject (Ranu, 1995)	15
2.9	Plantar pressure patterns for a diabetic patient (high pressures under the metatarsal head) (Ranu, 1995)	15
2.10	Gait cycle (Racic, Pavic, and Brownjohn, 2009)	17
2.11	Functional tasks and phases of gait (Racic, Pavic, and Brownjohn, 2009)	18

2.12	The vertical force graph can identify with precision all five phases of gait occurring during stance (Racic, Pavic, and Brownjohn, 2009)	18
2.13	Spatial parameters of gait (Racic, Pavic, and Brownjohn, 2009)	19
2.14	Division of the foot into 10 areas (Martinez-Nova, Cuevas-Garcia, Pascual-Huerta, and Sanchez-Rodriguez, 2007)	21
2.15	Pedar insoles pressure output (Putti, Arnold, Cochrane, and Abboud, 2007)	22
2.16	The 10 regions of the left and right insoles (Putti, Arnold, Cochrane, and Abboud, 2007)	22
2.17	Location of the sensors (in right foot) required in the three regression models (in grey) (Fong, Chan, Hong, Yung, and Fung, 2008)	23
2.18	Normal stress distributions on the plantar surface for wearing the (a) flat insole, (b) three layers, and (c) two layers (Chen, Ju, and Tang, 2003)	24
2.19	The outline of the 3D force platform for plantar distribution measurement (Wang, Liu, and Chen, 2009)	25
2.20	The track of the plantar force distribution (Wang, Liu, and Chen, 2009)	26
2.21	Force Sensing Platform (Gouwanda, Senanayake, Marasinghe, Chandrapal, Kumar, Tung, et al, 2008)	27
2.22	Schematic diagram of arrangements of sensors into quadrants with connectivity to the ethernet (Gouwanda, Senanayake, Marasinghe, Chandrapal, Kumar, Tung, et al, 2008)	27
2.23	Placement of sensors in each insole (Grandez, Bustamante, Gurutzeaga, and Garcia-Alonso, 2009)	29
2.24	There are five measurement areas in the insole. The place and the size of the capacitive sensor elements inside the insole are illustrated with white colour (Salpavaara, Verho, Lekkala, and Halttunen, 2009)	29

2.25	Sphere shaped load cell (Muller, Brito, Pereira, and Brusamarello, 2010)	30
2.26	The key design parameters of bulk micro-machined pressure sensor (Wahab, Zayegh, Veljanovski, and Begg, 2008)	30
2.27	One of the MEMS transducer design fabricate. The transducer shown here is a full Wheatstone bridge configuration with two traces in tension and two in compression (Wheeler, Rohere, Kholwadwala, Buerger, Givler, Neely, et al, 2009)	31
2.28	Schematic of the Shoe-Integrated Gait Sensors (SIGS) (Morris and Paradiso, 2002)	32
2.29	Sole with the eight areas and exploded view of transducer (ring, box, aluminium plates) (Faivre, Dahan, Parratte, and Monnier, 2003)	32
2.30	Schematic diagram of one instrumented insole with the included components (Jagos, Oberzaucher, Reichel, Zagler, and Hlauschek, 2010)	33
3.1	A summary chart of design options	41
3.2	A general process flowchart of an instrumented insole system	42
3.3	A figure representation of an instrumented insole system design using force sensing resistors (FSRs)	43
3.4	A figure representation of sensors positioning of an instrumented insole system design	43
3.5	10 μ F electrolytic capacitor (10 μ F Electrolytic Capacitor, 2010)	44
3.6	100 μ F electrolytic capacitor (100 μ F Electrolytic Capacitor, 2010)	44
3.7	1.0 k Ω resistor (Resistor 1K Ohm $\frac{1}{4}$ Watt, 2010)	45
3.8	Rechargeable 9.0 V battery (Energizer Ni-Mh Rechargeable 9V Square Batteries, 2010)	45
3.9	Battery Snap (9V Battery Snap Connector, 2010)	45
3.10	PVC battery holder (9V Sealed Battery Holder with Wires, 2010)	45

3.11	Donut board (Donut Board, 2010)	46
3.12	Male connector (Male Connector, 2010)	46
3.13	Female connector (Female Connector, 2010)	46
3.14	10 ways ribbon cables (Electrical & Electronic Connectors, 2010)	46
3.15	Red and black wires (Wires, 2010)	47
3.16	Plastic casing (Aluminium Box Silver, 2010)	47
3.17	Polymer shoe insole (Shock Absorbing Sheet, 2010)	47
3.18	Belts (Cable Belt, 2010)	47
3.19	Multimeter (Multimeter, 2010)	48
3.20	Soldering tools (How to Solder, 2010)	48
3.21	Interlink Electronics FSR-402 (Force Sensitive Resistor 0.5'', 2010)	48
3.22	Interlink Electronics FSR-406 (Force Sensitive Resistor – Square, 2010)	49
3.23	Interlink Electronics FSR construction (FSR Force Sensing Resistor Integration Guide and Evaluation Parts Catalog, 2010)	49
3.24	LM7805 5.0 V voltage regulator (LM7805 5V Regulator, 2010)	51
3.25	Connection diagram of LM7805 (L7800 Series Positive Voltage Regulators, 2004)	51
3.26	Block diagram of LM7805 (LM78XX/LM78XXA 3-Terminal 1A Positive Voltage Regulator, 2010)	52
3.27	Schematic diagram of LM7805 (LM341/LM78MXX Series 3-Terminal Positive Voltage Regulators, 2005)	52
3.28	LM324 operational amplifier (Quad Operational Amplifier, 2010)	53
3.29	Pin diagram of LM324 (Low Power Quad Operational Amplifiers, 1999)	54

3.30	Schematic diagram of LM324 (Low Power Quad Operational Amplifiers, 1999)	54
3.31	Microchip PIC16F877A microcontroller (PIC16F877A, 2010)	55
3.32	Pin diagram of microchip PIC16F877A microcontroller (PIC16F87XA Data Sheet, 2003)	56
3.33	Top view of SK40C enhanced 40 pins PIC start-up kit with components (SK40C Enhanced 40 Pins PIC Start-Up Kit User's Manual V1.1, 2010)	58
3.34	Side view of SK40C enhanced 40 pins PIC start-up kit (SK40C Enhanced 40 Pins PIC Start-Up Kit User's Manual V1.1, 2010)	59
3.35	Bottom view of SK40C enhanced 40 pins PIC start-up kit (SK40C Enhanced 40 Pins PIC Start-Up Kit User's Manual V1.1, 2010)	59
3.36	Board layout of SK40C enhanced 40 pins PIC start-up kit (SK40C Enhanced 40 Pins PIC Start-Up Kit User's Manual V1.1, 2010)	59
3.37	SKXBee XBee starter kit with components (XBee Starter Kit SKXBee User's Manual V1.0, 2008)	62
3.38	Board layout of SKXBee XBee starter kit (XBee Starter Kit SKXBee User's Manual V1.0, 2008)	62
3.39	Process flow of hardware design	65
3.40	Circuit diagram of instrumented insole system	66
3.41	Circuit diagram of LM7805 5.0 V voltage Regulator	67
3.42	LM7805 5.0V voltage regulators are soldered on donut board	67
3.43	Circuit diagram of voltage divider and voltage follower using LM324 operational amplifiers	68
3.44	LM324 operational amplifiers are soldered on donut board to form circuit loops of voltage divider and follower.	69
3.45	Ribbon cables for force sensing resistors connecting from polymer insole to circuit board	69

3.46	Ribbon cables for force sensing resistors connecting from polymer insole to power supply and operational amplifiers inside circuit board	70
3.47	Ribbon cables for SK40C enhanced 40 pins PIC start-up kit with SKXBee XBee starter kit	70
3.48	PIC16F877A microcontroller placement on SK40C enhanced 40 pins PIC start-up kit board	71
3.49	Circuit diagram of FSRs connected to LM7805 5.0 V voltage regulator, LM324 operational amplifiers, and SK40C Enhanced 40 Pins PIC Start-Up Kit Board	72
3.50	FSRs are connected to LM7805 5.0 V voltage regulator and LM324 operational amplifiers	73
3.51	FSRs are connected to SK40C enhanced 40 pins PIC start-up kit board	73
3.52	Circuit diagram of SKXBee XBee starter kit connected to SK40C enhanced 40 pins PIC start-up kit board	74
3.53	SKXBee XBee Starter Kit is connected to SK40C Enhanced 40 Pins PIC Start-Up Kit Board	75
3.54	FSR-402 (circular shape) are attached at big toe (hallux), first, and fifth metatarsals region on polymer shoe insole	75
3.55	FSR-406 (square shape) is attached at heel region on polymer shoe insole	76
3.56	FSR-402 and FSR-406 attached on polymer shoe insole	76
3.57	The final product housed inside a plastic casing, waist belt, shoe belts, and polymer shoe insole with sensors.	77
3.58	Polymer shoe insole tightened under user's foot	77
3.59	User and the instrumented insole device	78
3.60	Process flow of hardware assembly design	79

3.61	SK40C enhanced 40 pins PIC start-up kit with UIC00B USB ICSP PIC programmer connected (UIC00B USB ICSP PIC Programmer User's Manual V1.1, 2010)	81
3.62	UIC00B USB ICSP PIC programmer connected to computer with USB connection cable (UIC00B USB ICSP PIC Programmer User's Manual V1.1, 2010)	81
3.63	Process flow of Microchip PIC programming design	89
3.64	XBee module (SKXBee) connected to computer with USB connection cable (XBee Starter Kit SKXBee User's Manual V1.0, 2008)	90
3.65	Process flow of XBee module (SKXBee) communication design	96
3.66	Process flow of HyperTerminal testing design	100
3.67	Process flow of National Instruments LabVIEW interactions design	104
3.68	Process flow of PIC microcontroller programming design	110
3.69	LabVIEW graphical user front panel interface version one	111
3.70	LabVIEW programming mode block diagram interface version one	112
3.71	LabVIEW graphical user front panel interface version two	112
3.72	LabVIEW programming mode block diagram interface version two	113
3.73	LabVIEW graphical user front panel interface version three	113
3.74	LabVIEW programming block diagram interface version three	114
3.75	Serial COM port configuration block diagram for all versions	115

3.76	Serial COM port configuration block diagram labelling for all versions	115
3.77	Configure serial port front panel interface for all versions	116
3.78	Configure serial port block diagram interface for all versions	117
3.79	Configure serial port block diagram A for all versions	117
3.80	Configure serial port block diagram B for all versions	118
3.81	Configure serial port block diagram C for all versions	118
3.82	Configure serial port block diagram D for all versions	118
3.83	Configure serial port block diagram labelling for all versions	118
3.84	VISA read and write incoming data block diagram A for all versions	120
3.85	VISA read and write incoming data block diagram B for all versions	120
3.86	VISA read and write incoming data block diagram C for all versions	121
3.87	VISA read and write incoming data block diagram labelling for all versions	121
3.88	Removal of initial character, conversion to integer, and formula block diagram version one and version three	123
3.89	Removal of initial character, conversion to integer, and formula block diagram version two	123
3.90	Removal of initial character, conversion to integer, and formula block diagram labelling for all versions	123
3.91	Result display block diagram version one and version two	125

3.92	Result display block diagram version three	125
3.93	Result display block diagram labelling for all versions	126
3.94	Configuration of filter for all versions	126
3.95	Storage of data in text file block diagram A for all versions	128
3.96	Storage of data in text file block diagram B for all versions	128
3.97	Storage of data in text file block diagram labelling for all versions	128
3.98	Errors handle block diagram for all versions	129
3.99	Errors handle block diagram labelling for all versions	129
3.100	Merge errors front panel interface for all versions	130
3.101	Merge errors block diagram interface for all versions	130
3.102	Merge errors block diagram A for all versions	131
3.103	Merge errors block diagram B for all versions	131
3.104	Merge errors block diagram labelling for all versions	131
3.105	Simple error handle front panel interface for all versions	132
3.106	Simple error handle block diagram interface for all versions	133
3.107	Simple error handle block diagram for all versions	133
3.108	Simple error handle block diagram labelling for all versions	133
3.109	Process flow of LabVIEW graphical programming design	134
3.110	Process flow of gait simulation design	141
3.111	Process flow of subject testing design	146

4.1	Graph position with display for each foot in LabVIEW version one	148
4.2	Display labelling for each foot in LabVIEW version one	148
4.3	Graph position with display for each foot in LabVIEW version two	149
4.4	Graph position with display for each foot in LabVIEW version three	150
4.5	Filter adjustment front panel interface	151
4.6	Filter adjustment block diagram interface	152
4.7	Read from text file front panel interface	153
4.8	Read from text file block diagram interface	154
4.9	Read from text file block diagram A	154
4.10	Read from text file block diagram B	155
4.11	Read from text file block diagram C	155
4.12	Read from text file block diagram labelling	155
4.13	Example of text file created	156
4.14	Initial testing of sensor L1	157
4.15	Initial testing of sensor L2	158
4.16	Initial testing of sensor L3	158
4.17	Initial testing of sensor L4	159
4.18	Initial testing of sensor R1	159
4.19	Initial testing of sensor R2	160
4.20	Initial testing of sensor R3	160
4.21	Initial testing of sensor R4	161
4.22	Combined readings for all sensors	161
4.23	Static device with no inputs results by LabVIEW	162

4.24	Static device with static forces inputs results by LabVIEW	163
4.25	Static device with static forces inputs results by HyperTerminal	164
4.26	Standing results by LabVIEW	165
4.27	Sitting results by LabVIEW	166
4.28	Walking results by LabVIEW	167
4.29	Running results by LabVIEW	168
4.30	Pie chart of gender statistical distribution for subject testing	172
4.31	Bar chart of age statistical distribution for subject testing	172
4.32	Pie chart of age statistical distribution for subject testing	173
4.33	Pie chart of course (year/trimester) statistical distribution for subject testing	173
4.34	Bar chart of height statistical distribution for subject testing	173
4.35	Pie chart of height statistical distribution for subject testing	174
4.36	Bar chart of weight statistical distribution for subject testing	174
4.37	Pie chart of weight statistical distribution for subject testing	174
4.38	Bar chart of size of shoe statistical distribution for subject testing	175
4.39	Pie chart of size of shoe statistical distribution for subject testing	175
4.40	Pie chart of brand of shoe statistical distribution for subject testing	175
4.41	Pie chart of group statistical distribution for subject testing	176

4.42	Output resistance of FSR-402 (big toe region) by multimeter	195
4.43	Output resistance of FSR-406 (heel region) by multimeter	195
4.44	Error message during compiling UART function	198
4.45	Error message during configuring serial port	199
4.46	Wires connections of electronic components	200
4.47	Noises generated by the devices (without filter)	201
4.48	Formula used for conversion factor	201
4.49	Delay function in LabVIEW	202
4.50	Write to spreadsheet file front panel interface	203
4.51	Write to spreadsheet file block diagram interface	204
4.52	An example of flexible bend sensor (Flexible Bend Sensor, 2010)	206
4.53	An example of triple axis accelerometer (Triple Axis Accelerometer Breakout – MMA7260Q, 2010)	206
4.54	An example of gyroscope (Gyro Breakout Board – ADXRS610 300 degree/sec, 2010)	206
4.55	An example of XBee-PRO starter kit (XBee Starter Kit SKXBee User’s Manual V1.0, 2008)	207
4.56	Write to spreadsheet file VI	209
4.57	An example of PCB (PCB Fabrication, 2010)	210
4.58	An example of RC filter	211
4.59	An example of lithium-ion battery (ThunderPower Lithium Polymer Battery – 480mAH 11.1V with JST Connector, 2010)	212
4.60	Possible of FSR sensors’ arrangements	213
4.61	Possible of sensors’ arrangements	214
4.62	Example formulas of Bayes rules (Morris, 2004)	215

4.63	Example formulas of Support Vector Machines (Morris, 2004)	216
4.64	Example formulas of neural network (Morris, 2004)	216

LIST OF SYMBOLS / ABBREVIATIONS

ISw	Initial swing
MSt	Midstance
MSw	Mid-swing
PSw	Preswing
TSt	Terminal stance
TSw	Terminal swing
V_{in}	Input voltage
V_{out}	Output voltage
AD	Area detection
ADC	Analogue-to-digital converter
ANN	Artificial neural network
CA	Contact area
CART	Classification and regression trees
COP	Centre of pressure
DAQ	Data acquisition
DAS	Data acquisition system
DOF	Degrees of freedom
ECG	Electrocardiography
EEPROM	Electrically-erasable read only memory
EFS	Equine F-Scan sensors
EMFI	Electromechanical film
ES	Electrical stimulation
FD	Force detection
FES	Functional electrical stimulation
FIS	Fuzzy inference system
FO	Foot off

FSR	Force sensing resistor
GCF	Ground contact forces
GDPS	Gait phase detection sensor
GND	Ground
GRF	Ground reaction forces
GUI	Graphical user interface
IC	Initial contact
IMU	Inertial measurement unit
IO	Input and output
LED	Light emitting diode
LR	Loading response
MCU	Multipoint control unit
MEMS	Mirco-electro-mechanical system
MF	Maximum force
MGMS	Mobile gait monitoring system
MSSP	Mater synchronous serial port
PANs	Personal area networks
PC	Personal computer
PCA	Principal component analysis
PCB	Printed circuit board
PD	Parkinson's disease
PDA	Personal digital assistant
PVDF	Polyvinlylidine fluoride
RAM	Random-access memory
RC	Resistor and capacitor
RF	Radio-frequency
RPROP	Resilient back-propagation
SECOSP	Sensorized-codivilla-spring
SEMG	Surface electromyography
SIMS	Smart insole measurement system
SVM	Support vector machine
TCI	Total contact insoles
TM	Electrodynogram
TTL	Transistor-transistor logic

USART	Universal asynchronous receiver transmitter
WHANs	Wireless home area networks
WPANs	Wireless personal area networks
VGRF	Vertical ground reaction forces

LIST OF APPENDICES

APPENDIX	TITLE	PAGE
A	Circuit Diagram of Instrumented Insole System	239
B	PIC Microcontroller Coding	241
C	LabVIEW Block Diagram	245
D	Subject Testing Consent Form	255
E	Subject Testing Protocol	260
F	Subject Testing Schedule	263
G	Subjects' Information	268
H	Summary of Results	271
I	Benchmarking of Results	282
J	Expenditure of Project	316

CHAPTER 1

INTRODUCTION

1.1 Background

Gait analysis is the study and investigation of the human locomotion pattern, which can be carried out by using visual observation, sensor technology, video or optical cameras or integration of these technologies (Senanayake, 2009). Gait analysis is used in many applications namely, sports performance analysis (Salpavaara, Verho, Lekkala, and Halttunen, 2009), product design (Ramanathan, Kiran, Arnold, Wang, and Abboud, 2010), gait rehabilitation (Bachschtmidt, Harris, and Simouneau, 1995), post injury assessments (Tiberi and Maccioni, 2008), and improvement of human walking orientation (Pappas, Keller, Mangold, Popovic, Dietz, and Moran, 2003).

In general, gait analysis is primarily carried out in two ways. First, it is carried out in a motion laboratory, with full analysis of the motion of all body segments using efficiently accurate optical or video camera systems. Second, it is carried out in a doctor's office with the physician making visual observations.

The first method is expensive, which requires the maintenance of a high-technology motion lab, and cumbersome equipment needs to be attached to the patient, however, this high-cost method produces well-quantified and accurate results for short distances. The second method is inexpensive compared to the first method and nothing needs to be attached to the patient, here, the results are qualitative and difficult to compare across multiple visits.

So, there is a need for a low cost device that falls in between these two methods, which can provide quantitative and repeatable results over extended time periods. In addition, there is a need for monitoring gait over long periods of time. This is crucial in enhancing the studies and monitoring process done outside of the motion lab, like Parkinson's disease (Grandez, Bustamante, Solas, Gurutzeaga, and Garcia-Alonso, 2009), cerebral palsy (Smith, Coiro, Finson, Betz, and McCarthy, 2002), or diabetes (Al-Tayyar, 1997; Zequera, Stephan, and Paul, 2007).

With such high demand of an inexpensive device for gait analysis monitoring, more research nowadays focus on sensor technology, due to the several drawbacks identified on video and optical camera systems beside force platform, such as high cost and the need for spatial gait laboratories. Many sensor technologies are available in the current industry, namely accelerometers, gyroscopes, foot switches, load cells, force sensing resistors, and the list goes on, which facilitate the accurate acquisition of the gait parameters.

Therefore, the motivation of this project is to design and develop a low cost, reliable, and portable instrumented insole system. An insole system will be investigated which is capable of real-time pressure analysis at decided locations of sensor beneath each foot. Besides, it is designed to provide qualitative and quantitative information on how the ground reaction forces distributed on the human foot.

This instrumented insole system will provide instrumented gait analysis outside of traditional, expensive motion labs. Such a system has the potential to be highly informative by allowing data collection throughout the day in variety of environments, thus providing a vast quantity of long-term data not obtainable with current gait analysis system where this analysis cannot be done by using force platform in current technology.

1.2 Aims and Objectives

1.2.1 Aim

The main aim of this project is to design and develop an instrumented insole using force sensing resistors which are used to detect Vertical Ground Reaction Forces (VGRF) of human movement with respect to locomotion and gait analysis.

This project is carried out with the aspiration of developing a cost effective instrumented insole made of components which are available all the times at a reasonable prices. There are some other requirements in developing this instrumented insole, as shown below:

- Cosmetically unobtrusive
- Maintainability and long-lived
- Provide real-time analysis and feedback
- Wearability and easily mounted or installed
- Reliability, durability, functionality, usability

1.2.2 Group Objectives

In order to achieve the project aim, there are some group objectives being set, as the following:

- To study the biomechanics of human locomotion via biomechanical analysis.
- To develop a cost-effective, reliable, and durable instrumented system for biomechanical analysis.
- To collect and analyze gait data collected by the system and benchmark against published data.

1.2.3 Individual Objectives

In a group of two, each of the group members has their own individual objectives to fulfil the group objectives, as followed:

- To understand the basic operating of the circuit system/software generation.
- To design and develop the hardware/software subsystems of the instrumented system.
- To collect/analyze gait data collected by the system.

1.3 Progress Report Outline

This section is dedicated to show the overall picture of how this thesis is structured. Besides, a brief outline of each chapter will be stated as followed:

CHAPTER 1: INTRODUCTION

This chapter is mainly about the overall of the conducted project. This chapter briefly discuss about the project background, aim, group objectives, individual objectives, scope, overviews, motivation, and thesis outline.

CHAPTER 2: LITERATURE REVIEW

This chapter gives some briefing about the history of gait analysis and the development of existed instrumented insole from time to time. Some research has been done by studying the background related to this project and being summarize into a table form of critical review.

CHAPTER 3: METHODOLOGY

This chapter indicates the methods which used to develop and implement design for this project. Next, parts of each components being used in hardware design and software codes generation in software design are shown clearly with the help of suitable schematic diagrams and layout, includes the equipments and step by step procedure in completing the prototype.

CHAPTER 4: RESULTS AND DISCUSSIONS

Test results and collected data are presented in this chapter based on methodology mentioned in previous chapter. In addition, data analysis is done with respect to the collected data. Some figures, graphs, and the measured data are included in this chapter. This chapter ends with a thorough discussion on the problems being faced, solutions and precautions being taken in this project.

CHAPTER 5: CONCLUSION AND RECOMMENDATIONS

This chapter draws a conclusion of the project, proposes ideas for future work, and recommendations to improve the implemented prototype.

CHAPTER 2

LITERATURE REVIEW

2.1 History of Gait Analysis

People have been thinking about how they walk since the earliest times. An article written by Baker (2007) traces the history of this process from time of Aristotle through the dawn of the modern era of computerised analysis techniques. Through recounting this history, it is possible to see how present understanding of walking has developed as a series of steps each based on previous developments in the field and on the scientific and cultural environment in which the individual contributors were living (Baker, 2007).

How major developments have often been a consequence of collaborations of individuals with different expertise? An aspect of the history of this field is particularly between those with expertise in the life and physical sciences (Baker, 2007). A list of major contributors to the field is shown in table below. From the table, entries in light type face refer to contributors to general scientific developments which have become important components of gait analysis but made no specific contribution to the field (Baker, 2007).

Aristotle (384-322 BCE) can be attributed with the earliest recorded comments regarding human walk, where he was the person who made the first known written reference to the analysis of walking. Unfortunately, none of his propositions were ever tested by experiment. As a consequence, almost all his other related conjectures are now known to be false whilst this observation is true.

Table 2.1: Time-line of major contributors to the history of gait analysis (Baker, 2007)

Date	Name	Location	Contribution
384-322 BCE	Aristotle	Athens, Greece	Theories on the movement of humans and animals.
1501-1576	Girolamo Cardan	Milan & Pavia, Italy	Consideration of 3-d joint angles.
1564-1642	Galileo Galilei	Piza, Florence & Padua, Italy	The modern scientific method.
1596-1650	Rene Descartes	Leiden, The Netherlands	Cartesian co-ordinates. 1 st test-book on physiology.
1608-1679	Giovanni Borelli	Pisa & Rome, Italy	Muscle and tendon biomechanics.
1642-1727	Isaac Newton	London, England	Newtonian mechanics.
1668-1738	Hermann Boerhaave	Leiden, The Netherlands	Application of Newtonian mechanics to human body.
1707-1783	Leonhard Euler	Basel, Switzerland & St Petersburg, Russia	Theory of 3-d joint angles.
1708-1777	Albrecht van Haller	France	Physiology of walking (ideas reviewed by Weber and Weber).
1734-1806	Paul Barthez	France	
1783-1855	Francoise Margendie	France	
1781-1840	Samuel Poisson	France	
1797-1856	Pierre Gerdy	France	
1804-1891	Willhelm Eduard Weber	Leipzig, Germany	Anatomy and mechanics of walking. <i>Mechanik der Gehwerkzeuge (1836)</i> .
1806-1871	Eduard Friedrich Weber	Leipzig, Germany	
1795-1878	Ernst Heinrich Weber	Leipzig, Germany	Brother of and probable collaborator with Eduard and Willhelm.
1806-1875	Guillaume Duchenne	Boulogne, France	Founder of electrophysiology. Reported <i>Duchenne</i> gait pattern.
1844-1924	Freiderich Trendelenberg	Berlin & Leipzig, Germany	Orthopaedic surgeon. Reported <i>Trendelenburg</i> gait pattern.
1830-1904	Jules Etienne Marey	Paris, France	Physiologist. Force and pressure measurement. Chronophotography.
1849-1892	Gaston Carlet	Paris, France	Student of Marey. First essentially correct description of gait cycle.
1850-1918	Georges Demeny	Paris, France	Student of Marey. Pioneer of photographic method.
1830-1904	Edward Muybridge	Stanford then Pennsylvania, USA	Photography of movement.
1831-1892	Willhelm Braune	Leipzig, Germany	First 3-d gait analysis. <i>Der Gang des Menschen (1895)</i> [9]
1861-1917	Otto Fischer		
1896-1966	Nikolai Bernstein	Moscow, Russia	Development of theories of motor control.
1879-1935	Jules Amar	Paris, France	Pneumatic three-component force plate.
1893-1971	Wallace Fenn	Rochester, USA	Mechanical one-component force-plate
Unknown	Herbert Eiftman	New York, USA	Mechanical three component force plate. Kinetics of walking
1905-1980	Verne Inman	Berkeley, USA	Founded biomechanics lab at University of California, Berkeley
1906-1993	Howard Eberhart	Berkeley, USA	
1925-1984	Pat Murray	Milwaukee, USA	Instrumented studies of normal walking in men and women
1918-	Jacquelin Perry	Downey, USA	Pioneer of clinical electromyography and observational gait analysis
1923-2006	David Sutherland	San Francisco then San Diego, USA	Digitisation of data from cine film. Development of walking in children
1926-2000	Jurg Baumann	Basel, Switzerland	Integration of cine photography with electromyography.

Later, mathematical basis of modern gait analysis were formed by a professor of both mathematics and medicine in Milan and Pavia, Girolamo Cardan (1501-1576). As well as being the first European mathematician to use complex numbers (based on the square root of a negative number), to study probability, and the properties of three-dimensional angles (Baker, 2007).

Next, Rene Descartes (1596-1650) was the first conceived of an orthogonal co-ordinate system for describing the position of objects in space. However, it is less well-known that he also wrote the first modern textbook on physiology, *De Homine* (Baker, 2007). His advanced thinking is clearly demonstrated by one of the book's figures as shown in figure below which clearly show closed loop motor control with the movement of the arm being controlled by muscular activity under the influence of nerves connected to the brain. Feedback is provided by the eyes (Baker, 2007).

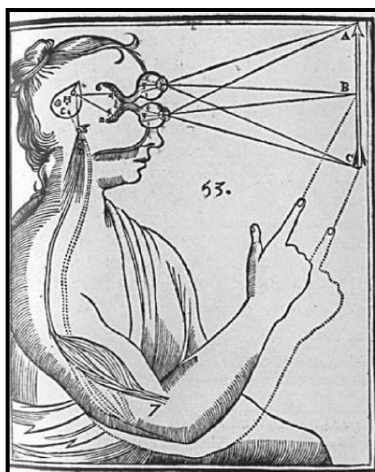


Figure 2.1: Illustration from Descartes textbook of physiology *De Homine* (1662) (Baker, 2007)

The first experiment in gait analysis was then performed by Giovanni Alfonso Borelli (1608-1679). Two poles were placed an unspecified distance apart and tried to walk towards them keeping one pole in front of the other (Baker, 2007). He found that when doing this, the near pole always appeared to move to the left and right with respect to the far pole (Baker, 2007). Borelli also studied the mechanics of muscle and was the first to conclude that the forces within the tendons and muscles are considerably greater than the externally applied loads (Baker, 2007).

Next major contribution was made by a team of brothers, namely Willhelm Eduard Weber (1804-1891), Ernst Heinrich (1795-1878), and Eduard Friedrich Willhelm (1806-1871). They did considerable experimental work using only a stop watch, measuring tape, and a telescope (Baker, 2007). They also attempted to work out the position of limbs at 14 different instants in the gait cycle and were the first to develop illustrations showing that attitude of the limb segments at these different instants (Baker, 2007) as shown in figure below.

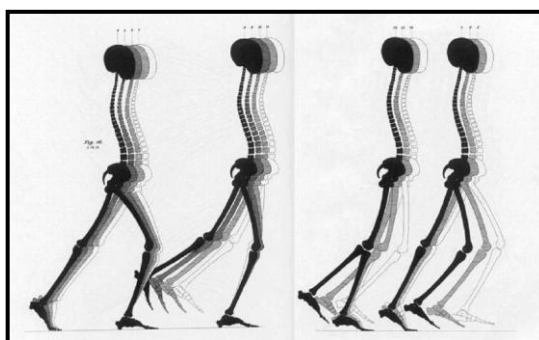


Figure 2.2: The alignment of the trunk and lower limbs at 14 instants during the gat cycle (Baker, 2007)

Gaston Carlet (1849-1892), a student of Jules Etienne Marey (1830-1904) had developed a shoe with three pressure transducers built into the sole and recorded the forces exerted by the foot on the floor. He was the first to record the double bump of the ground reaction (Baker, 2007) as shown in figure below. Besides, various other experimental techniques were used and Carlet's thesis, publisehd in 1872, concludes with a succinct description of the normal human gait cycle which is essentially accurate (Baker, 2007).

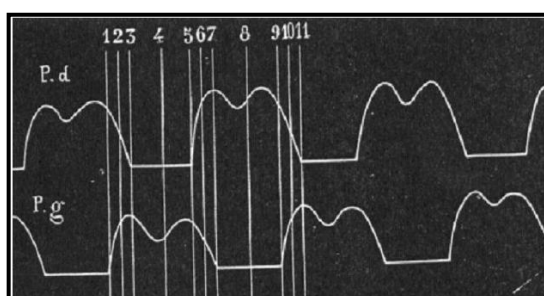


Figure 2.3: The characteristic shape of the vertical component of the ground reaction force as first recorded by Carlet (Baker, 2007)

The first three-dimensional gait analysis was conducted by a German mathematician, Otto Fischer (1861-1917). His work always associated with Wilhelm Braune (1831-1892). They used continuous exposures with the subject walking in the dark with Geissler tubes strapped to his body like figure below. A tuning fork was used to make and break the electrical circuit thus ensuring accurate timing of the flashes of light. But, they took between 6 and 8 hours to dress the experimental subject (Baker, 2007).

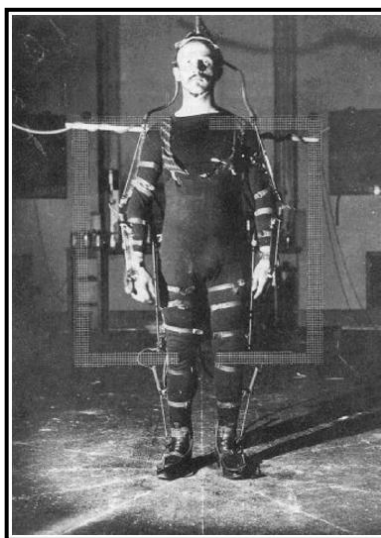


Figure 2.4: Braune and Fischer’s subject wearing the experimental suit (Baker, 2007)

Demeny’s force plate developed by Braune and Fischer only able to measure the vertical component, however it was clear that in order to fully understand walking knowledge of all three components of the ground reaction was required (Baker, 2007). After that, Jules Amar (1879-1935) was the first to develop a three-component force plate. This had a mechanical mechanism compressing rubber bulbs and pneumatic transmission of the signals similar to Demeny’s approach (Baker, 2007) which shown in figure below.

In 1930, another force plate being produced by Wallace Fenn for measure the horizontal component only and Elftman later made a full three-component mechanical force plate in 1983 (Baker, 2007). The next development in force plate technology was that of a full six-component force plate using strain gauges by

Cunningham and Brown is the late forties (Baker, 2007). The first commercially available force plates specifically designed for Biomechanics were however piezo-electric plates. These were developed by Kistler in 1969 (Baker, 2007).

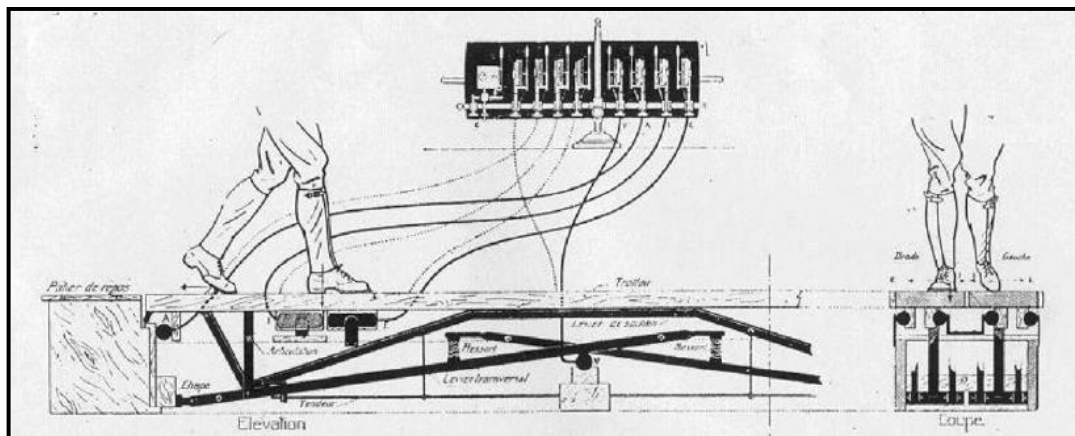


Figure 2.5: Amar's "Trottoire Dynamographique" (Baker, 2007)

For sure, a lot of research and developments have been done from time to time after that and perhaps the final development in gait analysis in the pre-computer era was the use of electrogoniometers to measure movement at specific joints, for example the work done by Ed Chao to measure three-dimensional knee movement using goniometers (Baker, 2007).

Even by the end of the 1970s, instrumented gait analysis had not really moved away from being a research tool only possible on a limited number of subjects (Baker, 2007). Equipment was generally cumbersome and time-consuming to use. Most importantly, the amount of time required to process data and the limited options for output prevented that data being presented in a format that was clinically meaningful (Baker, 2007).

Luckily, this was the dawn of the computer era with allowing for faster and faster processing of data and more and more options for output (Baker, 2007). The development of modern gait analysis was just waiting to happen, but that is another story (Baker, 2007).

2.2 Diseases and Disabilities

Gait stability is an important issue for safe locomotion, especially for the elderly and people with disabilities. To properly evaluate dynamic gait stability, stability measurements over a range of tasks and environments are needed, especially for uneven ground, stairs, ramps, and so forth (Lemaire, Biswas, and Kofman, 2006).

The feet are the foundation of the human body. They provide stability and support while standing, walking, and running (Karkokli and McConville, 2006). However, current foot pressure monitoring systems have been data capture intervals and permit recording of only a few consecutive steps with monitoring equipment frequently tethered to the subject by cable (Abu-Faraj, Harris, Anbler, Wertsch, and Smith, 1996).

These contemporary systems are unable to monitor in-shoe plantar pressures for more than a few minutes. Inherent gait variability requires that large numbers of steps be examined for reliable analysis and characterization (Abu-Faraj, Harris, Anbler, Wertsch, and Smith, 1996). This is an important requirement used in detecting the disabilities or diseases, such as cerebral palsy (CP), Parkinson disease, diabetes (with neuropathic feet), spinal cord injury, stroke, and so forth.

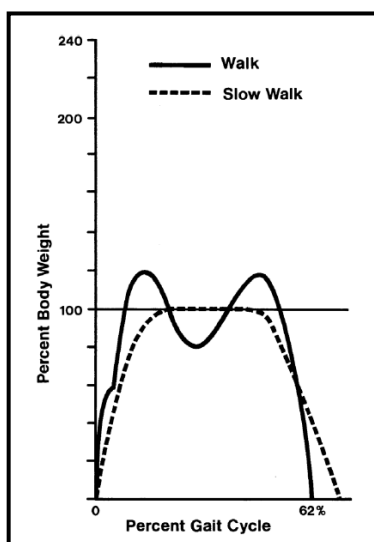


Figure 2.6: Characteristic pattern of the vertical ground reaction force during a gait cycle for a slow (patient) and the normal speed (Drerup, Szczepaniak, and Wetz, 2008)

For the child with spastic diplegia, cerebral palsy, the ability to ambulate is compromised. Walking for these children often requires an assistive device or orthoses to provide balance, support, and foot clearance. Children with CP exhibit motion disorders, including spasticity, athetosis or atoxia, result in imbalances between agonist and antagonist muscles, apparent muscle weakness, and a loss of selective muscle control (Smith, Coiro, Finson, Betz, and McCarthy, 2002). This results in poor stability during the stance phase of gait and inadequate foot clearance during the swing phase.

Currently, there is no definition of what constitutes a “satisfactory” surgical result. Additionally, there are no quantitative indexes which have been used to describe rehabilitative progress in a clinical series. In order to better understand the effectiveness of intervention in the correction and rehabilitative treatment of planovalgus foot deformity, it is essential to objectively describe plantar pressure characteristics during ambulation (Abu-Faraj, Harris, Anbler, Wertsch, and Smith, 1996).

Therefore, the role of instrumented insole system come into place in detecting the changes of forces, especially for electrical stimulation (ES) in improving the mobility by modulating spasticity, unmasking or improving volitional control, improving joint range of motion, strengthening weak muscles, and stimulation of muscle during activity (Smith, Coiro, Finson, Betz, and McCarthy, 2002).

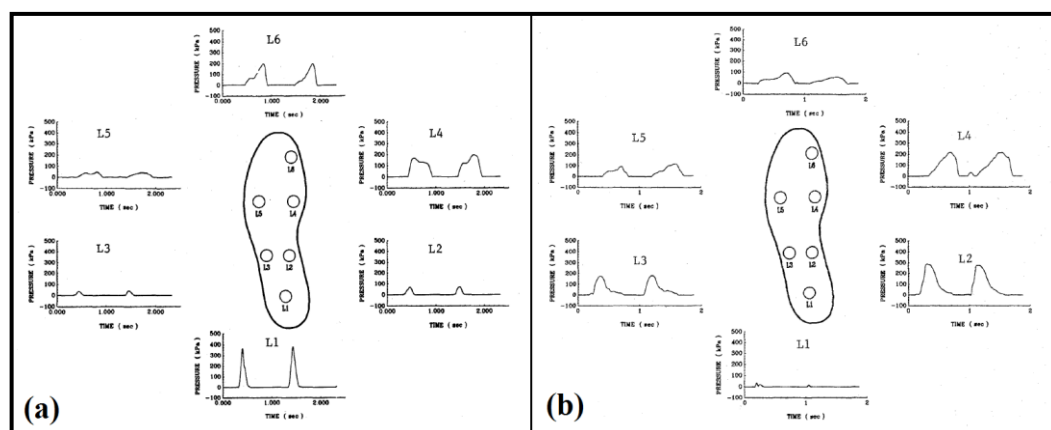


Figure 2.7: Left foot insole sensor location and sample output by sensor for the (a) normal child and (b) child with planovalgus foot deformity (Abu-Faraj, Harris, Anbler, Wertsch, and Smith, 1996)

Parkinson's disease is a progressive neurodegenerative disease. Gait disturbance is one of the major symptoms in patients with Parkinson's disease. Parkinson's disease patients walk slowly with shuffling and dragging steps diminished arm swing and flexed forward posture (Okuno, Fujimoto, Akazawa, Yokoe, and Sakoda, 2008). The progressive gait disturbance combined with postural instability finally deprives the patients of locomotion ability and yields medical as well as social problems (Okuno, Fujimoto, Akazawa, Yokoe, and Sakoda, 2008).

In previous studies, some researchers measured walking of Parkinson's disease people (PD) by using motion capture system with multi-camera and examined such gait parameters as step length, gait velocity, and so on (Okuno, Fujimoto, Akazawa, Yokoe, and Sakoda, 2008). In addition to differences in the gait motion, the way of heel contact and toe off motion in Parkinson's disease seems to be obviously different from that in normal subject (Okuno, Fujimoto, Akazawa, Yokoe, and Sakoda, 2008).

Therefore, it is necessary to develop a quantitatively evaluating system of the severity to measure the plantar pressure patterns during walking, like using embedded pressure sensors in shoe sole. Through this, the burden of Parkinson disease patients would be reduced if the features were measured in a gate experiment without sensors attached to the subjects.

Diabetic patients with peripheral neuropathy often suffer from tissue damage in their feet due to the loss of protective pain sensation (Zhu, Maalej, Webster, Tompkins, Bach-Y-Rita, and Wertsch, 1990). Repetitive plantar pressure has been listed as a strong risk factor for the development of plantar ulcers (Zhu, Wertsch, Harris, Price, and Alba, 1990). Therefore, foot pressure distribution measurement is important in the assessment of diabetic feet.

Undeniable, foot is the most frequent site of ulceration in individuals hospitalized for diabetes and infection (Al-Tayyar, 1997). Foot orthosis therapy is a common treatment used to relieve plantar pressure, in order to prevent ulceration and alleviate pain in rheumatic and neuropathic feet. But, no studies that have examined the relationship between plantar pressure and various orthosis components, such as

experimental shape variations, for 'off-the-shelf' shoes in low risk diabetic patients (Guldmond, Leffers, Schapper, Sanders, Nieman, Willems, et al, 2007).

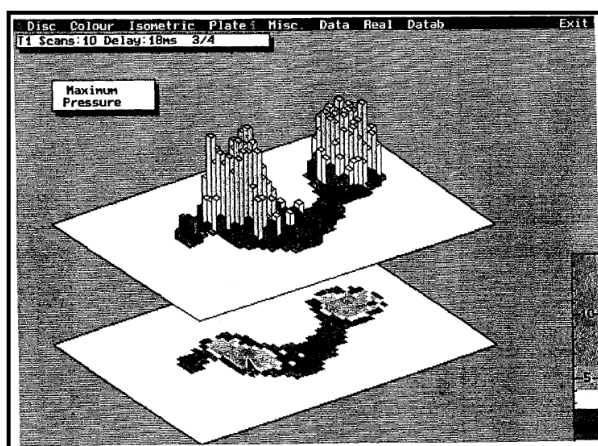


Figure 2.8: Three-dimensional and a flat display of plantar foot pressures for a normal subject (Ranu, 1995)

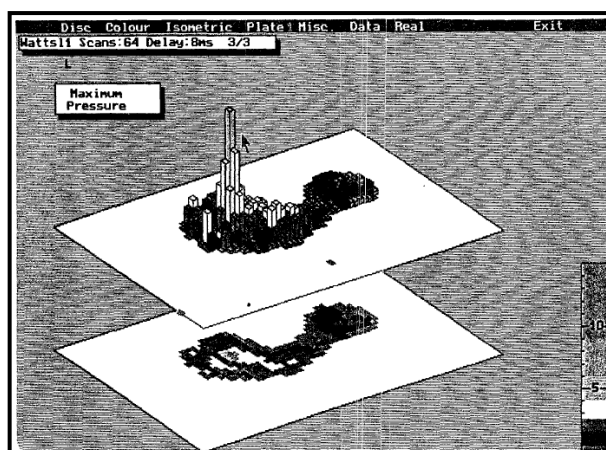


Figure 2.9: Plantar pressure patterns for a diabetic patient (high pressures under the metatarsal head) (Ranu, 1995)

There is a need to develop an insole-based system to quantify the conditions inside the shoe, to predict the progression of skin breakdown and ulceration in diabetic patients with peripheral neuropathy as well as spinal injury and stroke patients. Besides, this system can be tested with incomplete spinal injury and used to trigger functional electrical stimulation (FES), with demonstrated benefit for both subject (Bamberg, Benbasat, Scarborough, Krebs, and Paradiso, 2008).

2.3 Gait Cycle

Walking is one of the most common human physical activities and plays an important role in daily activities. It can be performed in a variety of ways and directions and is furthermore a highly energy-efficient method of locomotion (Rueterbories, Spaich, Larsen, and Andersen, 2010).

The gait cycle is the period of time between any two nominally identical events in the walking process. The term 'cycle duration' or 'cycle time' stands for the length of time that the complete gait cycle lasts (Racic, Pavic, and Brownjohn, 2009). Any event could be marked as the beginning since the gait has to be performed in a particular sequence where cycles follow each other continuously and smoothly (Racic, Pavic, and Brownjohn, 2009). Therefore, the instant at which one foot hits the ground has been generally selected as starting (and completing) event.

The duration of a complete gait cycle is divided into two periods, they are stance and swing phase as shown in figure below. For each foot, the stance phase, also called the support or contact phase, it is the phase when the foot is on the ground. It is initiated with 'heel strike' and ends with 'toe off' of the same foot, constituting approximately 60 percent of the gait cycle (Racic, Pavic, and Brownjohn, 2009).

Heel strike, also known as heel stance phase, also known as heel contact is a distinct impact between the heel and the ground at initial contact. Toe off is an event in the gait cycle when the foot leaves the ground. The swing phase lasts from toe off to the next initial contact, constituting approximately the remaining 40 percent of the gait cycle (Racic, Pavic, and Brownjohn, 2009). It denoted the time in which the foot is off the ground, moving through the air when all parts of the foot are in forward progression (Racic, Pavic, and Brownjohn, 2009).

There is a period of time when both feet are in contact with the ground, thus right foot initial contact occurs while the left foot is still on the ground, and vice versa. This period is known as double support or double limb stance and occurs twice in the gait cycle which at the beginning and end of the stance phases (Racic, Pavic, and Brownjohn, 2009).

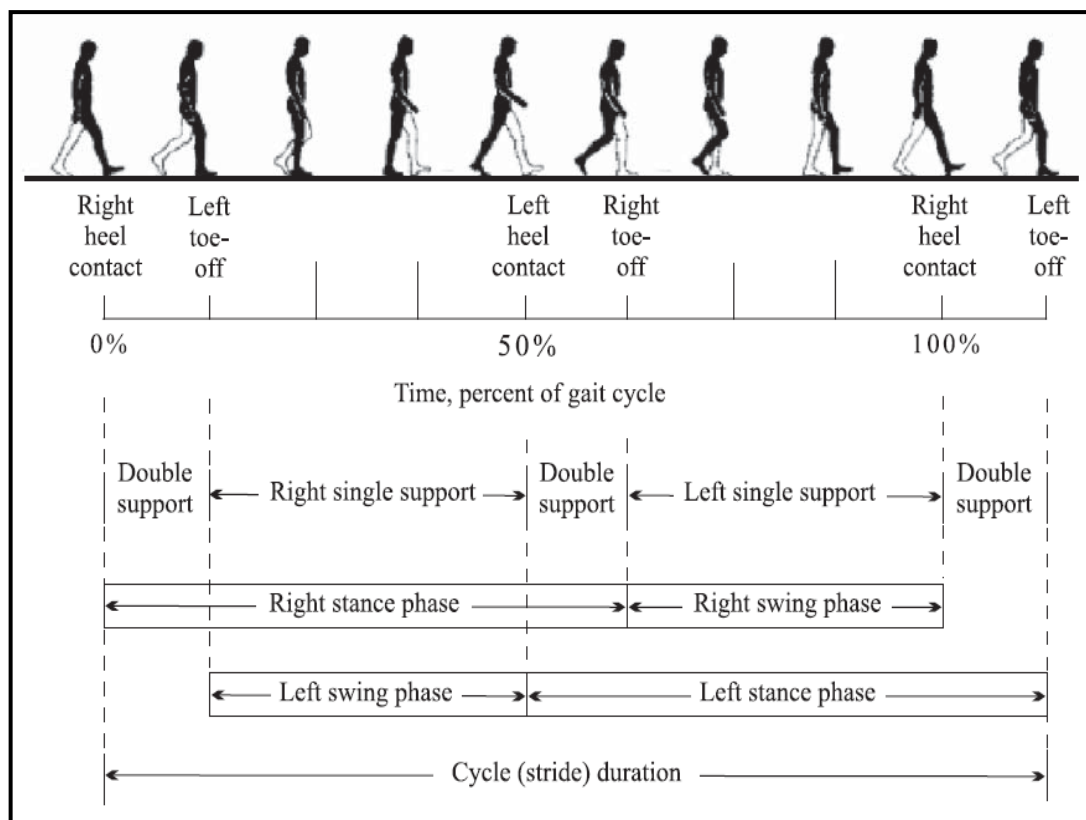


Figure 2.10: Gait cycle (Racic, Pavic, and Brownjohn, 2009)

Both the initial double limb support and the terminal double limb support take up about 10 percent of the gait cycle, or about 20 percent all together (Racic, Pavic, and Brownjohn, 2009). However, this varies with the speed of walking. The duration of double support becomes proportionally shorter as the speed increases (Racic, Pavic, and Brownjohn, 2009). Finally, single support is the period of time when only one foot is in contact with the ground and when the opposite limb is simultaneously in its swing phase (Racic, Pavic, and Brownjohn, 2009).

The stance period can be further divided into five functional sub-phases occurring in the following sequences, they are initial contact (IC), loading response (LR), midstance (MSt), terminal stance (TSt), and preswing (PSw). Similarly, the swing phase is broken down into three sub-phases occurring in the orders, namely initial swing (ISw), mid-swing (MSw), and terminal swing (TSw) (Racic, Pavic, and Brownjohn, 2009). An overview of the phases of the gait cycle is given in figure below.

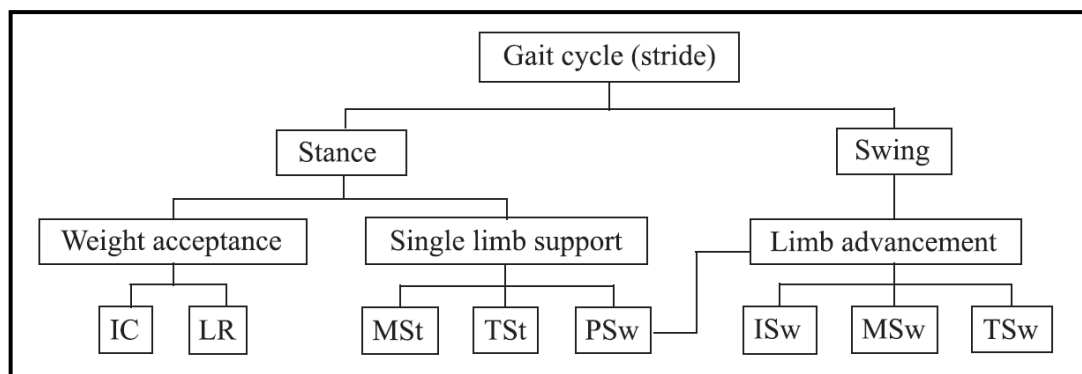


Figure 2.11: Functional tasks and phases of gait (Racic, Pavic, and Brownjohn, 2009)

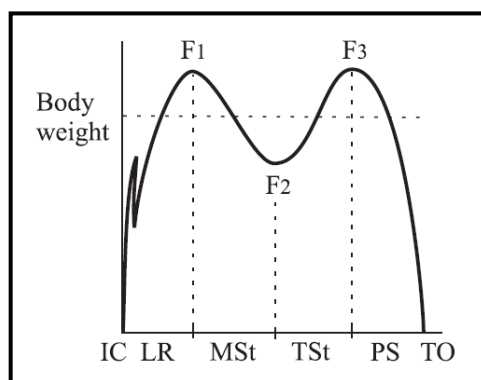


Figure 2.12: The vertical force graph can identify with precision all five phases of gait occurring during stance (Racic, Pavic, and Brownjohn, 2009)

Although the PSw is the final stage of the stance, it can be also regarded as preparatory phase for the swing period (Racic, Pavic, and Brownjohn, 2009). Therefore, it is usually considered as an intermediate phase between the stance and swing. Each of these sub-phases enables lower limbs to accomplish the three basic functional tasks of gait; they are weight acceptance, single-limb support, and limb advancement (Racic, Pavic, and Brownjohn, 2009).

The physical ways to analyze gait are based on kinetics and kinematics. The term kinetics describes the study of forces and moments that cause a movement or motion of objects and systems (Rueterbories, Spaich, Larsen, and Andersen, 2010). Those are the example gravitational, ground reaction, other external forces, or forces produced by muscle contractions (Rueterbories, Spaich, Larsen, and Andersen, 2010).

Kinetics usually used in foot contact measurement where a reaction force is generated from the ground. This reaction force is distributed under the plantar surface of the foot and its effect is to accelerate individual body segments and transmit force to adjacent segments (Billing and Hayes, 2005). Plantar pressure measurement techniques offer a visual description of how these forces are distributed under the foot as well as providing quantitative information about the timing and loading of individual foot structures (Billing and Hayes, 2005). However, plantar pressure distribution does not provide information regarding the non-planar forces which may be applied by the foot (Billing and Hayes, 2005).

As opposed to kinetics, the term kinematics is used to describe movement not taking into account the forces that cause the movement (Rueterbories, Spaich, Larsen, and Andersen, 2010). One approach to measure movement is the direct measurement of linear and angular displacements provided by joint angles, limb velocities or accelerations. A second established method is the indirect measurement of movement with cameras or tracking systems (Rueterbories, Spaich, Larsen, and Andersen, 2010).

In kinematics, there are few target variables, which includes stride length, stride frequency, contact time, and flight time (Billing and Hayes, 2005). Running speed is the product of stride length and stride frequency. However, these two variables are interdependent and their optimisation is the key to improve performance (Rueterbories, Spaich, Larsen, and Andersen, 2010). The sum of contact time and flight time equals stride time which is the determinant of stride frequency (Rueterbories, Spaich, Larsen, and Andersen, 2010).

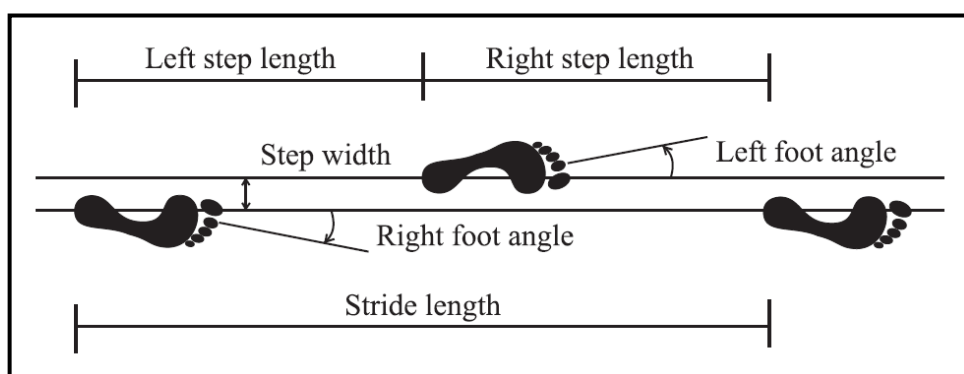


Figure 2.13: Spatial parameters of gait (Racic, Pavic, and Brownjohn, 2009)

2.4 Force Distributions

The average person takes 3 to 3.5 million steps per year (Putti, Arnold, Cochrane, and Abboud, 2007) and it is therefore no surprise that a variety of foot problems can occur. The foot is the only anatomical structure that comes in contact with the ground during the gait cycle and also while standing. Hence, it has to withstand any impact generated as a result of the body weight and in turn the ground reaction force produced (Putti, Arnold, Cochrane, and Abboud, 2007).

Force distribution measurements not only allow force changes under localized regions to be examined, but can also be used to extract foot position and orientation. In standing balance tests, foot position and orientation have been found to affect postural sway and the mean position of the centre of pressure (COP) (Yip and Prieto, 1996).

The process generally takes about one to two minutes. This is not a problem for normal individuals. However, subjects with problems maintaining a stable stance, such as Parkinson patients, may not be able to keep their feet in position long enough for the tracing to be completed (Yip and Prieto, 1996). Force distribution measurements will be able to provide the subject's foot position and orientation in a fraction of the time needed for manual tracing (Yip and Prieto, 1996).

In addition, information about the pressure distribution and active foot contact area during walking is considered to be important for the practice of neurology and physical medicine (Titianova, Mateev, and Tarkka, 2004). It is known that high pressure in the forefoot area occurs during the push-off phase of gait when the heel leaves the ground, and the entire body weight is borne on the forefoot and toe (Titianova, Mateev, and Tarkka, 2004).

Various methods have been used for estimation of gait parameters, however, only few can provide reliable information about foot pressure distribution during gait. Most of the techniques are labour-intensive, time consuming or otherwise insufficient for collecting reliable data (Titianova, Mateev, and Tarkka, 2004). Recent technology has resulted in flexible and portable walkways with embedded

pressure sensitive sensors with an instrumented insole system (Titianova, Mateev, and Tarkka, 2004).

To obtain accurate data, it is essential to identify the placement of the sensors in the body. There are many methods in identifying the suitable placement of the sensors, like from research, testing with subjects, or from the foot print techniques such as APEX foot imprinter, microcapsule socks, Fuji Pres-sensor Mat, and Shustrack system for locating sensors are investigated (Wertsch, Webster, and Tompkins, 1992). All of those methods should work best for applications in terms of accuracy, simplicity, and cost.

One of the measuring systems used was the Biofoot in-shoe system. The insoles are available in different sizes, permitting a good match to the shoe interface. Plantar pressures were distributed by the software into major areas by creating 10 areas corresponding to heel, mid-foot, whole forefoot, first to fifth metatarsal heads, hallux, and lesser toes as shown in figure below (Martinez-Nova, Cuevas-Garcia, Pascual-Huerta, and Sanchez-Rodriguez, 2007).

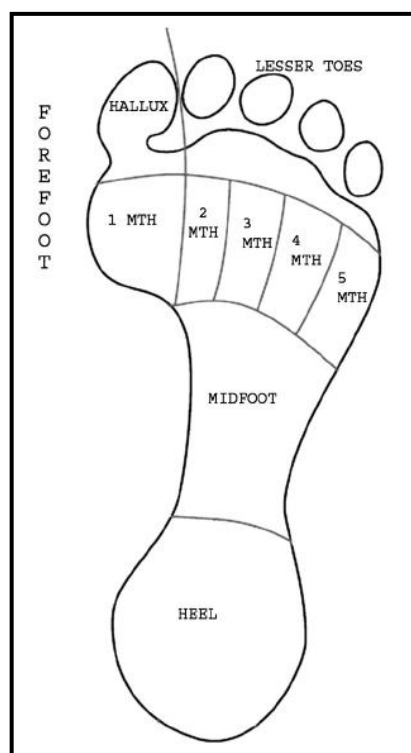


Figure 2.14: Division of the foot into 10 areas (Martinez-Nova, Cuevas-Garcia, Pascual-Huerta, and Sanchez-Rodriguez, 2007)

Another method would be the Pedar system, which is the one of the most commonly used systems for in-shoe pressure measurement (Putti, Arnold, Cochrane, and Abboud, 2007). This system has insoles comprising 99 capacitive sensors. Same as Biofoot, the foot was divided into 10 regions. The software for the Pedar system calculates information on 18 parameters where six of the most clinically relevant parameters were evaluated (Putti, Arnold, Cochrane, and Abboud, 2007).

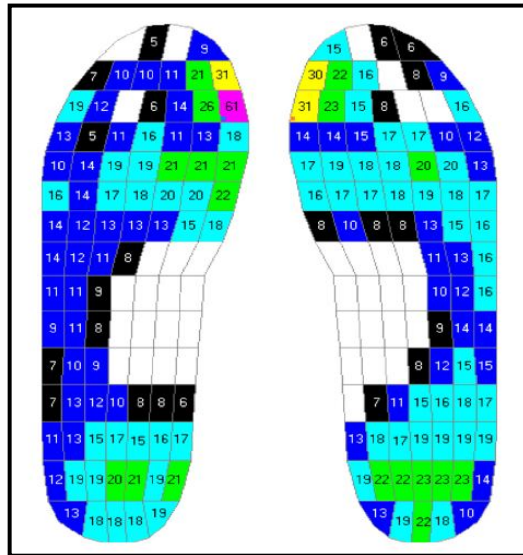


Figure 2.15: Pedar insoles pressure output (Putti, Arnold, Cochrane, and Abboud, 2007)

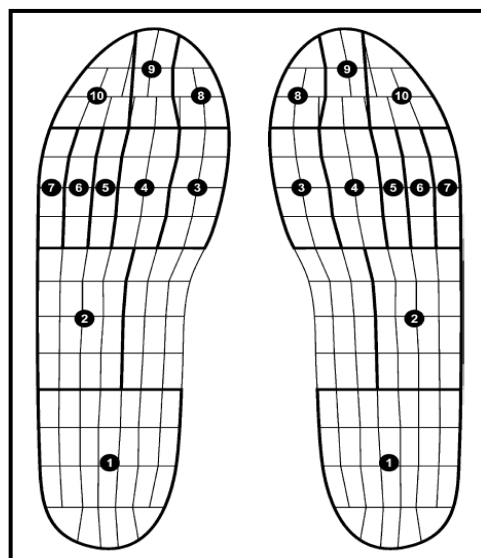


Figure 2.16: The 10 regions of the left and right insoles (Putti, Arnold, Cochrane, and Abboud, 2007)

A method to estimate the complete ground reaction forces from pressure insoles in walking was created by Fong, Chan, Hong, Yung, and Fung (2008). The complete ground reaction forces were collected during a right foot stride by a force plate at 1000 Hz (Fong, Chan, Hong, Yung, and Fung, 2008). Stepwise linear regressions were performed to individually reconstruct the complete ground reaction forces in three directions from the pressure data until redundancy among the predictors occurred (Fong, Chan, Hong, Yung, and Fung, 2008).

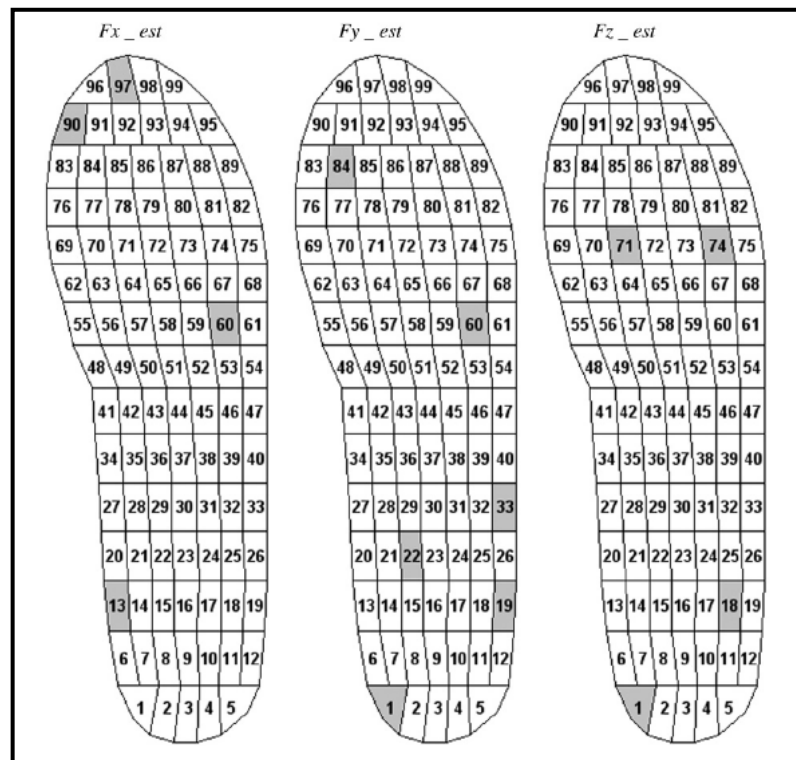


Figure 2.17: Location of the sensors (in right foot) required in the three regression models (in grey) (Fong, Chan, Hong, Yung, and Fung, 2008)

Finite models is one of the method for common flat insole and two sets of specially designed total contact insoles (TCI) were created directly underneath the foot model by Chen, Ju, and Tang (2003). After the material properties and the boundary conditions were set up in each of the three foot-insole models, finite element analyses were performed (Cheng, Ju, and Tang, 2003). The analysis results were retrieved to a local workstation for the post-processing of the stress distributions at the foot-insole interfaces. A comparison of values reported in other studies is shown in table below.

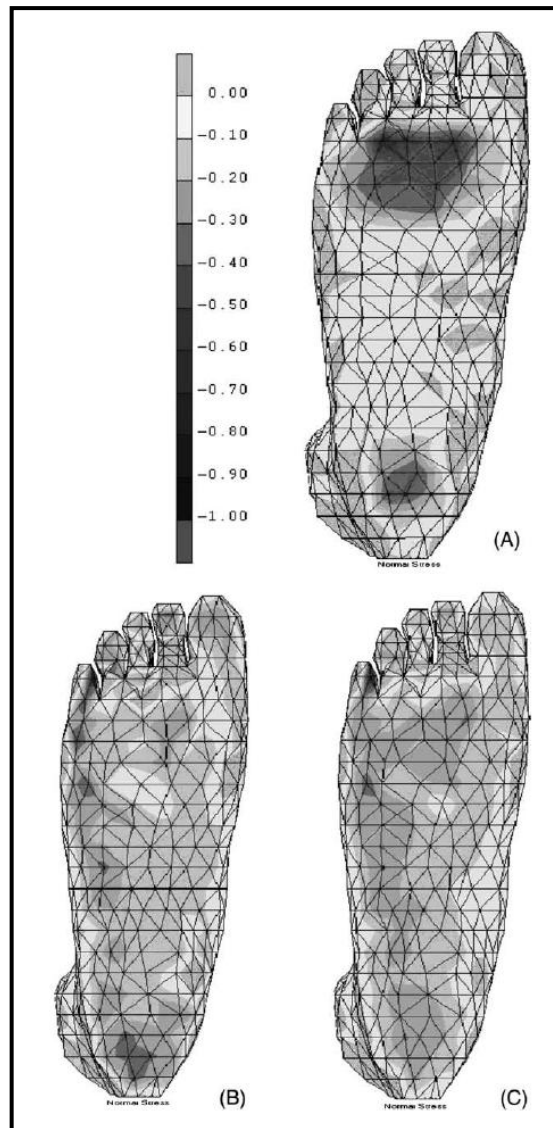


Figure 2.18: Normal stress distributions on the plantar surface for wearing the (a) flat insole, (b) three layers, and (c) two layers (Chen, Ju, and Tang, 2003)

Table 2.2: Comparison of values reported in other studies (Martínez-Nova, Cuevas-García, Pascual-Huerta, and Sánchez-Rodríguez, 2007)

Area	Martínez-Nova [8]	Putti et al. [3]	Bryant et al. [27]
Mean pressure			
Heel	253.1 ± 20.2	264.3 ± 44.1	167 ± 24
Midfoot	65.9 ± 16.8	109.0 ± 38.5	39 ± 25
Met Head 1	308.2 ± 36.1	248.0 ± 70.1	122 ± 33
Met Head 2	405.8 ± 57.4	246.5 ± 48.3	188 ± 41
Met Head 3	394.1 ± 37.7	224.7 ± 50.4	154 ± 32
Met Head 4	203.6 ± 22.5	161.0 ± 49.7	114 ± 39
Met Head 5	118.4 ± 18.3	141.6 ± 58.4	89 ± 43
Hallux	146.5 ± 22.5	280.4 ± 83.0	139 ± 38
Lesser Toes	105.3 ± 14.3	130.3 ± 55.3	83 ± 25

2.5 Current Method/Technology

2.5.1 Force Platform

Force platforms represent the gold standard method for determining these gait events. However despite their recognized accuracy, the method is usually restricted to gait laboratory environments and the number of force platforms available (often two or three) limits the number of steps per trial that can be recorded (Razian and Pepper, 2003).

As the study on biomechanics is growing, various methods and tools have been developed to collect either kinematics or kinetics parameters of the human gait. And force platform emerges as one of the most common tools used to provide information on three orthogonal forces and moments exerted by human body. It is widely used in engineering and medical research, orthopaedics, rehabilitation evaluation, prosthetics, and other general industrial uses (Gouwanda, Senanayake, Marasinghe, Chandrapal, Kumar, Tung, et al, 2008).

A novel 3D platform system has been developed by Wang, Liu, and Chen (2009). This system is suitable for the measurement of human foot pressure distribution has been presented in their research. The system measures plantar pressure between the foot and force platform during dynamic movement in real-time, which can be used in clinical gait analysis (Wang, Liu, and Chen, 2009).

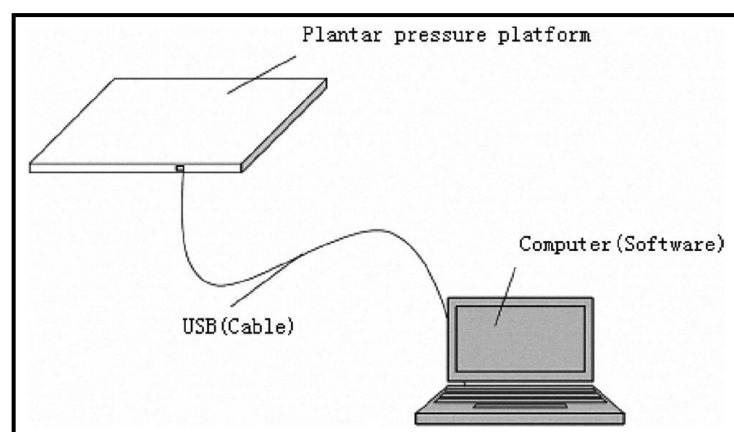


Figure 2.19: The outline of the 3D force platform for plantar distribution measurement (Wang, Liu, and Chen, 2009)

This system consists of a 3D force measuring platform and user-friendly software to graph and analyze the data (Wang, Liu, and Chen, 2009). Furthermore, a new type of Butterworth low-pass filter is being designed to employ for the signals preconditioning, the interference signals of the pressure sensor signal can be effectively filtered (Wang, Liu, and Chen, 2009).

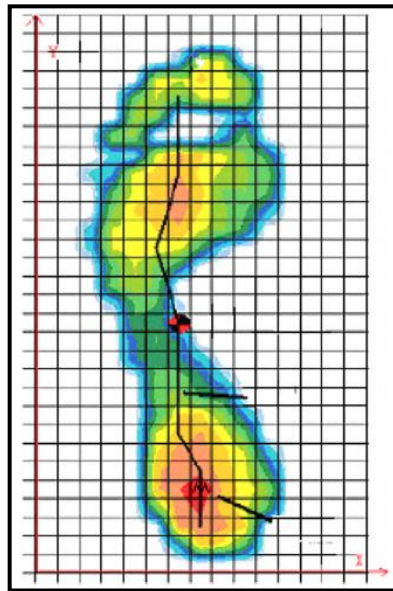


Figure 2.20: The track of the plantar force distribution (Wang, Liu, and Chen, 2009)

However, despite of its capabilities and performances, force platform has several limitations. One of its limitation is that force platform does not provide either qualitative or quantitative information on how the ground reaction forces are distributed on the human foot, from toe to heel (Gouwanda, Senanayake, Marasinghe, Chandrapal, Kumar, Tung, et al, 2008).

Therefore, due to this reason, a force sensing mat has been designed and developed that is capable to visualize the force distribution of the human feet. Polyvinylidene Fluoride polymer (PVDF) wires are used to develop a magic carpet that is capable of measuring human foot pressure by Paradiso. Then, another researcher, Srinivasan and his colleagues developed a pressure sensing floor that has one sensor per square centimetre, with sensor spaced apart and each sensor has active area of certain parts.

With similar functionalities as the force sensing mat being developed earlier, a real time force sensing instrument that has different concept is introduced by Gouwanda, Senanayake, Marasinghe, Chandrapal, Kumar, Tung, and Yulius (2008). This instrument contains an array force sensing elements as shown at figure below that is capable of monitoring and recording the movement pattern of a test subject in standing, walking, jumping, and running (Gouwanda, Senanayake, Marasinghe, Chandrapal, Kumar, Tung, et al, 2008).

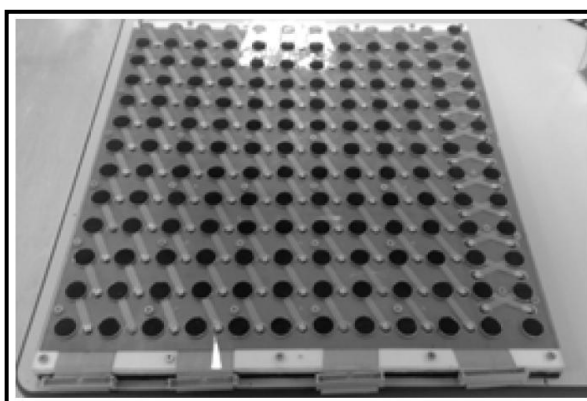


Figure 2.21: Force Sensing Platform (Gouwanda, Senanayake, Marasinghe, Chandrapal, Kumar, Tung, et al, 2008)

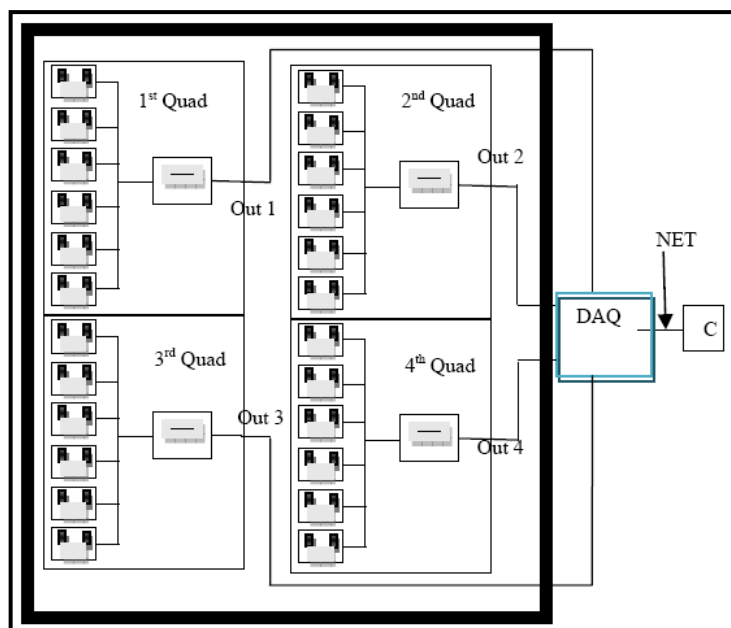


Figure 2.22: Schematic diagram of arrangements of sensors into quadrants with connectivity to the ethernet (Gouwanda, Senanayake, Marasinghe, Chandrapal, Kumar, Tung, et al, 2008)

2.5.2 Instrumented Insole

To monitor and analyze the gait of a person, it is necessary to identify and understand the movements (kinematics) of humans (Jagos, Oberzaucher, Reichel, Zagler, and Hlauschek, 2010) and the forces (kinetics) (Fong, Chan, Hong, Yung, Fung, and Chan, 2008) that are applied on the human joints.

Compared with floor-mounted or force platform systems, the in-shoe devices show more advantages. Subjects are able to wear the in-shoe device while walking in their normal gait without thinking about where the force platform is. Multiple steps can be monitored by in-shoe system but not with the force platform.

Despite the force platform system can provide both the shear and vertical information of the ground reaction force, little loading information about the plantar surface with respect to the supporting surface mentioned. Besides, with the development of wireless communication, the in-shoe device can be used not only in the clinic or laboratory, but also in the outdoor environment, which extends the usable locations for patients.

Up-to-date, research has been carried out to obtain the orientation velocity and acceleration of joints using accelerometers, and gyroscopes. Foot pressure patterns are also widely used in research using force sensing resistors (Grandez, Bustamante, Gurutzeaga, and Garcia-Alonso, 2009), capacitive (Salpavaara, Verho, Lekkala, and Halttunen, 2009), load cells (Muller, Brito, Pereira, and Brusamarello, 2010) or foot switches. Combination of the abovementioned sensor types are also used to obtain parameters of both kinematic and kinetic data for a detailed gait analysis (Faivre, Dahan, Parratte, and Monnier, 2003; Benbasat and Paradiso, 2005).

Recent advances on gait analysis of diseases, like Parkinson's disease patients include portable digital monitoring systems which are instrumented insole systems. These system allow gathering data by the patient themselves, wearing sensors at home and outside home. One of the example instrumented system being developed by Grandez and his colleagues (2009) based on tiny electronic circuits which gather and transmit data coming from force sensing resistors.

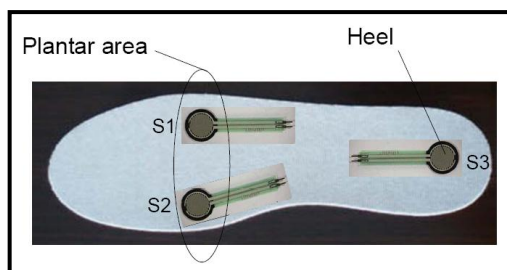


Figure 2.23: Placement of sensors in each insole (Grandez, Bustamante, Gurutzeaga, and Garcia-Alonso, 2009)

Besides the application in medical field, this instrumented insole system has been developed for the sport events. An insole system was being developed by Salpavaara and his colleagues (2009). The idea is to measure the forces between foot and insole with a low-cost laminated capacitive sensor matrix and embedded read-out electronics.

In comparison to other existing in-shoe measurement systems like F-Scan systems and Pedar systems, they are trying to make more application-oriented device that can be easily integrated to larger ambient measurement network (Salpavaara, Verho, Leikkala, and Halttunen, 2009).

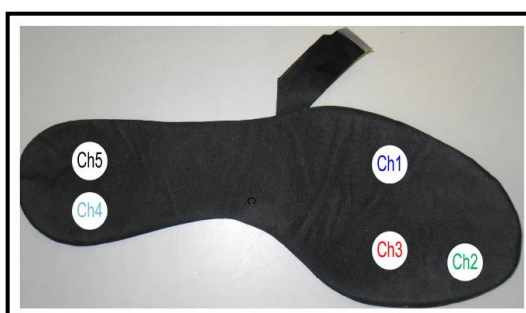


Figure 2.24: There are five measurement areas in the insole. The place and the size of the capacitive sensor elements inside the insole are illustrated with white colour (Salpavaara, Verho, Leikkala, and Halttunen, 2009)

Another sensors, like load cells have long been used to sense and measure force and torque. When properly designed and used, they are very accurate and reliable sensors. Load cells are applied in several different fields, usually for

weighing measurement like in pressure measurement. Among many other things, food, vehicles, and animals are weighed daily in load cells (Muller, Brito, Pereira, and Brusamarello, 2010).



Figure 2.25: Sphere shaped load cell (Muller, Brito, Pereira, and Brusamarello, 2010)

Other sensors like micro-electromechanical system (MEMS) and electromechanical film (EMFI) are used as well in designing the instrumented insole system. The mature bulk micro-electromechanical system technology provides a great opportunity to further advance the specification of foot pressure measurement devices (Wahab, Zayegh, Veljanovski, and Begg, 2008).

Moreover, it is proven that a silicon MEMS based pressure sensor able to measure biomechanical pressure. There are some research or experiments have been carried out to build the instrumented insole system using this MEMS sensors, for example in designing the insole pressure sensing for lower extremity exoskeleton (Wheeler, Rohere, Kholwadwala, Buerger, Givler, Neely, et al, 2009) and for foot plantar pressure measurement (Wahab, Zayegh, Veljanovski, and Begg, 2008).

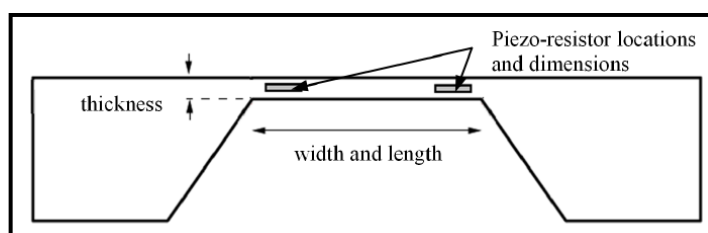


Figure 2.26: The key design parameters of bulk micro-machined pressure sensor (Wahab, Zayegh, Veljanovski, and Begg, 2008)

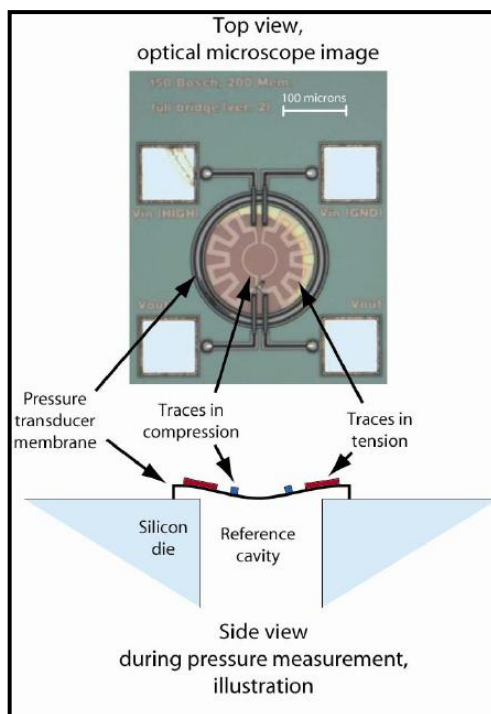


Figure 2.27: One of the MEMS transducer design fabricate. The transducer shown here is a full Wheatstone bridge configuration with two traces in tension and two in compression (Wheeler, Rohere, Kholwadwala, Buerger, Givler, Neely, et al, 2009)

On the other hands, Hannula, Sakkinen, and Kylmanen (2007) developed an instrumented insole system based on EMFI-film sensor. The EMFI-film is a highly sensitive transducer which can be used in pressure or force measurement (Hannula, Sakkinen, and Kylmanen, 2007). In real world, is has been applied in various applications, for example in blood pressure pulse detection and in touch screen systems. The advantages of EMFI-film material are its high sensitivity, flexibility, versatility, and low cost (Hannula, Sakkinen, and Kylmanen, 2007).

Recently, there are few designed being proposed with the combination of variety type of sensors in order to generate different values of foot pressure measurement at the same time. One of the famous studies is done by Morris and Paradiso (2002) where they combine the force sensing resistors (FSRs), piezoelectric material, Polyvinlylidine fluoride (PVDF), and two pairs of resistive bend sensors placed back to back to provide bi-directional bend as shown in figure below.

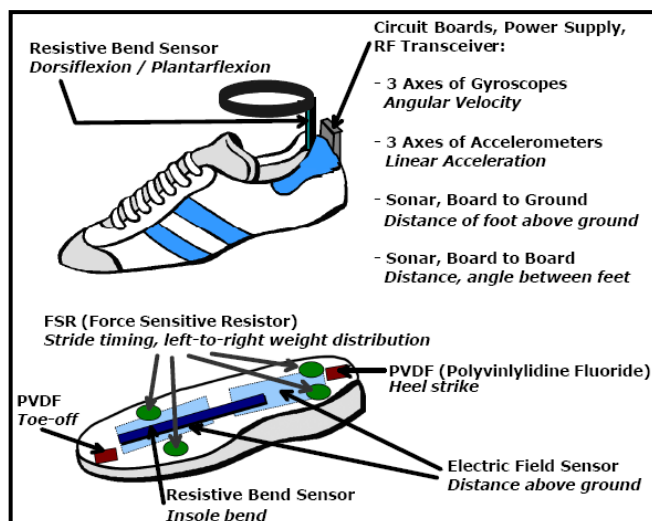


Figure 2.28: Schematic of the Shoe-Integrated Gait Sensors (SIGS) (Morris and Paradiso, 2002)

After that, a homemade shoe with an instrumented insole was being designed by Faivre, Dahan, Parratte, and Monnier (2003). It authorizes the dynamic recording of ground reaction force and plantar pressure during gait. The sole of this shoe contains several holes designed to receive force transducers. Each homemade transducer is composed of a metallic dynamometric ring (Faivre, Dahan, Parratte, and Monnier, 2003). A precision strain gauge is fixed on its external face as shown in the diagram below. The sensors which are used in this design include the piezoelectric, capacitive, and resistive sensors.

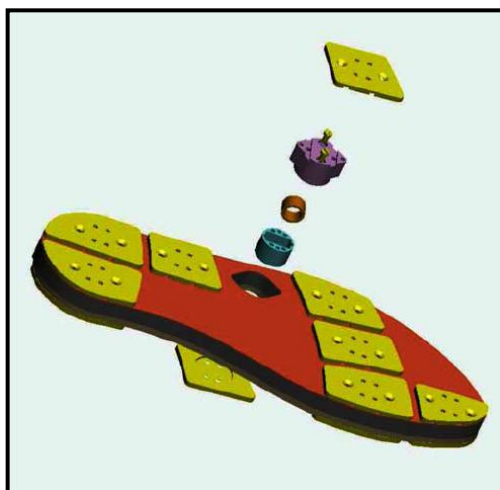


Figure 2.29: Sole with the eight areas and exploded view of transducer (ring, box, aluminium plates) (Faivre, Dahan, Parratte, and Monnier, 2003)

Apart from that, a multimodal approach for insole motion measurement and motion was developed as shown in the figure below. The instrumented insole system consists of an array of force sensing resistors (FSRs), a dual-axis gyroscope, and a tri-axis accelerometer. This combination of sensors allow for the plantar pressure measurement and detect the necessary motion patterns for further analysis in the fields of fall risk detection and physical activity measurement (Jagos, Oberzaucher, Reichel, Zagler, and Hlauschek, 2010)

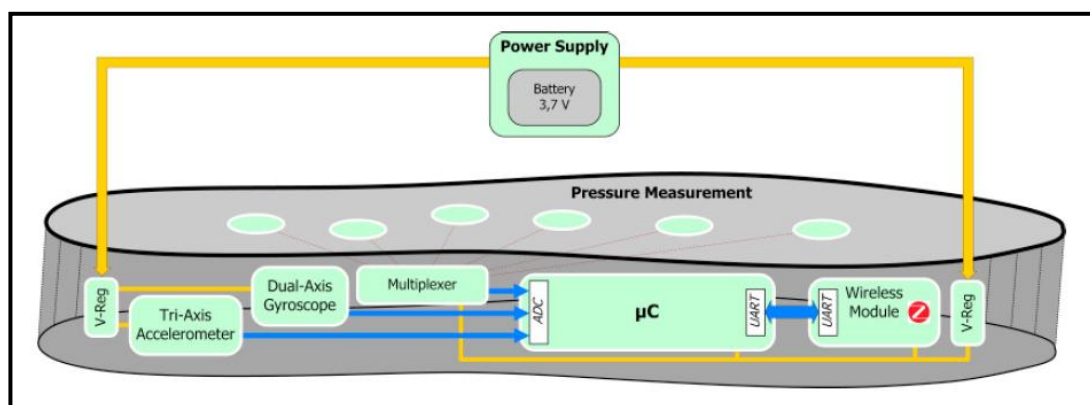


Figure 2.30: Schematic diagram of one instrumented insole with the included components (Jagos, Oberzaucher, Reichel, Zagler, and Hlauschek, 2010)

Not only that, there still a lot of instrumented insole designs with the combination of several sensors, function to measure different kinematics and kinetics force based on their requirement of the research or study, like a technique for conditioning and calibrating force-sensing resistors for measurement of compressive force (Hall, Desmoulin, and Milner, 2008), wireless gait analysis system by digital textile sensors (Yang, Chou, Hu, Hung, Wu, Hsu, et al, 2009), wireless modular sensor architecture and its application in on-shoe gait analysis (Benbasat, Morris, and Paradiso, 2003), compact modular wireless sensor platform (Benbasat and Paradiso, 2005), and the list goes on.

CHAPTER 3

METHODOLOGY

3.1 Introduction

An instrumented insole varies in different ways of design and development depends on the aim, objectives, and applications accordingly. Today, there are plenty of researches, tests, and trials being conducted to discover the most effective, simplest, and cost effective instrumented insole to play the crucial role in pressure detection beneath foot. In general, an instrumented insole consists of different design options, they are type of sensors, position of sensors, electronic circuit, data transmission, and so on. For sure, each design components has own specific functions, advantages, and disadvantages compared to others. Therefore, the purpose of this chapter is to deliver the first hand conceptual ideas by the group concerning the vital criteria such as the most suitable, user-friendly, light-weighted, and commercial available design of instrumented insole for this project.

In this chapter, a brief introduction of the selected design options will be discussed. For the hardware section, each selected component and tools used in this design will be listed clearly regarding their specification, characteristics, and assembly procedures. Next, the procedures of setting up the software are included in the software section. This chapter will be ended with the coding and graphical programming explanation for the design.

3.2 Preferred Design

To design an instrumented insole, there are several main aspects which need a great amount of attention in order to obtain the most idea design. These main aspects are type of sensors, sensor positions, power supply, signal conditioning, data logging, data transmission, data storage, data display, and data analysis. In this subsection, all the aspects as mentioned above will be further discussed and explained clearly.

3.2.1 Sensors

The usage of sensor is one important consideration in developing this instrumented insole where they detect and draw the overall foot pressure distributions of the system. They are the essential devices in converting a physical measurement to an electrical output. Forces are being generated by pressing or pressuring the sensors between instrumented insole and ground during human's walking or running activities. Changes in pressure distributions underneath different regions of foot can be observed by using the following sensors for further analysis:

In this design, two different sizes and shapes of Force Sensing Resistors (FSRs) manufactured by Interlink Electronics are used, which are in the circular and square sensing shapes. It is an ideal for designers, researchers, or anyone who needs to measure forces without disturbing the dynamics of their tests. This sensor can be used to measure both static can dynamic forces and are thin enough to enable non-intrusive measurement.

Force Sensing Resistors are a polymer thick film (PTF) device which use the resistive-based technology. The application of a force to the active sensing area of the sensor results in a change in the resistance of the sensing element in inverse proportion to the force applied, which shared similar properties with load cell or strain gauge (Interlink Electronics, 2010).

3.2.2 Position of Sensors

Position or placement of sensors beneath the foot varies with the foot pressure measurement. Different positions of sensors have to match with different foot pressure measurement. However, position of sensors might be affected by different aspects such as genders, ages, races, diseases, and so forth.

In this project, it is considered as one of the design options where the sensors are being distributed under foot regions respectively. These sensors are the main key in this project on how to measure the applied forces beneath foot during gait simulation. The circular shape sensors will be placed along the big toe (hallux), first, and fifth metatarsals where the square shape sensors will be attached under the heel area.

3.2.3 Power Supply

Without power supply, the whole instrumented system cannot function with the correct circuit connections and programs. Therefore, providing enough electrical power to make the force measurement working in a good condition is one of the crucial factors in operating the whole system. Meanwhile, attention should be paid in selecting the voltage source which is going to supply the correct range of required voltages for the electrical and electronic circuitry in the system. Hence, electronic components such as voltage regulator is being implemented to ensure there is no extra voltage or current flow that will cause overflow or damage to circuitry.

Rechargeable batteries are used to provide the required voltage to the whole design for smooth operating along the gait simulation. The 9.0 V batteries are attached as the input power supply for the whole design system. Voltage regulators are used in this design to regulate and maintain the input voltage at a constant level. Difference between the actual output voltages with the internal fixed reference voltage is amplified and used to control the regulation element in order to correct the voltage error.

3.2.4 Signal Conditioning

Signal conditioning is a process where the analogue signal from the output of sensor is being manipulated in order to meet the requirement for further processing. Signal conditioning includes several processes which are filtering, amplification, range matching, isolation and some other processes required to make the sensor output suitable for processing. In other words, all the output from sensors is only able to be processed and analyzed after they undergo a signal conditioning process.

Filtering is the most common signal conditioning function as not all the signal frequency spectrum contains valid data. This can be done by using filters to remove all the unwanted noises or signals, either by using the high pass filter on the higher threshold, low pass filter on the lower threshold, or the band pass filter for the intermediate signals.

Amplifiers are used to amplify or modify the signals by increasing or decreasing the amplitude of signals. Signal amplification performs two important functions which are increasing the resolution of the input signal and its signal-to-noise ratio.

Signal isolators must be used in order to pass signal from the source to the measurement device without a physical connection. It is often used to isolate possible sources of signal perturbations. Also, it is important to note that isolation needs to be done to the expensive equipments which used to process signal after signal conditioning from the sensors.

In this design, microcontroller is used to convert the analogue signals from the sensors to digital signals before further processing in the following subsystem. Noise filtering is done through software in the data display and data analysis instead of using RC circuits formed by capacitors and resistors in order to save costs and flexibility of the software.

3.2.5 Data Logging

Data logging is a subsystem which records, receives and stores data over time. It works in line with the microcontroller and serial port by collecting the analogue signals from sensors and converts them into digital signals so that can be transmitted to the processing unit. In general, there will be a temporary storage unit where the digital signals can be stored temporary before being transferred to a processing unit.

Microcontroller is used as the data logging facility in this design where it acts as the medium in collecting the analogue signals from the sensors. Then, the microcontroller will store the collected signals temporary before they are being converted into digital signals and ready to be sent to the processing unit, like computer or laptop.

3.2.6 Data Transmission

Normally, data transmission is divided into two types, wired and wireless for transmitting signals from the sensors to data loggers or from data loggers to processing unit. Both of these transmission types have their own advantages and disadvantages. Wires or ribbon cables are commonly used in wire communication for more connections through a circuit, while there are many types of wireless communications which is specific and harmless to human, for example Bluetooth, radio frequency (RF), radio frequency identification (RFID), Zigbee, and others.

For a better performance in transmitting the data, wireless communication is chosen as the data transmission in this design. XBee (ZigBee) module is used instead of other wireless network which is a specification for a suite of high level communication protocols using a small, low-power digital radios based on the IEEE 802.15.4-2003 standard for wireless home area networks (WHANs). It has capacity of 250 Kbits at 2.4 GHz, 40 Kbits at 915 MHz, and 20 Kbits at 868 MHz with a range of 10 m to 100 m. It is targeted at applications which require a low data rate, long battery life, and secure networking.

3.2.7 Data Storage

Data storage, a subsystem which is required by the instrumented insole system to save the transmitted file into an internal memory or temporary file for further analysis purposes. It can refer to computer or any other data storage devices, for instance computer system, laptop, PDA, remote devices, and mobile phones. It is a process of records (stores) or retrieves (reads) information or data from instrumented insole system through either wires or wireless communications before further analysis can be made.

Computer or laptop is use primarily in this design with the purpose of help in recording the real time data and store the data collected in the form of text files by using particular software. Other than that, computer or laptop is mostly used now where they are easy, portable, and convenient for data collecting, processing, storage, and analysis.

Normally, computer and laptop consist of a quite large internal memory compare to other device. Hence, more information and results from each analysis can be stored securely for further processing, comparison, and analysis. Besides, computer and laptop are capable of receiving and sending the data wireless anytime and anywhere.

3.2.8 Data Display

Data can be displayed only after being collected and stored in the internal memory or temporary file of processing unit. It is an output subsystem for presentation of information for visual, tactile or auditive reception, acquired, stored, or transmitted in various forms. When the input information is supplied as an electrical signal, the display is called electronic display. Display subsystem of data can be built by using programming logic codes, software, or combination of both. Certain parameters can be shown by setting up specific configuration of the system regarding to data collected in graphical or tabular forms.

In this design, National Instrument LabVIEW is used for the data display by installing into a computer or laptop. LabVIEW is a graphical programming software developed for measurement, test, and control system by using intuitive graphical icons and wires which resemble a flowchart. Therefore, the result of data collected can be displayed where the measurement of forces can be estimated along with a graph representation in real time.

3.2.9 Data Analysis

Analysis of data is a process of inspecting, cleaning, transforming, and modelling data with the goal of highlighting useful information, suggesting conclusions, and supporting decision making. Normally, analysis system can be built by using programming logic codes, software, algorithms, or combination of both. By using analysis system, data can be judged or analyzed with specific parameter requirements. Data can be filtered by removing unwanted, overlapping, or redundant information which lead to a conclusion of data collected.

Same as data display, National Instrument LabVIEW is used for the data analysis where particular settings can be made to the software to meet the measurement requirements for the design. Before data analysis, data can be filtered as well by using the software according to the level of amplitude and frequency for better and accurate results.

3.2.10 Summary of Preferred Design

All the selected design options which being discussed are summarized and illustrated clearly in the chart below:

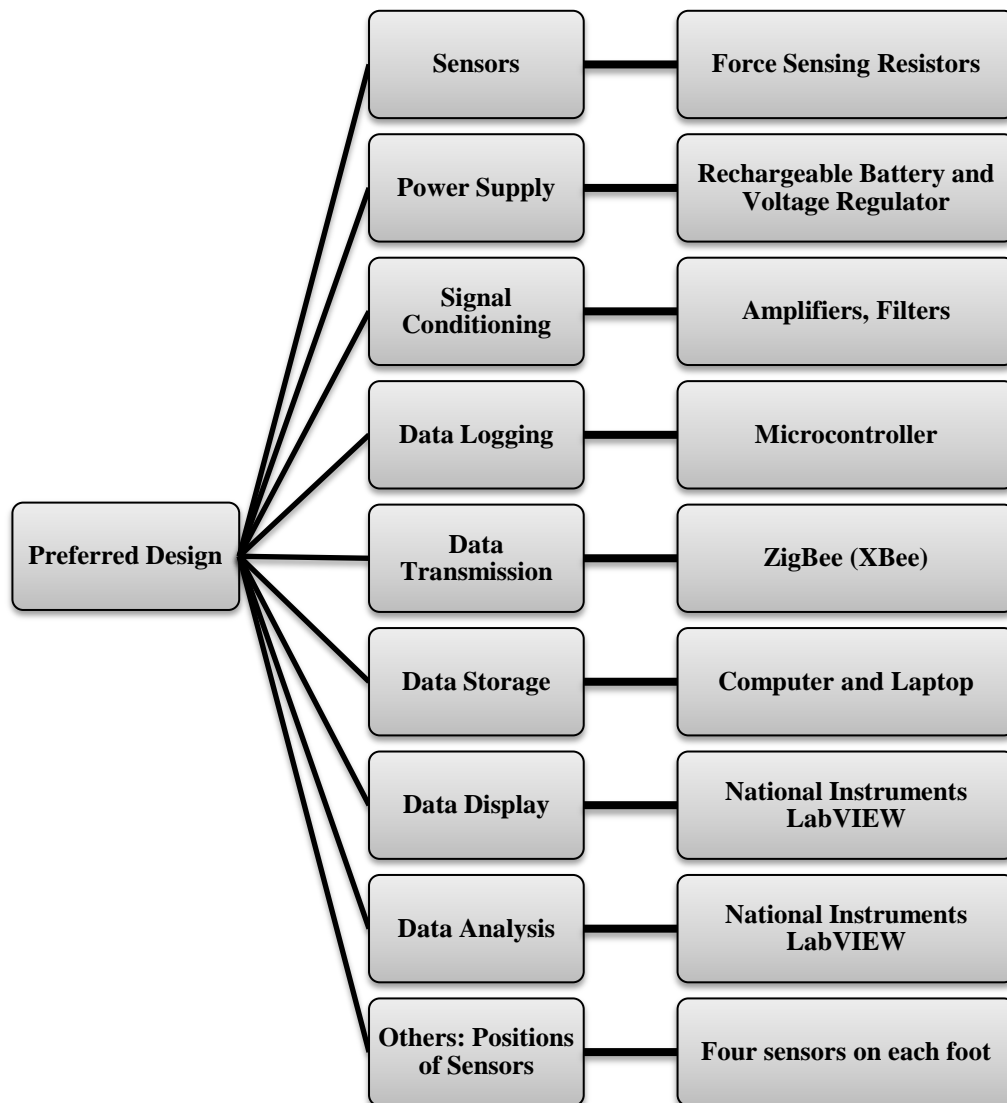


Figure 3.1: A summary chart of design options

3.3 Process Flow

The overall process of how the instrumented insole system functions in measuring the pressure distribution beneath foot is summarized in the flowchart shown below:

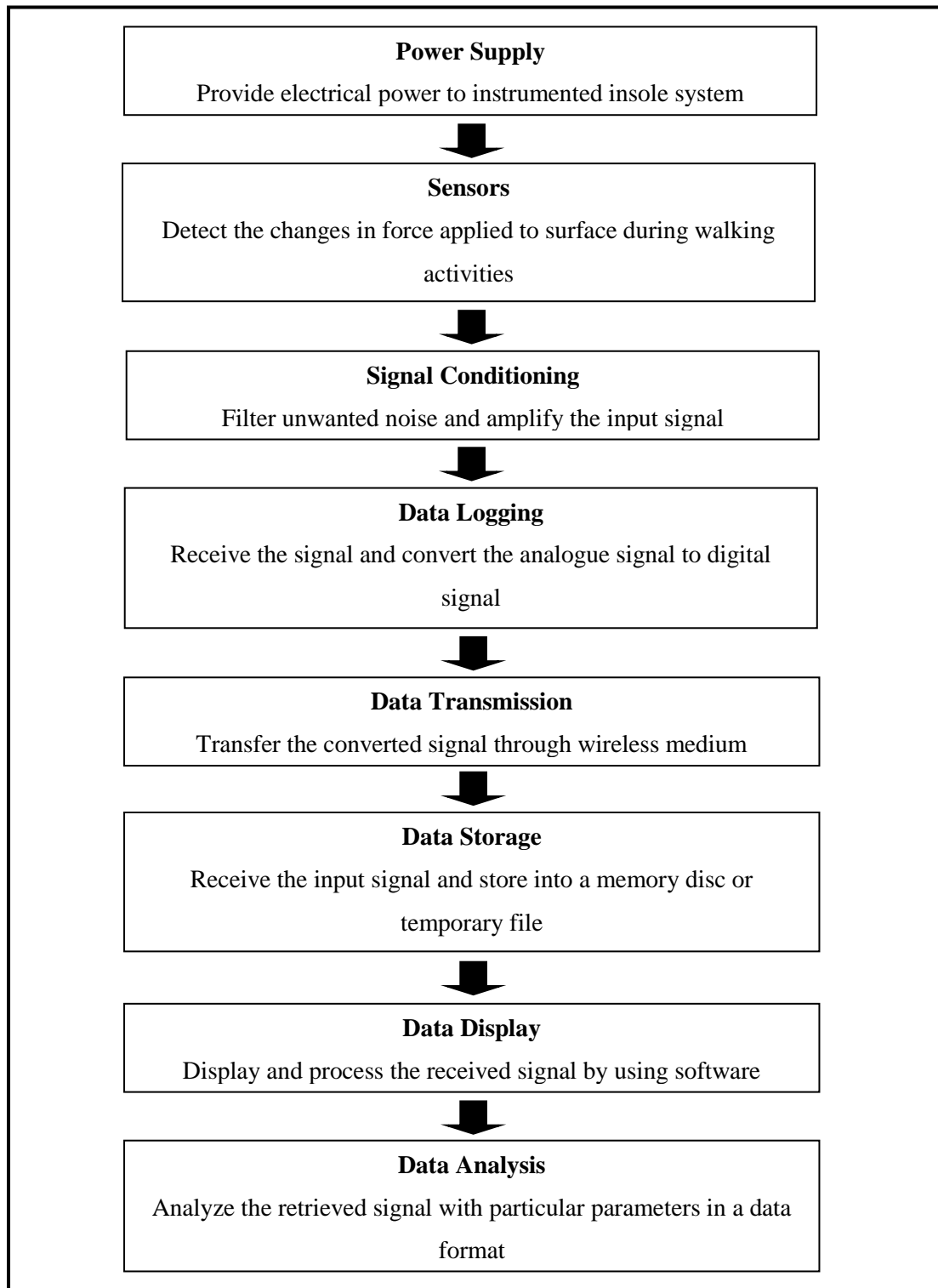


Figure 3.2: A general process flowchart of an instrumented insole system

In addition, block diagram below is used to summarize the flow of the instrumented insole system as shown below, where it consists of power supply, signal conditioning, data logging, data transmission, data storage, data display, and data analysis. This followed by a schematic diagram of the positions of sensors beneath each foot.

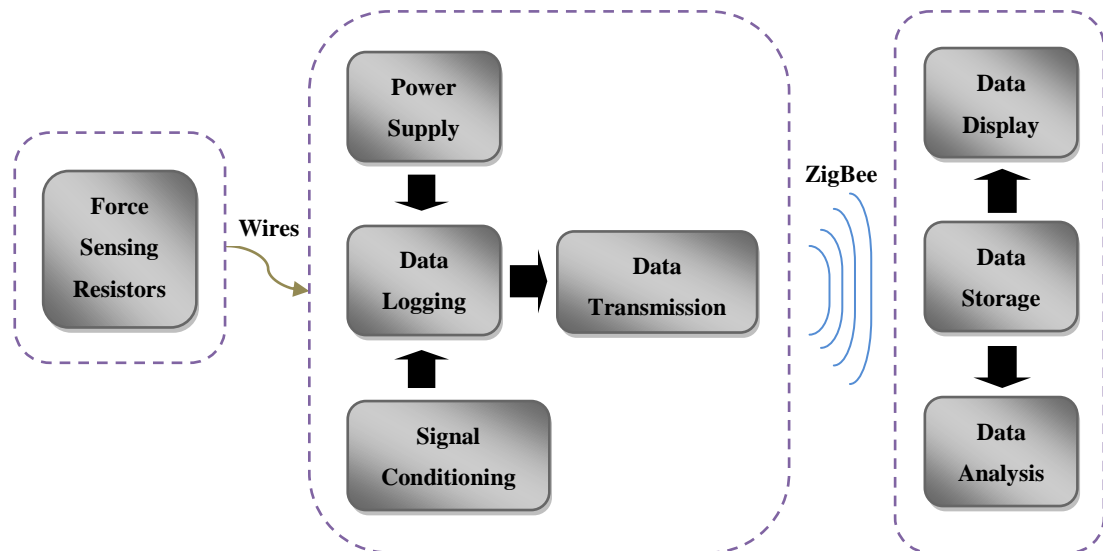


Figure 3.3: A figure representation of an instrumented insole system design using force sensing resistors (FSRs)

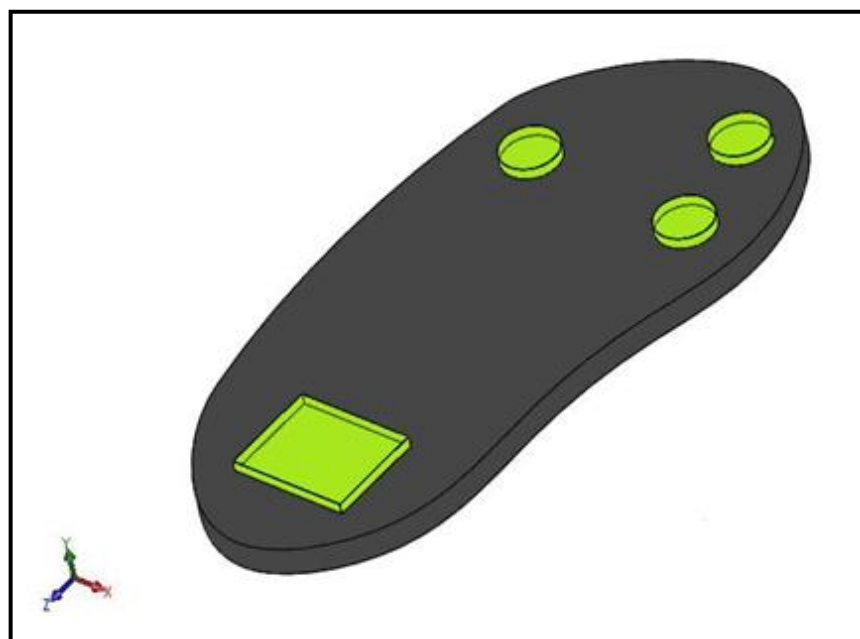


Figure 3.4: A figure representation of sensors positioning of an instrumented insole system design

3.4 Hardware

3.4.1 Components and Tools

In this section, the specification, characteristics, and technical data of each component used in the design are listed. The main hardware components in developing the instrumented insole system are as followed:

1. Force Sensing Resistors (FSR-402 and FSR-406 Interlink Electronics)
2. Voltage Regulator (LM7805)
3. Operational Amplifiers (LM324)
4. Microcontroller (Microchip PIC16F877A)
5. PIC Start-Up Kit (SK40C Enhanced 40 Pins)
6. XBee Starter Kit (SKXBee)

There are still some essential components and tools used in completing this design, such as 10 μF electrolytic capacitor, 100 μF electrolytic capacitor, 1 k Ω resistors, rechargeable 9.0 V batteries, battery snaps, PVC battery holders, donut board, male and female connectors, 10 ways ribbon cables, red and black wires, plastic casing, polymer shoe insole, belts, multimeter, and soldering tools.



Figure 3.5: 10 μF electrolytic capacitor (10 μF Electrolytic Capacitor, 2010)



Figure 3.6: 100 μF electrolytic capacitor (100 μF Electrolytic Capacitor, 2010)

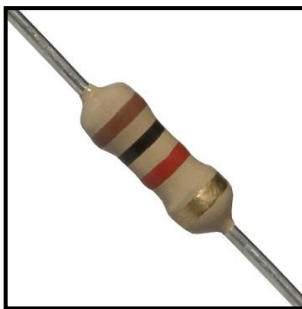


Figure 3.7: 1.0 kΩ resistor (Resistor 1K Ohm ¼ Watt, 2010)



Figure 3.8: Rechargeable 9.0 V battery (Energizer Ni-Mh Rechargeable 9V Square Batteries, 2010)



Figure 3.9: Battery Snap (9V Battery Snap Connector, 2010)



Figure 3.10: PVC battery holder (9V Sealed Battery Holder with Wires, 2010)

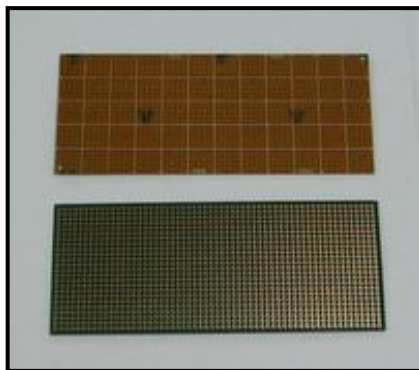


Figure 3.11: Donut board (Donut Board, 2010)

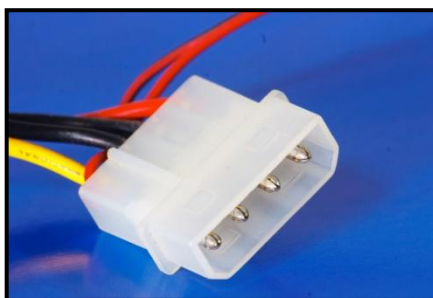


Figure 3.12: Male connector (Male Connector, 2010)

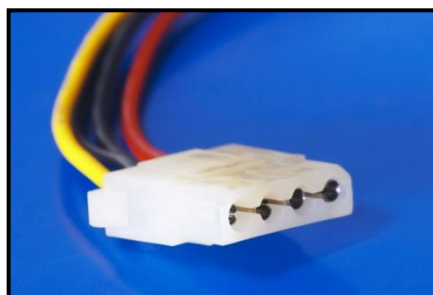


Figure 3.13: Female connector (Female Connector, 2010)

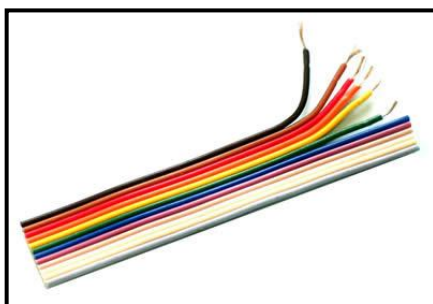


Figure 3.14: 10 ways ribbon cables (Electrical & Electronic Connectors, 2010)



Figure 3.15: Red and black wires (Wires, 2010)



Figure 3.16: Plastic casing (Aluminium Box Silver, 2010)



Figure 3.17: Polymer shoe insole (Shock Absorbing Sheet, 2010)



Figure 3.18: Belts (Cable Belt, 2010)



Figure 3.19: Multimeter (Multimeter, 2010)



Figure 3.20: Soldering tools (How to Solder, 2010)

3.4.1.1 Force Sensing Resistors (FSR-402 & FSR-406 Interlink Electronics)

There are two kinds of Force Sensing Resistors (FSRs) being used in this design; they are FSR-402 which have a circular sensing area with a diameter 12.7 mm and FSR-406 with a square sensing area of 38.1 mm x 38.1 mm. They both have the same thickness around 0.46 mm (FSR Force Sensing Resistor Integration Guide and Evaluation Parts Catalog, 2010). A force sensing resistor has variable resistance as a function of applied pressure.



Figure 3.21: Interlink Electronics FSR-402 (Force Sensitive Resistor 0.5'', 2010)

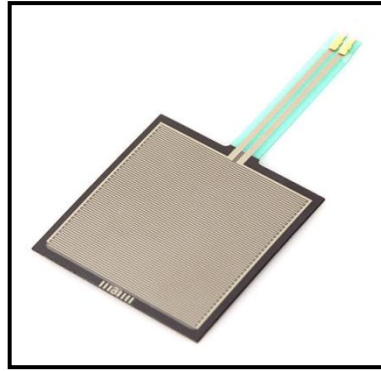


Figure 3.22: Interlink Electronics FSR-406 (Force Sensitive Resistor – Square, 2010)

The resistance is inversely proportional to the force applied. This FSR is fabricated using elastic material and formed by several layers. The inner layer is electrically insulating plastic where it has an active area consisting of a pattern of conductors which is connected to the leads on the tail to be charged with an electrical voltage. Besides, it has an intermediate layer of plastic spacer which induces an opening aligned with the active area as well as an air vent through the tail. The outer layer would be a flexible substrate coated with a thick polymer conductive film which is aligned with the active layer.

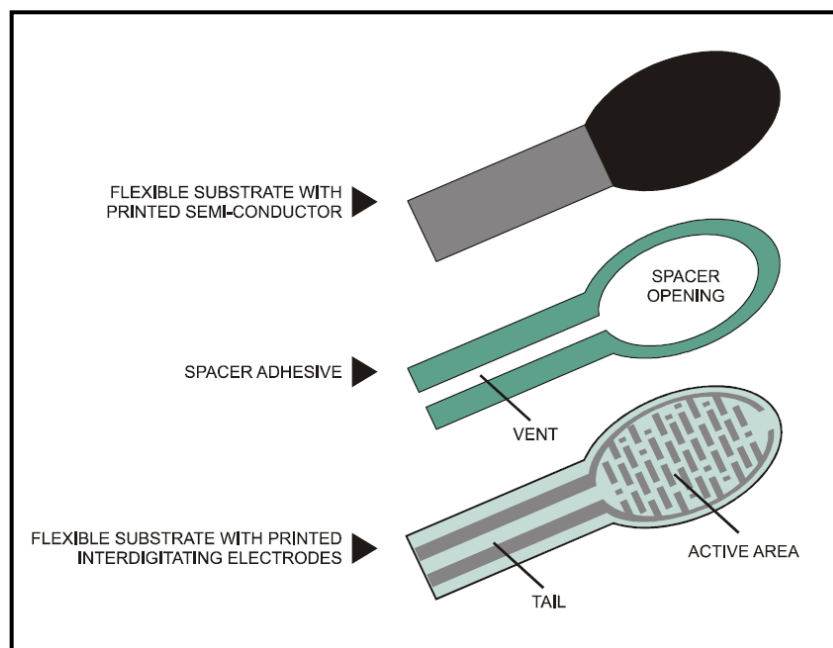


Figure 3.23: Interlink Electronics FSR construction (FSR Force Sensing Resistor Integration Guide and Evaluation Parts Catalog, 2010)

When external force is applied to the sensor during a human locomotion activity, the resistive element is deformed against the substrate. The air from the space opening is being pushed through the air vent into the tail. At the same time, the conductive material on the substrate comes into contact with parts of the active area.

The more the active areas touch the conductive element, the lower the resistance. Generally, FSRs have a “Switch-like Response” where some amount of the force is necessary to break the sensors resistance at rest and push it into the measurement range. Like load cell or strain gauge devices, FSRs have similar properties and can provide a cost effective alternative.

Force accuracy ranges from approximately $\pm 5\%$ to $\pm 25\%$ depending on the consistency of the measurement and actuation system, the repeatability tolerance held in manufacturing ranges from $\pm 15\%$ to $\pm 25\%$ of an established nominal resistance, and the use of part calibration (FSR Force Sensing Resistor Integration Guide and Evaluation Parts Catalog, 2010). The force resolution of FSR device is better than $\pm 0.5\%$ of full use force (FSR Force Sensing Resistor Integration Guide and Evaluation Parts Catalog, 2010).

In this design, six FSR-402 (circular shape) and two FSR-406 (square shape) sensors will be used beneath the foot region respectively. The purpose of using total number of eight sensors is to ensure the accuracy of the results in measuring the force distribution under foot region during human locomotion activity. The readings from these sensors are capable of identifying the types of walking patterns in order to detect the disabilities or diseases being faced by tested subjects.

3.4.1.2 Voltage Regulator (LM7805)

In this design, a 9.0 V battery is used to supply power to the electronic components. Normally, the operating power for most electronic components ranged from 2.0 V to 5.5 V where too high of input voltage may cause damage to them. Therefore, a LM7805 5.0 V voltage regulator is used to lower down the input voltage before the voltage is supply to the whole circuit.

Basically, LM7805 5.0 V voltage regulator consists of three terminal pins; they are input, ground, and output pin. It employs built-in internal current limiting, thermal shutdown, and safe-operating area protection which make it virtually immune to damage from output overloads. Although designed primarily as fixed voltage regulators, these devices can be used with external components to obtain adjustable voltages and currents (LM341/LM78MXX Series 3-Terminal Positive Voltage Regulators, 2005).

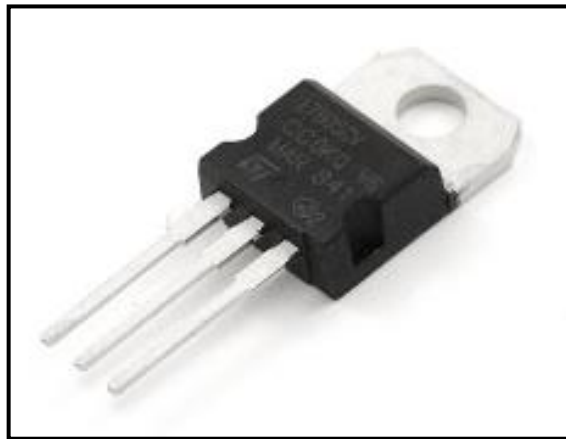


Figure 3.24: LM7805 5.0 V voltage regulator (LM7805 5V Regulator, 2010)

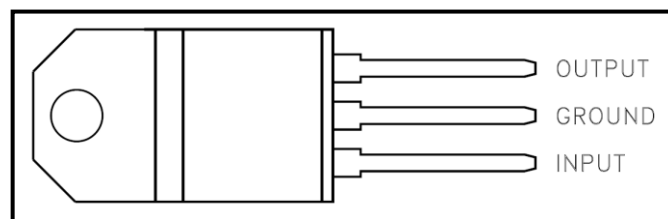


Figure 3.25: Connection diagram of LM7805 (L7800 Series Positive Voltage Regulators, 2004)

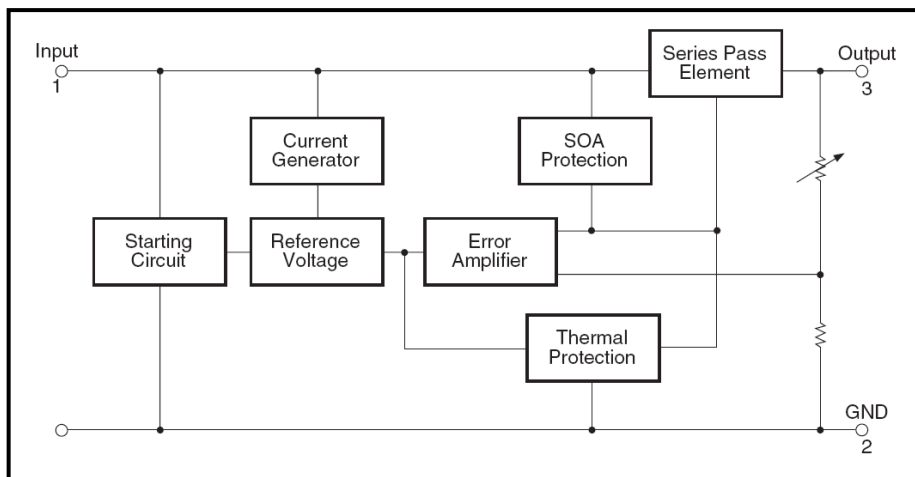


Figure 3.26: Block diagram of LM7805 (LM78XX/LM78XXA 3-Terminal 1A Positive Voltage Regulator, 2010)

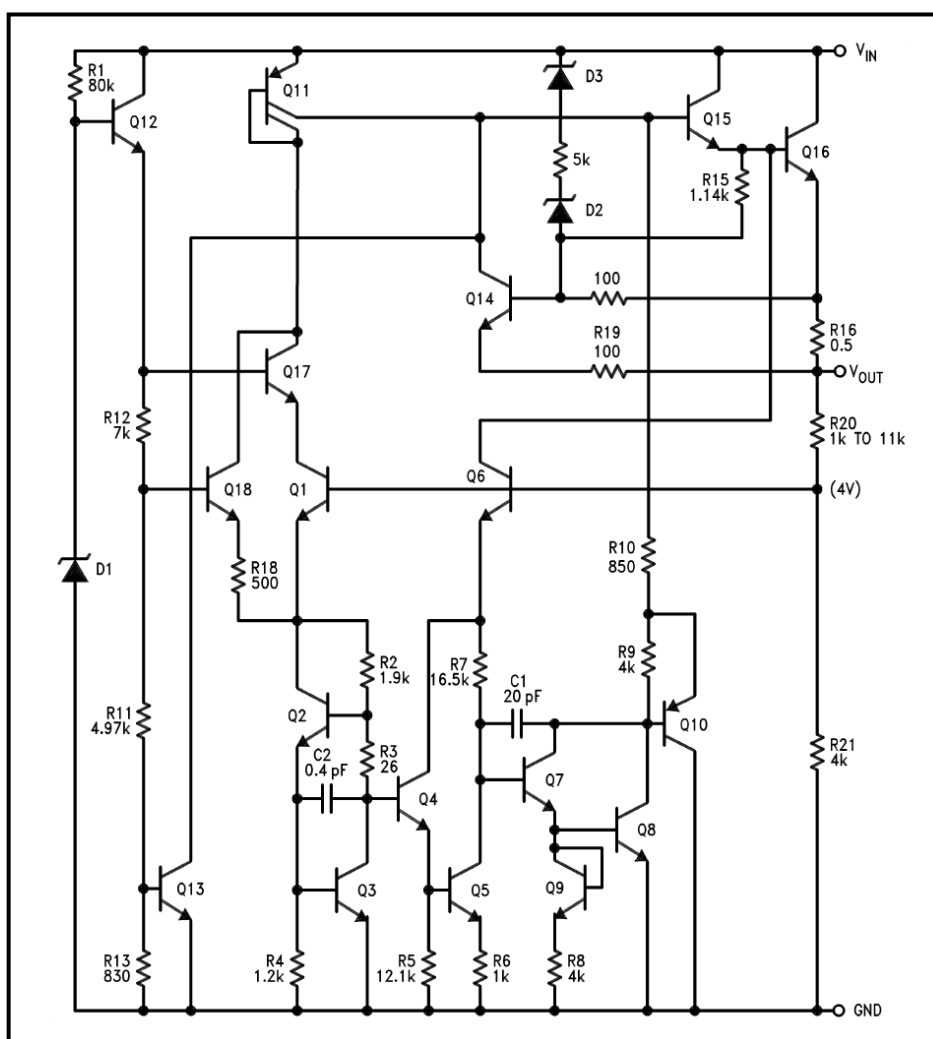


Figure 3.27: Schematic diagram of LM7805 (LM341/LM78MXX Series 3-Terminal Positive Voltage Regulators, 2005)

3.4.1.3 Operational Amplifiers (LM324)

Operational amplifier is an amplifier where the output voltage is proportional to the negative of its input voltage. The LM324 is a low power quad operational amplifier which consists of four independent, high gain, internally frequency compensated operational amplifiers.

LM324 operational amplifiers are used in a voltage divider configuration of the design to achieve a “switch-like” response where a certain amount of force is required to break the sensors resistance to allow a proportional voltage to leak through it. The resistance value of the pull-down resistor is inversely proportional to the force sensitivity range of the FSR and limits the current. The lower the resistance is used, the higher the voltage saturated at forces.

It is designed specifically to operate from a single power supply over a wide range of voltages. Operation from split power supplies is also possible and the low power supply current drain is independent of the magnitude of the power supply voltage. The details on how to assemble the LM324 operational amplifiers will be discussed in the later part of this topic.

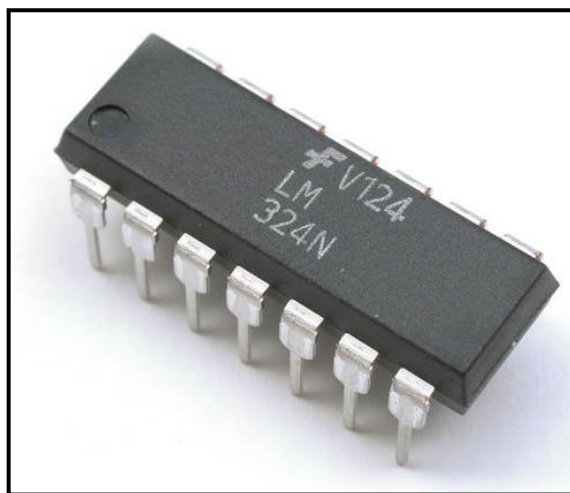


Figure 3.28: LM324 operational amplifier (Quad Operational Amplifier, 2010)

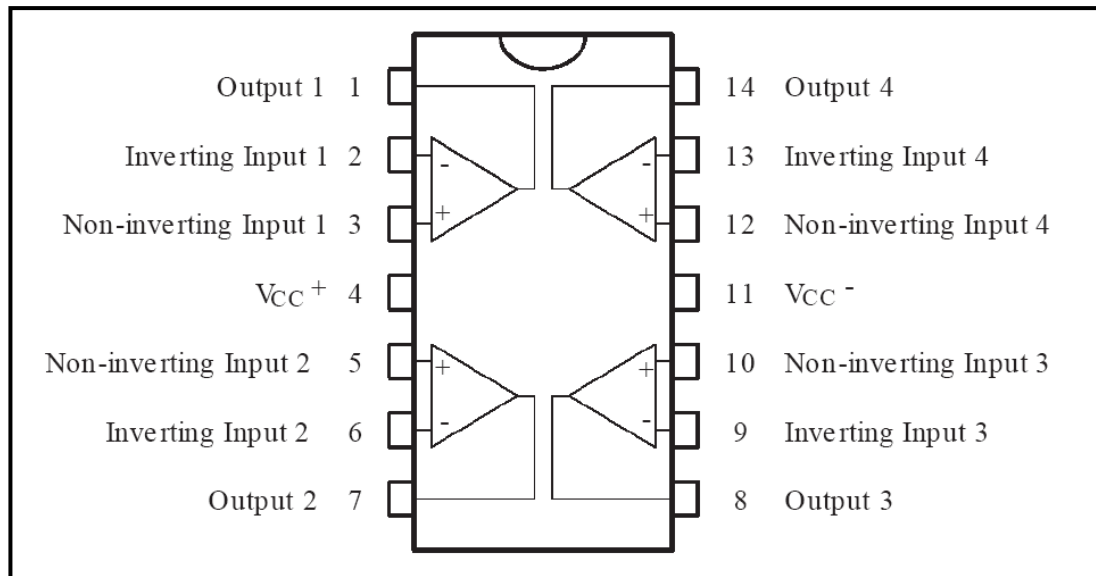


Figure 3.29: Pin diagram of LM324 (Low Power Quad Operational Amplifiers, 1999)

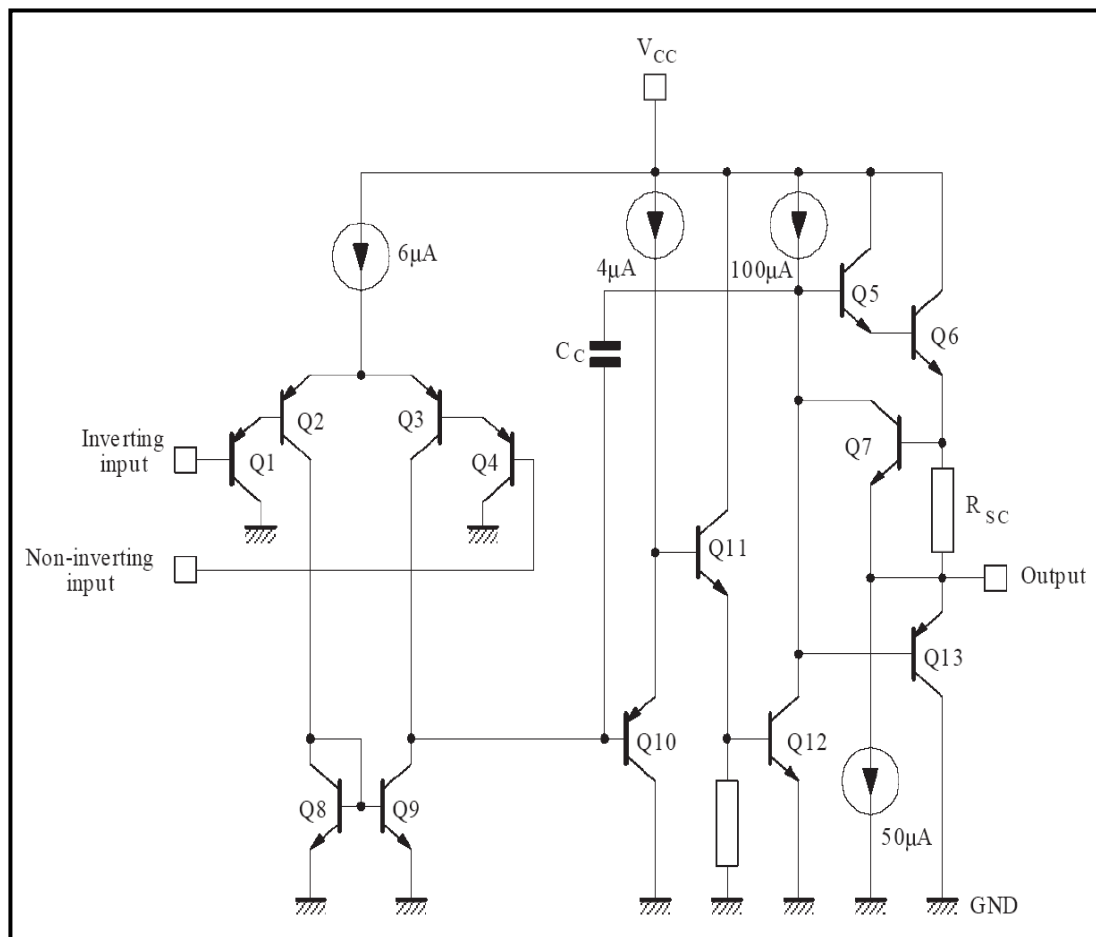


Figure 3.30: Schematic diagram of LM324 (Low Power Quad Operational Amplifiers, 1999)

3.4.1.4 Microcontroller (Microchip PIC16F877A)

Microcontroller serves as an important medium in this design between the sensing element and computer for software analysis. Few types of microcontroller can be used depending on the desired specification needed. Different type of microcontroller provides different pins number, input channel, and functions.

In this project, 40 pins Microchip PIC16F877A is a very powerful microcontroller with easy-to-program features and high computational performance at an economical price. Besides, it has electrically erasable programmable read-only memory (EEPROM) data memory, three timer modules, two capture/compare/PWM (CCP) modules, universal asynchronous receiver transmitter (USART) module, master synchronous serial port (MSSP) module, and dual analogue comparators with input multiplexing (PIC16F87XA Data Sheet, 2003).

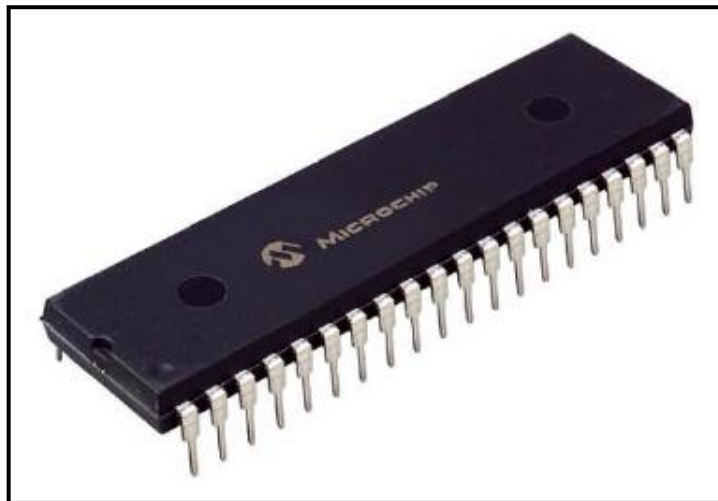


Figure 3.31: Microchip PIC16F877A microcontroller (PIC16F877A, 2010)

The Microchip PIC16F877A is used in this design as it consists of 10-bit, up to 8-channels analogue-to-digital converter (ADC) with programmable acquisition time, which is sufficient for all eight FSRs inputs used in the design. The ADC module has high and low-voltage reference input which can be software selectable. In this microcontroller, USART is presented.

This USART enables transmission of data serially through serial communication interface, which has a multiprocessor communication capability using 9-bit address detection. This will be served as an essential connection formed between microcontroller and computer processing unit through wireless transmission in this design.

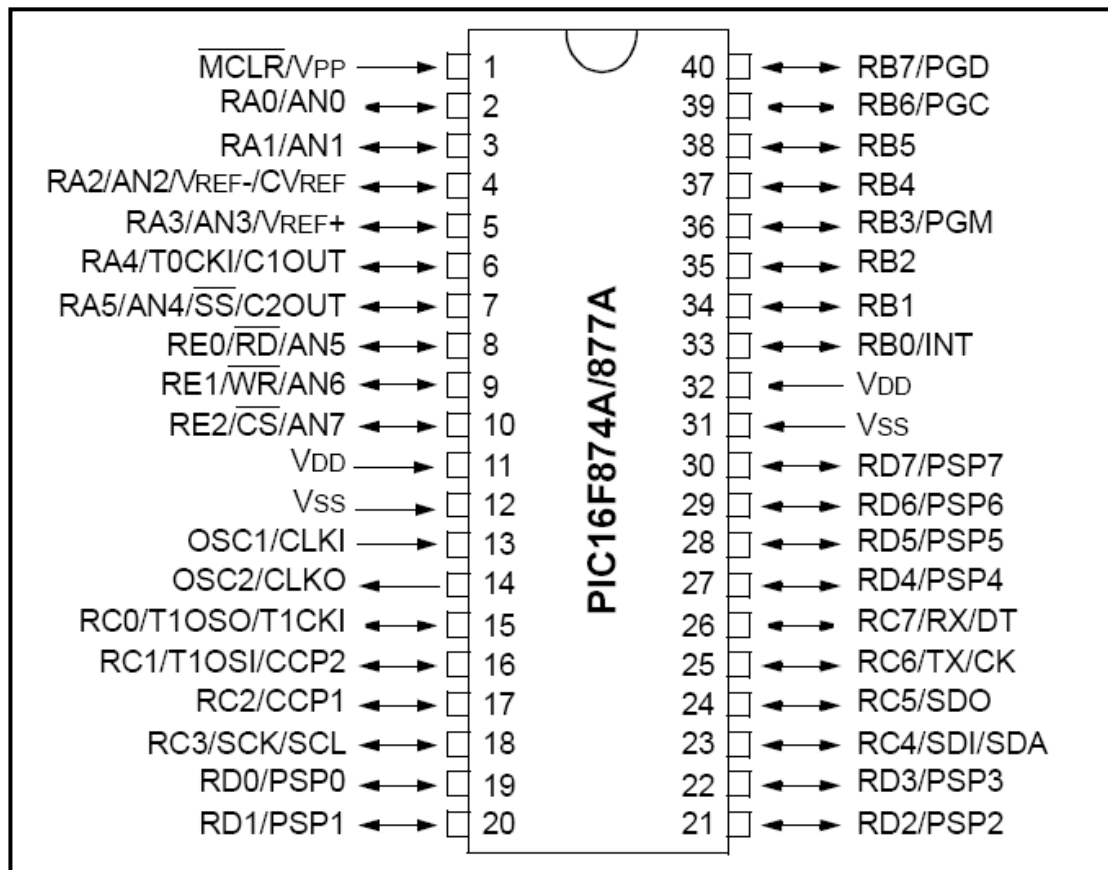


Figure 3.32: Pin diagram of microchip PIC16F877A microcontroller (PIC16F87XA Data Sheet, 2003)

From the diagram shown above, there are notably four ports in the microcontroller which is from A to D. Port A and E are being activated in this design system which consist of the ADC channels labelled from AN0 to AN7. So, this microcontroller functions to read eight analogue input signals from sensing element and converting them into digital signals. The signals are then sent to the XBee module to transmit the data to computer processing unit for storage and analysis. The details on how to assemble the Microchip PIC16F877A will be discussed in the later part of this topic.

Table 3.1: Microchip PIC16F877A microcontroller device features

Key Features	Microchip PIC18F4550
Operating Frequency	DC – 20 MHz
Working Voltage	2.0 to 5.5 V
Flash Program Memory (Bytes)	8K
Data Memory (Bytes)	368
EEPROM Data Memory (Bytes)	256
Interrupt Sources	15
I/O Ports	Port A, B, C, D, E
Timers	3
Capture/Compare/PWM Modules	2
Serial Communications	MSSP, USART
Parallel Communications	PSP
10-bit Analogue-to-Digital Module	8 Input Channels
Comparators	2
Resets (and Delays)	POR, BOP (PWRT, OST)
Instruction Set	35 Instructions
Packages	40-pin PDIP 44-pin PLCC 44-pin TQFP 44-pin QFN

Source: PIC16F87XA Data Sheet, 2003

3.4.1.5 PIC Start-Up Kit (SK40C Enhanced 40 Pins)

Unlike traditional method of microcontroller configuration, SK40C is a new technology that can be used in this design. It is another enhanced version of 40 pins PIC microcontroller start-up kit which is designed to offer an easy assembling as start-up board for PIC users (SK40C Enhanced 40 Pins PIC Start-Up Kit User's Manual V1.1, 2010). This board comes with all the necessary basic components required which is being soldered for PIC to function.

This device is able to utilize the function of PIC by directly plugging in the input and output (IO) components in whatever way that is convenient. With UIC00B (USB ICSP PIC Programmer) connector on board, program can be wrote or loaded to the PIC in a simplest and fastest way without plugging the PIC in and out. Furthermore, UART provided in SK40C can be used for communication to microcontroller or computer. Unlike previous starter kit (SK40B), serial communication between microcontroller and computer can be done without the need of RS232 serial port.

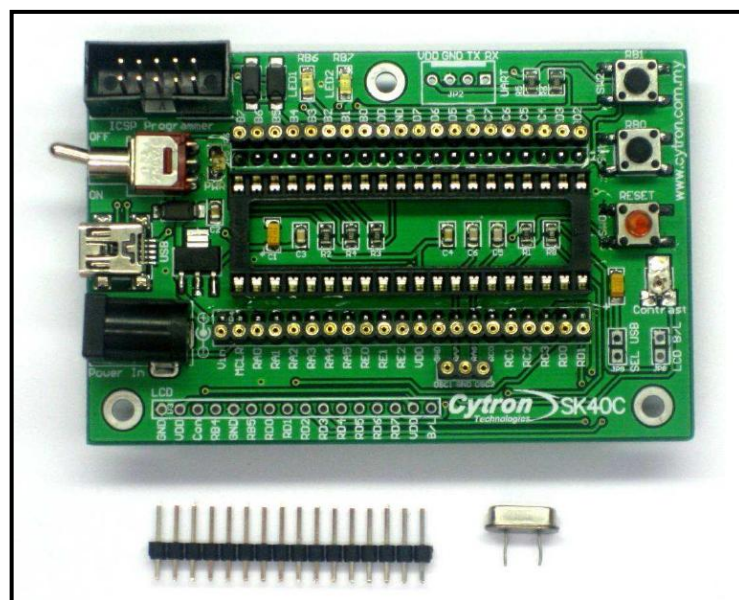


Figure 3.33: Top view of SK40C enhanced 40 pins PIC start-up kit with components (SK40C Enhanced 40 Pins PIC Start-Up Kit User's Manual V1.1, 2010)

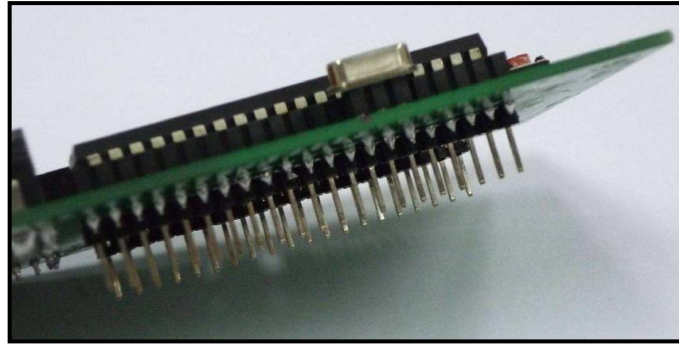


Figure 3.34: Side view of SK40C enhanced 40 pins PIC start-up kit (SK40C Enhanced 40 Pins PIC Start-Up Kit User's Manual V1.1, 2010)

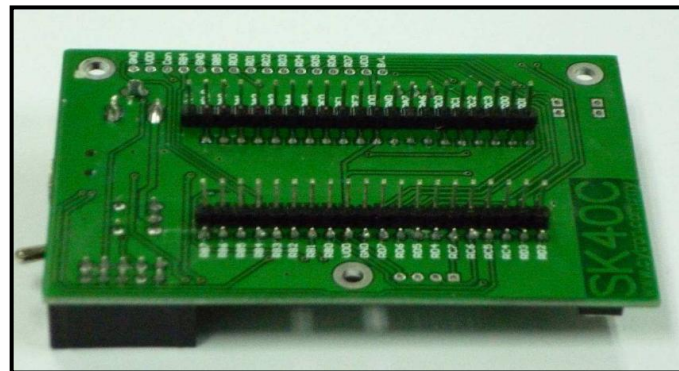


Figure 3.35: Bottom view of SK40C enhanced 40 pins PIC start-up kit (SK40C Enhanced 40 Pins PIC Start-Up Kit User's Manual V1.1, 2010)

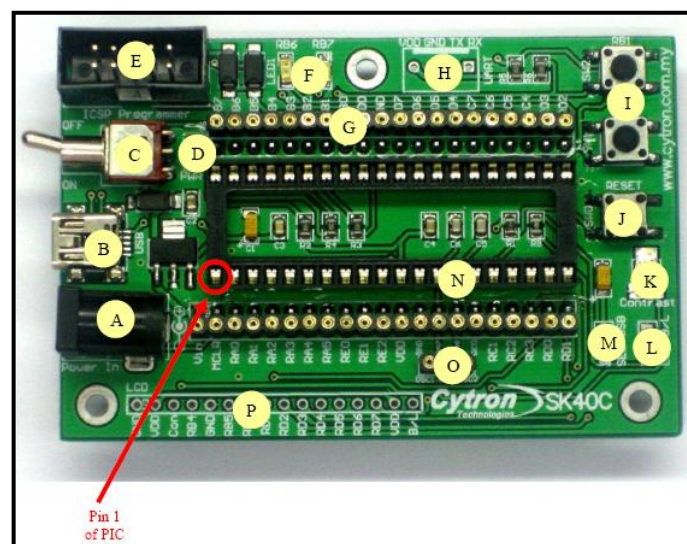


Figure 3.36: Board layout of SK40C enhanced 40 pins PIC start-up kit (SK40C Enhanced 40 Pins PIC Start-Up Kit User's Manual V1.1, 2010)

Table 3.2: Functions of each labelled components in SK40C enhanced 40 pins PIC start-up kit

Label	Function
A	DC power adaptor socket for user to plug in DC adaptor. The input voltage should be ranged from 7 to 15 V.
B	USB connector for communication between devices and a host controller (usually personal computers). This function is only valid for certain model of PIC microcontroller. Please refer to USB interface section. The power LED will light ON when the USB cable is connected.
C	Toggle switch to On/Off the power supply from DC adaptor.
D	Power indicator LED for on board. It will light ON as long as the input power is correctly connected.
E	2 x 5 box header for UIC00A, USB ICSP PIC Programmer.
F	2 LEDs (connected to RB6 and RB7) as active High output for PIC MCU. These LEDs are controllable from PIC MCU.
G	Consist of several line of header pin and turn pin. Header pin provide connector for user to solder SK40C to prototype board and use the I/O of PIC MUC. 40 pins of PIC MCU except OSC (connected to crystal) are extended out to these pin. There is an extra pin on top of MCLR which is labelled as V_{in} , is connected to the input power.
H	Reserved for UART communication. Tx and Rx pin of SK40C are connecting to RC6 and RC7 respectively. Ensure PIC use have the correct UART pin (RC6 and RC7).
I	A 2 x Push button connected to RB0 and RB1 of PIC MCU. This is an extra input button for user. It can be programmed as an input switch.
J	Push button with the function of Reset for PIC MCU.
K	5K of trimmer to set LCD contrast.
L	JP8 is provided for LCD Backlight. LCD Display will have backlight if this pin is shorter.
M	JP9 is provided for USB. Connect this pin if users use USB port.

N	40 pin IC socket for user to plug in any 40 pin PIC MCU (8bit). It can be either be 16F or 18F PIC. Of course the IC package should be PDIP. Inside IC socket, there some electronics components, it include a 20 MHz Crystal.
O	Turn pin is provided for crystal. 20 MHz is default crystal provided in SK40C. However, the 20 MHz crystal can be removed and replace with other crystal. Just remove the crystal and put other crystal on turn pin without soldering.
P	Reserved for 2 x 16 LCD Display. User may solder 2 x 16 LCD display at this space if want to use it.

Source: SK40C Enhanced 40 Pins PIC Start-Up Kit User's Manual V1.1, 2010

SK40C enhanced 40 pins PIC start-up kit is used in this design as it is compact, small, low cost, portable, and user-friendly. Each of the SK40C is around 85 mm x 55 mm (small size) and 50 grams (light weight) which allows to be carried around. As all components being soldered compactly on the board, there is no extra soldering needed which might have the risks of having disconnection between wires or damage to the electronic components. Moreover, SK40C is built to function with XBee starter kit module. Hence, it saves a lot of developing time and removes the need of complicated wire connections.

3.4.1.6 XBee Starter Kit (SKXBee)

XBee is a simple yet reliable wireless communication for embedded applications. This XBee starter kit module is engineered to meet IEEE 802.15.4 standards and support the unique needs of low cost and low power wireless sensor networks (XBee Starter Kit SKXBee User's Manual V1.0, 2008). With this device, no more searching for surrounding device and request for connection, it can send data wireless after powering up without any extra configuration.

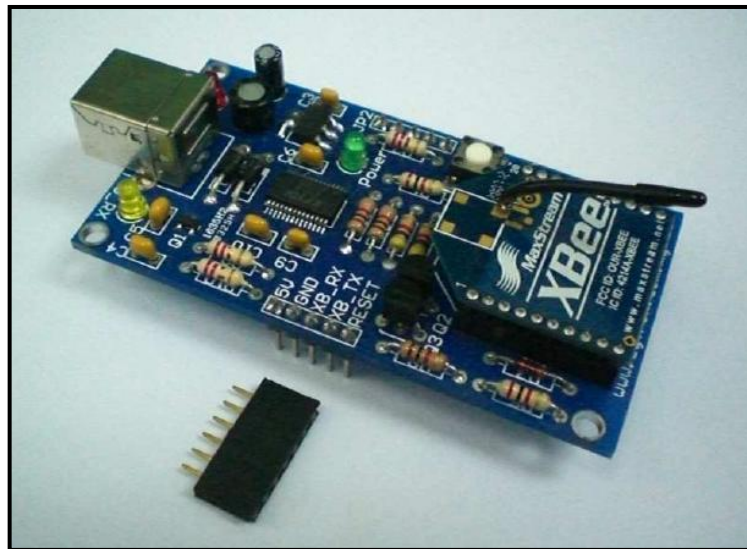


Figure 3.37: SKXBee XBee starter kit with components (XBee Starter Kit SKXBee User's Manual V1.0, 2008)

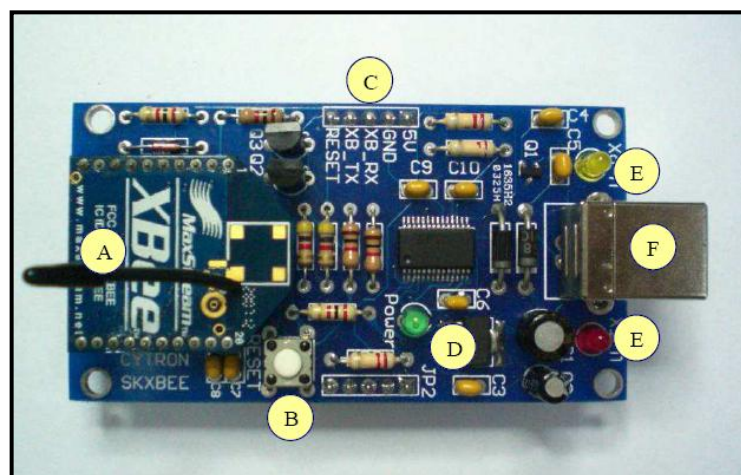


Figure 3.38: Board layout of SKXBee XBee starter kit (XBee Starter Kit SKXBee User's Manual V1.0, 2008)

For XBee, it offers indoor communication range up to 30 m and outdoor line of sight range up to 100 m. Besides, it consists of power down current less than 10 μ A. While XBee start kit have been developed to convert 3.3 V required by XBee into 5.0 V operation and offer connection to computer with USB for more user friendly solution to ease the process of exploring the possible development application (XBee Starter Kit SKXBee User's Manual V1.0, 2008).

Table 3.3: Functions of each labelled components in SKXBee XBee starter kit

Label	Function
A	Connector for either XBee or XBee-Pro module.
B	Reset button for XBee module.
C	5 ways header pin for external power supply and interface to microcontroller. If this kit is connected to microcontroller board, it should be powered with 5 V.
D	3.3 V power indicator. This small green LED indicates the status of 3.3 V from on board voltage regulator. It should be ON if either 5 V power or USB connection is connected to SKXBee.
E	These are a pair of small LED, red and yellow in color. These LEDs are connected to on board USB to UART converter. It indicates the receiver and transmitter activity. It will only work if SKXBee is connected to PC or laptop through USB cable. Red LED indicates USB's transmitter activity; while yellow LED indicate USB's receiver activity.
F	USB B type socket. If connection to PC or laptop is required, please connect one end of USB cable (B type) to this socket, while the other end to PC or laptop USB port.

Source: XBee Starter Kit SKXBee User's Manual V1.0, 2008

Table 3.4: Product specification of SKXBee XBee starter kit

Label	Definition	Function
5 V	Power input for SKXBee	External power source for SKXBee, the typical voltage is 5 V. On board 3.3 V voltage regulator will regulate the voltage to 3.3 V for XBee module. The power is not necessary if SKXBee is connected through USB cable.
GND	Ground or negative	Ground of power and signal.
XB_RX	XBee UART receive signal	This is XBee module's receiver pin, it should be interfaced to 5 V logic UART, no divider is necessary. This is an input pin to SKXBee. It should be connected to microcontroller's transmitter pin.
XB_TX	XBee UART transmit signal	This is XBee module's transmitter pin, it should be interfaced to 5 V logic UART. This is an output pin from SKXBee. It should be connected to microcontroller's receiver pin.
RESET	XBee Reset pin	Reset pin of XBee module. It should be connected to push button to Gnd, or NPN transistor.

Source: XBee Starter Kit SKXBee User's Manual V1.0, 2008

In this design, XBee starter kit is used due to its reliability and cost effectiveness as wireless transmission module. It has a long range data integrity and low power consumption compare to other transmission devices, such as Bluetooth. Each XBee starter kit is around 80 mm x 40 mm (small size) and 160 grams (light weight) which is portable for user to carry around within the range. In additional, there is no worry about missing components or disconnection between wires as all of the necessary components are being soldered perfectly on board.

3.4.1.7 Process Flow

The overall process flow of hardware design is shown as followed:

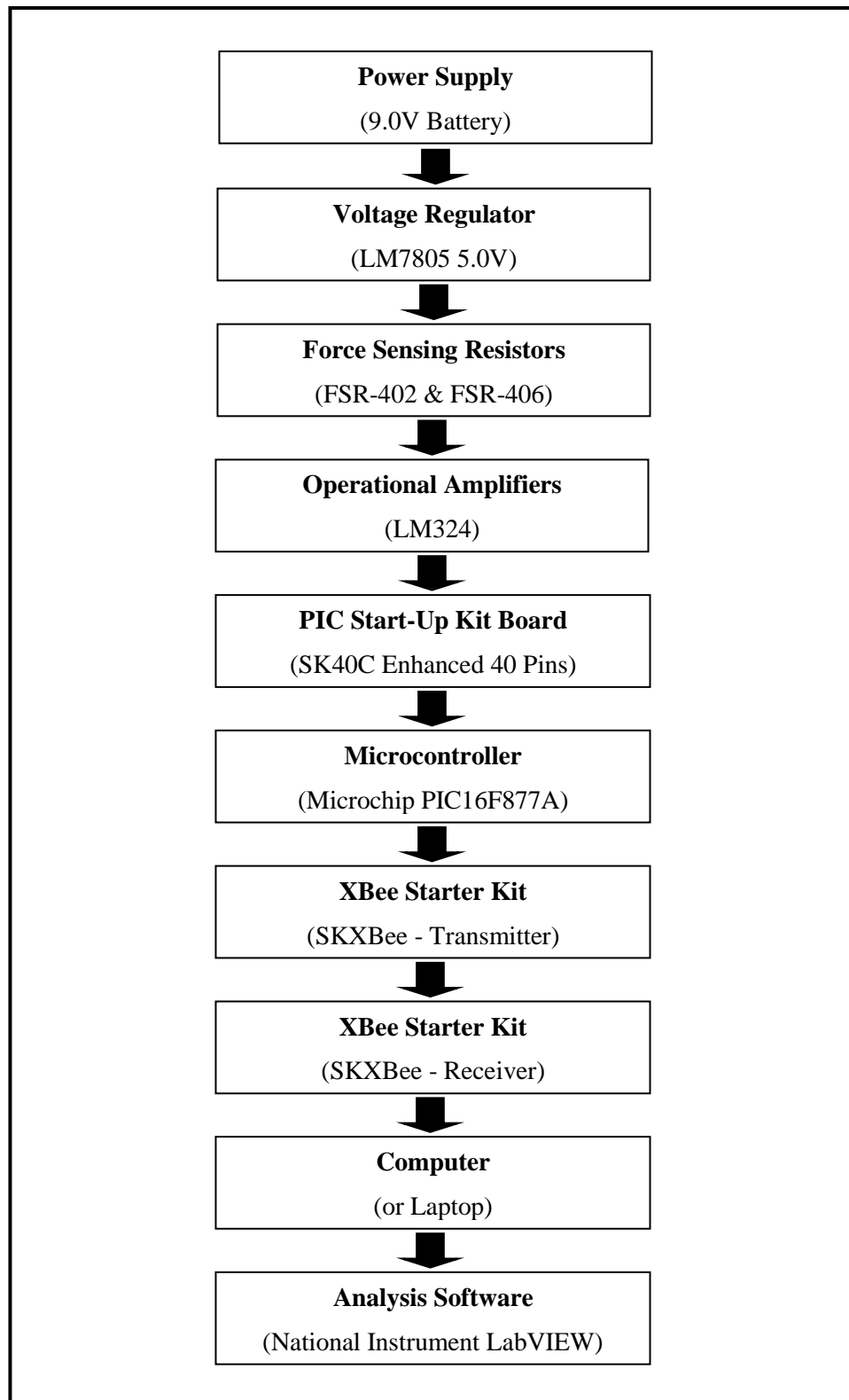


Figure 3.39: Process flow of hardware design

3.4.2 Hardware Assembly

3.4.2.1 Circuit Diagram

The circuit diagram used to assembly the design of this project is shown as followed. A better version can be found in Appendix A.

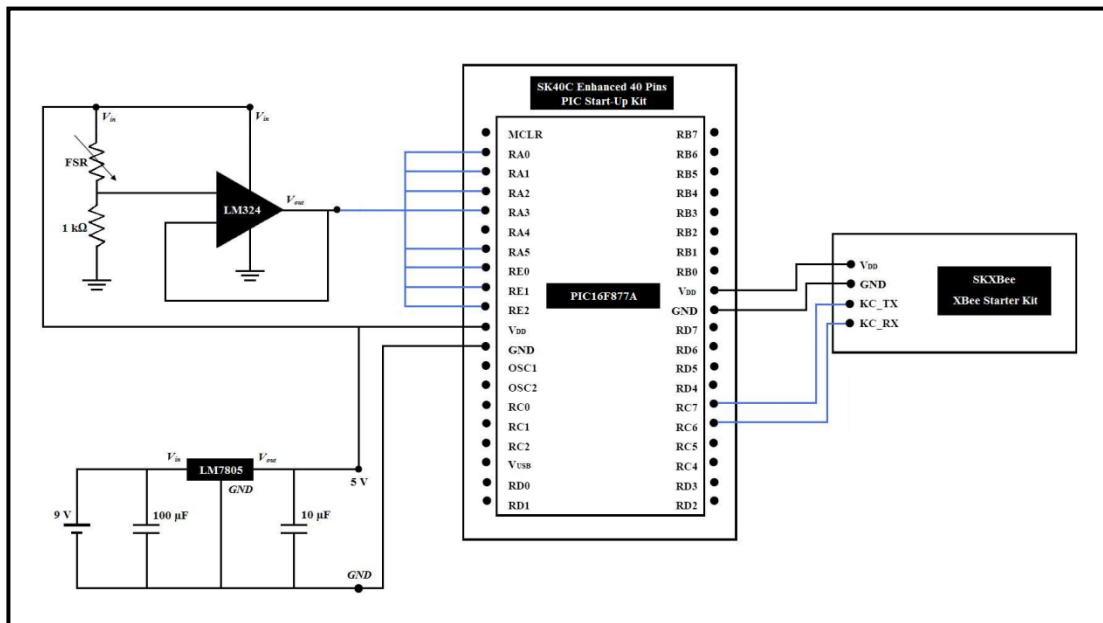


Figure 3.40: Circuit diagram of instrumented insole system

3.4.2.2 Construction of Voltage Regulator (LM7805)

In order to prevent over supply of voltage which might cause damage to the electronic circuits, LM7805 5.0V voltage regulator is used just right after the power supply with 100 μF (from the battery) and 10 μF (output) connected in parallel and grounded as shown in figure below:

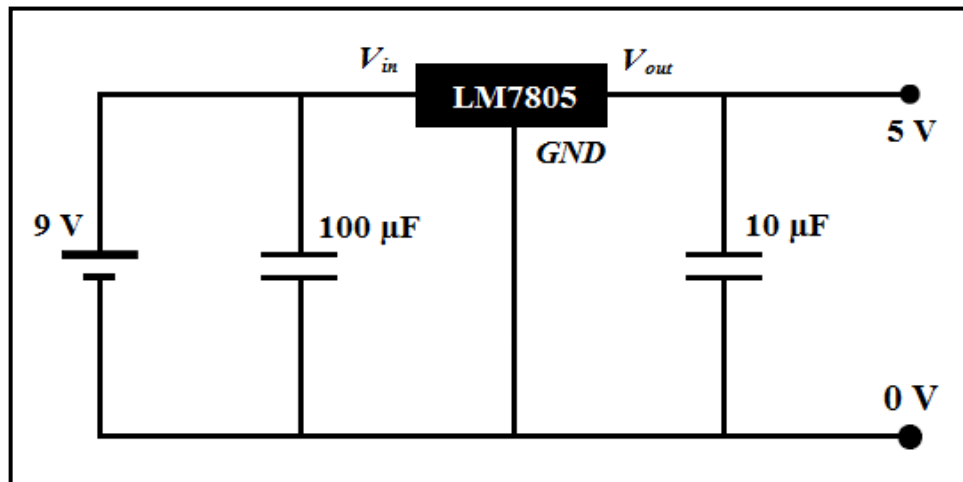


Figure 3.41: Circuit diagram of LM7805 5.0 V voltage Regulator

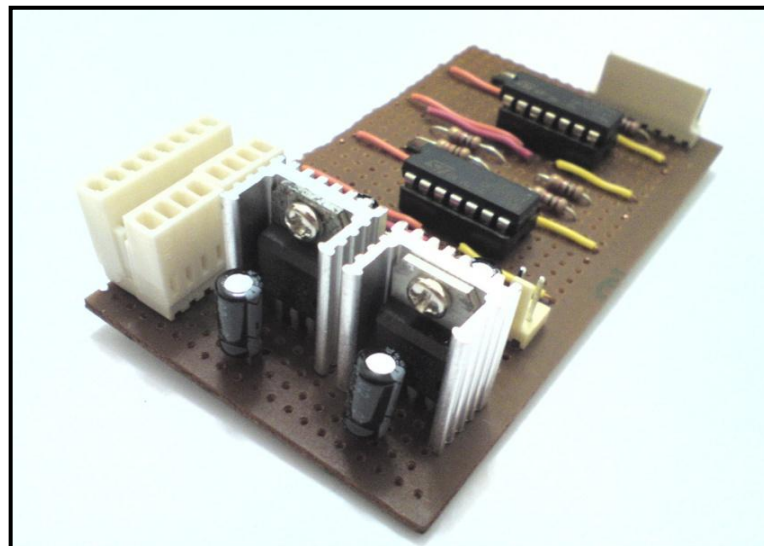


Figure 3.42: LM7805 5.0V voltage regulators are soldered on donut board

3.4.2.3 Construction of Operational Amplifiers (LM324)

Each FSR consists of two non-polar leads, one will be connected to voltage input of 5.0 V and the other one will attach to a 1.0 k Ω pull-down resistor to ground to form a voltage divider circuit. The point between the fixed pull-down resistor and the variable FSRs are connected to the LM324 operational amplifier in order to form a circuit loop of voltage follower.

Two LM324 operational amplifiers are used in this design system as there are ten sensors connection of the electronic components. The output voltage of the voltage divider is channelled to the microcontroller on SK40C enhanced 40 pins PIC start-up kit board, which will be discussed in the following subsection.

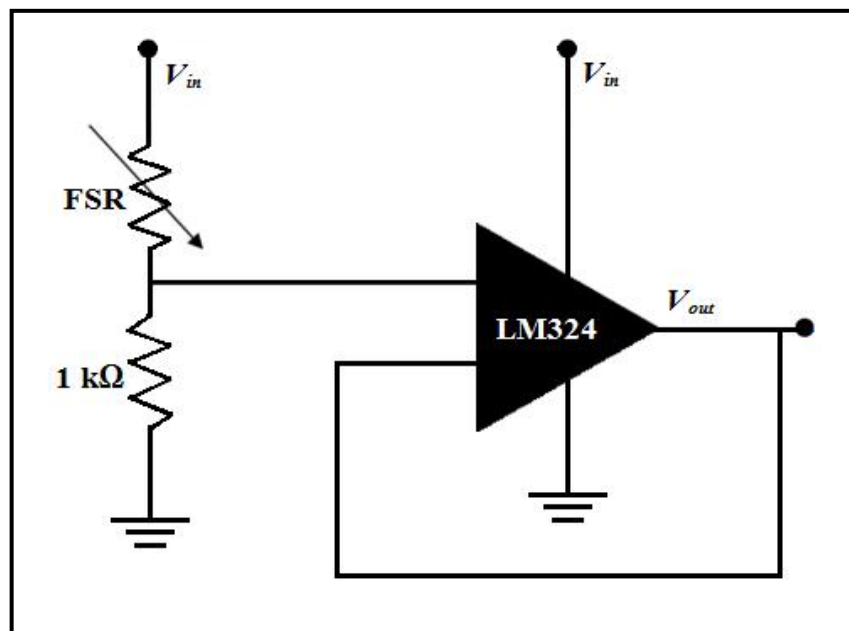


Figure 3.43: Circuit diagram of voltage divider and voltage follower using LM324 operational amplifiers

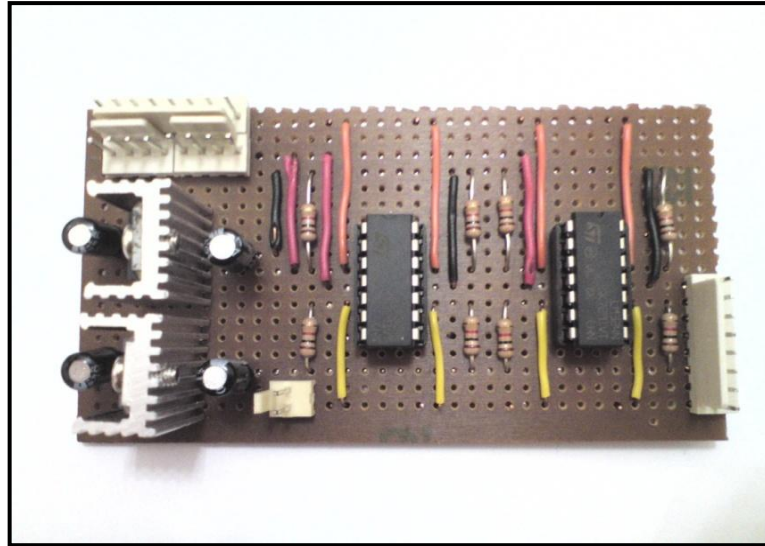


Figure 3.44: LM324 operational amplifiers are soldered on donut board to form circuit loops of voltage divider and follower.

3.4.2.4 Preparation of Ribbon Cables as Connectors

Ribbon cables are used to connect between FSRs and electronic circuit in order to reduce the complexity and messy condition of wires for the whole design. Apart from that, ribbon cables are used as well for the connection between SK40C enhanced 40 Pins PIC start-up kit with SKXBee starter kit.

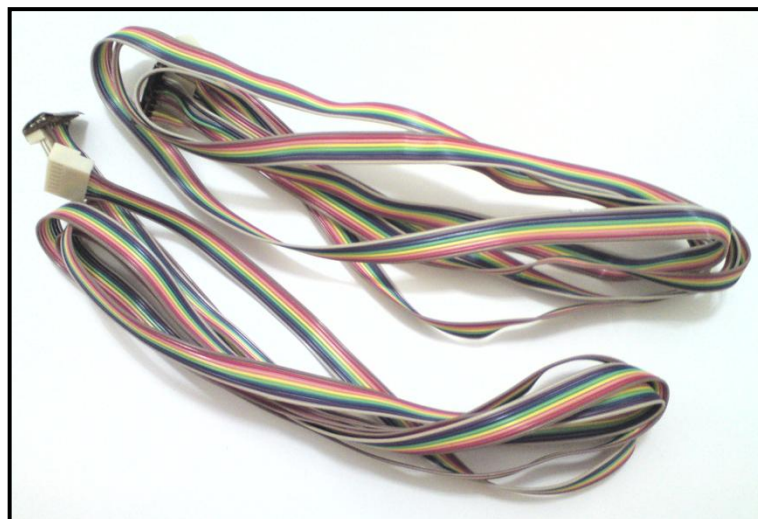


Figure 3.45: Ribbon cables for force sensing resistors connecting from polymer insole to circuit board

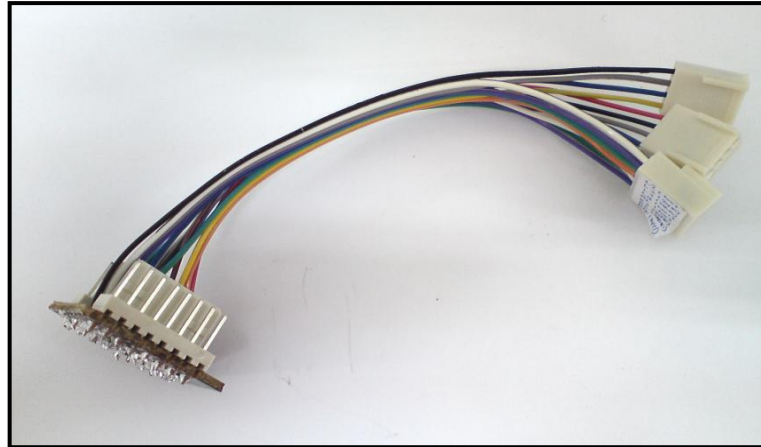


Figure 3.46: Ribbon cables for force sensing resistors connecting from polymer insole to power supply and operational amplifiers inside circuit board

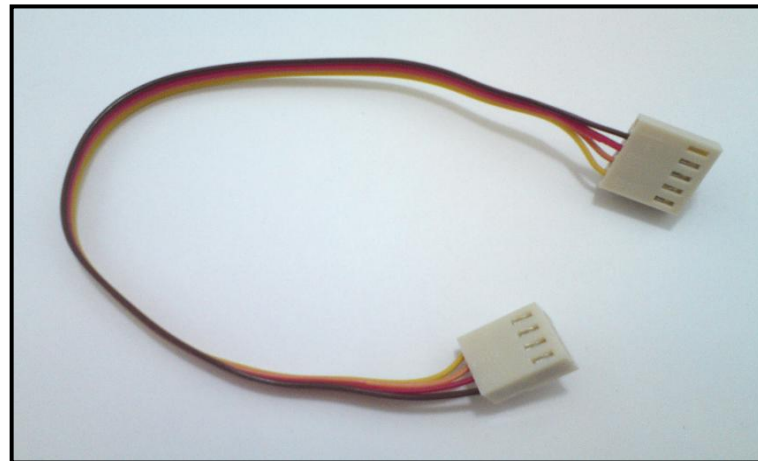


Figure 3.47: Ribbon cables for SK40C enhanced 40 pins PIC start-up kit with SKXBee XBee starter kit

3.4.2.5 Placing Microprocessor (Microchip PIC16F877A) on PIC Start-Up Kit Board (SK40C Enhanced 40 Pins)

The introduction of a convenient and affordable PIC microcontroller start-up kit comes with a simplified design that includes built-in voltage regulator, crystal oscillator, and MAX232 is utilised as part of this project. Hence, the PIC16F877A will be placed on this 40 pin start-up kit as most of the basic components are already setup and configured by the manufacturer.

For the pins configuration, pin (11) labelled V_{DD} will be connected to 5.0 V voltage supply and pin (12) will be grounded. Ten pins at Port A and Port B are connected to FSRs as ADC channels into the microcontroller respectively. Other than that, pin (13) and (14) are connected to the 20 MHz crystal oscillator grounded after two parallel 22 pF capacitors.

The output pins for the microcontroller will be configured at pins (25) and (26) which are the TX (transmitter) and RX (receiver) respectively. Output pins of TX and RX are connected from the PIC16F877A microcontroller to the SKXBee XBee starter kit function to transmit data wireless. Caution has to be taken to locate the position of the first pin on SK40C enhanced 40 pins PIC start-up kit and PIC16F877A microcontroller. Misplacement of the microcontroller onto the board might cause trouble of damaging both components. Besides, the occurrence of bend leads of should be determined which might affect the functionality of the microcontroller.

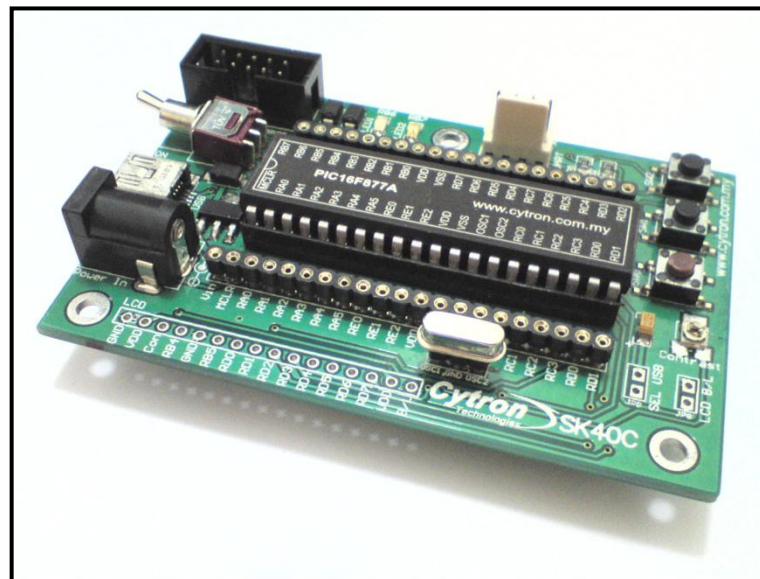


Figure 3.48: PIC16F877A microcontroller placement on SK40C enhanced 40 pins PIC start-up kit board

3.4.2.6 Connecting Force Sensing Resistors (FSR-402 & FSR-406) to Voltage Regulator (LM7805), Operational Amplifiers (LM324), and PIC Start-Up Kit Board (SK40C Enhanced 40 Pins)

As mentioned earlier, almost all of the electronic components require operating voltage between 2.0 V to 5.5 V. Therefore, the 9.0 V input voltage supply (positive power supply, V_{CC}) and ground (ground or negative power supply, GND) are connected to LM7805 5.0V voltage regulator to turn 5.0 V standard voltage supply to the circuit.

After the voltage supply is regulated, the output of the voltage regulator is connected to the one lead of each FSR as mentioned in the construction of voltage divider and follower circuit. Besides, the regulated voltage is being connected to the input voltage supply of LM324 operational amplifiers and PIC16F877A microcontroller on SK40C enhanced 40 pins PIC start-up kit board.

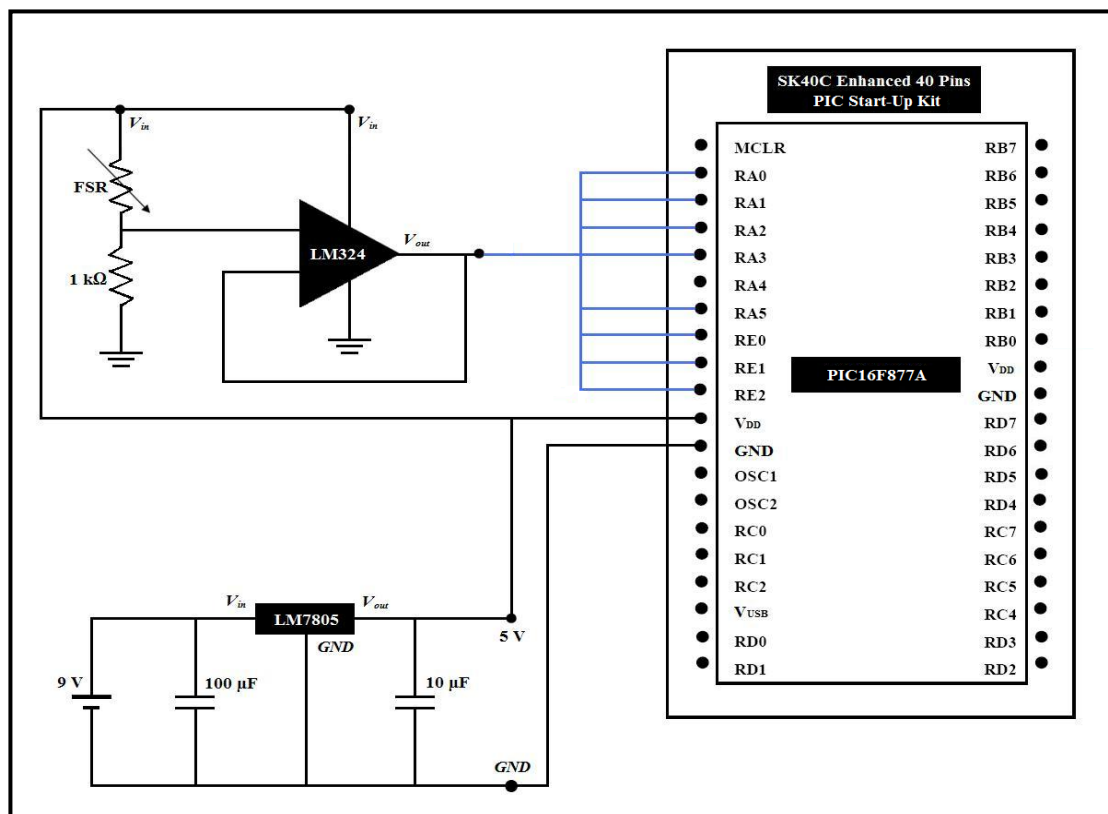


Figure 3.49: Circuit diagram of FSRs connected to LM7805 5.0 V voltage regulator, LM324 operational amplifiers, and SK40C Enhanced 40 Pins PIC Start-Up Kit Board

From the operational amplifiers, the outputs of them will be connected to the SK40C enhanced 40 pins PIC start-up kit board. Since Port A and E of PIC16F877A are activated as input pins. The outputs are connected to RA0, RA1, RA2, RA3 of Port A and RA5, RE0, RB1, RB2 of Port B. The analogue signals changes are collected from the FSRs by the PIC16F877A microcontroller and converted into digital signals.

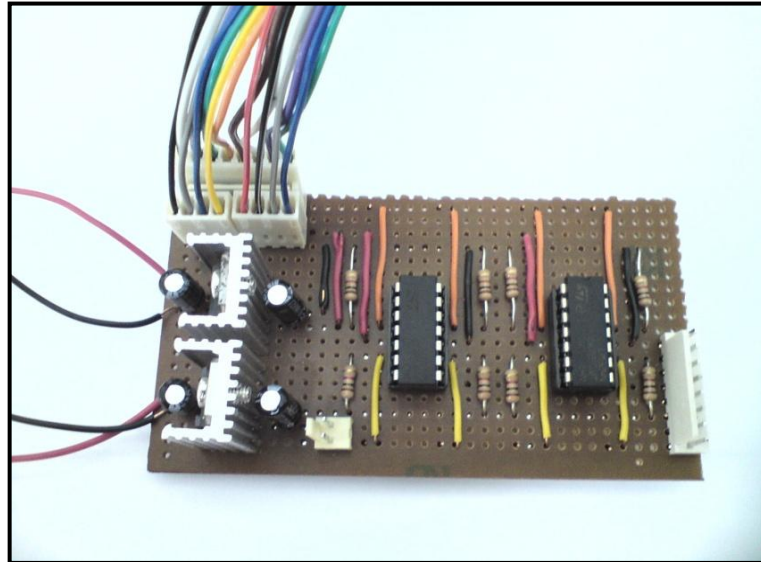


Figure 3.50: FSRs are connected to LM7805 5.0 V voltage regulator and LM324 operational amplifiers

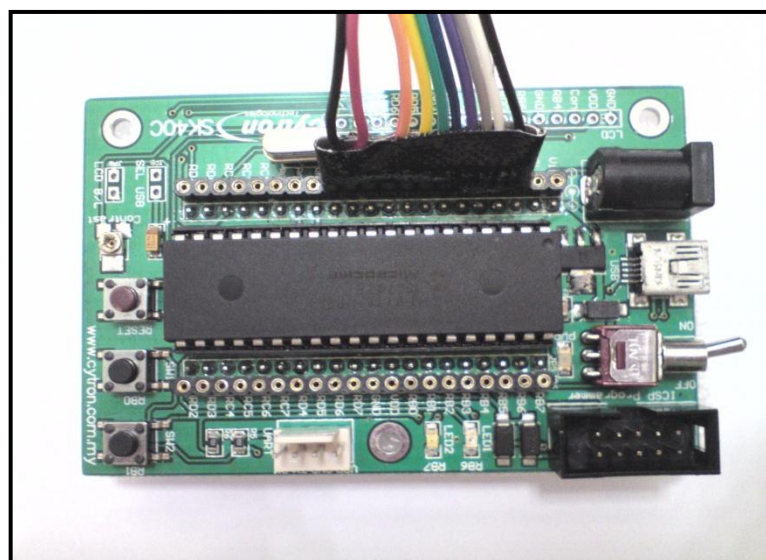


Figure 3.51: FSRs are connected to SK40C enhanced 40 pins PIC start-up kit board

3.4.2.7 Connecting SKXBee (XBee Starter Kit) to PIC Start-Up Kit Board (SK40C Enhanced 40 Pins) and computer

The UART connector outputs (V_{DD} , GND, TX, and RX) of SK40C enhanced 40 pins PIC start-up kit are connected to the input pins (V_{DD} , GND, XB_RX, XB_TX) of SKXBee XBee starter kit. It has to be ensured that the TX and RX pins of SK40C enhanced 40 pins PIC start-up kit is connected to the XB_RX and XB_TX pins of SKXBee XBee starter kit correctly.

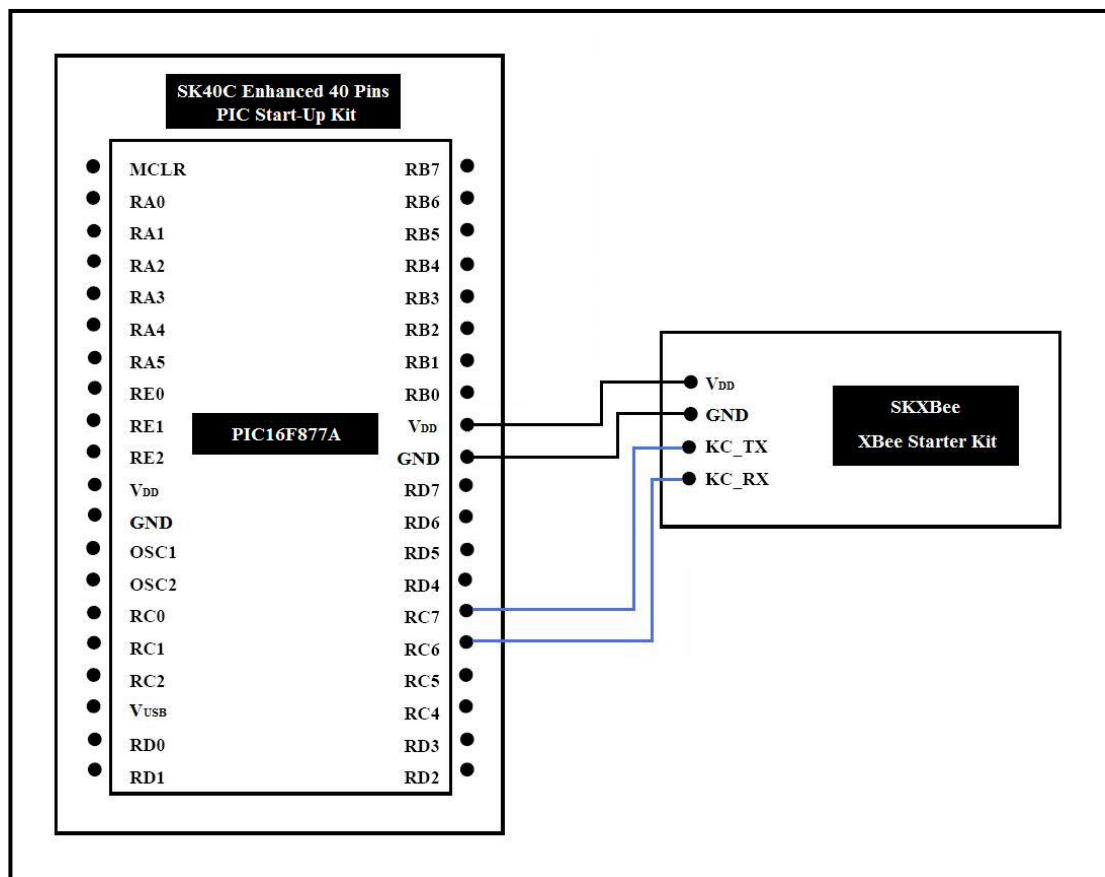


Figure 3.52: Circuit diagram of SKXBee XBee starter kit connected to SK40C enhanced 40 pins PIC start-up kit board

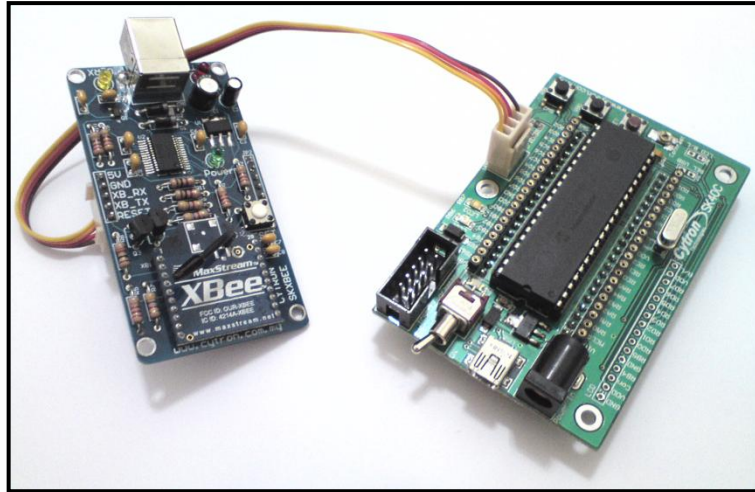


Figure 3.53: SKXBee XBee Starter Kit is connected to SK40C Enhanced 40 Pins PIC Start-Up Kit Board

3.4.2.8 Positioning Force Sensing Resistors (FSR-402 & FSR-406) to polymer shoe insole

As mentioned earlier, four FSR-402 (circular shape) and one FSR-406 (square shape) are attached to each side of polymer shoe insole. FSR-402 will be attached to big toe (hallux), first, and fifth metatarsals whereas FSR-406 will be attached to heel region on the shoe insole. Total of eight sensors will be attached to polymer shoe insole and connecting to the electronic circuit via soldered wires.

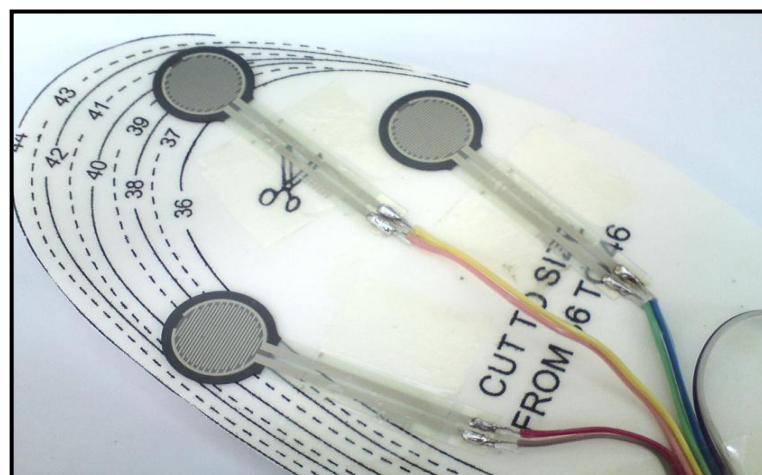


Figure 3.54: FSR-402 (circular shape) are attached at big toe (hallux), first, and fifth metatarsals region on polymer shoe insole

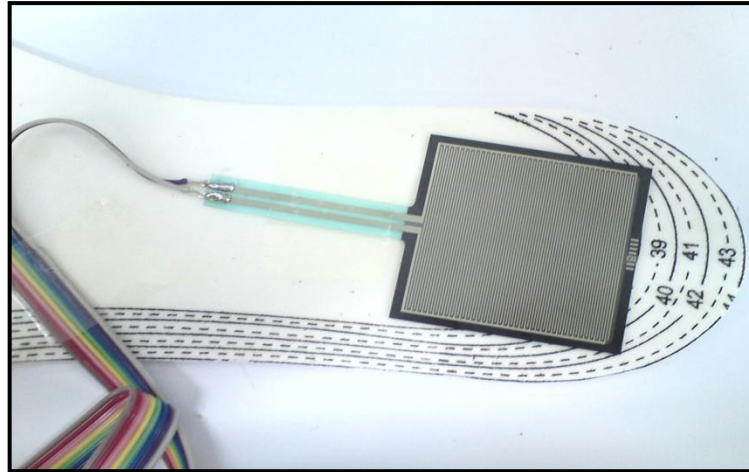


Figure 3.55: FSR-406 (square shape) is attached at heel region on polymer shoe insole

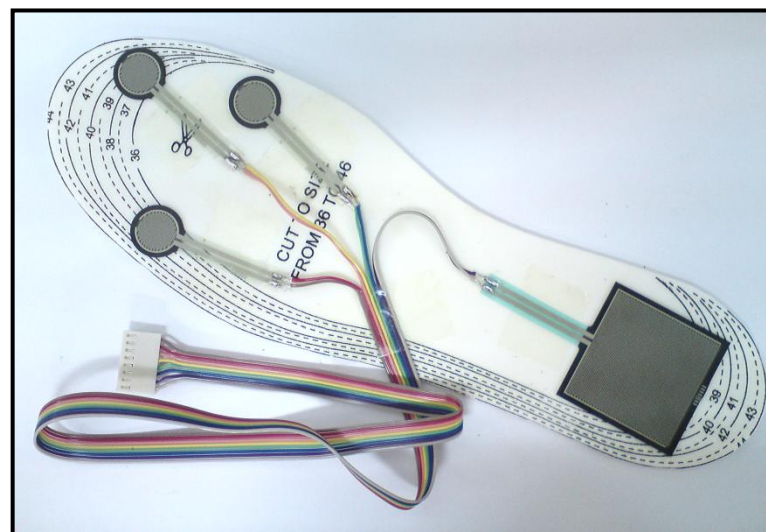


Figure 3.56: FSR-402 and FSR-406 attached on polymer shoe insole

3.4.2.9 Final Product

All the components are housed inside a plastic casing to serve as a protection to the connections between electrical components in order to increase the portability and effectiveness. The polymer shoe insole is being tightened on user's foot and the plastic casing on user's waist using belts to avoid them from failing or dislocation out of place. The final product is shown as following:

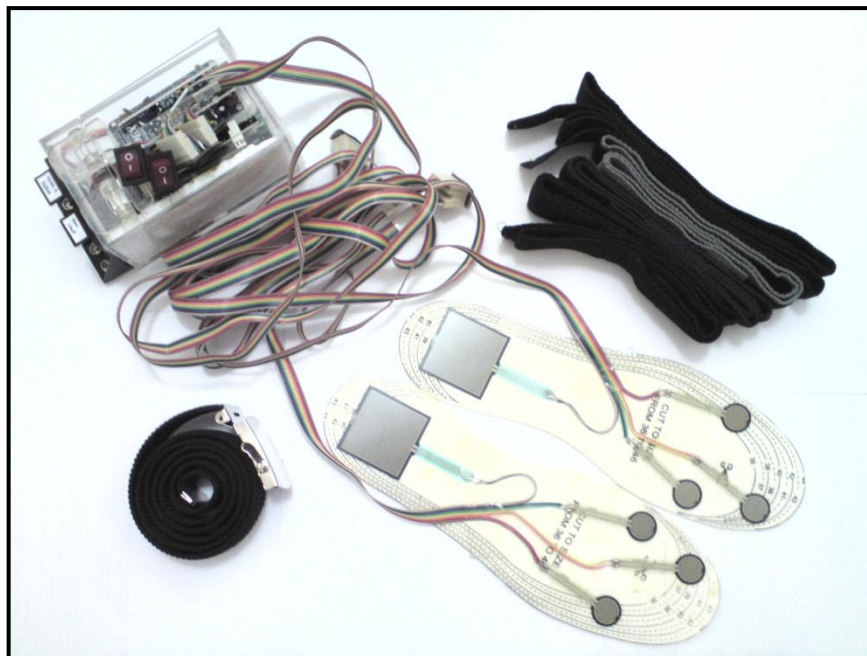


Figure 3.57: The final product housed inside a plastic casing, waist belt, shoe belts, and polymer shoe insole with sensors.



Figure 3.58: Polymer shoe insole tightened under user's foot



Figure 3.59: User and the instrumented insole device

3.4.2.10 Process Flow

The overall process flow of hardware assembly design is shown as followed:

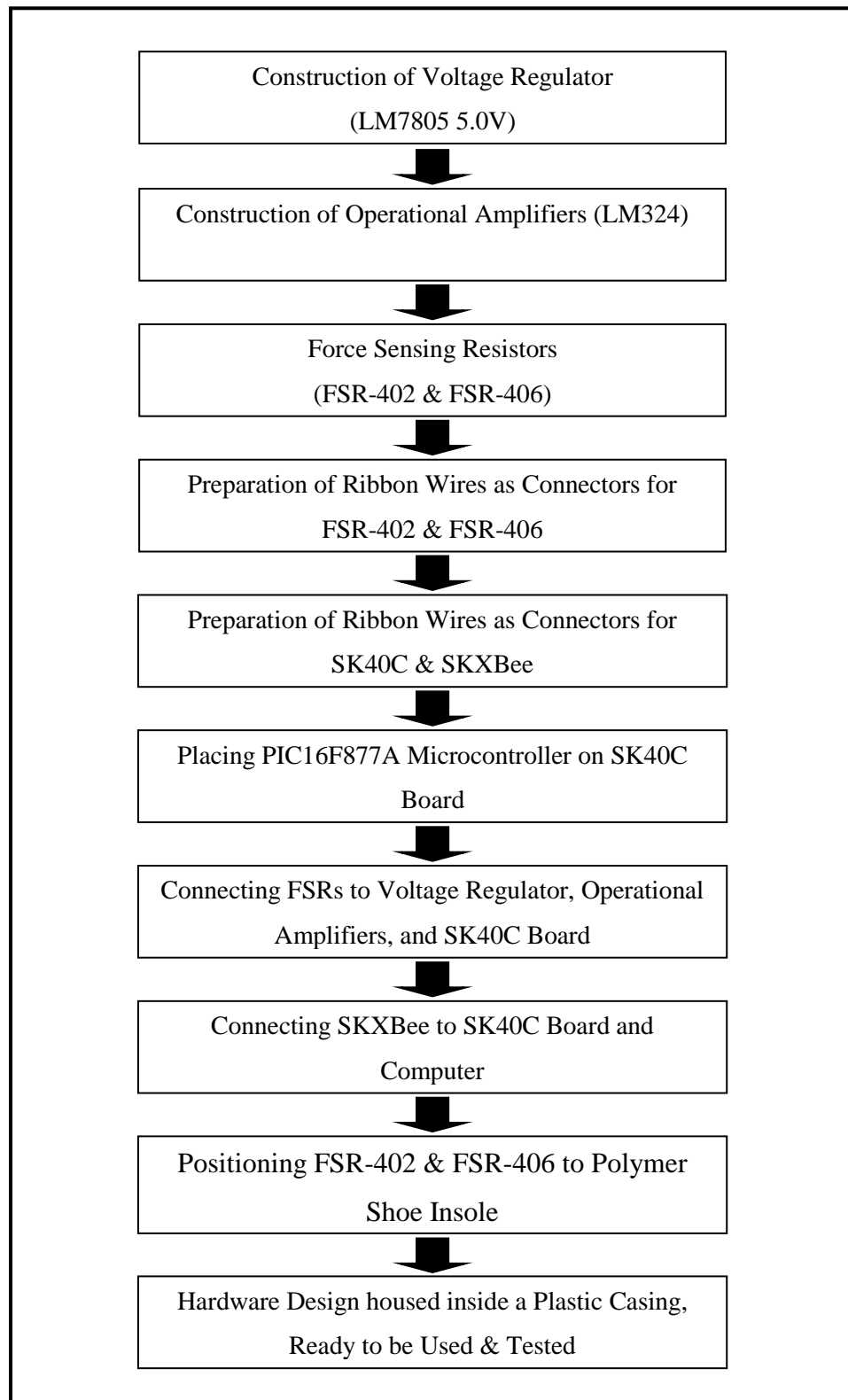


Figure 3.60: Process flow of hardware assembly design

3.5 Software

3.5.1 Microchip PIC Programming

In order for the instrumented insole system to perform the required task, software is used. Generally, a microcontroller's function is based on the program writing to support, operate, and obtain the data. Software contributes one of the essential parts of this project especially for the data analysis. There are two software are being used to compile the programming language (mikroC Compiler) and to load or burn it into the microcontroller (PICkit 2). The steps and procedures of mikroC Compiler and PICkit 2 will be discussed thoroughly in following sections.

3.5.1.1 Setting Up PIC Start-Up kit (SK40C Enhanced 40 Pins) and USB ICSP PIC Programmer (UIC00B)

SK40C enhanced 40 pins PIC start-up kit is a board with unique design which allowed program to be loaded or burned into the microcontroller without the need of removing it from the board. It comes with UIC00B USB ICSP PIC programmer connector to offer simple way for downloading program and save a plenty of development time.

USB connection is used to connect the SK40C enhanced 40 pins PIC start-up kit and UIC00B USB ICSP PIC programmer to computer. Then, compiled programming file (HEX code) can be loaded into the microcontroller in less than a minute. Besides, SK40C enhanced 40 pins PIC start-up kit has to be powered by the DC power adaptor socket. After that, the compiled programming file (HEX code) is ready to be loaded to SK40C enhanced 40 pins PIC start-up kit.

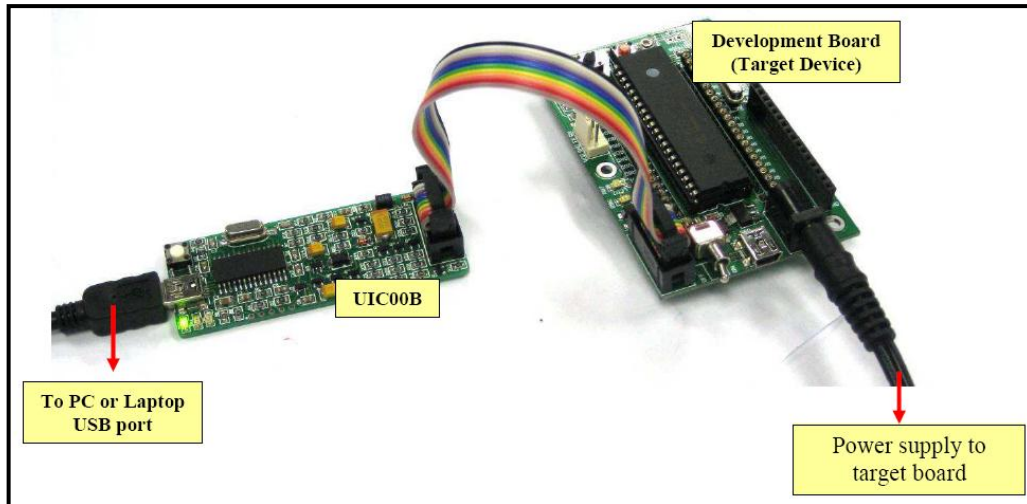


Figure 3.61: SK40C enhanced 40 pins PIC start-up kit with UIC00B USB ICSP PIC programmer connected (UIC00B USB ICSP PIC Programmer User's Manual V1.1, 2010)

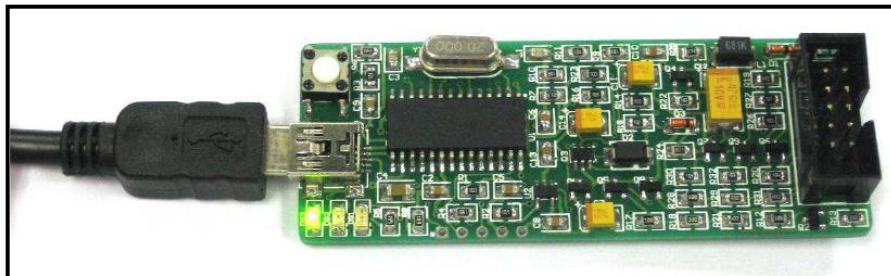
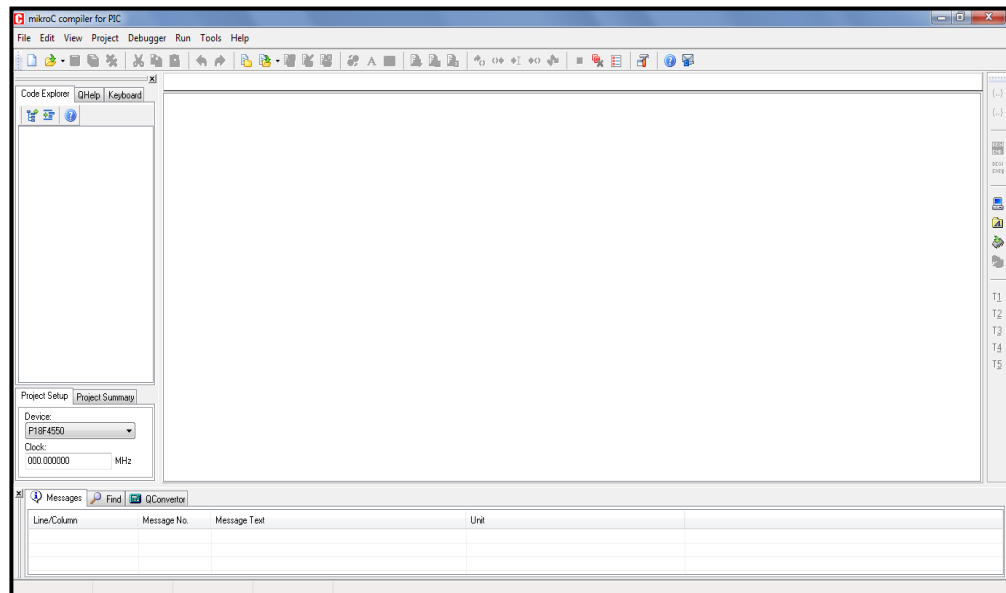


Figure 3.62: UIC00B USB ICSP PIC programmer connected to computer with USB connection cable (UIC00B USB ICSP PIC Programmer User's Manual V1.1, 2010)

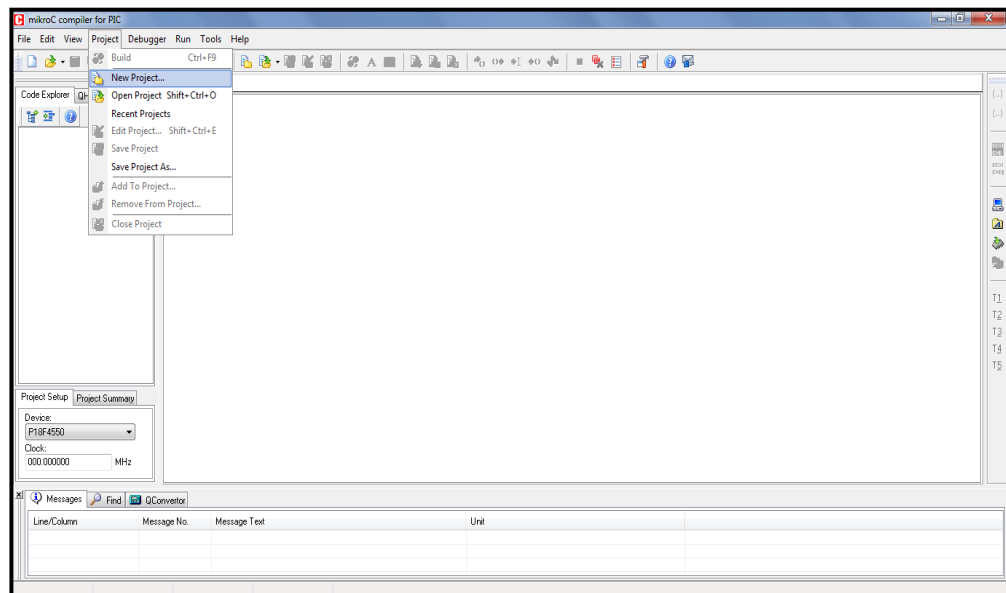
3.5.1.2 MikroC Compiler

There are two fundamental coding languages used to program a microcontroller, they are Assembly and C language. Both languages compile in a different ways, format, and complexity but will generate the same outcome. In this project, C language is chosen to be used to program the microcontroller from mikroC Compiler. The procedures of compiling the compiled programming file into HEX code are explained as followed:

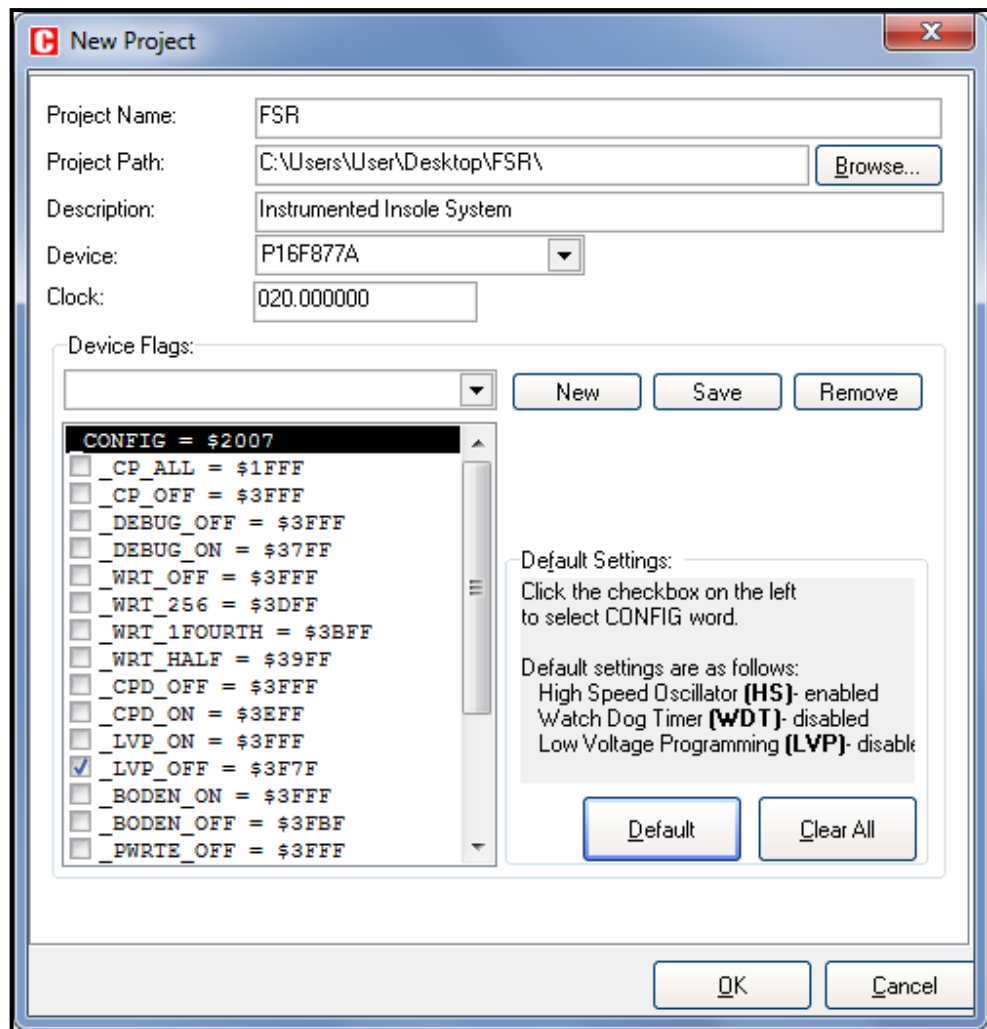
1. Double-click on the “mikroC Compiler” icon to launch the software.



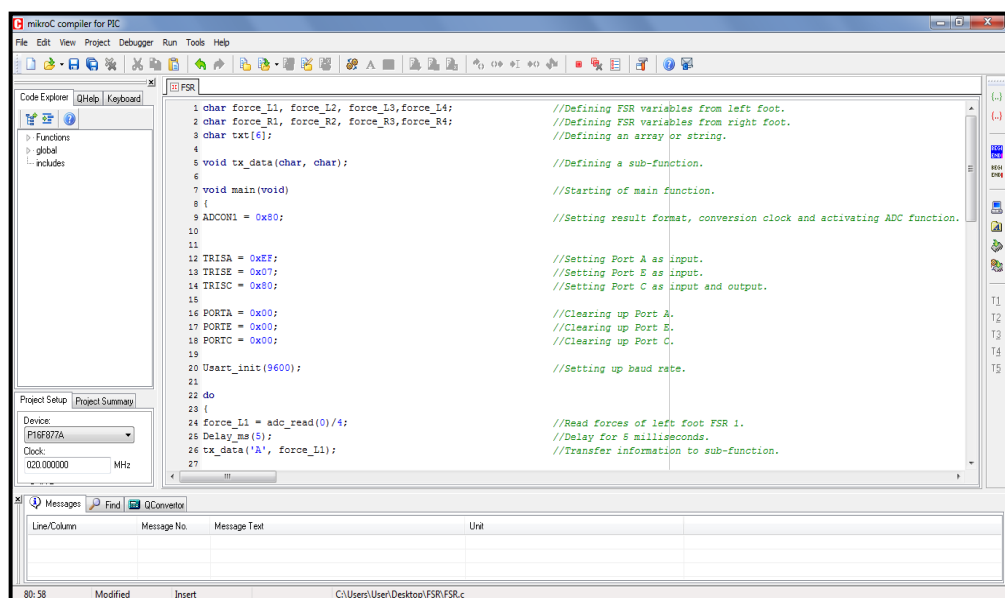
2. Go to “Project” tab and browse the drop-down menu, select “New Project”.



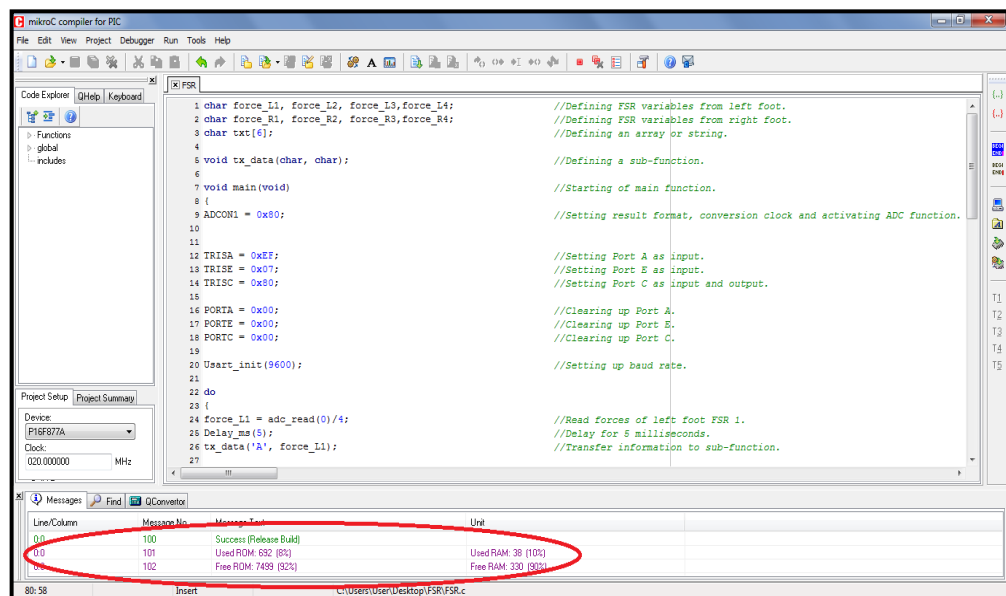
3. A window of “New Project” will be prompted out. Fill in the “Project Name” and “Description”. Browse the ‘Project Path” and for the “Device” drop-down menu, select “PIC16F877A”. “Clock” blank space should be entered with “020.00000” which means 20MHz. Click on the “Default” button once and then click “OK”.



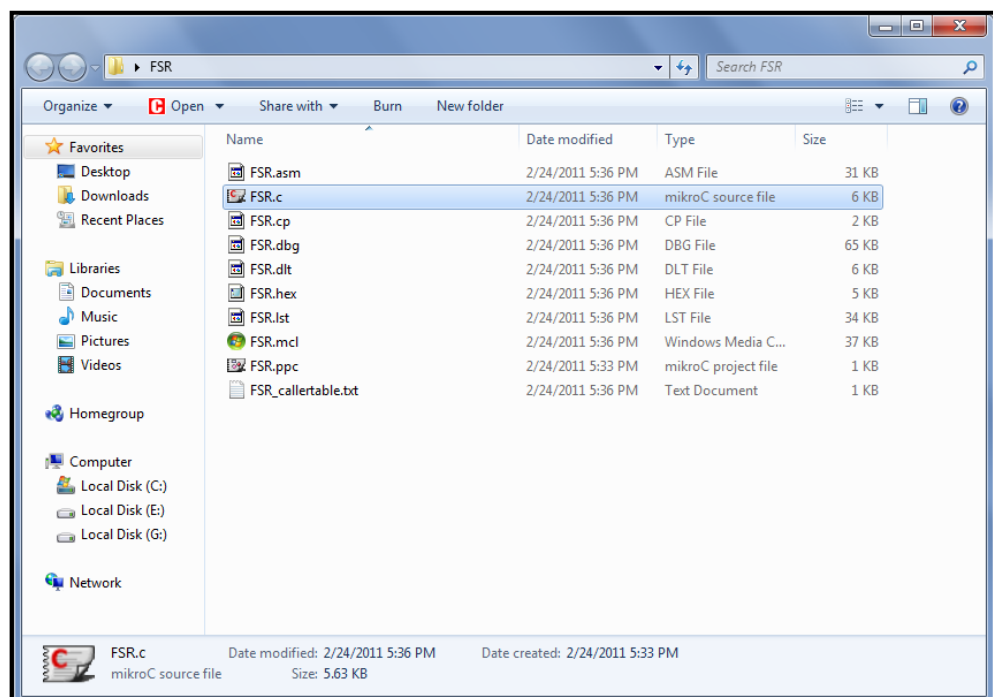
4. After creating a new project, a new project workspace is created successfully and programme writing can be started on the blank area.



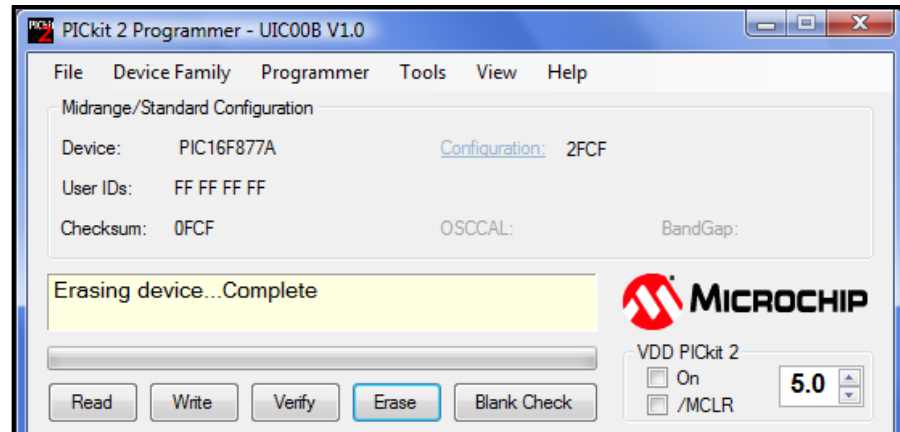
- Once finished writing programme, go to “Build” tab and select “Build” in the drop-down menu. This action is going to compile the program creating .hex (HEX code) file to be loaded into the microcontroller. If there are any errors, warning will be mentioned at the bottom area under “Messages”. If it is successfully built, the program is ready to be loaded into the microcontroller.



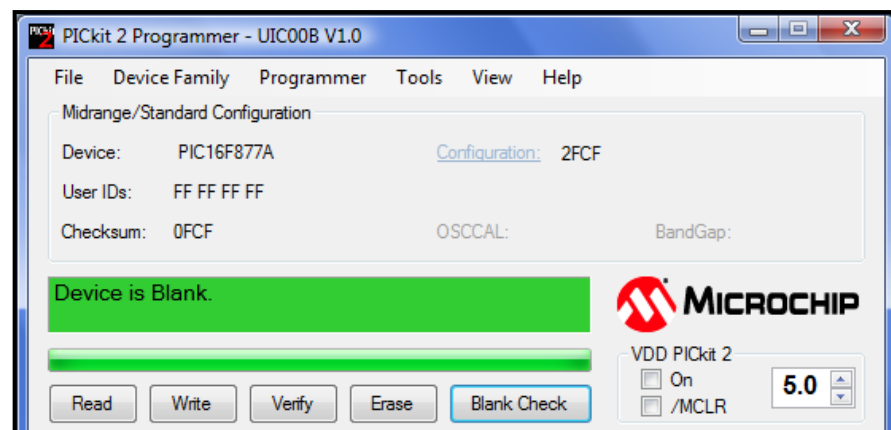
- A list of files is created after compiling the program. The FSR.hex is going to be loaded into the microcontroller.



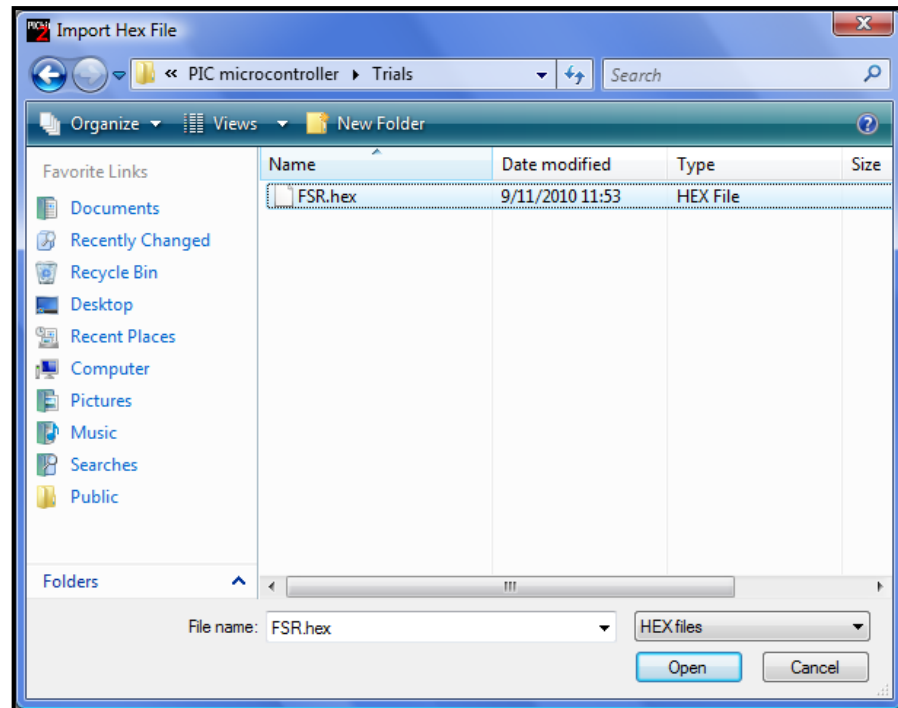
3. First, microcontroller has to be making sure that it is empty before loading any program to it. If no, click on “Erase” to wipe off everything in the microcontroller.



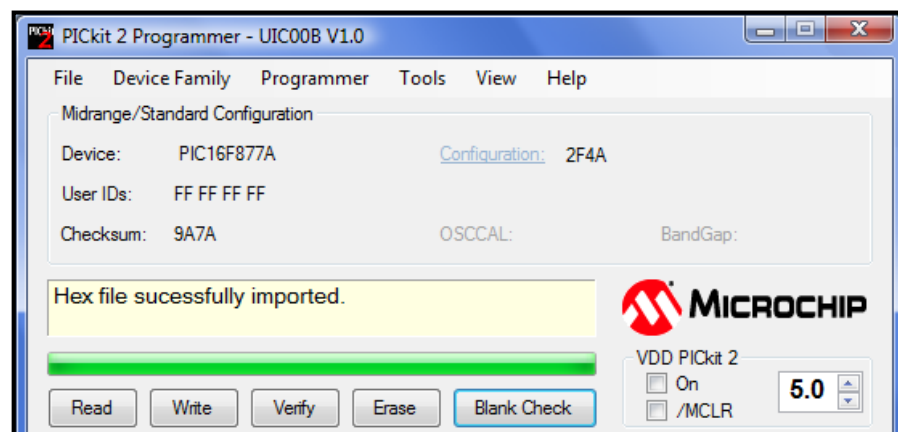
4. Then, click on “Blank Check” to check the microcontroller if it is empty.



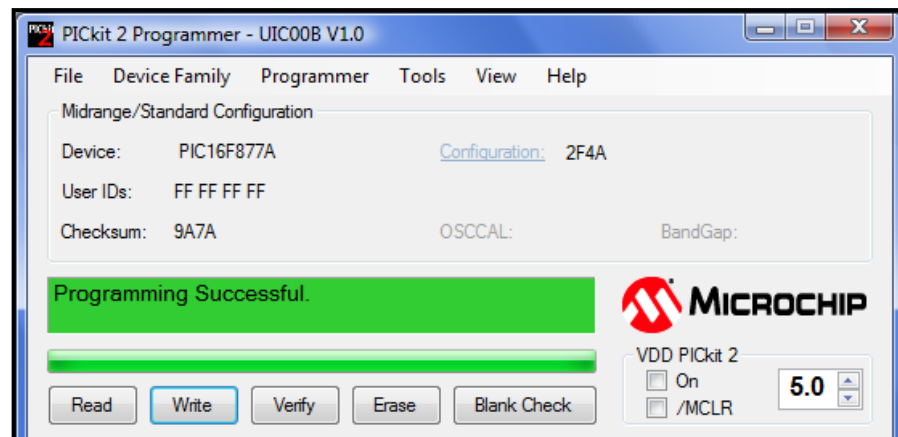
5. To load the created HEX file into the microcontroller, go to “File” tab and browse the drop-down menu, select “Import Hex”. From the prompt menu, find the HEX file location in the directory. Click on the file and then click “Open” to start importing the HEX file.



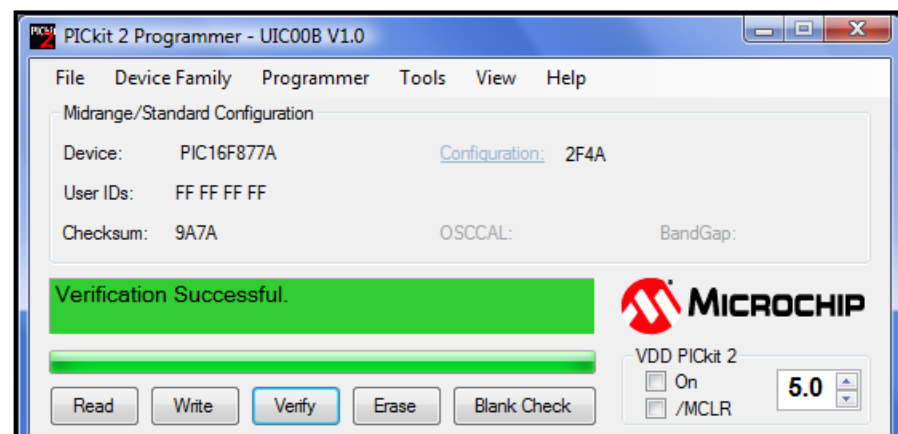
6. If the HEX code is supported and match with the device, PICKit 2 programmer will successfully import the HEX code.



7. After HEX file has been imported, click on “Write” to load or burn the programme into the microcontroller. The operation status will display on the “Status Bar” and the “Status Bar” will turn to green if writing is successful.



- Next, click on "Verify" to check if the program is properly loaded into the microcontroller.



- The microcontroller is now ready to be used.

3.5.1.4 Process Flow

The overall process flow of Microchip PIC programming design is shown as followed:

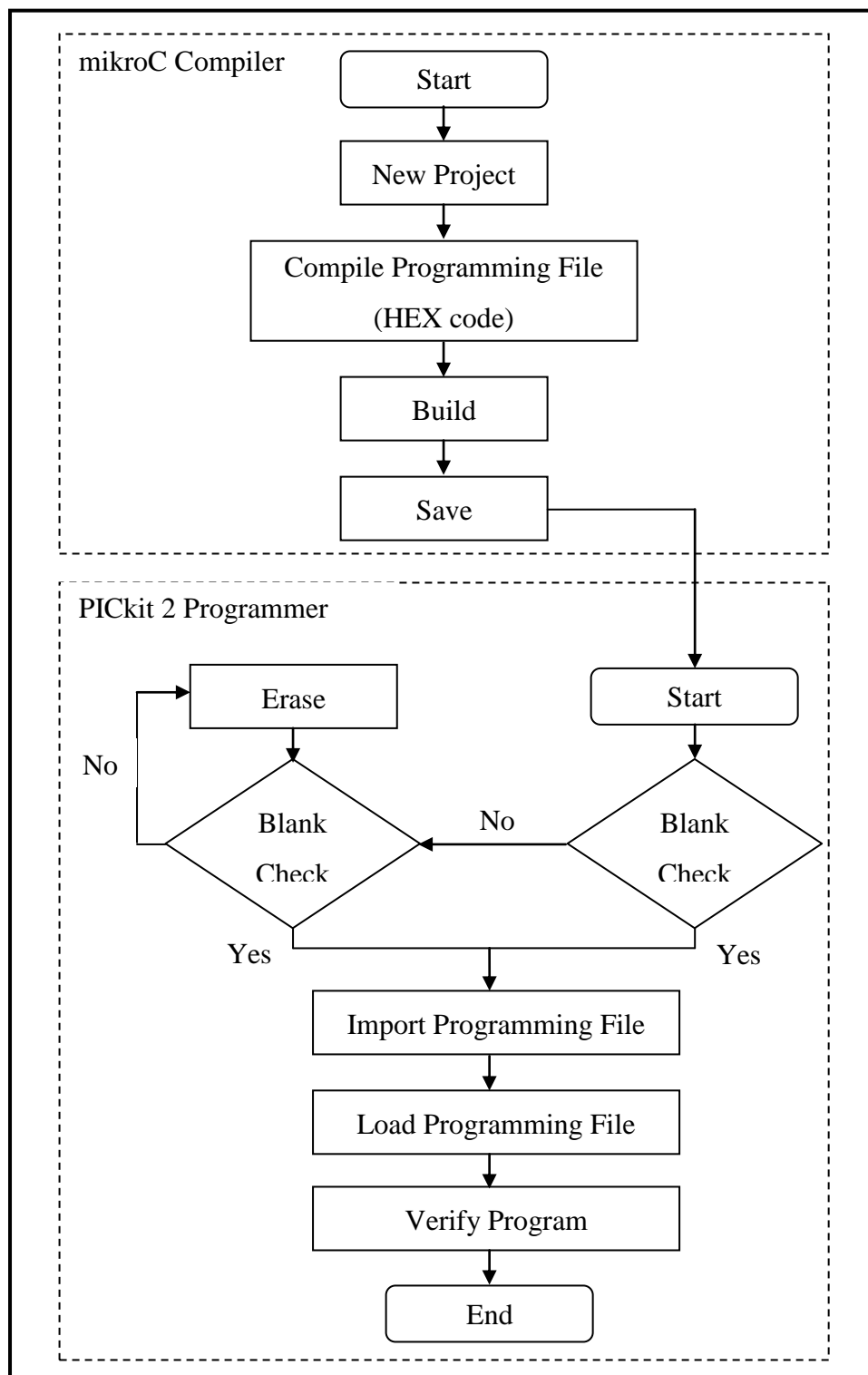


Figure 3.63: Process flow of Microchip PIC programming design

3.5.2 XBee Module (SKXBee) Communication

SKXBee is a module that specially designed compact yet easy and reliable platform. It has filtered the hardware flow control and other IO for TTL logic interface where no extra voltage divider is necessary. With minimum interface, it is ready to connect to microcontroller for embedded XBee development. Moreover, on board USB to UART converter offer easy yet reliable communication to computer for functionality test and as XBee dongle. This enables the SKXBee works well together with SK40C enhanced 40 Pins PIC start-up kit to either transmit or receiver data in this project.

Both SKXBee (circuit and computer side) should be supplied with voltage so that they can carry out the data transmitting process. Circuit side SKXBee can be powered up with an external voltage supply of 5.0 V and computer side SKXBee (XBee dongle) can be powered up by connecting to computer with USB connection cable. It is also has to be ensured that X-CTU is installed in the computer.

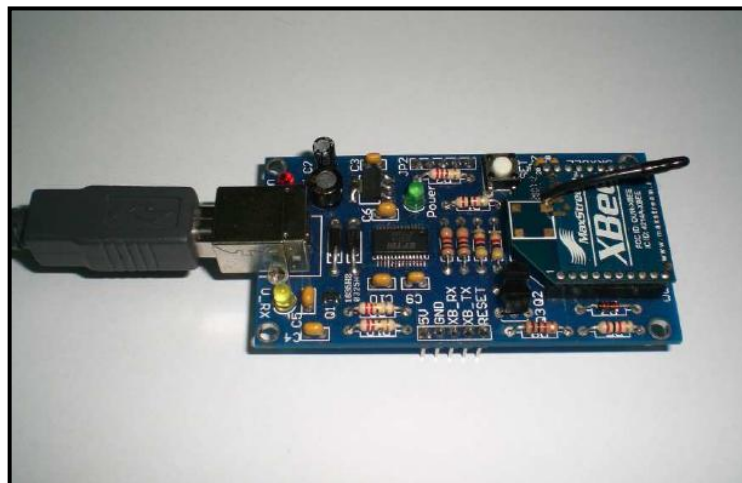
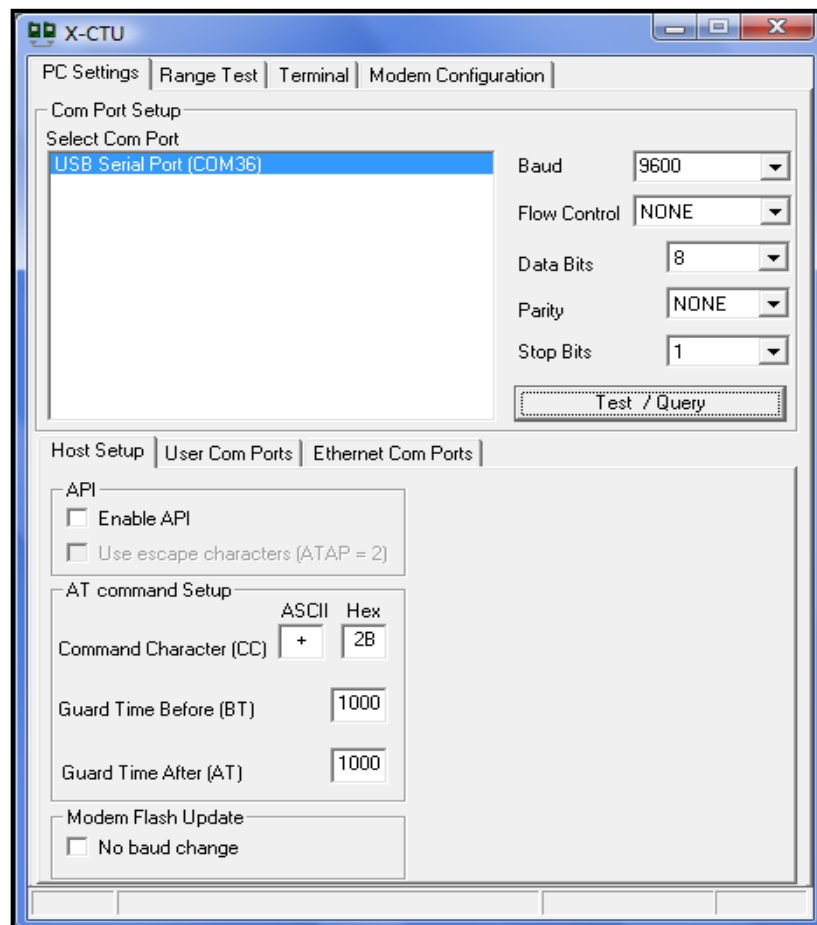


Figure 3.64: XBee module (SKXBee) connected to computer with USB connection cable (XBee Starter Kit SKXBee User's Manual V1.0, 2008)

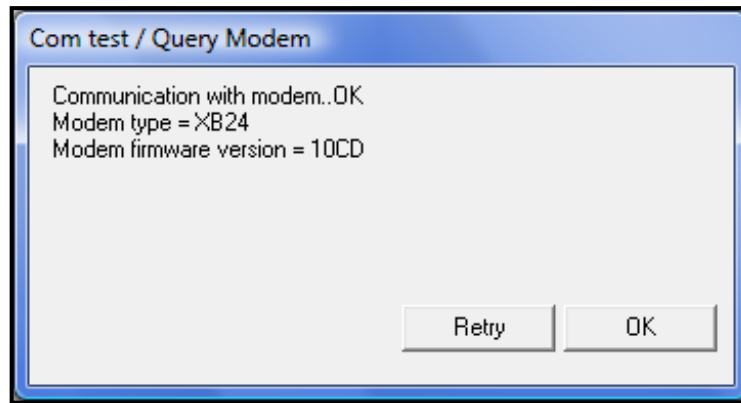
3.5.2.1 Setting UP XBee Module (SKXBee)

An established connection is needed between SKXBee and computer is needed in order to receive the inputs from FSRs. To achieve the connection, X-CTU software is used specially for this SKXBee data transmission. The software should be installed into computer and settings have to be adjusted before collection of data can be carried out. The procedures of connecting the SKXBee with computer or laptop are explained as followed:

1. Click on the icon “X-CTU” to launch the software. Select the “PC Settings” tab to select the virtual “Com Port” from the drop-down menu. Besides, fill in the parameters, like “Baud” as ‘9600’, “Flow Control” as ‘None’, “Data Bits” as ‘8’, “Parity” as ‘None’, and “Stop Bits” as ‘1’.

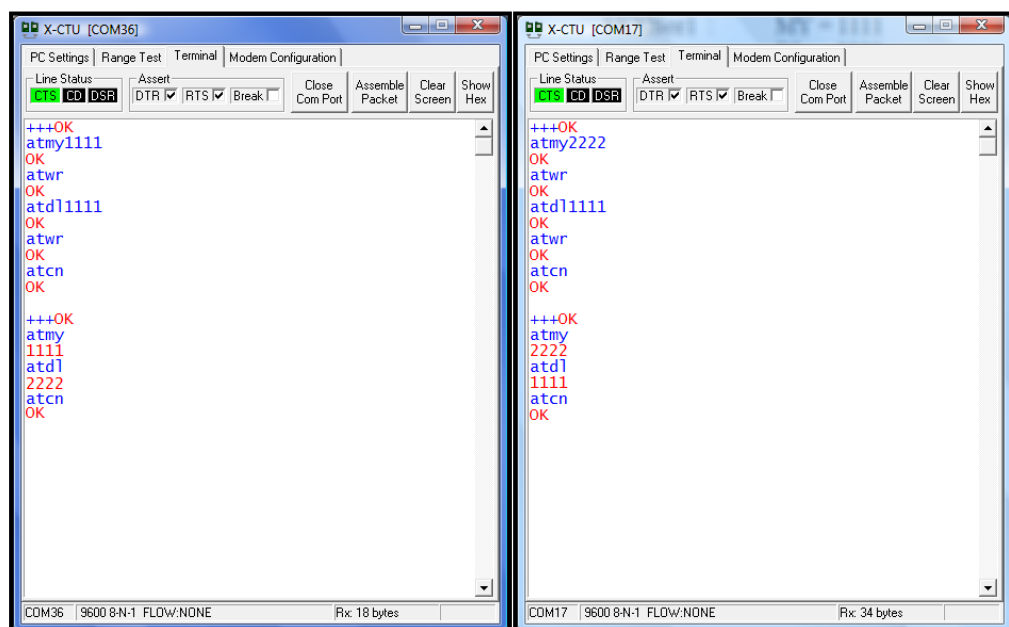


2. Choose the COM Port and click on “Test/Query” tab. A window will prompt out and show the status of communication with modem, modem type, and modem firmware version as followed. Click on “OK”.

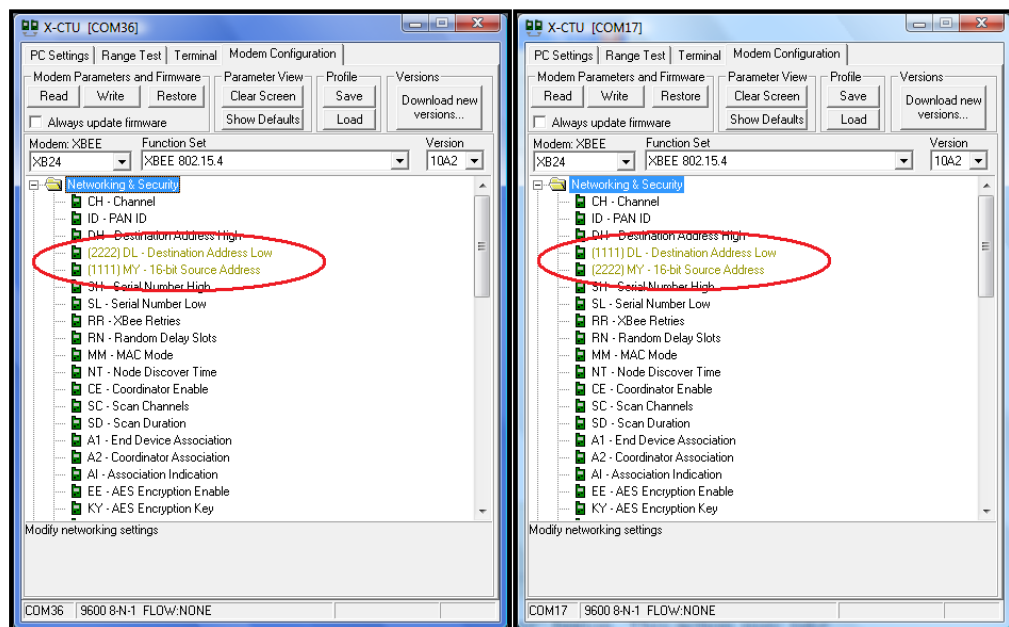


3. Next, set the address for each module as source address (MY) of circuit side SKXBee must be match to destination address (DL) of computer side SKXBee and destination address (DL) of circuit side SKXBee must be match to source address (MY) of computer side SKXBee.
4. Select the “Terminal” tab on X-CTU software. To enter AT Command Mode, send the 3-character command sequence ‘+++’ and SKXBee will response ‘OK’ which means that it has already enter the Command Mode. For this project, the source address (MY) and destination address (DL) of circuit and computer side SKXBee are set as below:

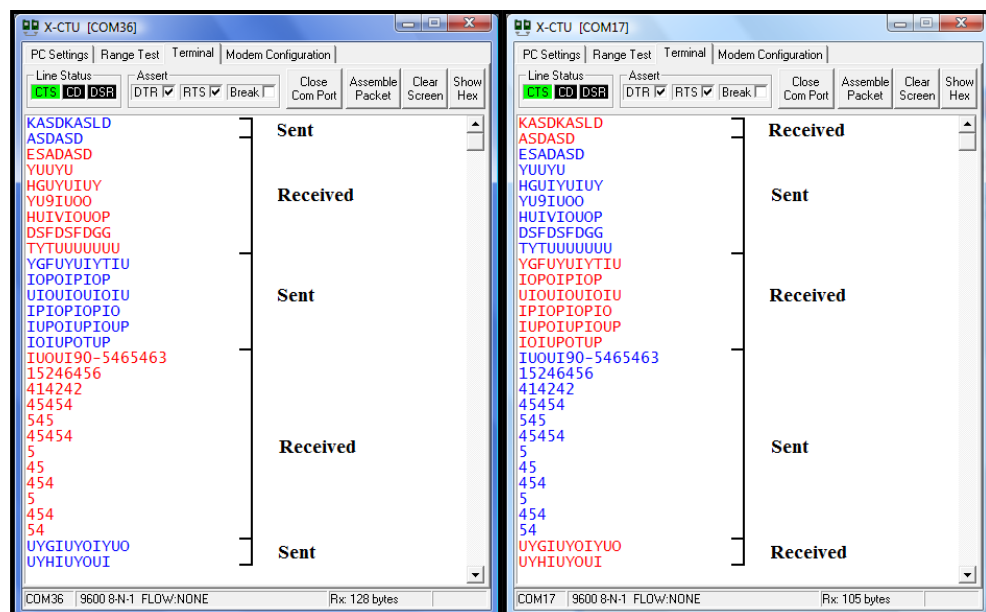
SKXBee1:	MY = 1111	SKXBee2:	MY = 2222
(Circuit)	DL = 2222	(Computer)	DL = 1111



5. There is an alternative way to change the source address (MY) and destination address (DL). Go to “Modem Configuration” tab, click on “Read”, information gather from SKXBee will be displayed after a few seconds. Click on “MY” and “DL” to key in new address. After changing the address, click on “Write” to load the new configuration into SKXBee.



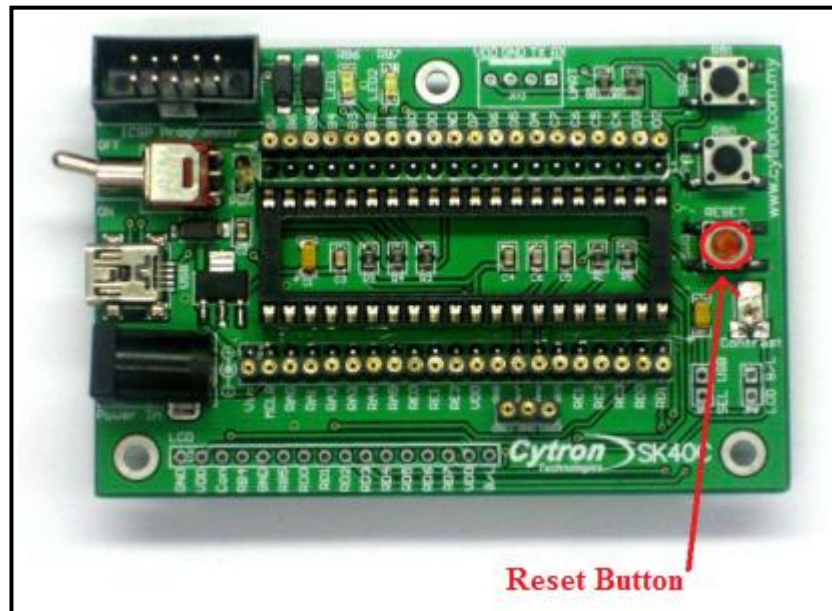
6. After built the connection between these two SKXBee, they can communicate among each other. Data sent by circuit side SKXBee is ready to receive data from FSRs and send to computer side SKXBee now.



3.5.2.2 XBee Module (SKXBee) with Microcontroller

More work will be needed if microcontroller is used as host of SKXBee. The procedures of connecting the SKXBee with microcontroller are explained as followed:

1. Setup SK40C enhanced 40 pins PIC start-up kit with PIC18F4550. All the components required are being configured and soldered onto a donut board.
2. Load the programming to microcontroller using SK40C enhanced 40 pins PIC start-up kit with UIC00B USB ICSP PIC programmer. The default rate for SKXBee is 9600 and therefore, set the baud rate of the PIC to be same as SKXBee.
3. Then, SK40C enhanced 40 pins PIC start-up kit is powered up with external voltage supply. “Reset” button of SK40C enhanced 40 pins PIC start-up kit is pressed and released.



4. If all connections and setup are correctly done, SKXBee is ready to receive and send data through wireless XBee dongle from computer.

3.5.2.3 XBee Module (SKXBee) as XBee Dongle

Compare to communication between SKXBee and microcontroller, SKXBee acts as XBee dongle is much easier. The procedures of connecting the SKXBee with computer as XBee dongle are explained as followed:

1. SKXBee is connected to computer using USB connection cable. The address is set for each module as explained before. Click on the icon “X-CTU” to launch the software. Go to “Terminal” setting tab to test the communication.
2. Reset button of SK40C enhanced 40 pins PIC start-up kit is pressed as mentioned before, followed by pressing “OK” and a sentence of ‘Cytron Press any number’ will appear.
3. Next, press any number. Data in red color is data received while data in blue color is data sent.



4. XBee dongle is ready to receive and send data through wireless SKXBee from microcontroller.

3.5.2.4 Process Flow

The overall process flow of XBee module (SKXBee) communication design is shown as followed:

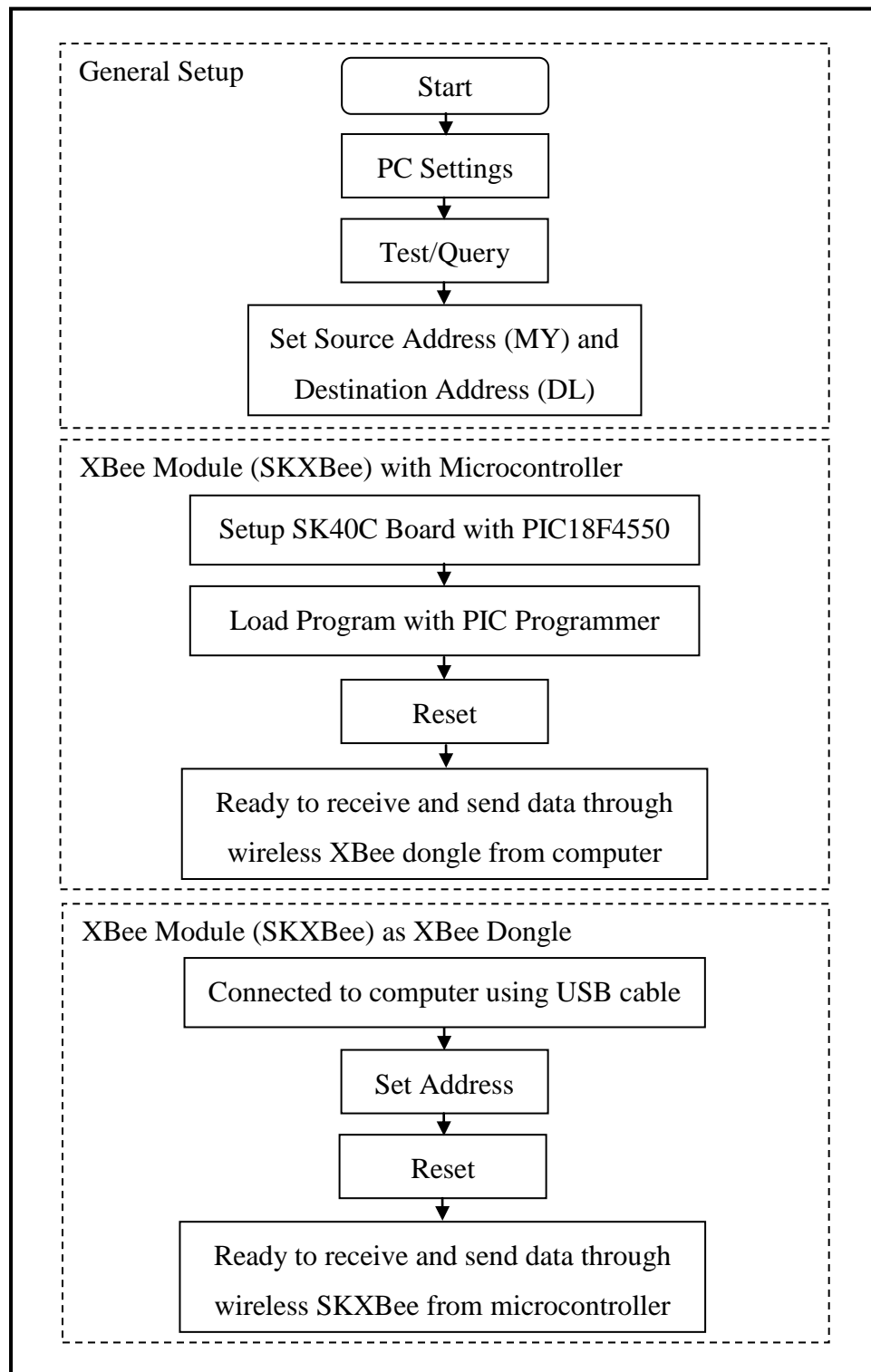
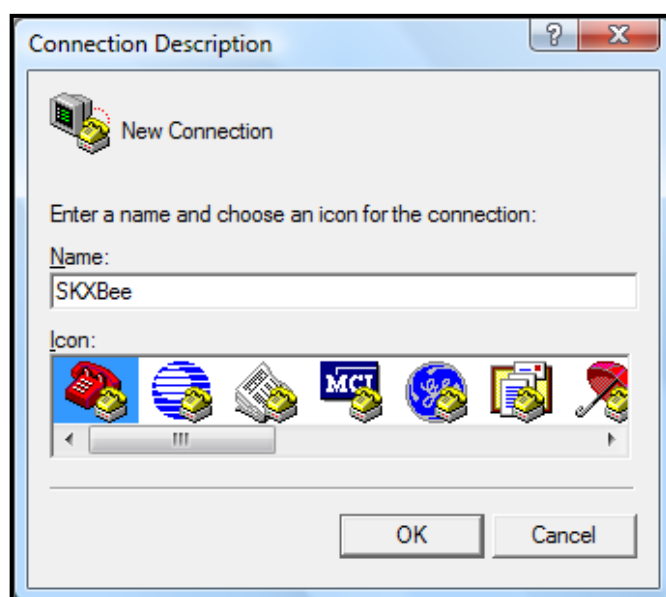


Figure 3.65: Process flow of XBee module (SKXBee) communication design

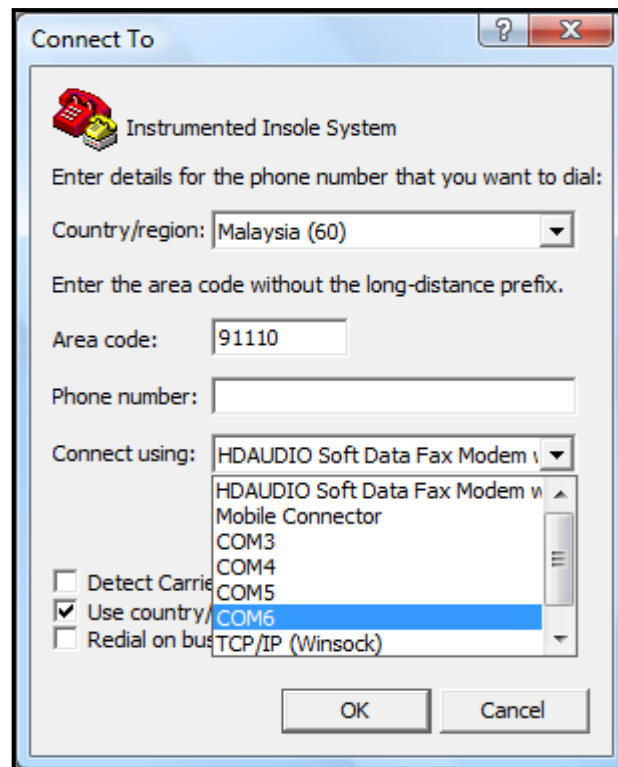
3.5.3 HyperTerminal Testing

The most efficient way to determine whether the SKXBee is connected and sending signals to computer is through HyperTerminal setup. This setup for UART communication with computer using can be done by connecting SKXBee to computer directly as new feature of USB to UART has been added to it. It is not valid for USB connection at SK40C enhanced 40 pins PIC start-up kit. The procedures of HyperTerminal testing are explained as followed:

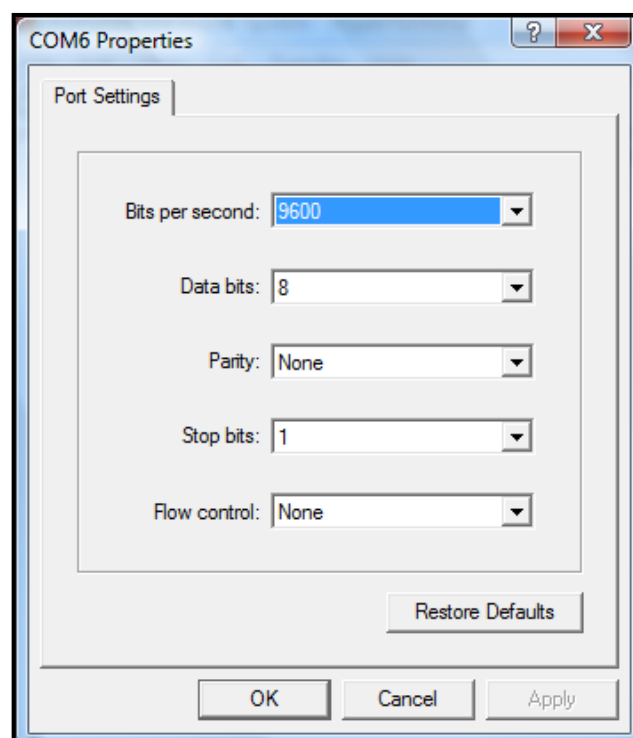
1. Go to “Start-up”, then “Accessories”, then “Communications” and select “HyperTerminal” to launch the program. For Windows Vista and Windows 7, HyperTerminal Private Edition 7.0 has to be downloaded and installed into computer.
2. After plug in the UC00A to computer and installation of driver, the functionality of SKXBee is ready to be tested. Open the HyperTerminal “Connection Description” dialogue box will prompt out. Enter a name in the space provided, choose an icon for connection, and click “OK”.



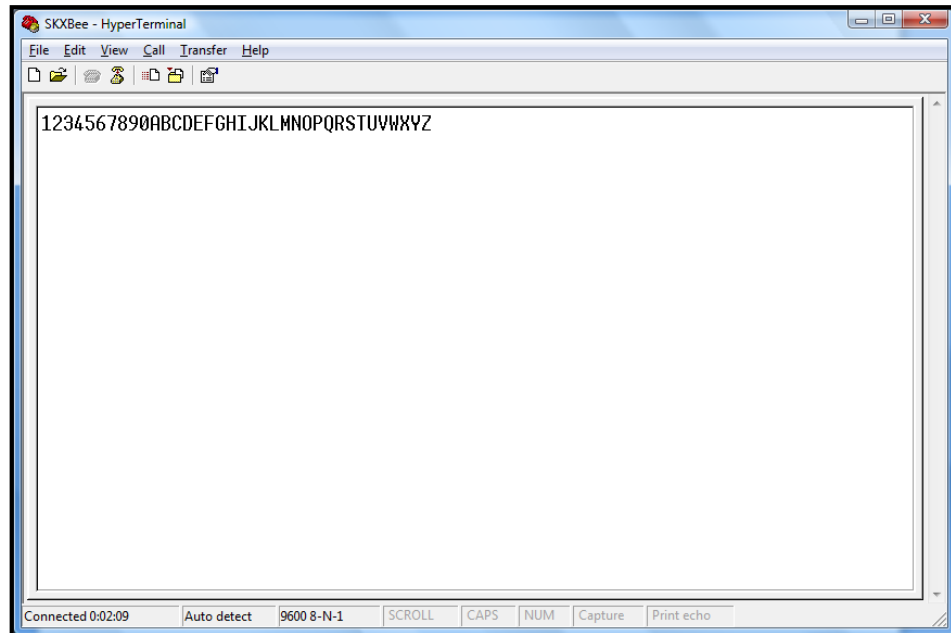
3. Next, the “Connect To” dialogue box prompted out. Choose the appropriate communication port for the computer (this port is referring to the virtual COM port created by X-CTU). In this example, COM11 is assumed to be the virtual COM port, and then click “OK”.



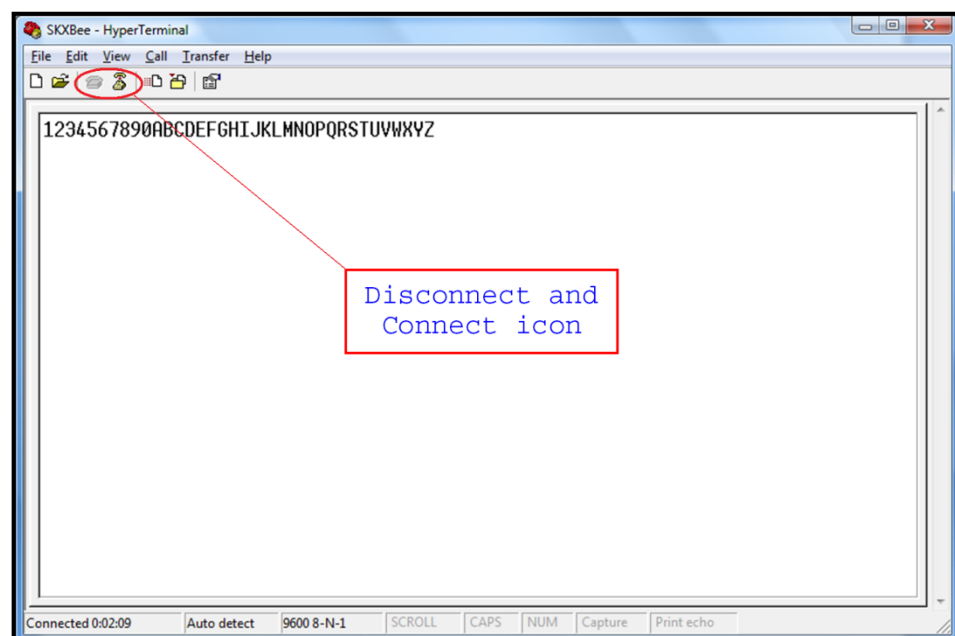
4. The “COM Port Properties” dialogue box will prompt out. Choose appropriate settings for the device and click “OK”. The default baud rate of SKXBee is 9600 Kbps. Change the “Bits per second” to ‘9600’ and “Flow control” to ‘None’.



5. After all settings are completed, SKXBee is ready to communicate with computer and the communication will be shown on HyperTerminal. As default (if SKXBee is not connected to any inputs), the results are shown as followed:



6. The communication between computer and SKXBee can be terminated by clicking the icon "Disconnect" and can be turned on again by clicking the icon "Connect".



The overall process flow of HyperTerminal testing design is shown as followed:

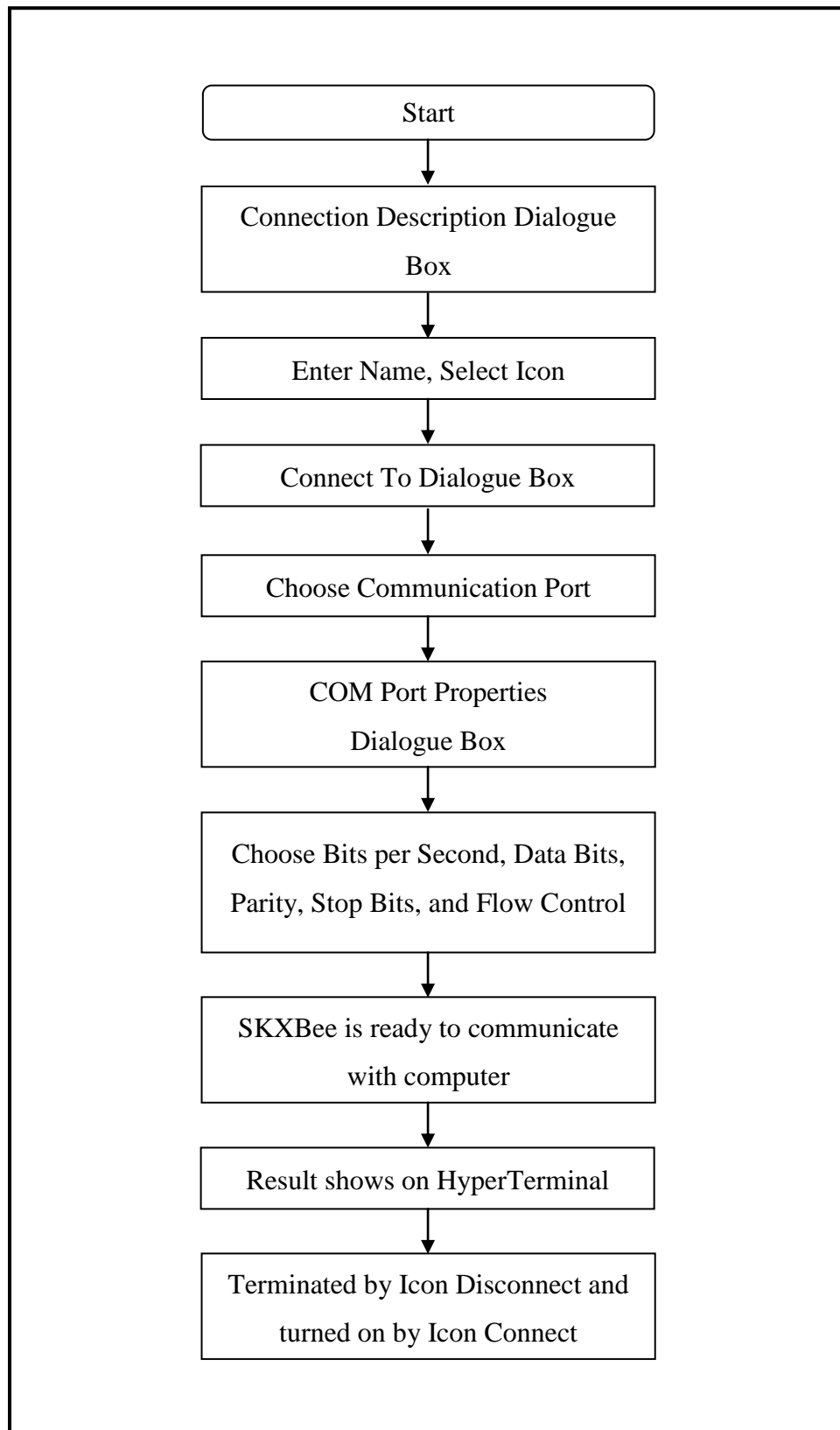
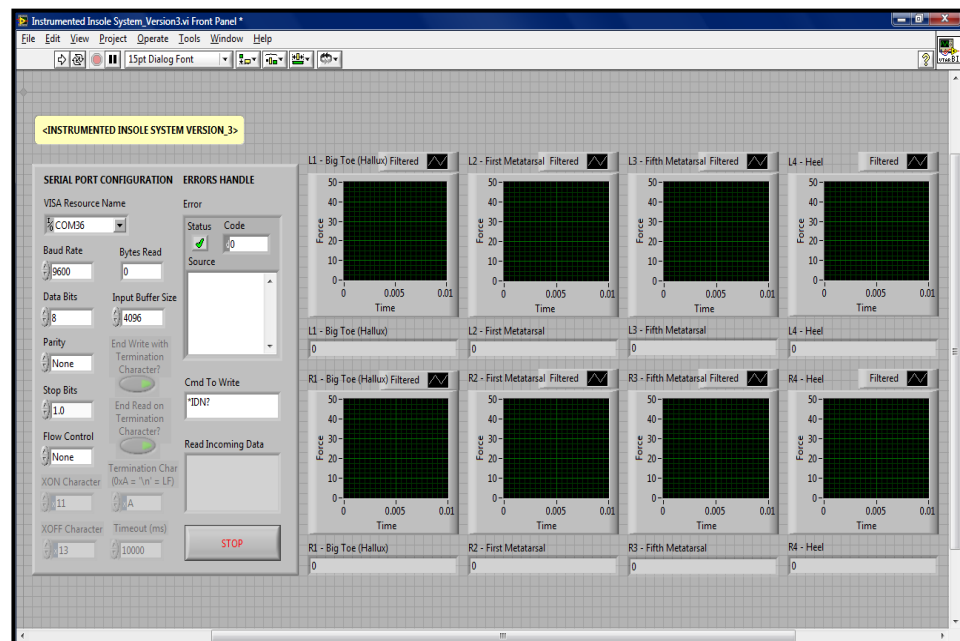


Figure 3.66: Process flow of HyperTerminal testing design

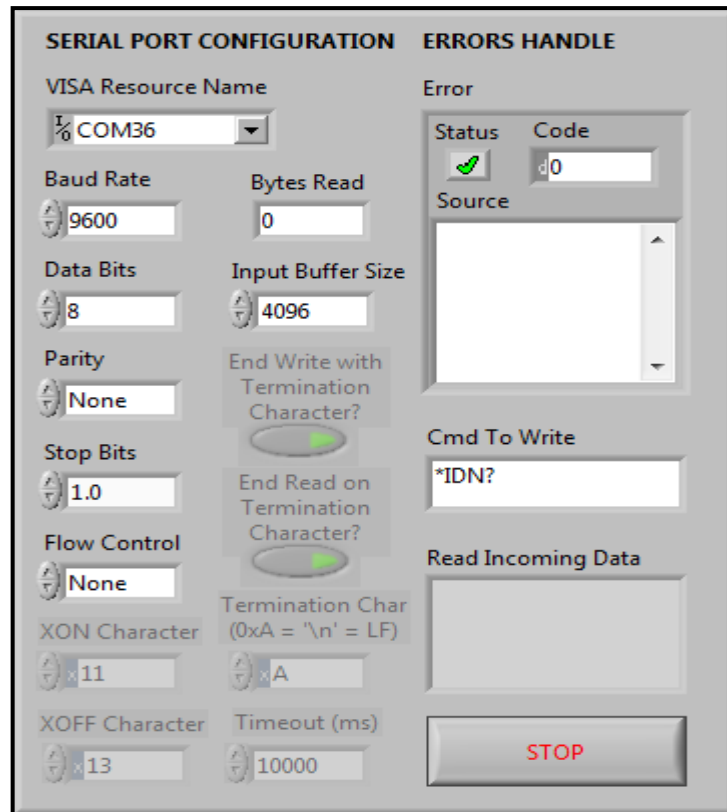
3.5.4 National Instruments LabVIEW Interactions

Once the SKXBee is connected with computer, data can be read (as well as storage of data) using a software called National Instruments LabVIEW 2009. The procedures of setting up the configuration are explained as followed:

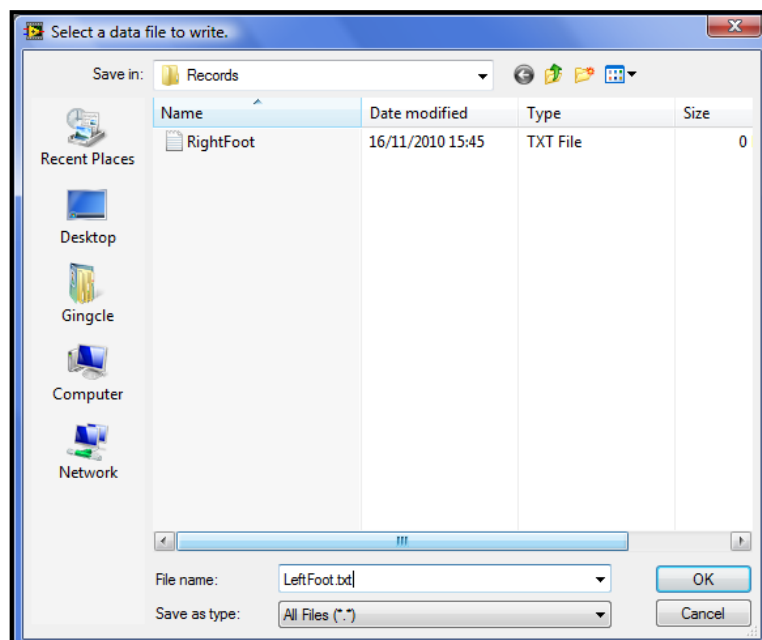
1. After installing the software into the computer, click on the icon “LabVIEW” to launch the software.
2. To open a saved file, go to “File” tab, from the drop-down menu, select “Open”. Browse the file “Instrumented Insole System.vi” from the appropriate folder.



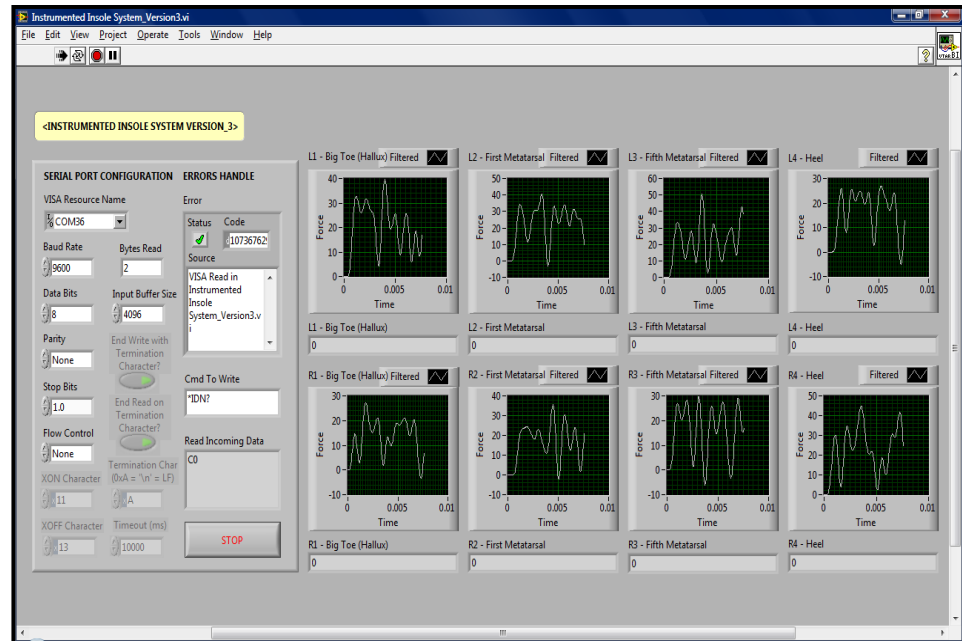
3. Then, under the “Serial Port Communication”, select the virtual COM port created by X-CTU software between SKXBee and the computer from the drop-down menu of “Visa Resource Name”. In this example, COM1 is used and the “Baud rate” is set to ‘9600’.



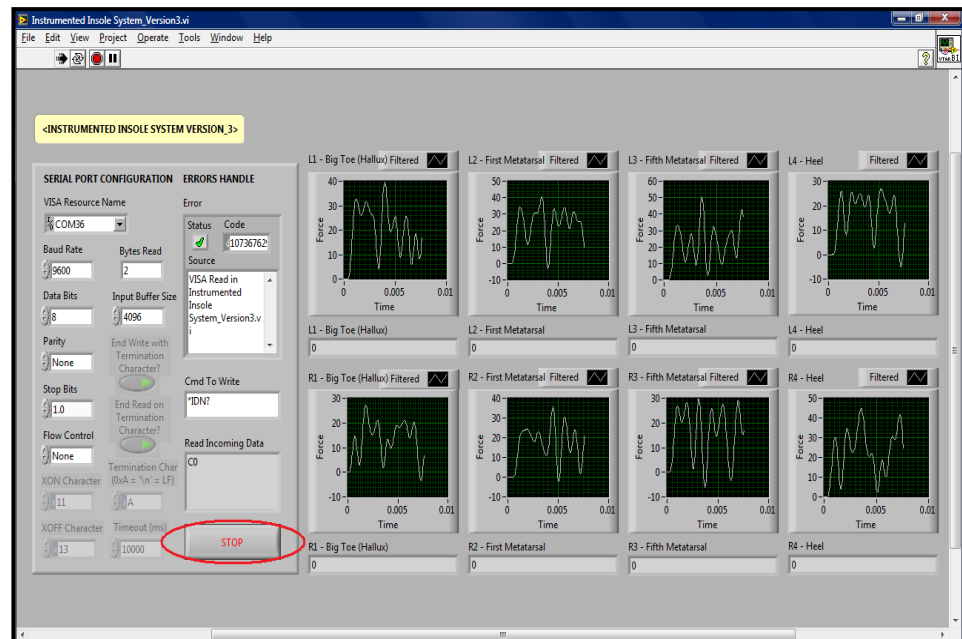
4. Next, to run the visual instrumentation, go to the “Operate” tab, and select “Run”. A dialogue box will appear to ask the selection of a text file to write the data (for storage purposes). A name (example: LeftFoot.txt) is entered and click “OK”. Repeat this for the next dialogue box with different file name.



5. After that, the program will start displaying graphs and collecting data into the text files. Now, the software is ready to monitor the changes in the FSRs.



6. To stop the program, click on the “Stop” button in the interface.



The overall process flow of National Instruments LabVIEW interactions design is shown as followed:

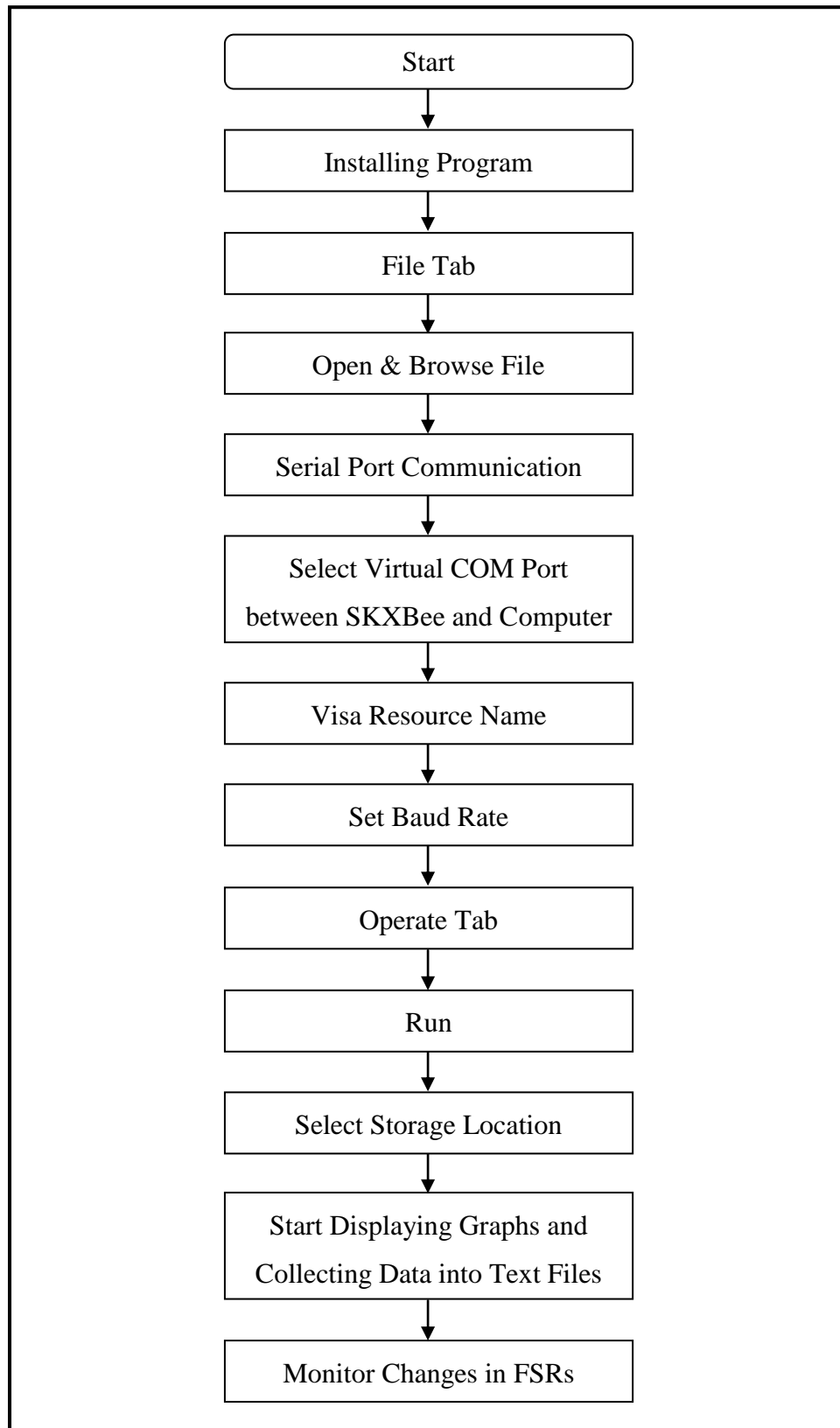


Figure 3.67: Process flow of National Instruments LabVIEW interactions design

3.6 PIC Coding and LabVIEW Graphical Programming

This section is divided into two parts, which are the PIC coding and LabVIEW graphical programming. The first part refers to the PIC coding used to load or burn into the microcontroller. It is important to know how the microcontroller converts the analogue voltages into digital signals so that the data analysis and processing can be done. The coding will be explained step by step in the next section thoroughly.

The second part in this section explains the graphical programming of LabVIEW in collecting the data, displaying the output graphs, and storing the results for future purpose. In this project, LabVIEW is used as part of the data processing where functions to convert the string into values and filtering low frequency noises. Same as PIC coding, this analytical system will be explained as well in the next section in a more clear and detail way.

3.6.1 PIC Microcontroller Programming

The complete PIC microcontroller coding is attached in Appendix B. The procedures of PIC microcontroller coding are explained line by line as followed.

Similar to other C language coding software, the first part of the PIC coding is a declaration part. This part defines the variables which are going to be used in the later part of the program. All spelling of the defined variables should not be similar to the library function names, such as “Call”, “Return”, and so on. The variables are defined as character or in short, “*char*”.

```
char force_L1, force_L2, force_L3, force_L4;  
char force_R1, forcer_R2, force_R3, force_R4;  
char txt[6];  
void tx_data(char, char);
```

The library function “*char*” declares the defined variable such as from *force_L1* to *force_L4* and *force_R1* to *force_R4* refers to the force sensing resistors output. The function type “*char*” indicates the variables are alphanumerical. *force_L1* to *force_L4* refers to the sensors from left foot and *force_R1* to *force_R4* refers to the sensors from right foot. The third line defines an array or string of seven characters called *txt*. This variable is going to be used as a string to store up the converted values and transmit it as output. The last line refers to a sub-function called *tx_data*, which is used to write the transmitted data and sends it out to the output pins. Details are explained in later part of this topic.

```
void main(void)
```

This *void main(void)* indicates the starting point of the main function. The coding in this main function has the priority to be first executed and any other sub-functions are linked directly from this main function.

```
ADCON1 = 0x80;
```

ADCON1 register at the address 9Fh is a feature used to activate the microcontroller’s analogue-to-digital converter (ADC). The *ADCON1* is used to configure the A/D result format select bit, A/D conversion clock select bit, and A/D port configuration control bits on the microcontroller. After the A/D conversion is complete, the result sits in registers ADRESL (A/D Result Low Byte) and ADRESH (A/D Result High Byte) (Mazidi, 2008). The *ADCON1* configuration is shown as followed:

ADFM	ADCS2	-	-	PCFG3	PCFG2	PCFG1	PCFG0
where	ADFM	:		A/D Result Format Select Bit			
	ADCS2	:		A/D Conversion Clock Select Bit			
	PCFG	:		A/D Port Configuration Control Bits			

For *ADCON1*, it is assigned with 0x80 (means “10000000” in binary). The *ADFM* result format select bit is set to “1”, which is right justified (6 most significant bits of *ADRESH* are read as ‘0’). For the A/D conversion clock select bit, *ADCS2* is set to “0” as default. Hence, the clock conversion is set to $F_{OSC}/2$. The *PCFG* configuration bits are set as “0000”, which means all of the ADC channels are activated as analogue inputs and the V_{REF+} and V_{REF-} are set to V_{DD} and V_{SS} correspondingly.

```
TRISA = 0x2F;
TRISE = 0x07;
TRISC = 0x80;
```

The next step is to configure the input and output pins (I/O) of the ports that are being used. In this configuration, “0s” is assigned to the *TRISx* register to act as an output port and “1s” is assigned to the *TRISx* register to act as an input port. Port A, C, and E are being utilized in this project. It must be noted that unless *TRISx* bit is being activated, the data will not go from the port register to the pins of the PIC (Mazidi, 2008). From above, 0x2F (means “00101111” in binary) is assigned to *TRISA* and 0x07 (means “00000111” in binary) is assigned to *TRISE* to make them as input ports. Port A and Port E is used as input for the eight FSRs.

As for *TRISC*, 0x80 (means “10000000” in binary) is assigned which indicates that one output of the eight pins in Port C is set as input pin, which is the RC7. This pin serves as a RX pin to be used as the communicator between the microcontroller and the XBee module. The TX pin (RC6 of Port C) is assigned with “0” to make it as an output port so that it can transfer data to the XBee module. Therefore, other pins on Port C are set as output port but only TX pin will be used and this instrumented insole system does not require taking any inputs from computer.

```
PORTA = 0x00;
PORTE = 0x00;
PORTC = 0x00;
```

The three lines above are used to clear any values that are being stored in Port A, E, and C previously before initiating the program.

```
Usart_init(9600);
```

This command sets the baud rate of the microcontroller to 9600 kbps, which means that asynchronous data communication is using 9600 baud rate, eight bit, one stop bit, and non-parity. This baud rate should match with XBee module's baud rate in order to transmit the data correctly.

```
do
{
force_L1 = adc_read(0)/4;
Delay_ms(5);
tx_data('A', force_L1);
...
...
}while(1);
```

In this *do-while* loop, the analogue voltages generated by the FSRs are being converted into digital signals. This is done by calling *adc_read(0)* function. The microcontroller will start to read from channel "0" of the input port, converts the analogue voltages, and then stores it into the variable of *force_L1* defined earlier in the program. The next line of command is used to transfer two data to the sub-function *tx_data*, which is a character "A" (arbitrary value to indicate the first sensor) and the converted value of *force_L1*. A *Delay_ms* function is used to delay the execution of 5 milliseconds.

The following line of commands is similar and repeated for *force_L2* until *force_R4*. This is done by putting the "1" into the *do-while* loop, which indicates that the function is always true and repeat the process continuously. Now, the microcontroller has the data and ready to send it out to the XBee module. The sub-

function *tx_data* holds a *char a* as “A” and *char b* as the value of *force_L1*. Part of the sub-function from the main program is shown as followed:

```
void tx_data(char a, char b)  
{  
  Usart_write(a);  
  bytetostr(b, txt);  
  if(txt[0] == ‘ ’)  
    Usart_write(‘0’);  
  else  
    Usart_write(txt[0]);  
  ...  
  ...  
  Delay_ms(50);  
}
```

The function *Usart_write(a)* is used to send the data out from microcontroller. For example, *char a* is obtained from the main body and send to the TX pin of the microcontroller, where *char a* is the alphabet “A”. Therefore, the first output from the microcontroller is expected to be the letter “A”.

The library function *bytetostr(b, txt)* is used to convert *char b* into a string of values and store it inside an array called *txt* which is created in the early part of the program. If string is detected, the string will be sent but if there is no value detected from the string, a “0” is sent and displayed as a horizontal straight line.

The *if-else* command is used to determine the array *txt* whether it stores any characters. If the array stores nothing (represented by the bracket ‘ ’), the microcontroller will send out the value of “0”. Else, if the array stores a value, the microcontroller will send out that value to the TX pin for transmission. This same command is carried out for the next few characters and all these ended with a delay of 50 milliseconds using the function of *Delay_ms(50)*. This function ensures that the microcontroller has enough time to do all the data reading, conversion, and transmitting before another set of values come into the sub-function.

The overall process flow of PIC microcontroller programming design is shown as followed:

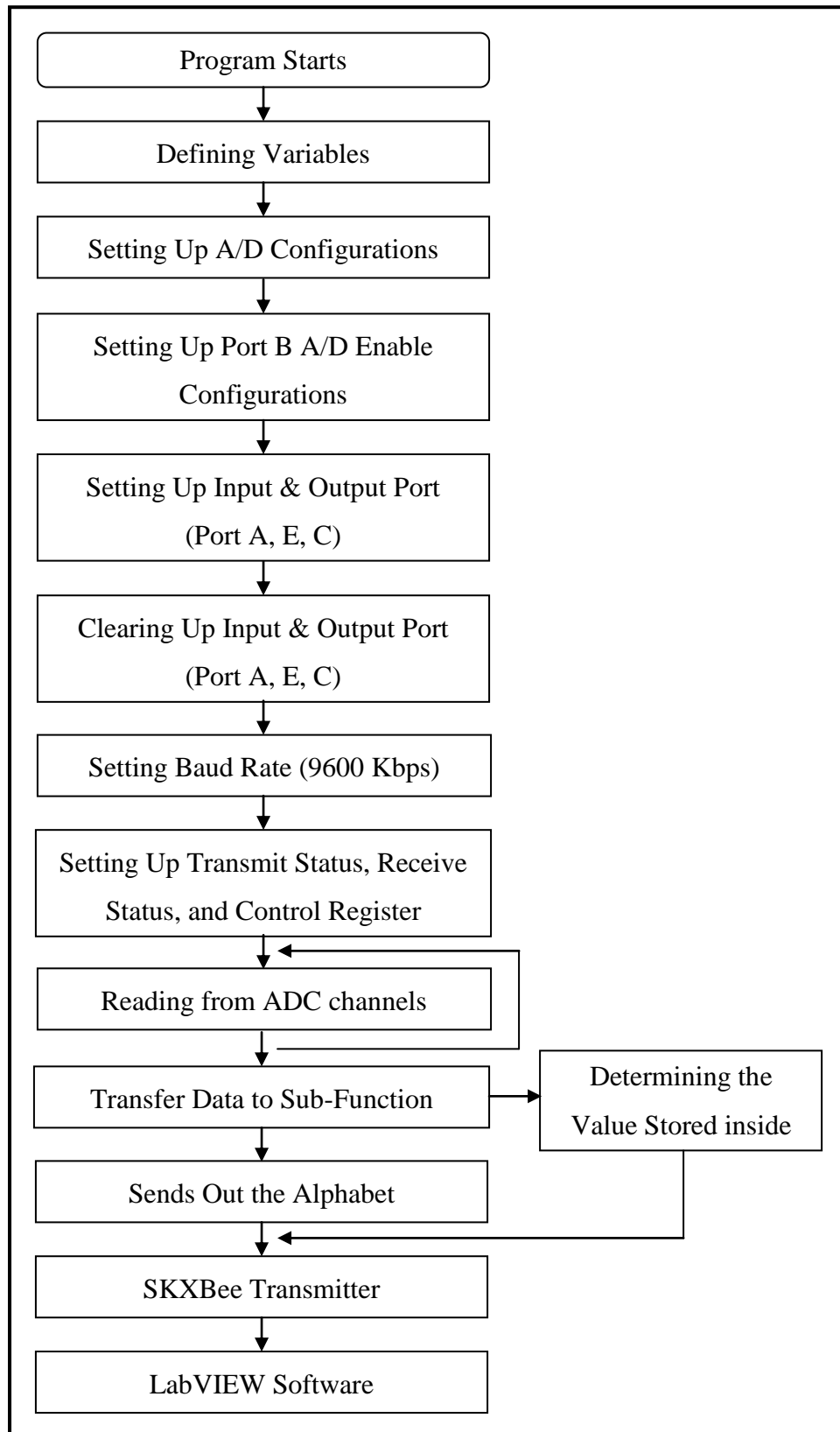


Figure 3.68: Process flow of PIC microcontroller programming design

3.6.2 LabVIEW Graphical Programming

National Instruments LabVIEW is a powerful development environment for signal acquisition, measurement analysis, and data presentation. This software gives the flexibility of a programming language without the complexity of traditional development tools. Typically, measurement and automation applications can be broken up into three primary pieces that are acquiring data, analyzing it, and then presenting it to the enterprise.

Therefore, this software offers much user-friendly functions like drag and drop buttons to form block diagrams without having complicated coding and programming language. Basically, it runs on two windows, one is recognized as the “Front Panel” which is used as an interface for displaying data, and another window is for “Block Diagram” which is used for graphical programming.

There are three different functional systems have been developed for this project. Most of the block diagrams are the same, only the formula and graph display are slightly different. The complete block diagram is separated into parts to reduce the complexity due to large size of the system. For more details, the complete block diagram is found in Appendix C.

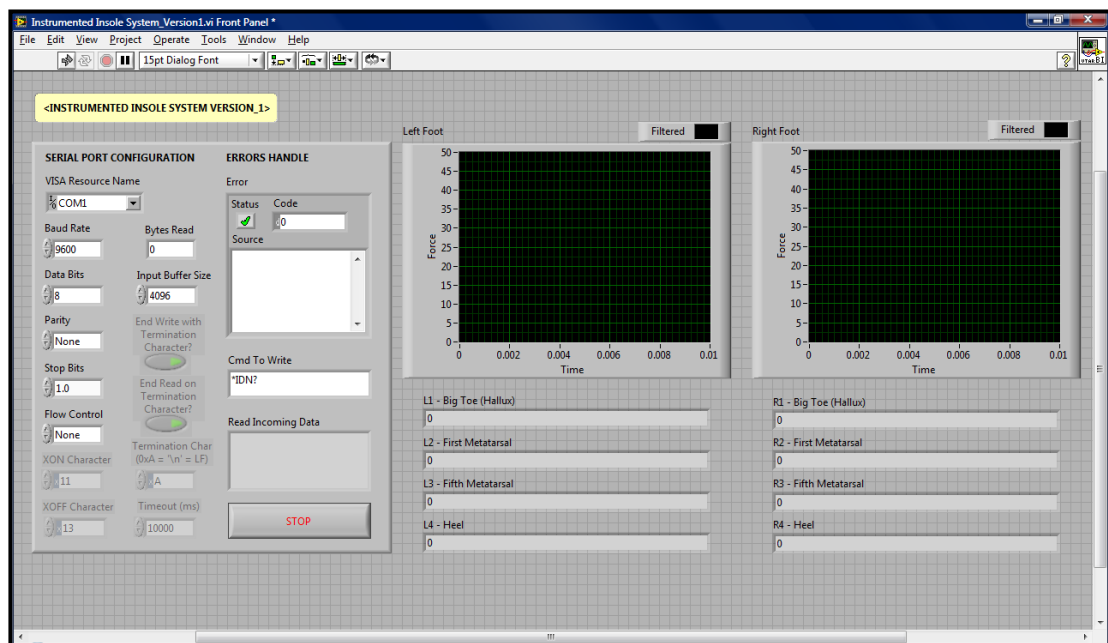


Figure 3.69: LabVIEW graphical user front panel interface version one

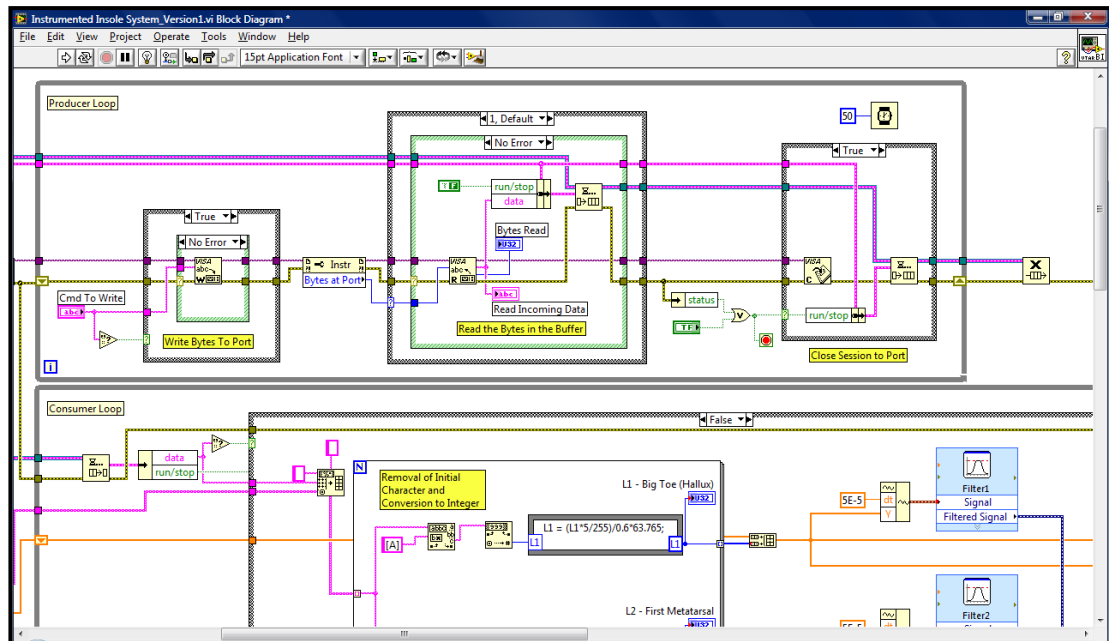


Figure 3.70: LabVIEW programming mode block diagram interface version one

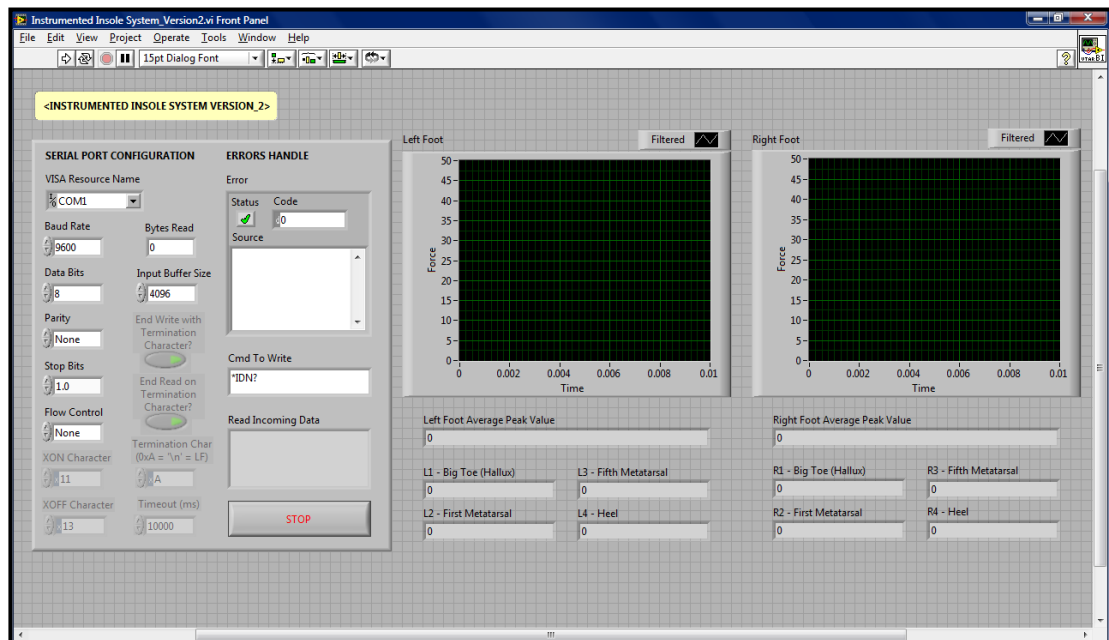


Figure 3.71: LabVIEW graphical user front panel interface version two

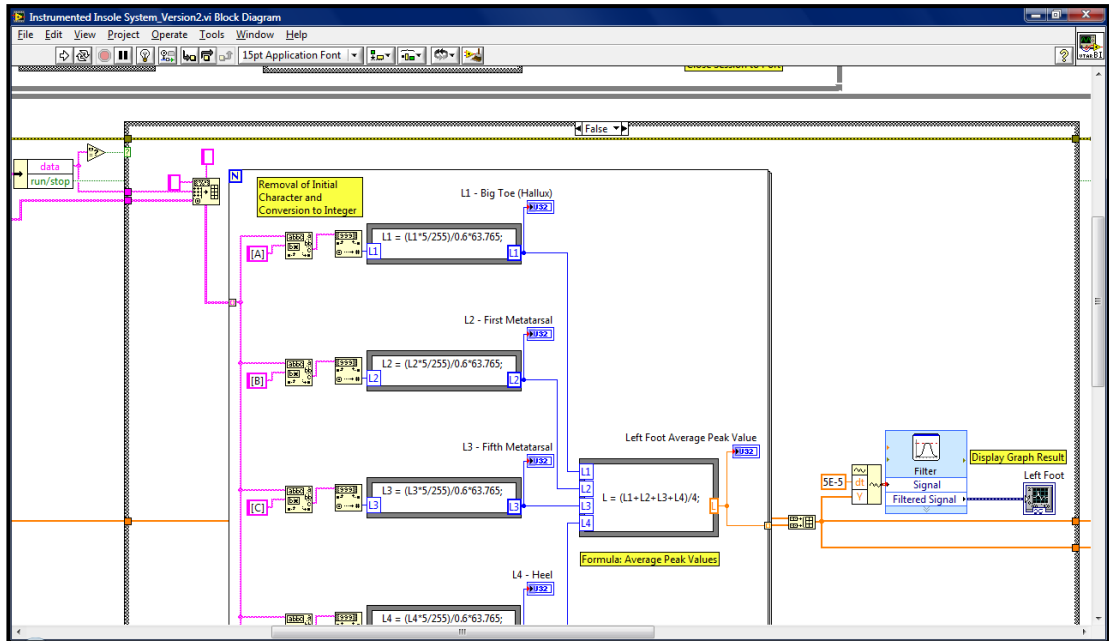


Figure 3.72: LabVIEW programming mode block diagram interface version two

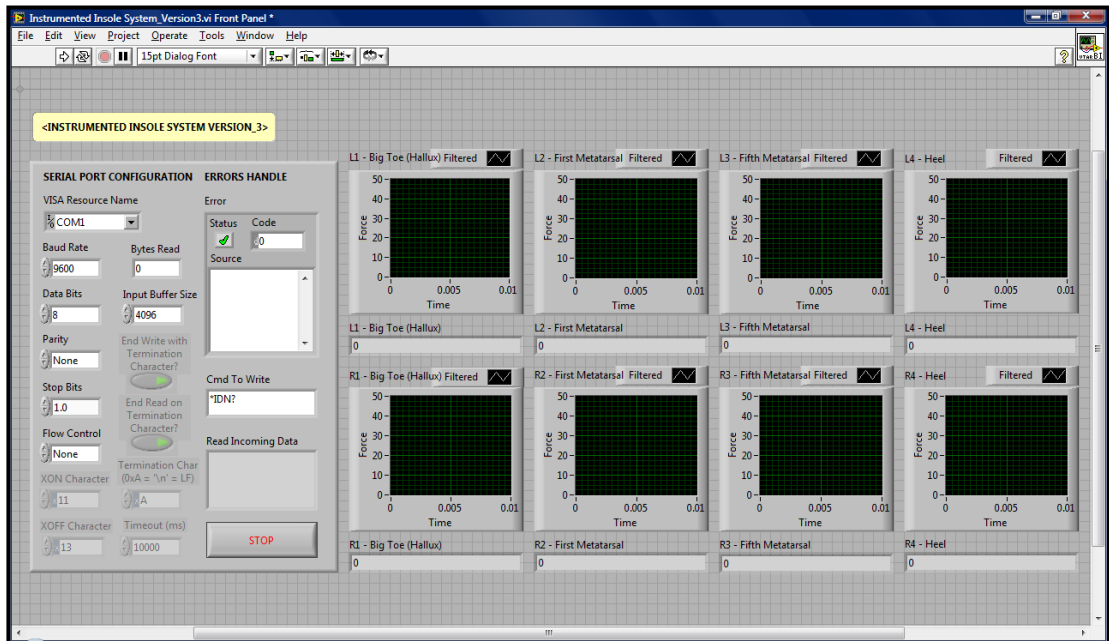


Figure 3.73: LabVIEW graphical user front panel interface version three

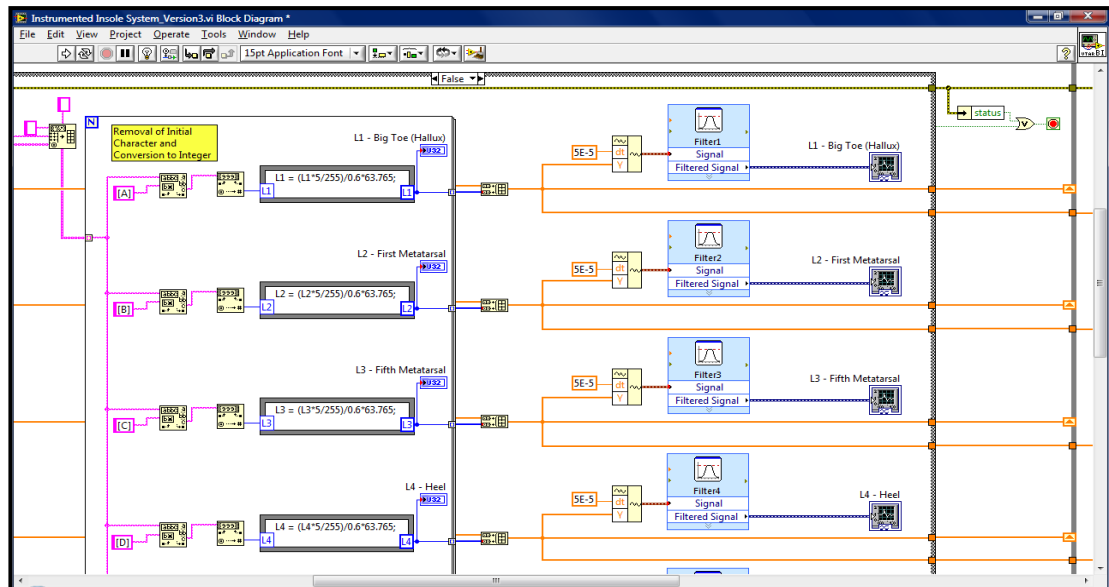


Figure 3.74: LabVIEW programming mode block diagram interface version three

In this section, the block diagram interface is discussed. However, only major parts of the block diagram are being explained due to the complicated system created. The work flow of data acquiring, conversion, analyzing, and result presenting are focused in this section rather than the function of each component in the block diagram. The major parts of block diagram are as followed:

1. Serial COM Port Configuration
2. VISA Read and Write of Incoming Data
3. Removal of Initial Character, Conversion to Integer, and Formula
4. Result Display
5. Storage of Data in Text File
6. Errors Handler

3.6.2.1 Serial COM Port Configuration

The serial COM port configuration sets up LabVIEW to communicate with XBee module. It plays an important role to synchronize the streams of eight signal inputs from the sensors through XBee module for real-time monitoring and analysis.

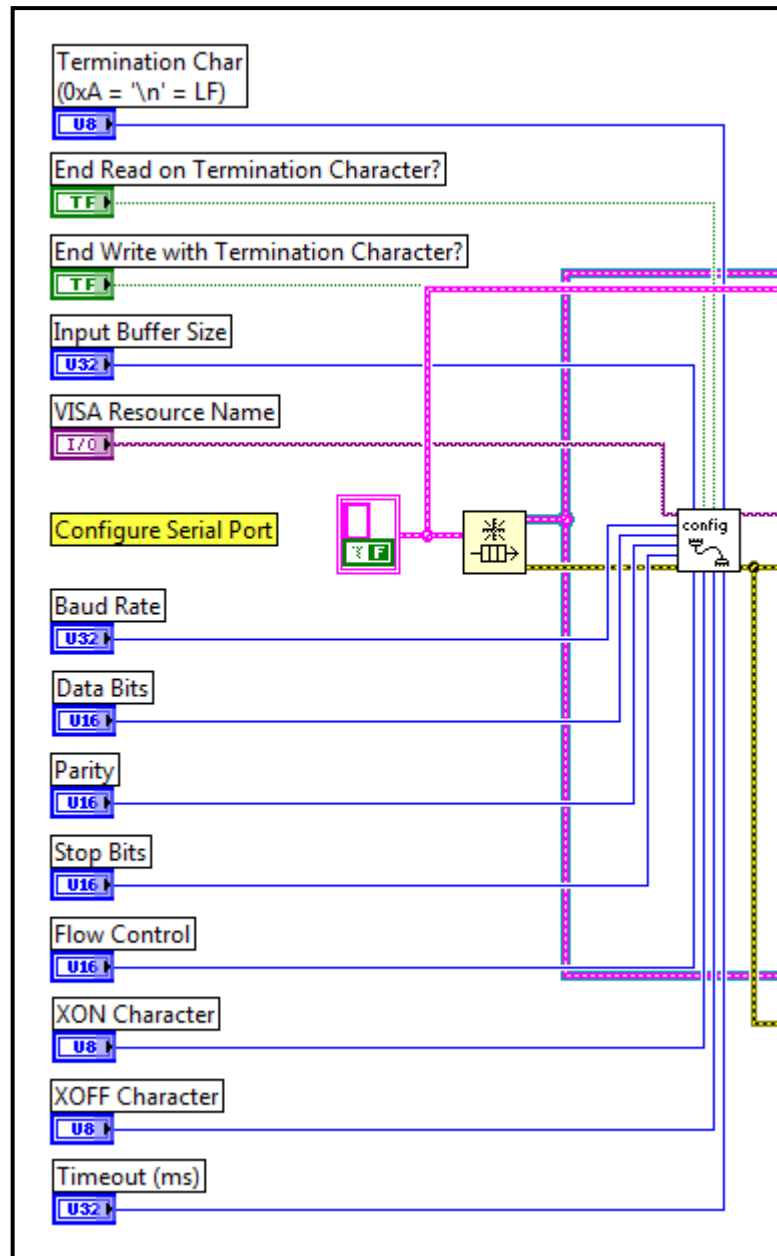


Figure 3.75: Serial COM port configuration block diagram for all versions

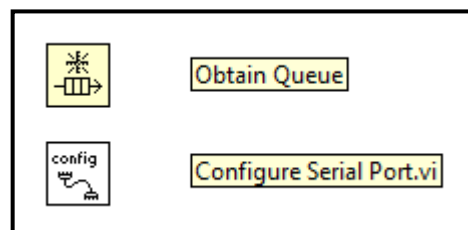


Figure 3.76: Serial COM port configuration block diagram labelling for all versions

In this configuration, settings must be first adjusted to suit the configuration of XBee module incoming port before any data processing, monitoring, and analysis can be done. However, there are some important parameters to be taken into consideration such as VISA resource name, baud rate, data bits, parity, stop bits, and flow control.

Besides, the terminal character and timeout period are set for the read operation. VISA resource name refers to the virtual COM port created by the XBee module. Other parameters of each setting are being configured according to XBee module specifications as discussed in the previous section of LabVIEW interactions.

“Obtain Queue” is used in this serial COM port configuration, which is functioned to return a reference to a queue. By using this queue operations functions, it can create a queue for communicating data between sections of a block diagram or from another VI. As shown in the serial COM port configuration block diagram labelling, there is a sub-VI called “Configure Serial Port”. The front panel and block diagram is shown as bellow.

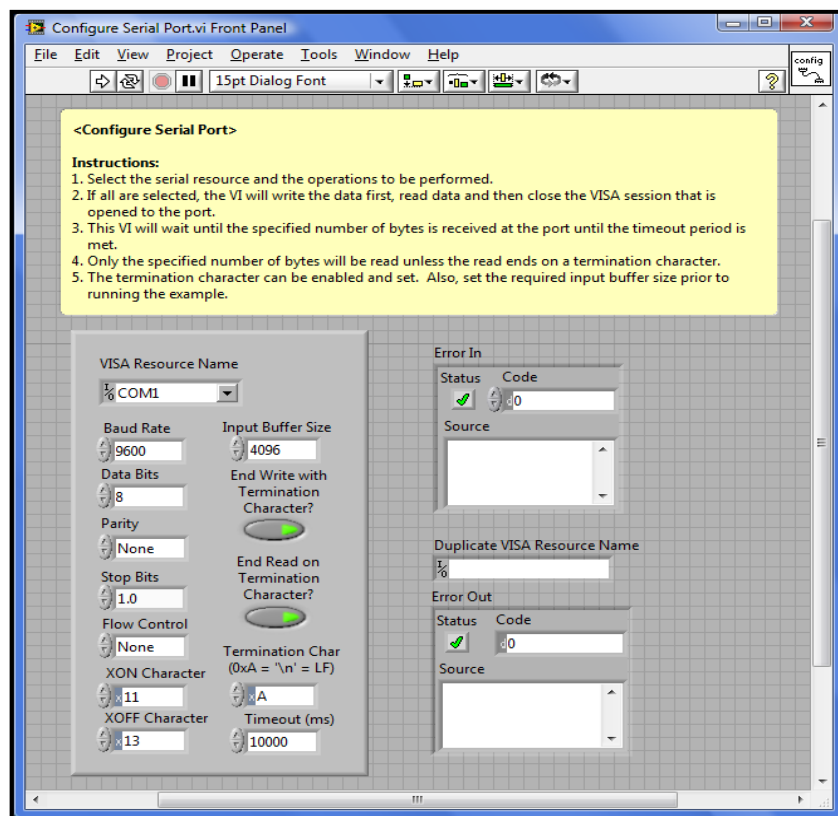


Figure 3.77: Configure serial port front panel interface for all versions

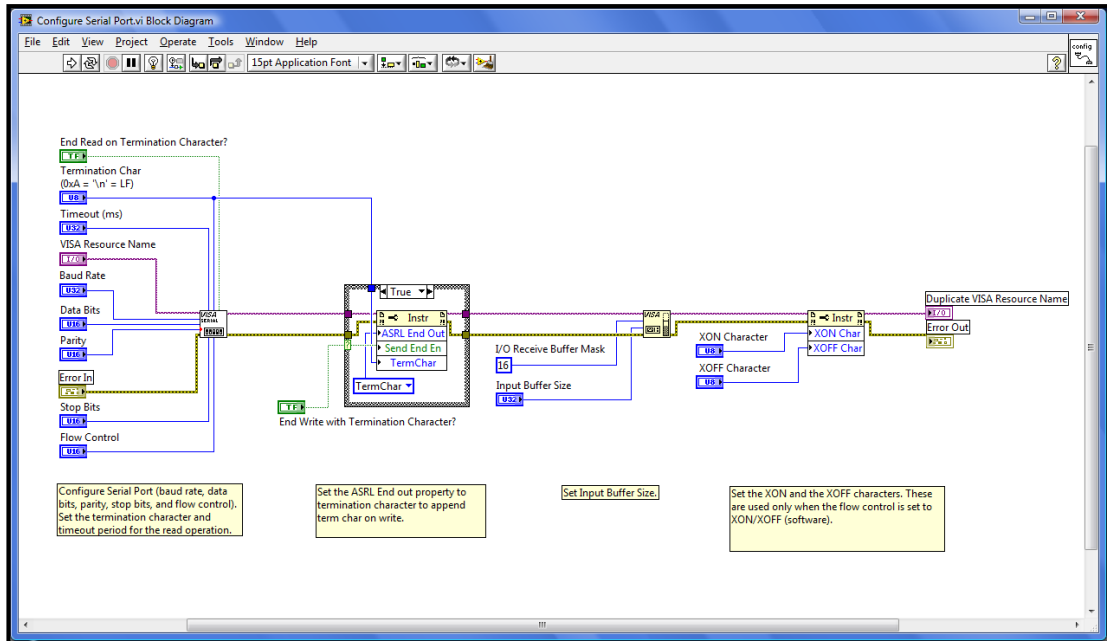


Figure 3.78: Configure serial port block diagram interface for all versions

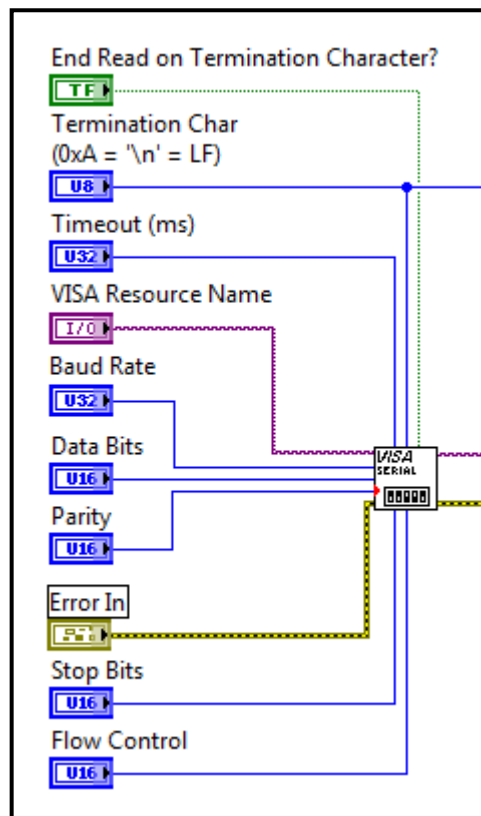


Figure 3.79: Configure serial port block diagram A for all versions

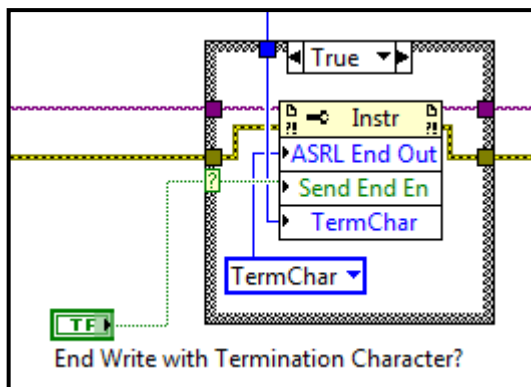


Figure 3.80: Configure serial port block diagram B for all versions

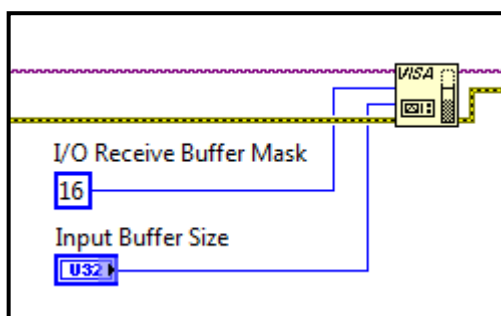


Figure 3.81: Configure serial port block diagram C for all versions

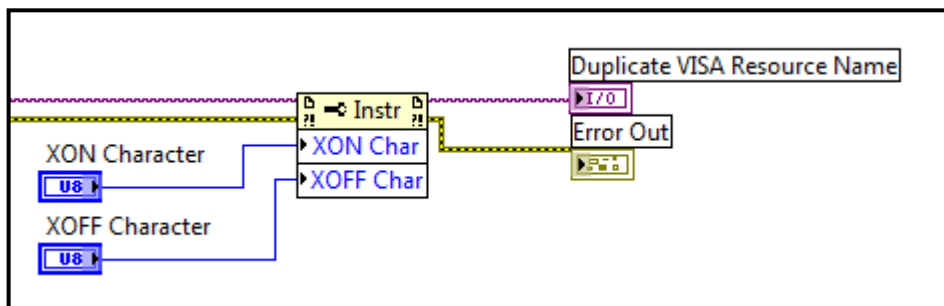


Figure 3.82: Configure serial port block diagram D for all versions

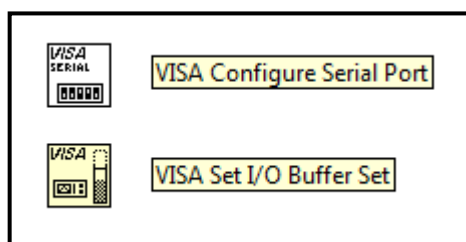


Figure 3.83: Configure serial port block diagram labelling for all versions

Each part carried out their own working operation, like to set the input buffer size, set the XON and XOFF characters. These are used only when the flow control is set to XON or XOFF. From the block diagram, “VISA Configure Serial Port” is functioned to initialize the serial port specified by VISA resource name to specified settings. With this function, data can be wired to the VISA resource name input to determine the polymorphic instance to use or manually select the instance.

For “VISA Set I/O Buffer Set”, it is used to set the size of the I/O buffer and run the VISA configure serial port. Commonly, not all serial drivers support user-defined buffer sizes. Therefore, some implementations of VISA might not be able to perform this operation. If an application requires a specific buffer size for performance reasons and the VISA implementation cannot guarantee that size, some form of handshaking is used to prevent overflow conditions.

3.6.2.2 VISA Read and Write Incoming Data

The VISA (Virtual Instrument Software Architecture) read and write incoming data part consists of a while loop which continuously obtain the incoming data from COM port. This part is connected to the “Configure Serial Port” from the serial COM port configuration as discussed before.

This loop will repeat the sub-diagram inside it until the conditional terminal, and input terminal, receives a particular Boolean value. Hence, this VISA communication port will continuously read from the serial COM port. If necessary command is needed, the “VISA Write” function is available.

Obviously, the major function of this part is to ensure that LabVIEW keeps reading from the connected serial COM port without having any errors. This is done by using a few case structures built inside the loop to carry out the working operation efficiently and accurately.

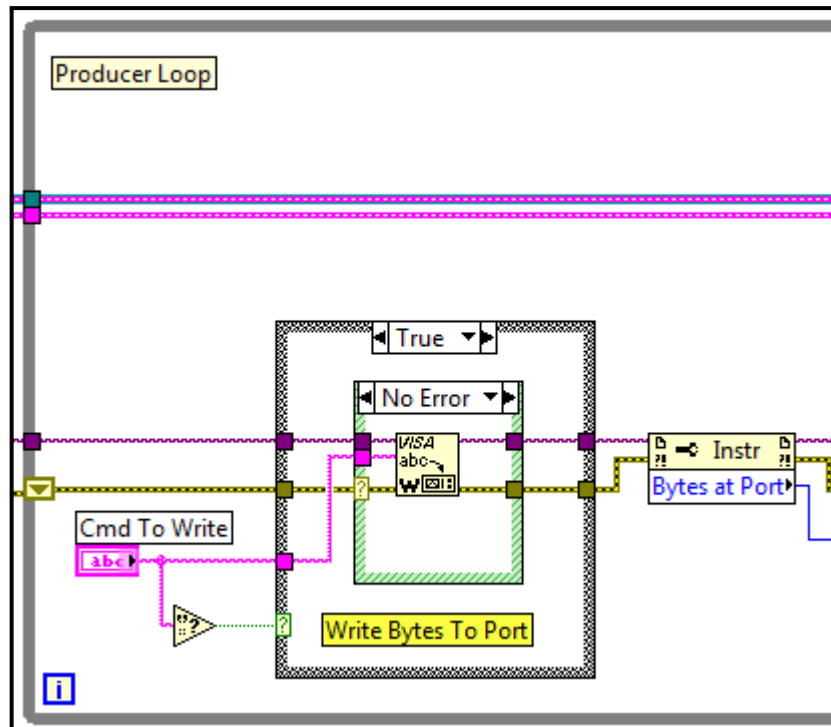


Figure 3.84: VISA read and write incoming data block diagram A for all versions

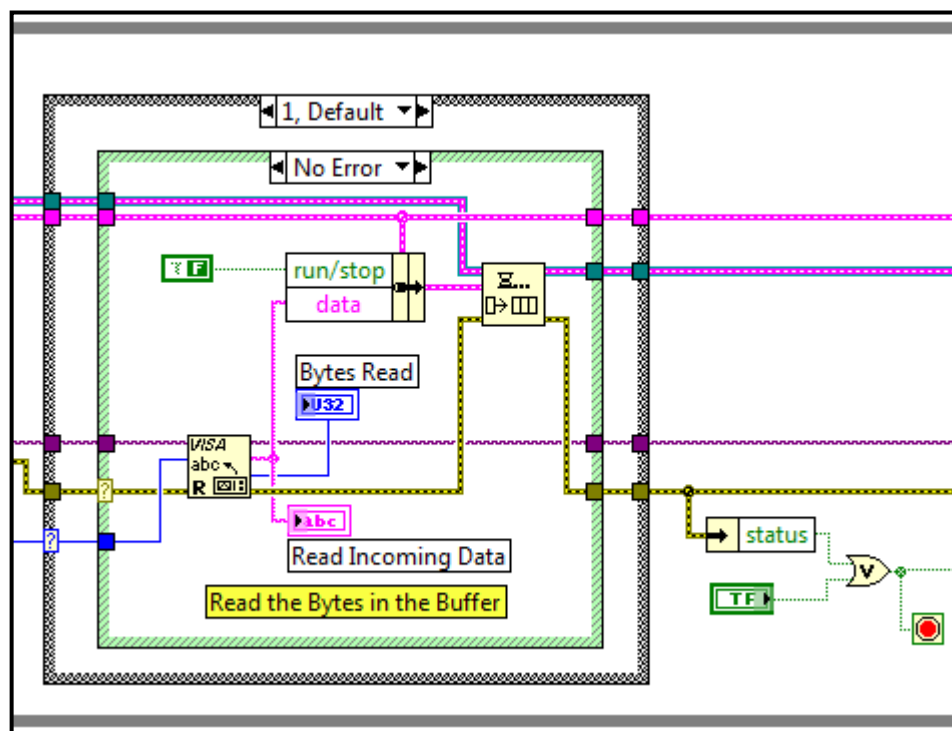


Figure 3.85: VISA read and write incoming data block diagram B for all versions

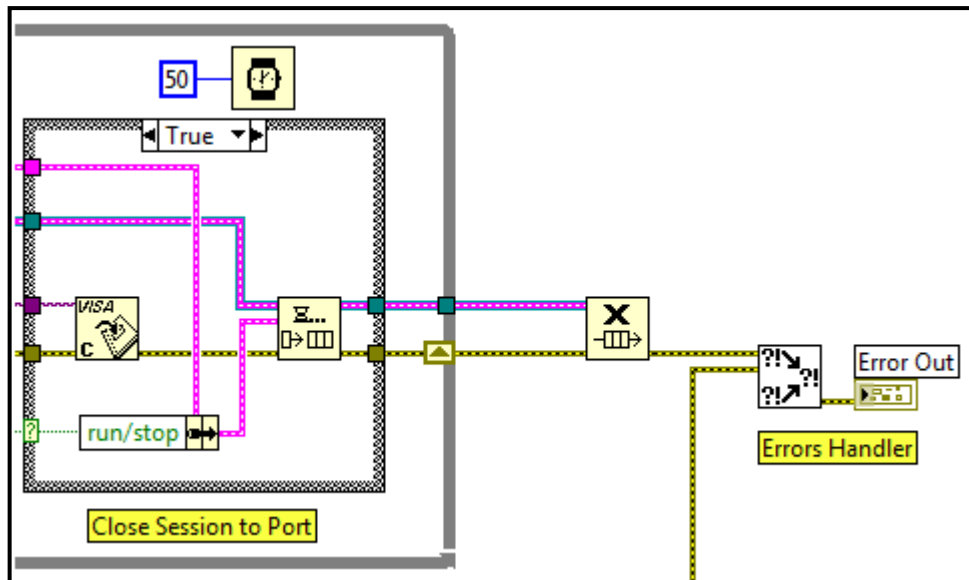


Figure 3.86: VISA read and write incoming data block diagram C for all versions

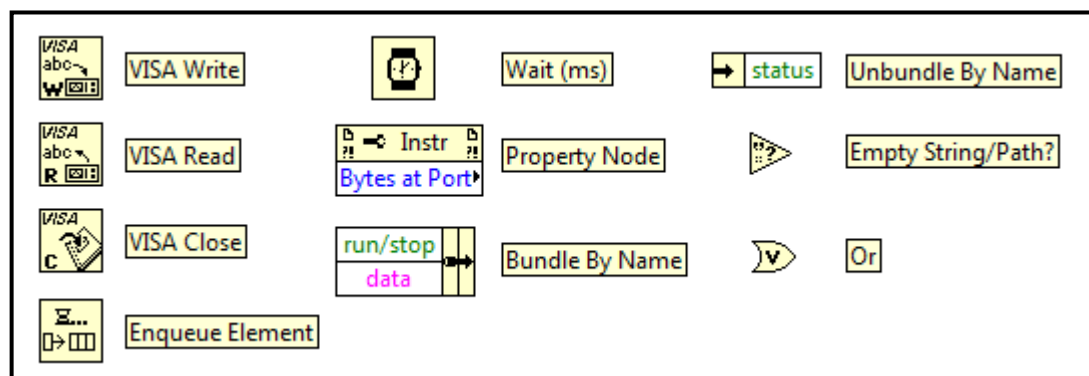


Figure 3.87: VISA read and write incoming data block diagram labelling for all versions

From the block diagram, the parts are being shown out for writing bytes to port, reading the bytes in the buffer, and close session to port. This is done by combining certain functions, like “VISA” functions. The “VISA Write” to write the data from write buffer to the device or interface specified by VISA resource name, “VISA Read” to read the specified number of bytes and returns the data in read buffer, and “VISA Close” for closing a device session or event object. This combination forms the VISA read and write incoming data working operation.

The “Enqueue Element” is to add an element to the back of a queue. If the queue is full, the function waits timeout in ms before timing out. If space becomes available in the queue during the wait, the function inserts the element and timed out is false. If queue becomes invalid such as when the queue reference is released, the function stops waiting and returns error code 1122.

Furthermore, a delay of 50 milliseconds is made by “Wait (ms)” function to ensure that the data is read completely by LabVIEW before any other incoming data is collected. This function will wait the specified number of milliseconds and return the value of the millisecond timer, which force the current thread to yield control of the computer.

“Property Node” is functioned to get or set properties of a reference. By using this function, the properties are get or set and methods on local or remote application instances, Vis, and objects. This node will automatically adapt to the class of the object that reference to. “Empty String/Path?” and “Or” expressions are used for Boolean algorithm.

Next, “Bundle By Name” is used to replace one or more and return the cluster element. This function refers to cluster elements by name instead of by their position in the cluster. While for “Unbundle By Name” is used to return the cluster elements. With the present of this function, there is no need to track the order of the elements within the cluster. This function does not require the number of elements to match the number in the cluster.

3.6.2.3 Removal of Initial Character, Conversion to Integer, and Formula

The initial character of A to H represents the input from which FSR sensors and which side of foot that is detected. Before plotting out the results, the initial character must be removed and the results must be in integer form. Formula conversion factor plays an important role to convert the input signals into required parameter for ready to be displayed out.

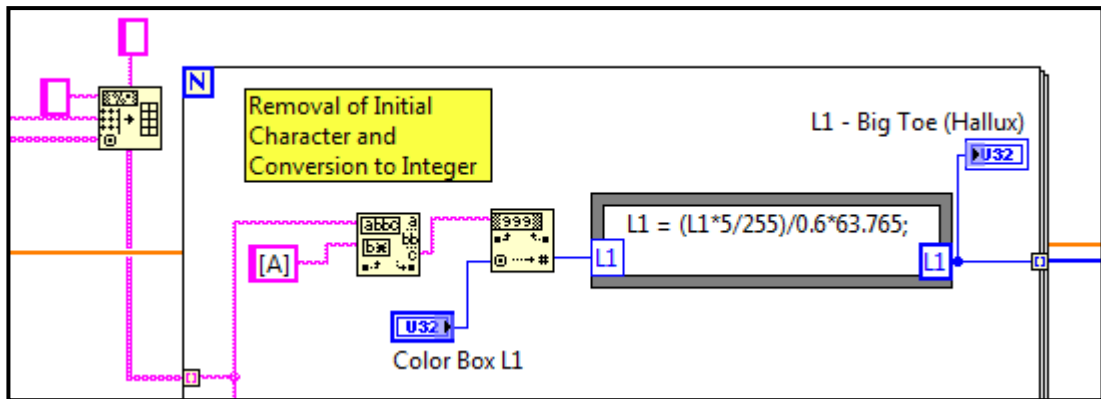


Figure 3.88: Removal of initial character, conversion to integer, and formula block diagram version one and version three

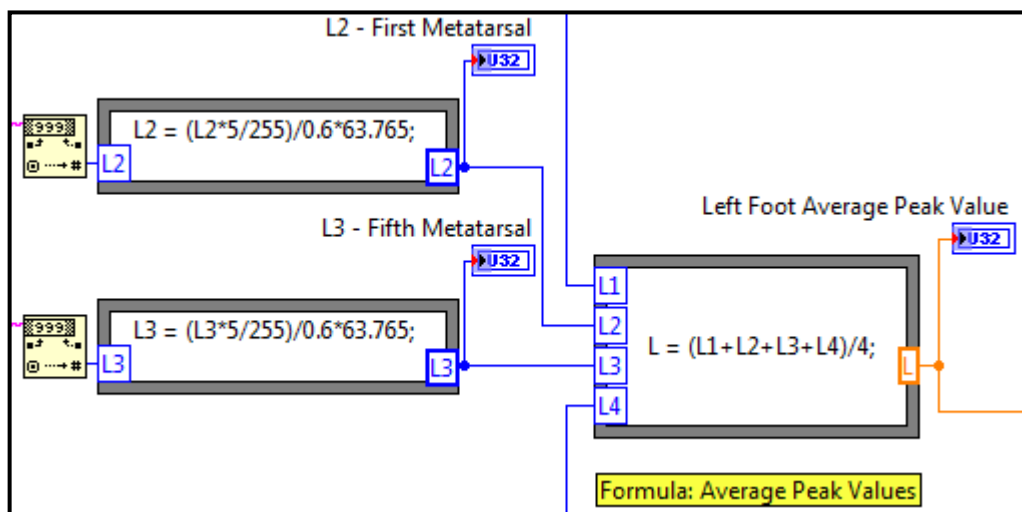


Figure 3.89: Removal of initial character, conversion to integer, and formula block diagram version two

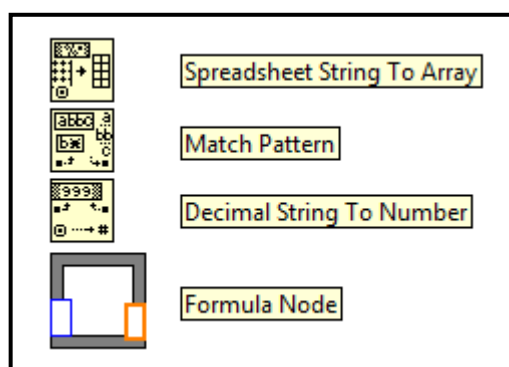


Figure 3.90: Removal of initial character, conversion to integer, and formula block diagram labelling for all versions

“Spreadsheet String To Array” is used to convert the spreadsheet string to an array of dimension and representation of array type. It works for arrays of strings or arrays of numbers. The purpose is to append the incoming string of data from the XBee module so that the system can execute all the functions with a given time before another string goes into the loop. Nowadays, the processing power of a computer can withhold the strings up to a large number, close to infinite.

For “Match Pattern”, this is functioned to search for regular expression in string beginning at offset, and if it finds a match, it will split the string into three substrings. A specific combination of characters is required by a regular expression for pattern matching. As shown in the PIC programming before, the initial character of the input is an alphabet. Thus, it is simple to match the pattern accurately. By matching the initial character, “after substring” is taken out (only the strings of numbers) and wired to integer conversion.

The “Decimal String To Number” is used to convert the numeric characters in string, starting at offset, to a decimal integer, and returns it in number. From here, integer can be obtained from string inputs and ready to be plotted in the graph. Another important function is the “Formula Node”, which evaluates mathematical formulas and expressions similar to C on the block diagram. In this node, the formula of conversion factor from output voltage into force is written. With this, all the incoming inputs are converted into the required parameter before displaying out the reading and plotting the graph.

There is some modification at this part for system version two where there is an extra formula node to sum up all the output forces from four sensors into one output to be displayed in a single graph for each side of foot. This is done by totalling up all the four inputs and divides them by four. Therefore, the output results that showed in the graph is the average peak force values by each side of the foot.

3.6.2.4 Result Display

For the result display part, there are a few functions used which include “Filter”, “Waveform Graph”, “Build Array”, “Build Waveform”, and “Merge Signals”. After getting the string readings from the microcontroller and being converted using formula, the results will be displayed through this part. Each side of five input signals will be merged together and displayed out with a waveform graph. So, there are total of two waveform graphs will be shown out at the front panel for left and right foot.

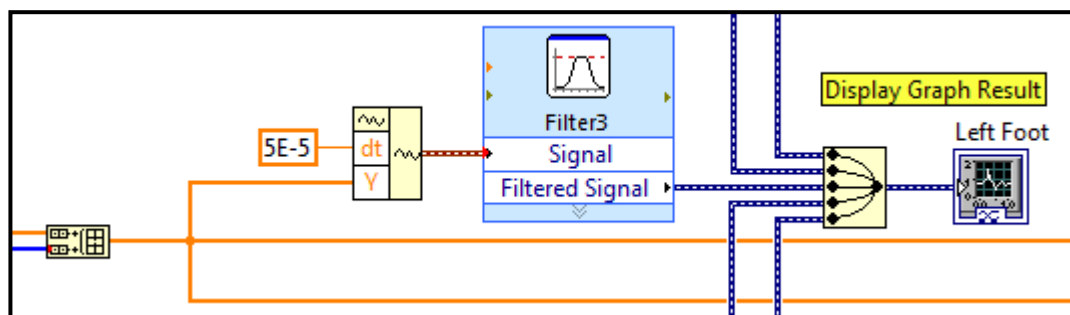


Figure 3.91: Result display block diagram version one and version two

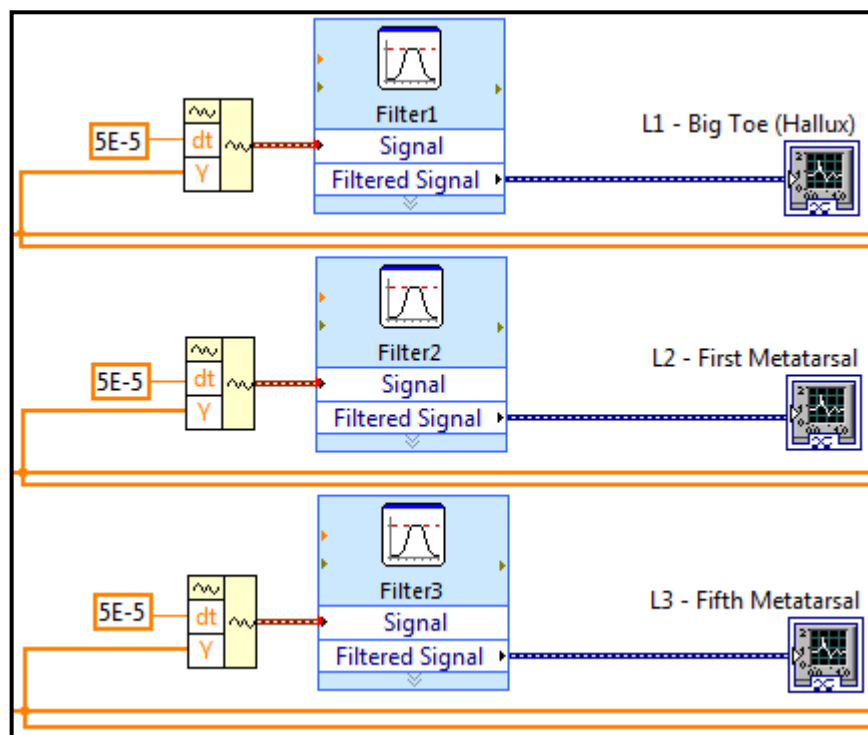


Figure 3.92: Result display block diagram version three

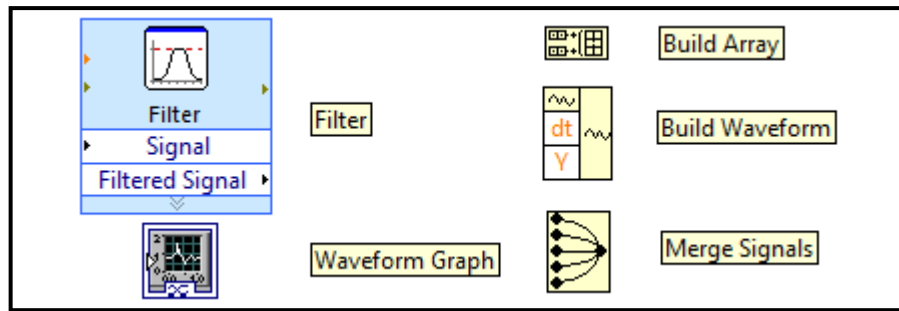


Figure 3.93: Result display block diagram labelling for all versions

“Filter” in LabVIEW functions to process signals through filters and windows. It is very powerful as it is capable of carrying normal filter topology, such as Butterworth, Chebyshev, Elliptic, and Bessel. Filtering can be done by choosing the type of filter functions, like lowpass, highpass, bandpass, bandstop, and even smoothing. For the filter specifications, the cutoff frequency (Hz), high cutoff frequency (Hz), and order of filter can be adjusted depending on the application. In this instrumented insole system, Butterworth filter with 1000 Hz cutoff frequency and 6 order of low pass filter characteristics is applied.

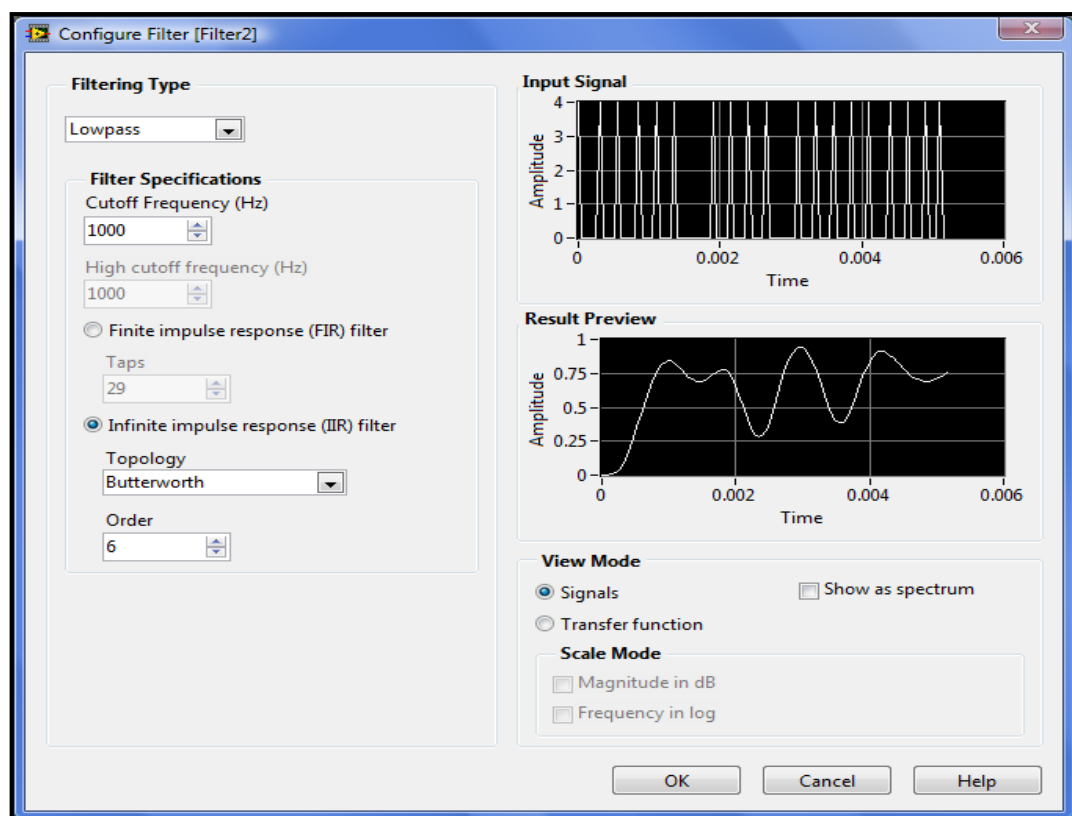


Figure 3.94: Configuration of filter for all versions

After the data is filtered, it will be displayed by using the “Waveform Graph” function. As mentioned before, five input signals from each side of foot will be gathered and displayed in a waveform graph. From there, results can be monitored continuously and checked for waveform patterns. Apart from that, “Build Array” is used to concatenate multiple arrays or append elements to n-dimensional array.

After the collected data passing through “Build Array”, it will come to “Build Waveform” which is functioned to build an analogue waveform or modifies an existing waveform based the components that connected. Before the results being displayed out, “Merge Signals” is used. This “Merge Signal” is functioned to merge all the input signals into a single output before connected to the “Waveform Graph”. It will help to resize the function to add inputs and appears on the block diagram automatically when a signal output is wired to the wire branch of another signal.

There is some modification at this part for system version three where there are total of eight different graphs will be displayed at the front panel. Unlike the system version one and two, those output graphs are not being merged into a single graph but choose to be displayed out in the corresponding graphs individually. Through this, the outputs that being generated can be observed and monitored clearly.

3.6.2.5 Storage of Data in Text File

Post-processing of data might be done sometimes by referring to the previous recorded results. This is why storage of data is needed in this system. There are a lot of data type can be stored, such as binary file, channel groups (TDMS), TDM, XML, datalog, and text file.

Well, text file data type is used for the data storage as it is easy, simple, and can be used in other analytical softwares, like Notepad, Microsoft Office, even LabVIEW itself. In this part, “File Dialog” is used to display a dialog box which can specify the path to a file or directory. By using this, user is allowed to select existing files or directories or to select a location and name for a new file or directory.

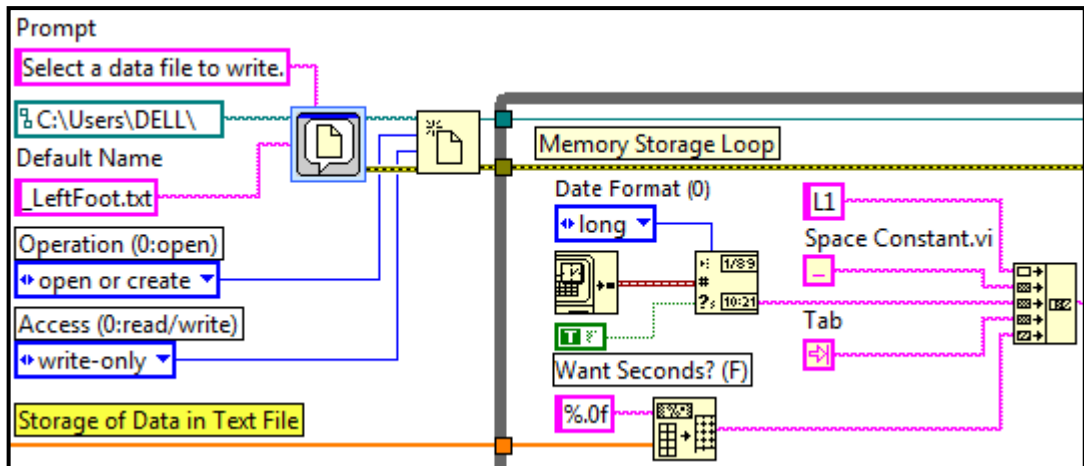


Figure 3.95: Storage of data in text file block diagram A for all versions

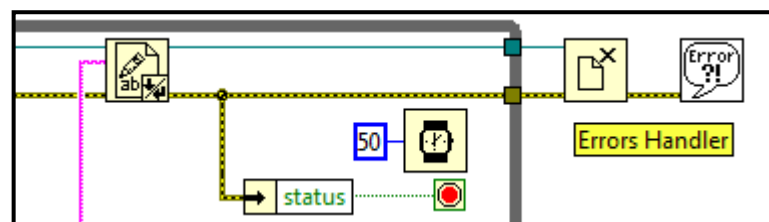


Figure 3.96: Storage of data in text file block diagram B for all versions

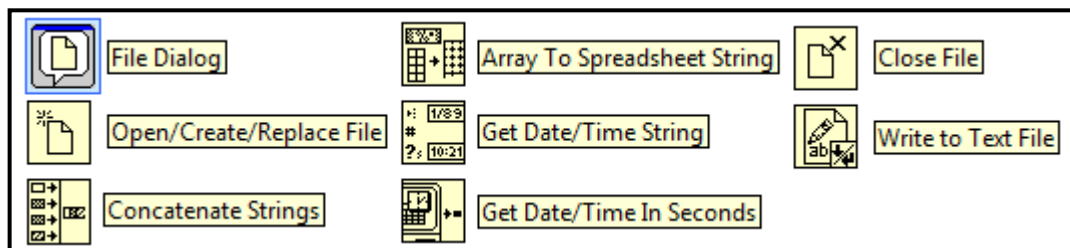


Figure 3.97: Storage of data in text file block diagram labelling for all versions

To open an existing file, create a new file or replace an existing file, “Open/Create/Replace File” is used programmatically or interactively. Next, “Write to Text File” will function to write a string of characters or an array of strings as lines to a file in a text file format. After that, “Close File” will close an open file specified by refnum and return the path to the file associated with the refnum. Error I/O can operate uniquely in this function, which close regardless of whether an error occurred in a preceding operation. This is to ensure that files are closed correctly.

Next, “Array To Spreadsheet String” is functioned to convert an array of any dimension to a table in string form, which containing tabs separating column elements, a platform-dependent EOL character separating rows, and, for arrays of three or more dimensions, headers separating pages. Through this, output from the “Build Array” is being converted back into string values in order to write in text file.

The “Get Date/Time String” and “Get Date/Time In Seconds” are used to convert a timestamp value or a numeric value to a date and time string in the time zone configured for the computer. The “Concatenate Strings” is used to concatenate input strings and 1D array of strings into a single output string. For array inputs, each element of the array is concatenated by this function.

3.6.2.6 Errors Handler

Error handle is an important part in this graphical programming to ensure that the system can be run in a stable and steady condition without any error occurred. This might be done by connecting each component with an error handle. In this system, two kind of error handler are used in sub-VI formats that are “Merge Errors.vi” and “Simple Error Handler.vi”.

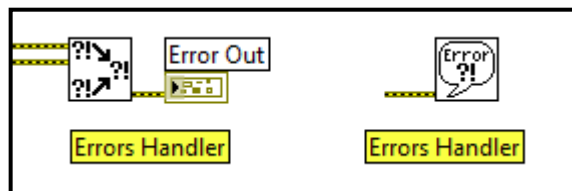


Figure 3.98: Errors handle block diagram for all versions

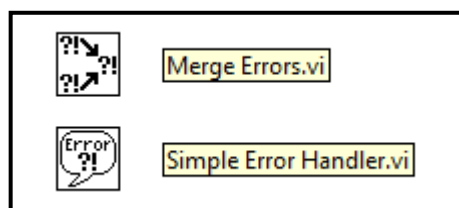


Figure 3.99: Errors handle block diagram labelling for all versions

For “Merge Errors”, this VI first look for errors among error in 1, error in 2, and error in 3. Then, the error array in and reports the first error found. If the VI finds no errors, it looks for warnings and returns the first warning found. But if the VI finds no warnings also, it returns no error.

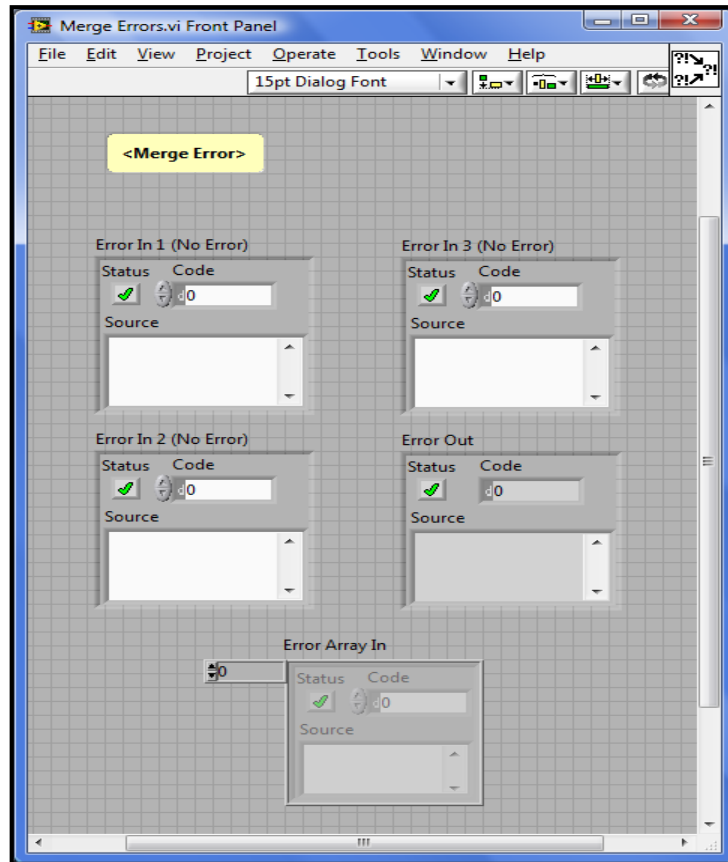


Figure 3.100: Merge errors front panel interface for all versions

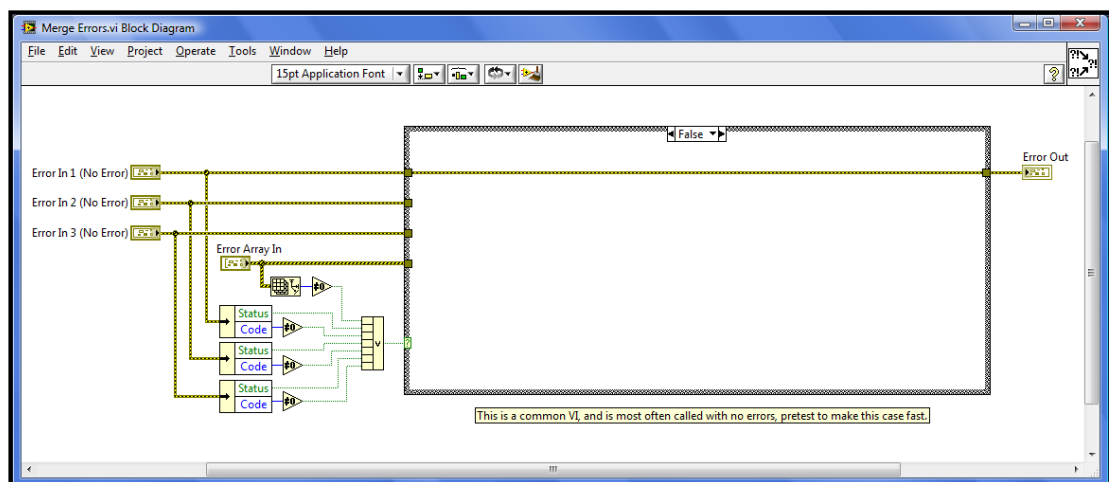


Figure 3.101: Merge errors block diagram interface for all versions

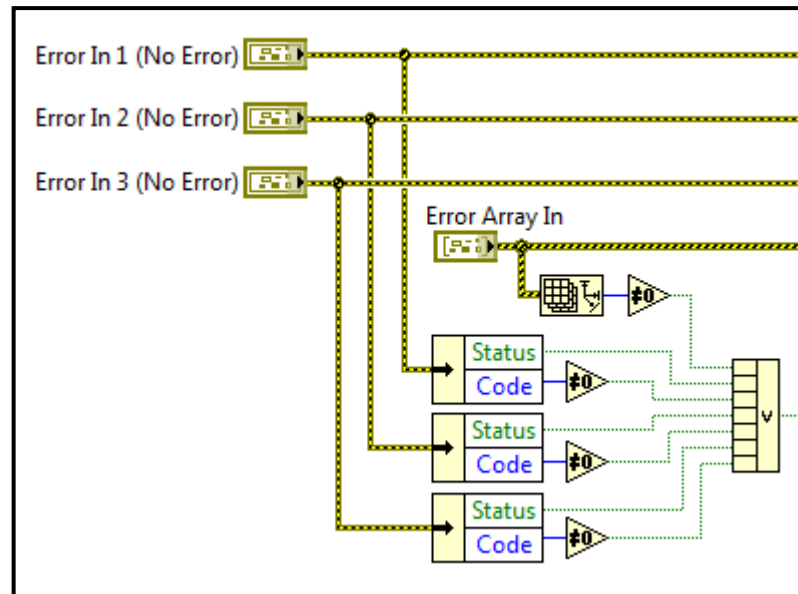


Figure 3.102: Merge errors block diagram A for all versions

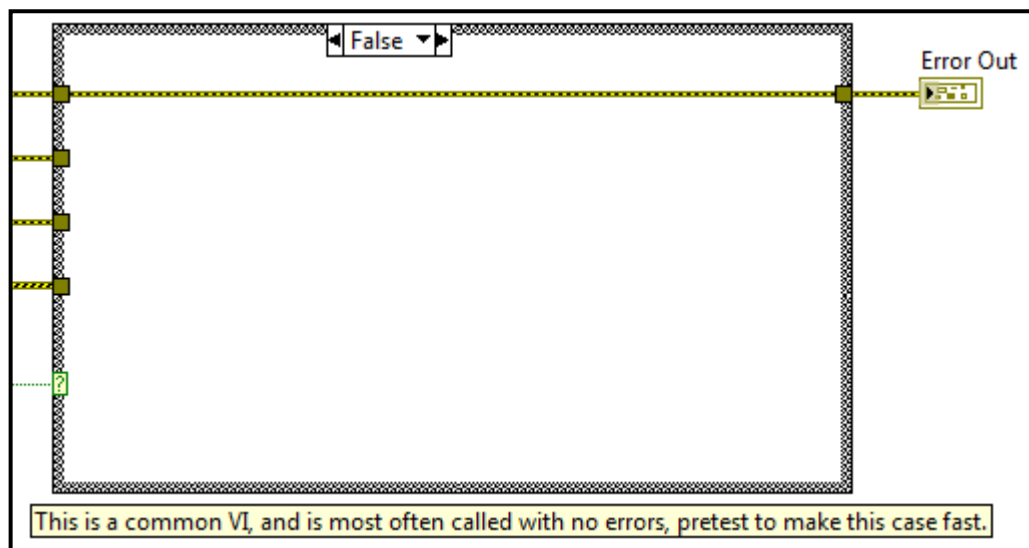


Figure 3.103: Merge errors block diagram B for all versions

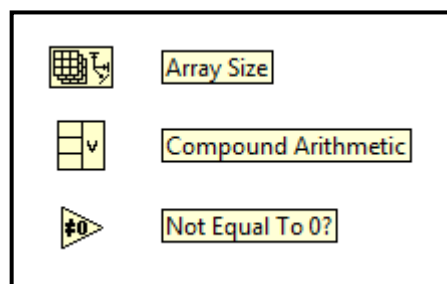


Figure 3.104: Merge errors block diagram labelling for all versions

“Array Size” is used in this sub-VI to return the number of elements in each dimension of array. Then, this function is connected to “Not Equal To 0?” Boolean expression. This expression functioned to return TRUE if the incoming data is not equal to zero. Otherwise, this function returns FALSE. For “Compound Arithmetic”, it is used to perform arithmetic on one or more numeric, array, cluster, or Boolean inputs.

Another sub-VI used in this error handler is “Simple Error Handler”. This VI helps in indicating whether an error occurred. If an error occurred, this VI will return a description of the error and optionally displays a dialog box. This VI will call the “General Error Handler” and has the same basic functionality as “General Error Handler” but with fewer options.

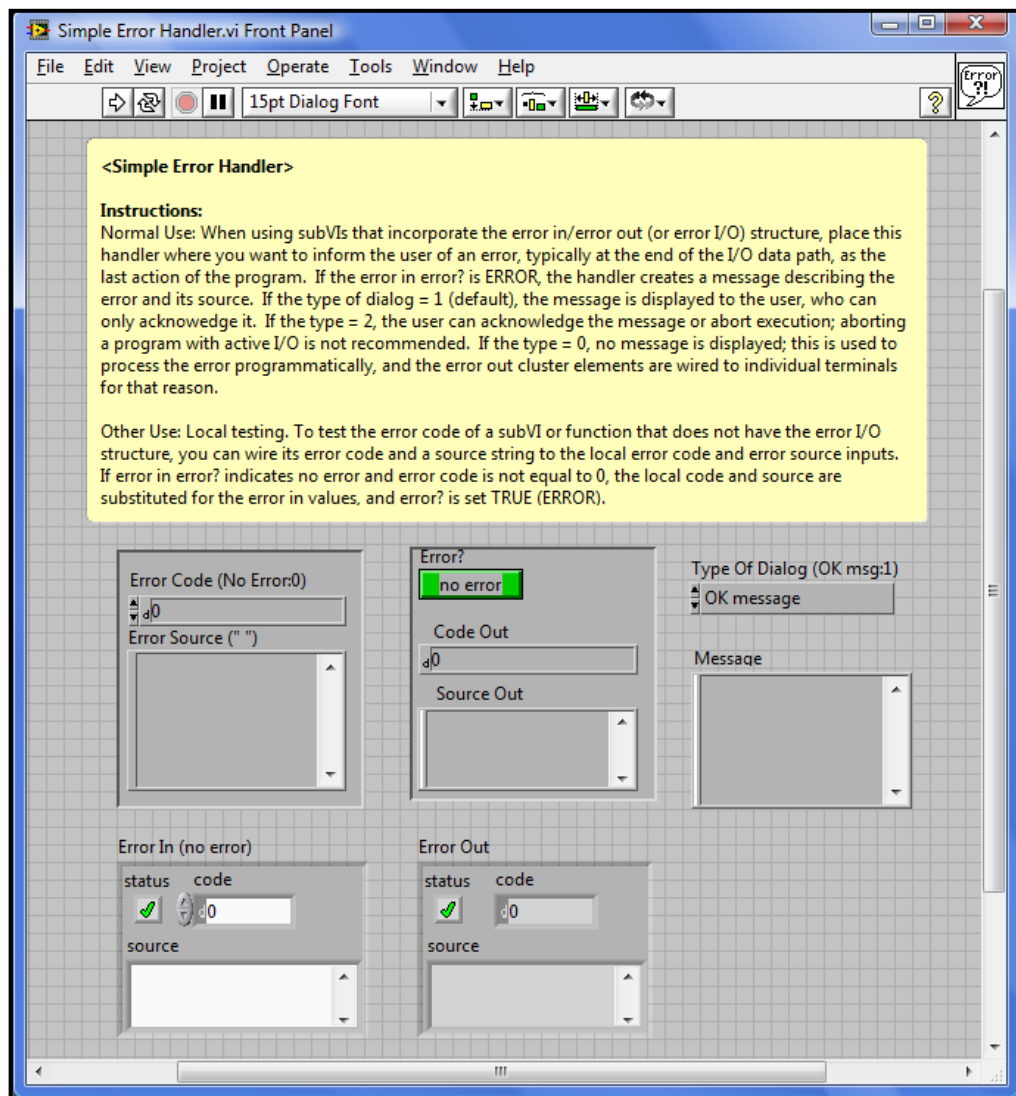


Figure 3.105: Simple error handle front panel interface for all versions

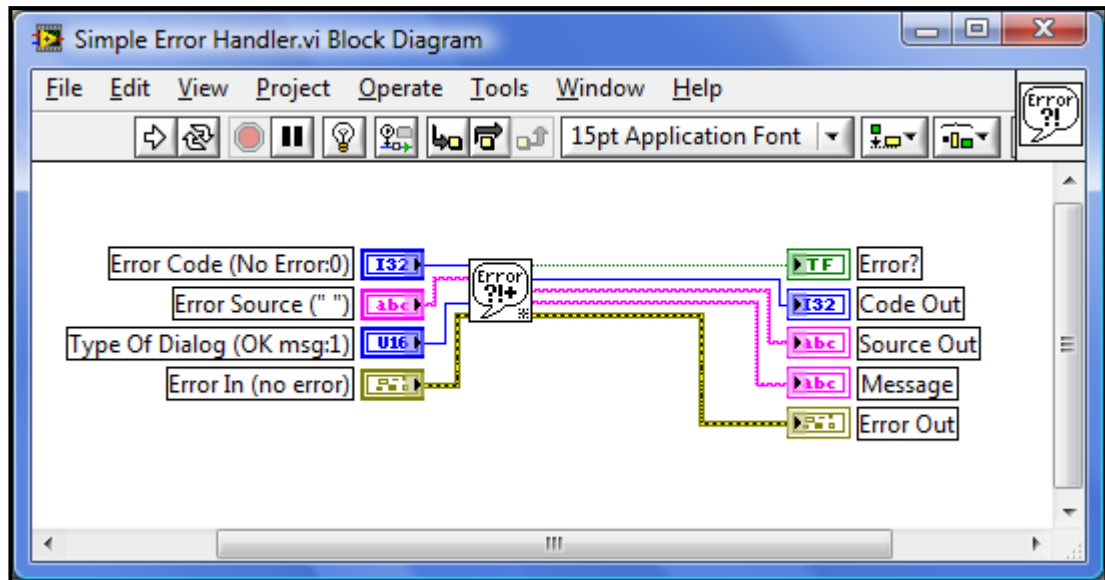


Figure 3.106: Simple error handle block diagram interface for all versions

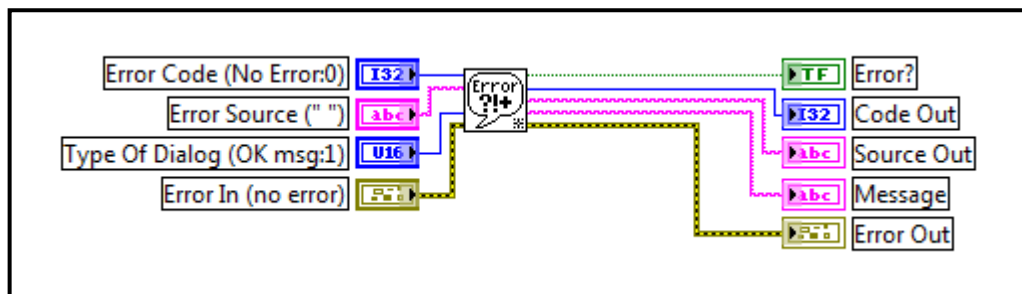


Figure 3.107: Simple error handle block diagram for all versions

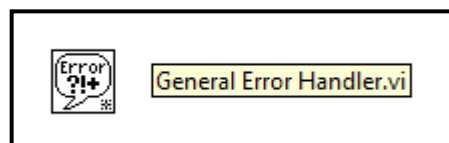


Figure 3.108: Simple error handle block diagram labelling for all versions

3.6.2.7 Process Flow

The overall process flow of PIC microcontroller programming design is shown as followed:

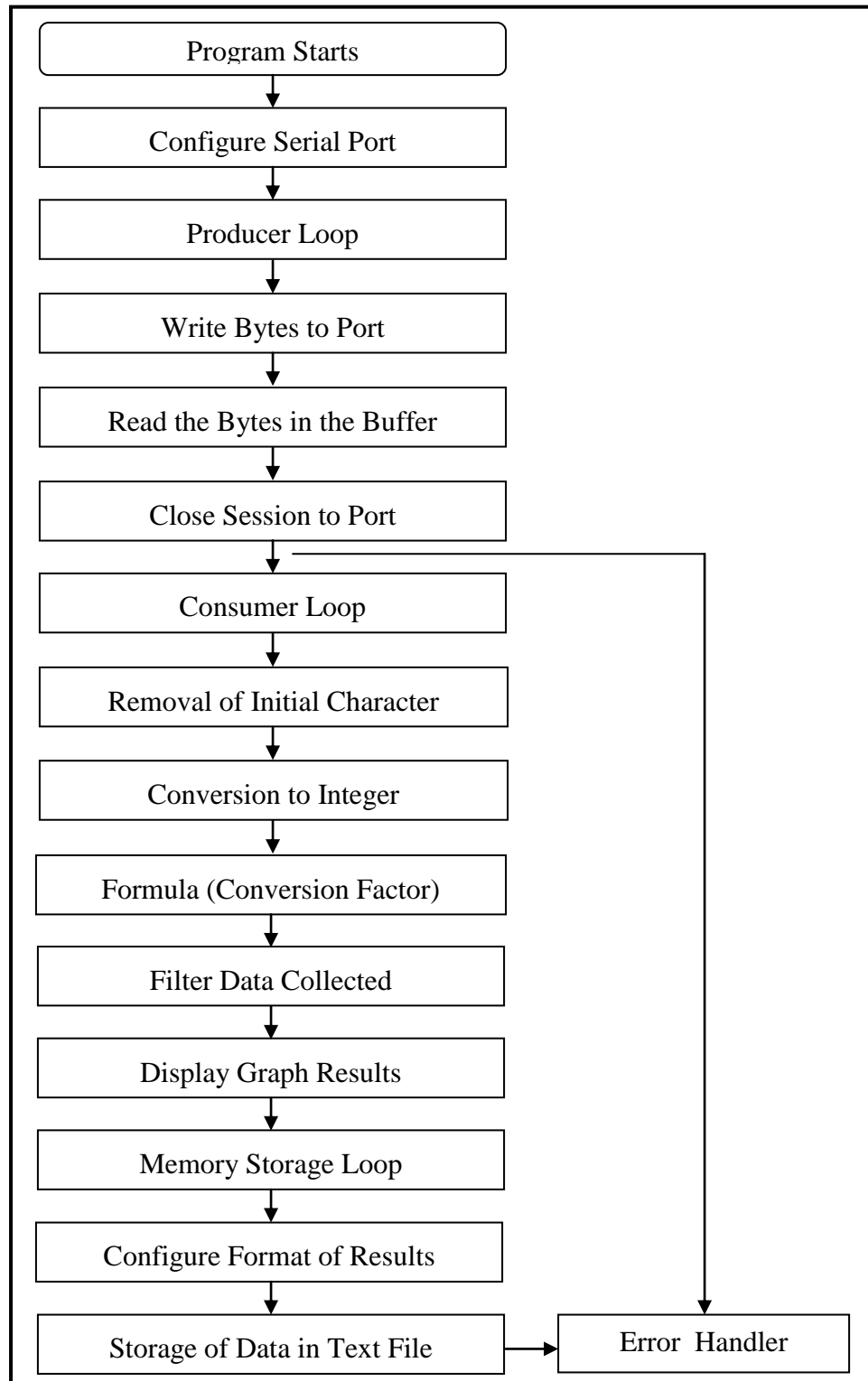


Figure 3.109: Process flow of LabVIEW graphical programming design

3.7 Gait Simulation and Subject Testing

In this testing section, it is divided into two parts, which are the gait simulation and subject testing. The first part refers to the gait simulations based on gait cycle (stance and swing phase) of each human locomotion activities. It is a simple gait simulation for collecting the gait characteristic results from the system which might serves as a reference to match or compare the results from the subject testing.

The second part in this section explains the subject testing specially conducted for this system. This subject testing is conducted to test the functionality, usability, reliability, and durability of the instrumented insole system. The design, including the recruitment, consent forms, and testing protocol will be discussed one by one at the following sub-section in a more clear and detail way.

3.7.1 Gait Simulation

A few simulations are chosen to be discussed in this project which involved in common human locomotion activities; they are standing, sitting, walking, and running. Besides, some testing has been carried out before the gait simulation; they are initial testing, static device with no inputs, and static device with static forces inputs. All the results will be showed and explained at the next chapter.

Those initial testing serves as a preparation for the gait simulations in order to test for the functionality of sensors. These testing are important for the sensors to get ready and stabilize before the gait simulations so that a more accurate and stable result can be obtained during the gait simulations.

For standing simulation, a subject is requested to stand still while information is collected from the FSR sensors. The subject is asked to look straight ahead, stand as still as possible with two hands lowered down on the sides and the knees should not bend (parallel to X-Axis).

In sitting simulation, the subject is requested to look straight ahead, sit 90° vertical position on a chair with two hands lowered down on the sides, the legs facing down, and slight contact with the floor. In this simulation, the subject is asked to maintain the same position along the period of simulation.

For walking simulation, subject is requested to look straight ahead, move forward in as straight a line as possible, and walking at a normal pace on a treadmill system with constant speed. The speed of walking must be moderate and not too fast. In this simulation, the steps taken within the period of simulation will be counted in a range of distances.

In running simulation, the subject is requested to look straight ahead, move forward without leaning any sides, and run faster than normal pace on a treadmill system with a constant speed. The speed of running must be faster than normal walking speed. Same as walking simulation, the steps taken within the period of simulation will be counted in a range of distances.

3.7.1.1 Gait Simulation Parameters

To carry out gait simulation, the subject needs to wear the system and ensure that the device and FSR sensors do not fall out of place. Simulation is carried out based on the ways and patterns of a human locomotion activity (gait cycle). Table below explained the type of simulation and parameters that will be used as a guideline in monitoring and analyzing the locomotion activities of the subject.

Table 3.5: Type of simulation and parameters based on human locomotion activity (Gait cycle)

Type of simulation	Description
Stance Phase	A period when the foot is with its entire length in contact with the ground.
Initial Contact (IC)	A period when the right heel hits the ground at the beginning of the contact phase.
Loading Response (LR)	A period of initial double-limb support and the foot is in the full contact with the surface.
Mid-Stance (MSt)	A period begins when the contralateral foot leaves the ground and ends when the right heel rises.
Terminal Stance (TSt)	A period begins with the heel rise and ends when the contralateral foot contacts the ground.
Preswing (PSw)	A period begins when the contralateral foot contacts the ground and ends with ipsilateral toe off.
Swing Phase	A period when the foot is in the air (not in contact with the ground) and swings forward.
Initial Swing (ISw)	A period begins the moment the right foot leaves the ground and continues until maximum knee flexion occurs.
Mid-Swing (MSw)	A period of maximum knee flexion and ends when the tibia is in vertical position.
Terminal Swing (TSw)	A period where the swing cycle ends and the right foot ready to contact with ground.
Others	
Walking speed	The rate of motion of walking. Natural or free speed refers to the subject's comfortable walking speed.
Cadence	The step rate of a subject.
Max Applied Force	The maximum force applied on the sensors in every single step.
Step Time	The time duration from the initial heel contact of one foot to the next initial heel contact of the opposing foot.
Stride Time	The time duration from the initial heel contact of one foot to the next initial heel contact of the same foot.
Step Length	The distance between the point of initial contact of one foot and the point of initial contact of the opposite foot.
Stride Length	The distance between successive points of initial contact of the same foot.

Source: Yang, Chou, Hu, Hung, Wu, et al, 2009.

3.7.1.2 Gait Simulation Formulas

Besides, the formulas used in the data analysing will be listed out and explained one by one for more understanding on how the data to be collected and analyzed. There are few main formulas are used in the data analysis and calculation for the results obtained from the subject testing.

Several spatial-temporal parameters and formulas are selected typically investigated in gait studies. As the system developed in this project does not allow the measurement more than two dimensional, the parameters and formula related to angle are not measured. Besides, camera is not equipped in this simulation, kinematic parameters and formulas like the joint angles of different parts are not measured too.

First of all, formula of velocity is used to obtain the walking speed of the subject during the gait simulations. This is done by recording the time with stopwatch and the distances travelled are being measured. The formula is formed by dividing the distance measured in meter unit with the time recorded in second unit which showed as followed.

$$v = \frac{s}{t} [m/s] \quad (3.1)$$

where

v = velocity, m/s

s = distance, m

t = time, s

The step length can be obtained by dividing the distances travelled in meter unit with number of steps taken by the subject along the simulation. As one stride length is equal to two steps length, the formula used to calculate the stride length can be formed by dividing the distances travelled in meter unit with two times of number of steps taken along the simulation.

$$\text{Step Length} = \frac{d}{n} [m] \quad (3.2)$$

$$\text{Stride Length} = \frac{d}{2n} [m] \quad (3.3)$$

where

d = distances, m

n = number of steps

After the step length and stride length can be calculated through the formulas above, the step time and stride time in second unit can be formed by replacing the distances travelled with the period of time of the simulation in the previous formulas. The formulas can be showed as followed.

$$\text{Step Time} = \frac{t}{n} [s] \quad (3.4)$$

$$\text{Stride Time} = \frac{t}{2n} [s] \quad (3.5)$$

where

t = time, s

n = number of steps

Next, the number of steps taken during the gait simulation is being counted for the purpose of calculate the cadence of subject at their natural walking speed and running speed. The cadence can be calculated by dividing the number of steps from the gait simulation with the time recorded in second unit. The formula of cadence can be simplified as followed.

$$\text{Cadence} = \frac{n}{t} [step/min] \quad (3.6)$$

where

n = number of steps

t = time, min

The third formula used in the results calculation is force weight ratio. This is a parameter which added to analyse the relations between the force and the weight of subject. The equation is formed by dividing the forces obtained from the gait simulation with subject's weight as followed.

$$\text{Force Weight Ratio} = \frac{\text{Force}}{\text{Weight}} [N/kg] \quad (3.7)$$

where

Force = Maximum applied force, N

Weight = Weight of subject, kg

Unlike force plate, instrumented insole system used in this project cannot obtain other extra parameters directly from the software. Through all the formulas discussed here, the extra data and results collected from the gait simulation can be obtained. The parameters like the average step length, average step time, average stride length, average stride time can be calculated by referring to the data recorded from the gait simulation and showed as part of the additional results of data analysis.

3.7.1.3 Process Flow

The overall process flow of gait simulation design is shown as followed:

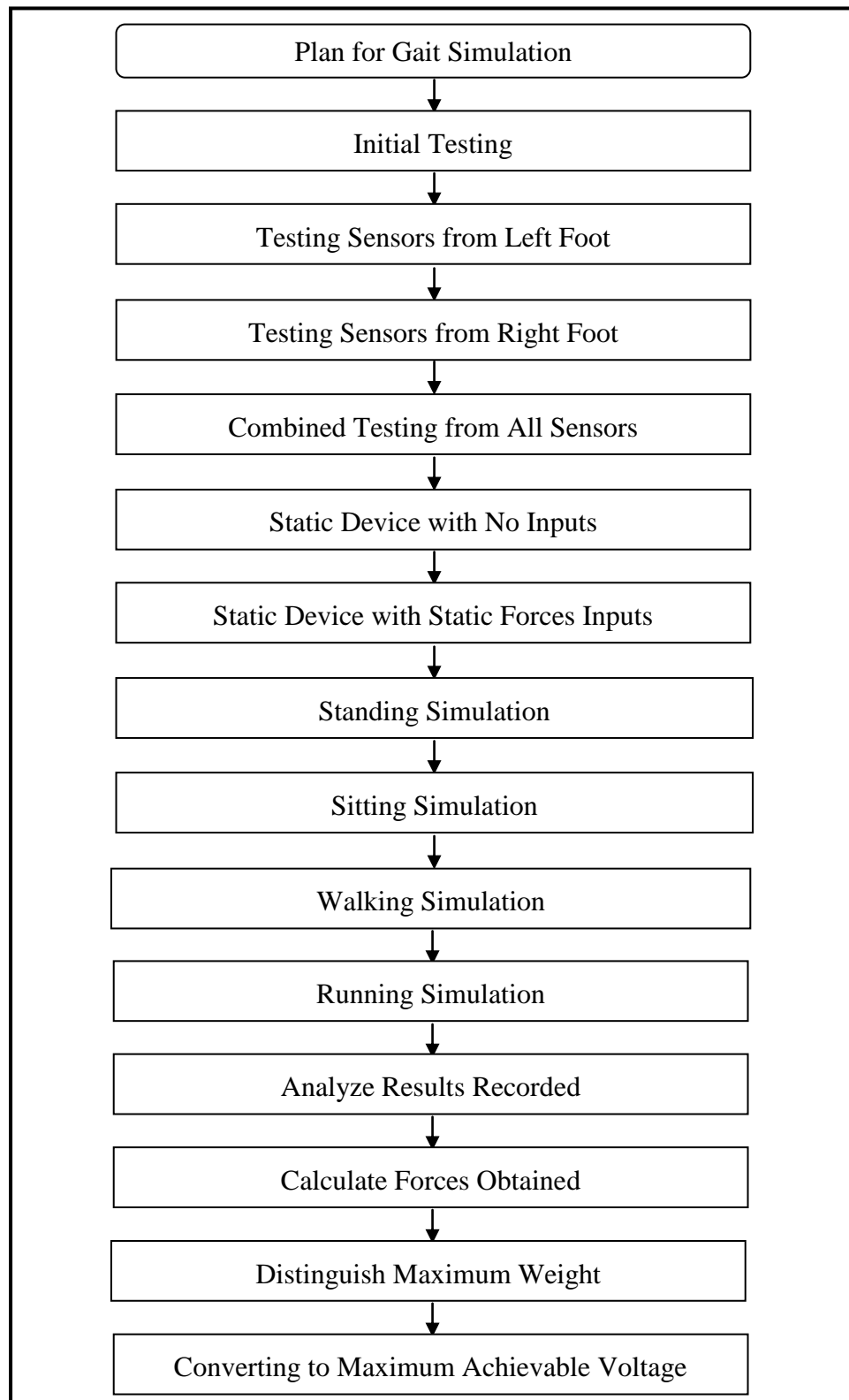


Figure 3.110: Process flow of gait simulation design

3.7.2 Subject Testing

A subject testing is being designed for this project to test the instrumented insole system. The overall procedures on how this subject testing to be designed, including the subject recruitment, and the testing protocol will be discussed thoroughly in the following sub-sections.

3.7.2.1 Subject Testing Design

The subject testing design is discussed about how the subject testing will be conducted, the flow of the subject testing, and the procedures in carrying each locomotion tasks. This subject testing involved in placing the instrumented insole inside the subject's shoe and the circuit board will be attached to the subject's waist by using an adjustable belt.

While the subject testing is being conducted, the sensors will detect the forces distribution beneath the foot. After that, the output signals from the sensors will be collected by microcontroller. The small antenna of XBee module on the circuit board will then transmit the output signals to the receiving transmitter at computer. All signals are digitized and saved on a laptop computer set within 10 feet of the instrumented insole system during subject testing.

Each subject is asked to perform a series of locomotion tasks, while the instrumented insole system simultaneously collects the generated data. The results collected from the system is being analyzed and compared to validate the analysis of gait parameters from the data acquired by the instrumented insole. The information gathered did not offer any direct benefits to the subjects tested. After the subjects complete the testing protocol, gait characteristics are compared to those reported in previously published studies.

3.7.2.2 Subject Recruitment

The recruitment is planned to be carried out after the design is being constructed successfully and tested well in gait simulation. The subjects with healthy gait are recruited via email and word of mouth. However, most of the recruitment is done via email where the course representatives of each courses are being informed about this subject testing.

The message is passed around and the consent form is distributed to every subject. When the subjects replied with the interest in the subject testing, they are provided with more details about the testing. After filling the consent form, an appointment is set up at the Biomechanics Lab according to each group with a corresponding date and time respectively.

At first, a brief introduction is given about the definition of gait analysis, the motivation of this project, the basic function of an instrumented insole system, and the purpose of the subject testing. In addition, the process flow of how the subject testing will be conducted and the locomotion tasks to be completed are being explained in order to provide a clear picture of this testing to the subjects.

Furthermore, a terminology is attached together with the consent forms. A simple diagram of gait cycle is provided together with some terms and explanations to describe how the gait cycle is formed during human locomotion activity, such as gait, heel strike, stance, step, stride, and so on. If subject has any questions about the subject testing or interest to know more about this project, contact number and e-mail address can be found in the consent form.

All subjects recruited are adults who could understand and follow basic directions throughout the subject testing. Subjects are excluded if they reported acute pain which prevented performance of their comfortable and typical movement. Similarly, subjects are excluded if they have an unstable medical condition, such as history of lower extremity symptoms, musculoskeletal or neurological disorders related to lower extremity obvious pathology.

3.7.2.3 Consent Form

A consent form is prepared for this subject testing. Basic personal information is required in this consent form, like name, gender, age, date of birth, address, and course. Contact number and email address are required in order to keep in touch with those subjects for the confirmation and preparation for subject testing from time to time. Every single latest news or actions regarding the subject testing will be informed through these ways.

Every subject is compulsory to attach a digital photo in the consent form. Apart from that, personal physical conditions, such as height and weight are asked as well inside the consent form. Furthermore, subjects are required to fill in the details about the size of shoe and brand of shoe which they are using. This information is needed in dividing those subjects into different group according to their size of shoes so that the subject testing can be carried out smoothly.

Next, history of falls in past year and past month are asked to know how frequent the subjects facing such problem in their current live to ensure that a healthy walking pattern is resulted from the gait simulation. Lastly, there is a space for the information regarding subjects' other medical records related to lower extremities. This is up most important as subjects with lower extremities problems or diseases are not recommended to participate in this subject testing. The format of the consent form is shown at Appendix D.

3.7.2.4 Subject Testing Protocol

After the subject recruitment, those subjects will be grouped into different small group where each group consists of certain amount of subjects. This grouping process is done by referring to the size of subjects' shoes where subjects with same size of shoes will be grouped together. Subject testing will be conducted group by group with date and time respectively.

A schedule of the subject testing is formed by listing out the date, time, and groups divided for subjects to check and attend the testing on time. Most of the date and time are chosen depends on the flexibility of subjects because priority is given to subjects in deciding the date and time that they are available for the testing.

A subject testing protocol is prepared for the subject testing as showed in Appendix E. Before the subject testing, the subjects are being informed about the preparations for the testing, like subjects are recommended to wear comfortable t-shirt, long pants, and sport shoe for the testing where other extra accessories, decorations, and slippers or scandals are not allowed.

Besides, subjects are advised to be punctual and they need to report themselves about 15 minutes earlier than their testing time. A short briefing will be given to all the subjects regarding the correct way to wear the instrumented insole system. Moreover, questioning section will be held to clear all doubts from subjects about the testing.

An agreement will be signed by the subject. This agreement is to ensure that the subjects understand the purpose and procedures of this testing; they are aware of the possible risks, discomfort, and potential benefits that they might experience throughout the subject testing. In other words, the signature indicates the willingness of subjects to participate in this testing.

During the subject testing, a photo of eight-segment representation is taken from the right side of the subjects. Next, body segment lengths and circumferences (anthropometric dimensions) will be measured. Next, a short period will be given to the subjects to accommodate the system at the natural pace prior to test the system besides letting them familiar with the system before any tasks are started.

After that, there are four locomotion tasks to be carried out, that are standing, sitting, walking, and running. Each locomotion task will be conducted for a certain period of time. Subjects are not given specific instruction to complete the tasks to avoid alterations in natural walking pattern during the testing. At last, subjects are asked to give comments about the system and the testing.

3.7.2.5 Process Flow

The overall process flow of subject testing design is shown as followed:

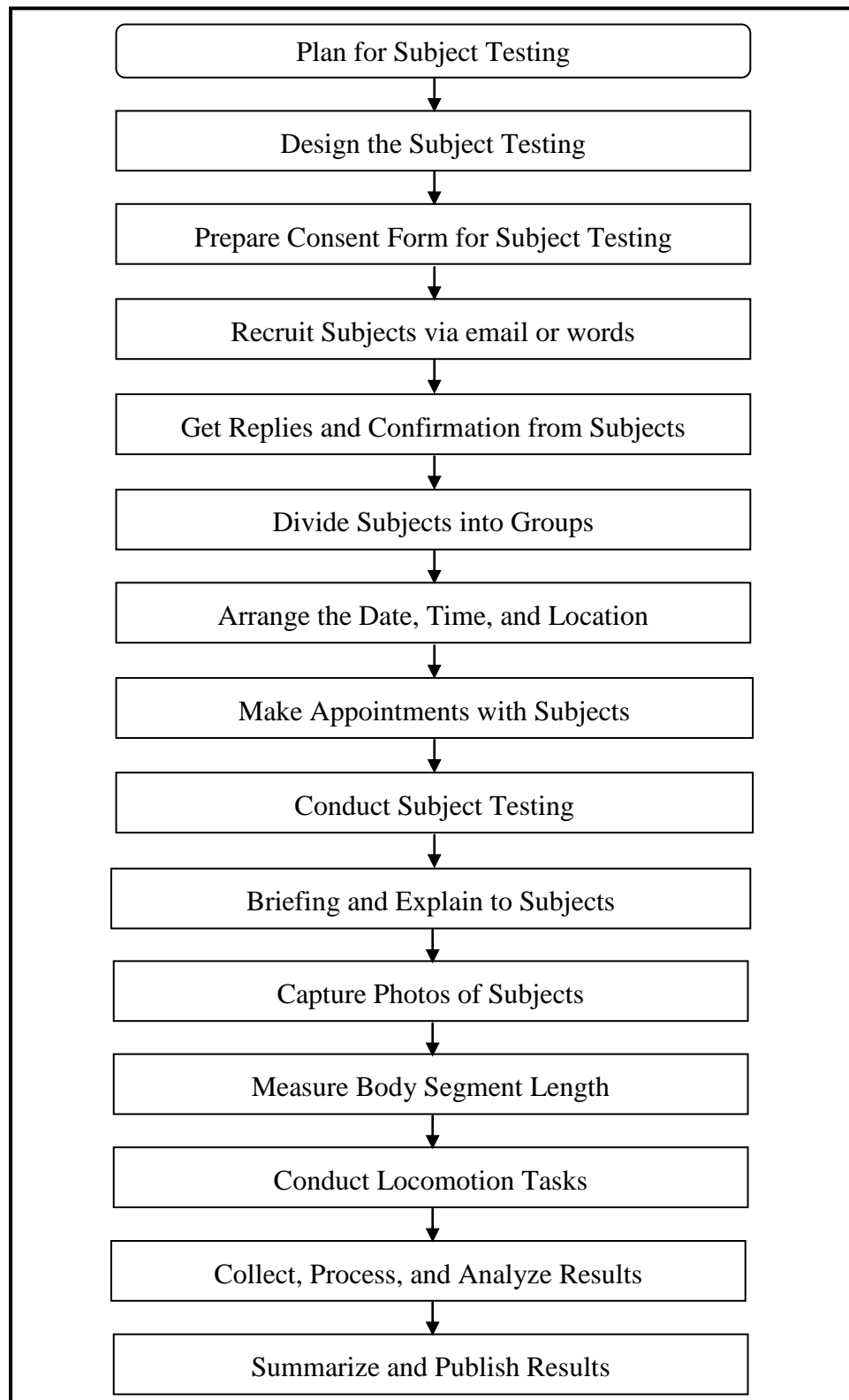


Figure 3.111: Process flow of subject testing design

CHAPTER 4

RESULTS AND DISCUSSIONS

4.1 Result Interface and Format

Before explaining the simulation and results obtained, there is a need to explain the interface and the format of the results shown in LabVIEW. In this project, there are eight FSR sensors used for human locomotion analysis. Four sensors are placed equally beneath each foot where they located around the region of bid toe (hallux), first metatarsal, fifth metatarsal, and heel.

As mentioned before, forces being generated during human locomotion activities are the main parameter to be concerned in this project. Therefore, each sensor has only one axis to be displayed that is force in Newton unit. Conversion will be done from output voltage into force and display in the form of graphs. In the graph, X-Axis represents the time taken (duration) in second for the human locomotion activities, while the Y-Axis represents the forces generated from the sensors.

As mentioned before, there are three different formats of LabVIEW systems being developed. The four sensors will be gathered together and display in a graph for each side of foot to reduce the complexity of result displaying in the first version system. The first column of graph result shows the FSR sensors outputs from left foot, and the second column of graph results shows the FSR sensors outputs from right foot. The graph position with readings for each foot in LabVIEW is shown in the next page.

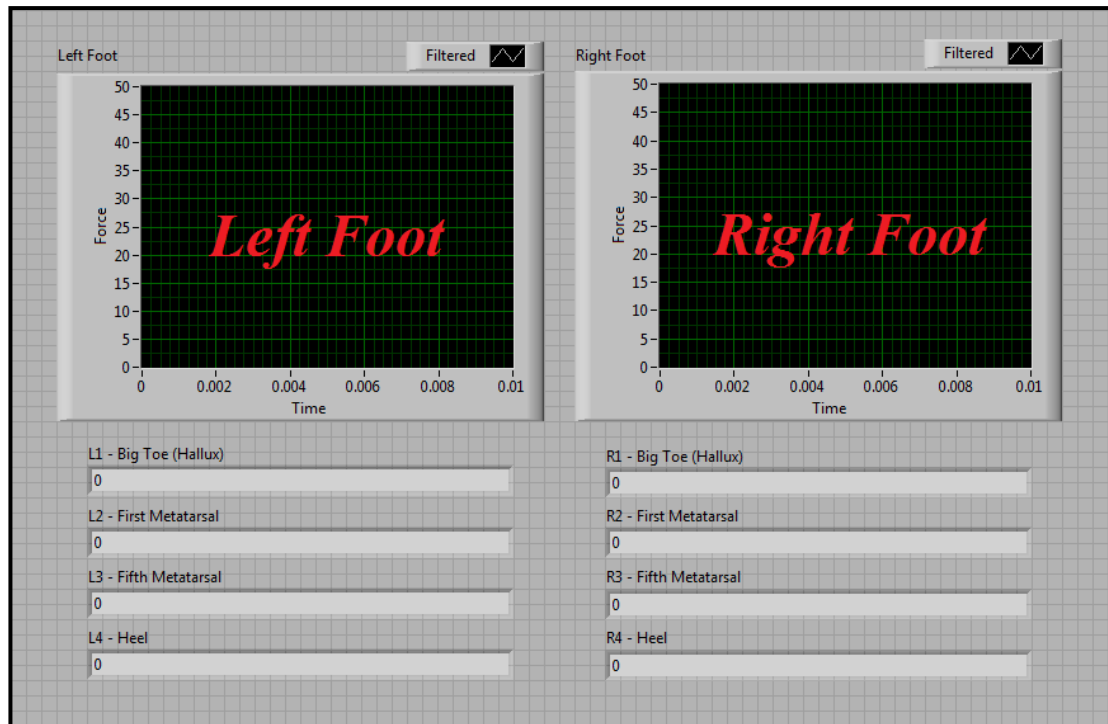


Figure 4.1: Graph position with display for each foot in LabVIEW version one

Sensors	Colors	Sensors Position
L1 & R1	White	Big Toe (Hallux)
L2 & R2	Yellow	First Metatarsal
L3 & R3	Orange	Fifth Metatarsal
L4 & R4	Red	Heel

where L : FSR Sensors from Left Foot (L1 – L4)
 R : FSR Sensors from Right Foot (R1 – R4)

Figure 4.2: Display labelling for each foot in LabVIEW version one

There are four different colors used at the first version to represent different input values from those sensors. Sensors from both left and right foot are being represented by white for big toe (hallux), yellow for first metatarsal, orange for fifth metatarsal, and red for heel region. Therefore, there will be four different lines showing at each graph to which represent to different sensors from both side of foot.

Next, there are two graphs showed at LabVIEW version two where each of them represents the average peak force values from left and right foot. In this version, no colors will be used to represent the output forces as all the forces from each side have been total up and divide equally to get an average output to be displayed. This generates an overall view of the forces detected during locomotion activities from time to time. Compare to the other versions, the average peak force values will be showed out under each graph.

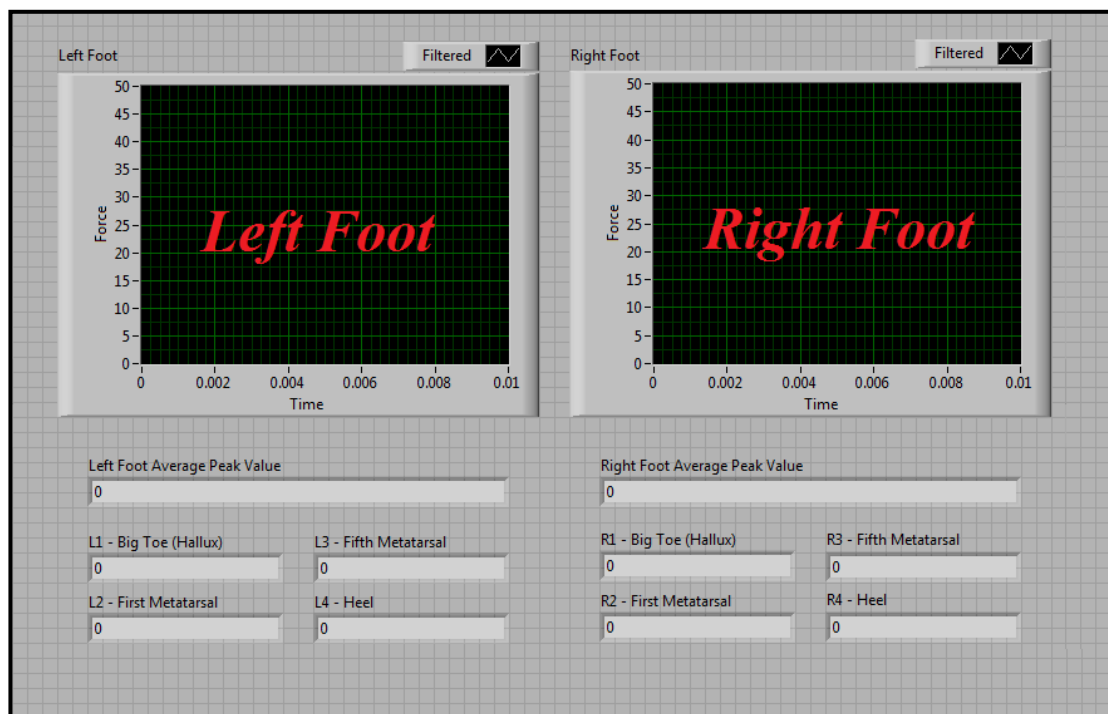


Figure 4.3: Graph position with display for each foot in LabVIEW version two

For the third version, more graphs will be used to display the output results from forces detection by sensors. Total of eight graphs will be showed at this version in order to represent each four sensors from each side of foot. Through this, each result from eight sensors can be viewed and monitored at the individual graphs without combining or merged with others outputs. This is useful and essential when the user is focused on the forces generated by each single sensor, such as checking the functionality of each sensor before starting any testing or measurement or to detect the abnormal forces generated beneath each part of foot.

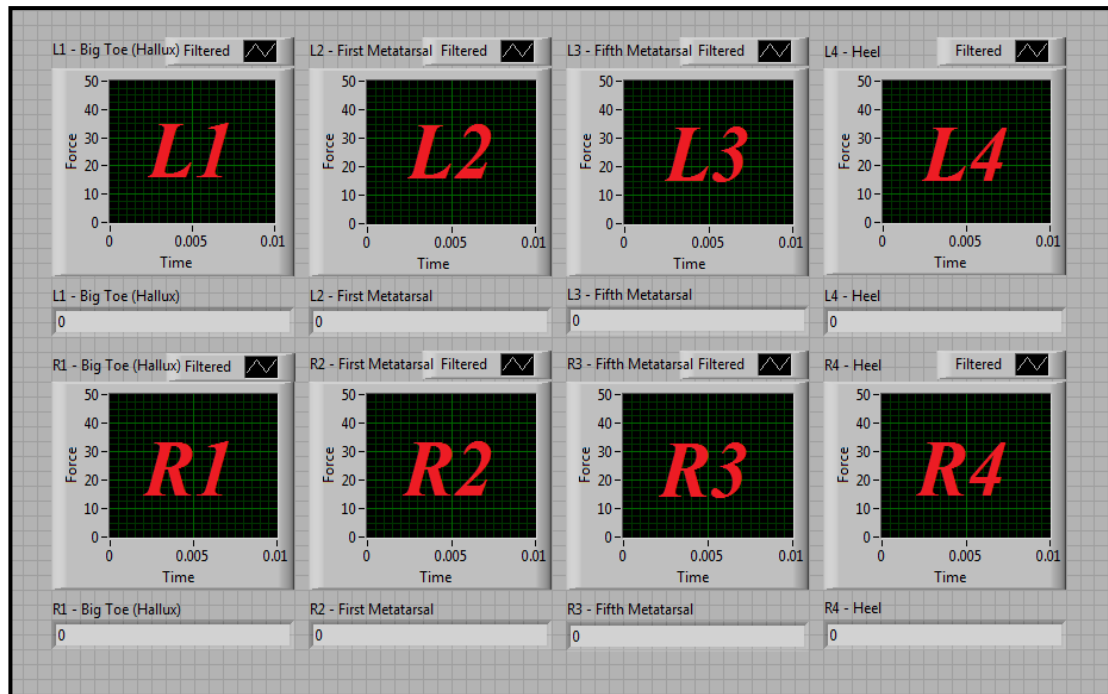


Figure 4.4: Graph position with display for each foot in LabVIEW version three

Each graph for all versions plots “Force” against “Time”, which is the main output parameter that being concerned in this project. In this case, “Force” means the digital signals converted from the analogue voltages from the output voltage of the FSR sensors. These digital signals are directly related to the changes in the analogue voltages when the FSR sensors detect the changes in force applied to surface during human locomotion activities.

However, the digital signals showed out in the graph are being formulated with the conversion factor of output voltage to force. Through this conversion factor, data monitoring and analysis can be done by looking at the peak amplitudes and by comparing the outputs with a consistent reading of normal human locomotion activities.

The scale for the unit “Time” in the graph is smaller than the original time. This is due the reason that some settings are made to plot the graph in LabVIEW. The scale has to be adjusted to suit the function of the component. In these graphs, each unit of 0.01 in scale represents 10 seconds in real time, which means by factor of 1000.

4.2 Analysis Tool

There is a need of some programs that can be used as analysis tool for the recorded data. Each analysis tool will be discussed on how they function to help in analysing data in following sub-section.

4.2.1 Adjustment Filter

Adjustment filter is essential in filtering the data generated from the FSR sensors. As not all of the data generated is smooth and presentable through LabVIEW, this tool is used so that the data can be filtered with correct order of particular type of filter before displaying out the data through LabVIEW. By using this filter, the suitable order of particular type of filter can be set with the purpose to display a better result for data monitoring and analyzing.

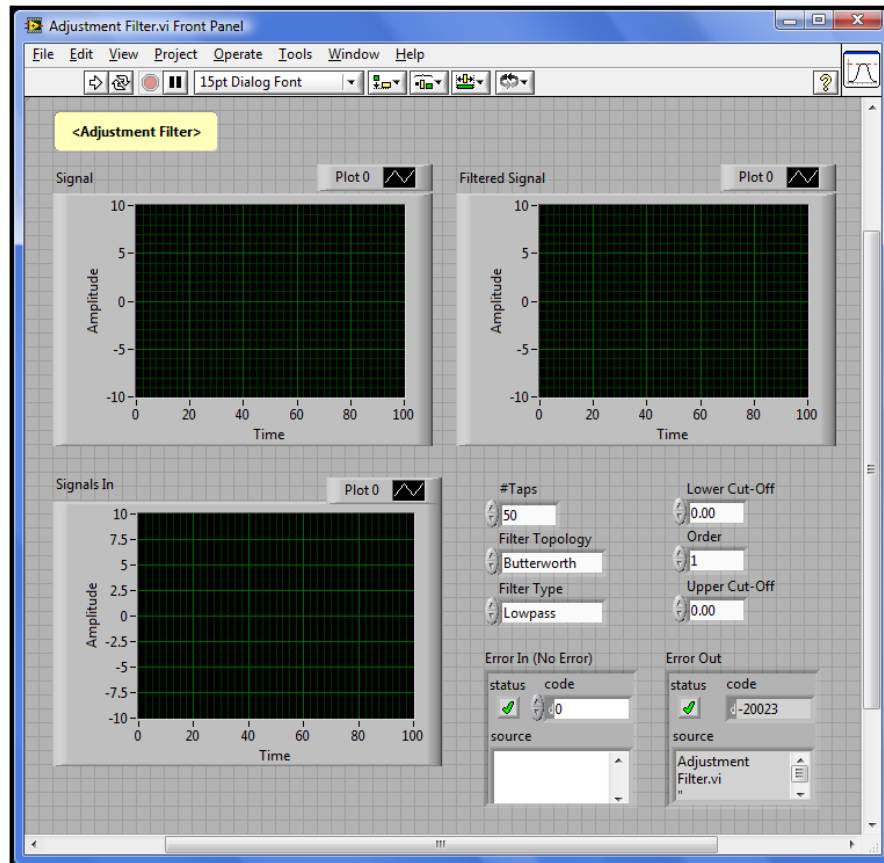


Figure 4.5: Filter adjustment front panel interface

From the front panel interface, there are three waveform graphs, which are “Signal”, “Signals In”, and “Filtered Signal”. The adjustment of the filter can be done in real-time by monitoring the changes and smoothing of the graphs. There are few options provided in the front panel to let user select the required parameters, such as filter topology, filter type, lower cut-off, upper cut-off, and order. Besides, there is “Error In” and “Error Out” provided for the alert function if there is any error occurred along the filtering process.

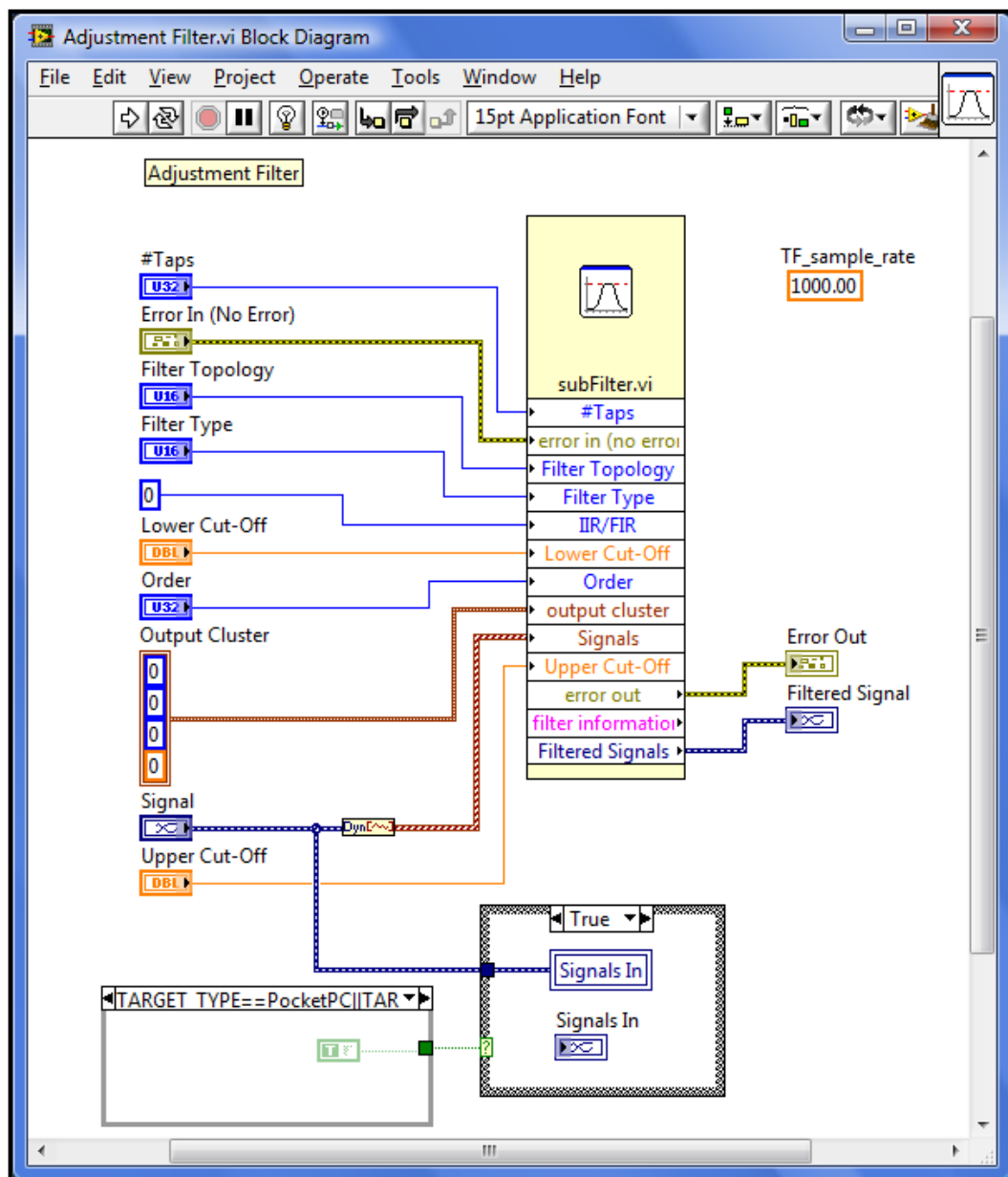


Figure 4.6: Filter adjustment block diagram interface

From the block diagram interface, there are some inputs need to be set to let the filter functions as normal, like what shown at the front panel. This can be consider as an advanced type of filter that can be used to figure out the suitable filter parameters before data processing and data analyzing can be carried out in order to produce a better and accurate results for this project.

4.2.2 Read From Text File

After recording the results, analysis tool is need to re-open or post-processing the data collected for future data analyzing or any advanced data analysis. This is important especially when errors or mistakes occurred; recorded data needs to be checked. This can be done by using the “Read From Text File” VI as shown below.

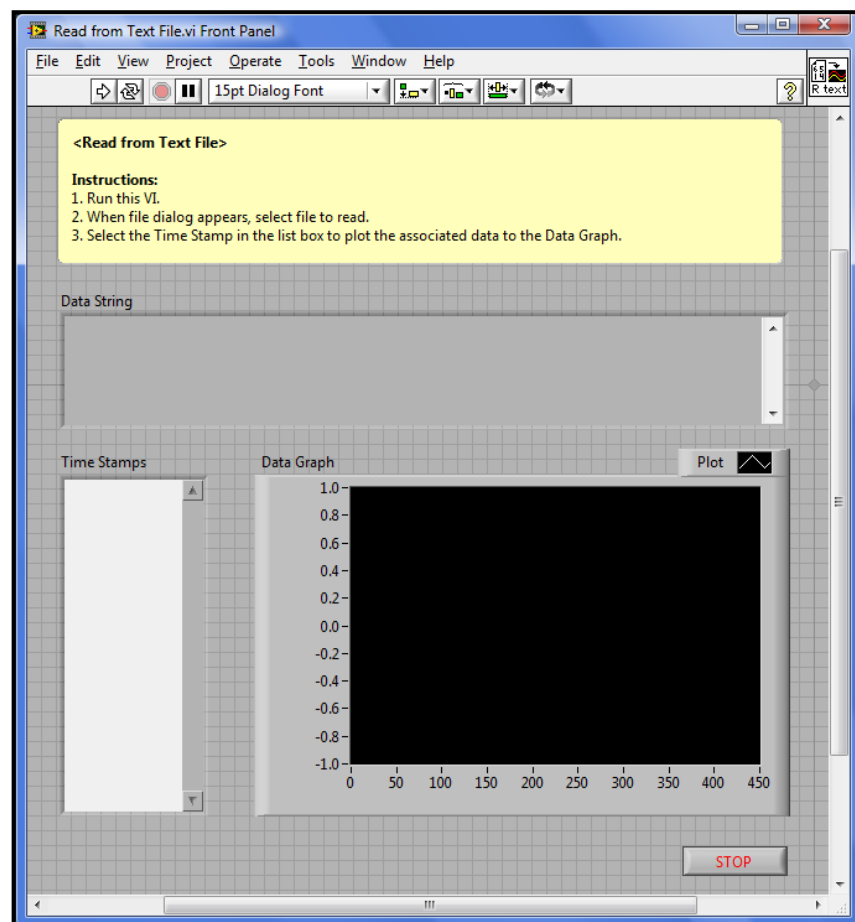


Figure 4.7: Read from text file front panel interface

From the front panel interface, the data that recorded in the text file format (output readings) will be showed at the “Data String” column which is normally the force peak values. For the “Data Graph”, it is used to convert the recorded results into a presentable graphical form. Well, the “Time Stamps” is functioned to displayed out all recorded results according to the recording time and the FSR sensors output. Hence, user can select the data to be viewed by clicking the required period inside the “Time Stamps”.

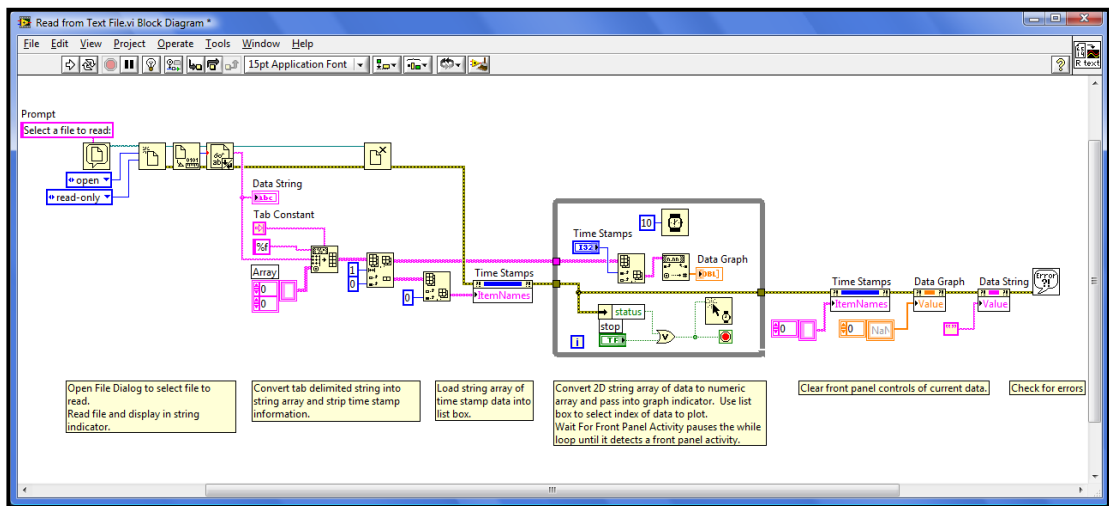


Figure 4.8: Read from text file block diagram interface

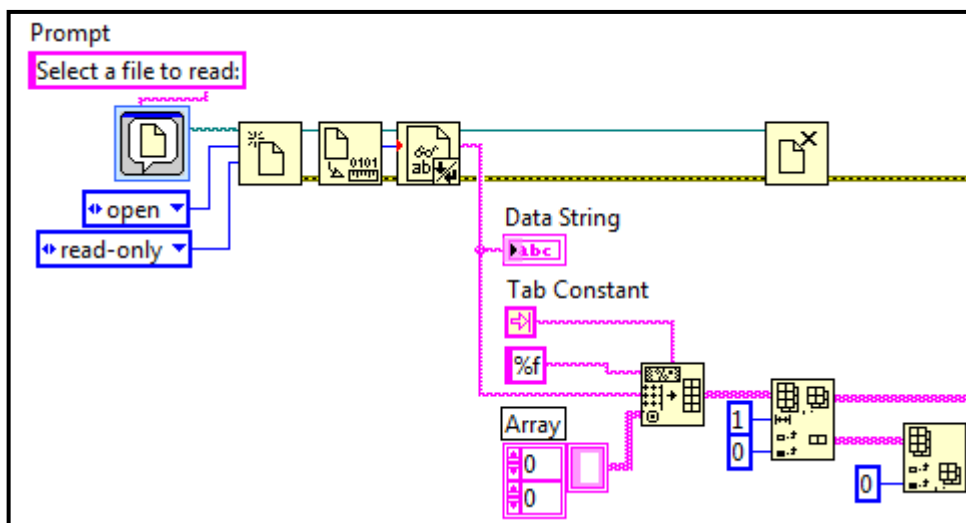


Figure 4.9: Read from text file block diagram A

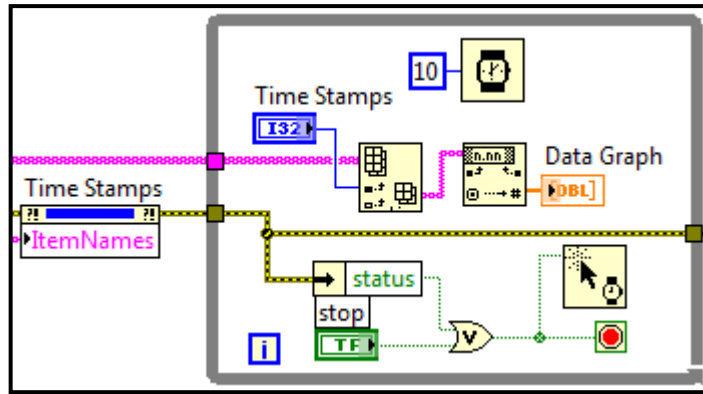


Figure 4.10: Read from text file block diagram B

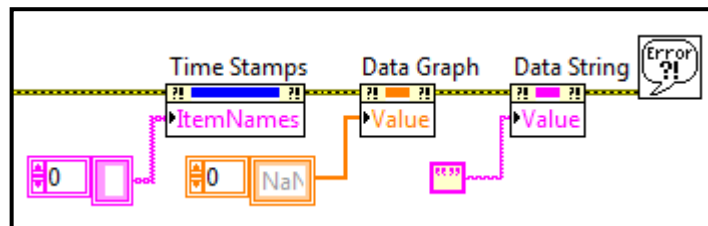


Figure 4.11: Read from text file block diagram C

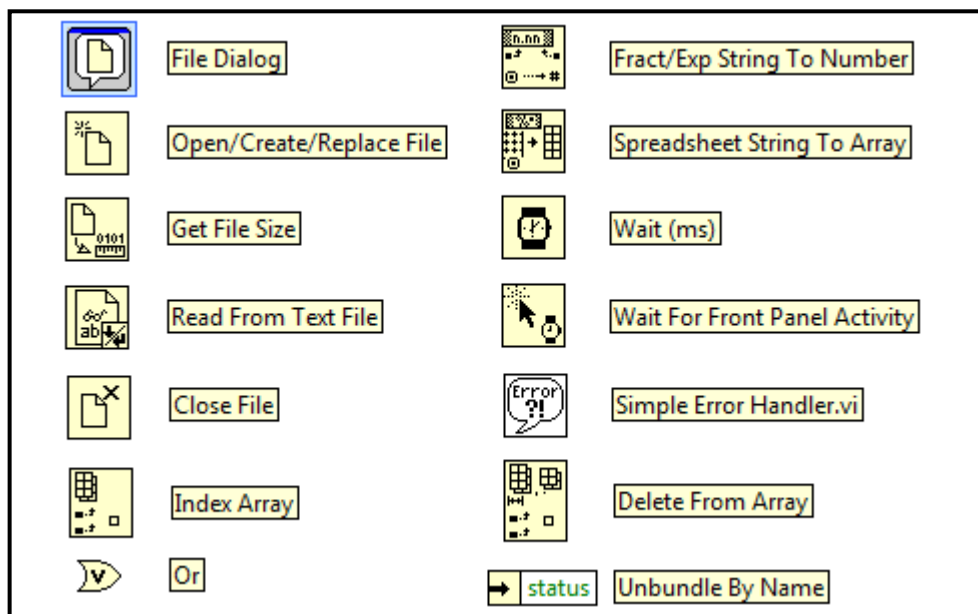


Figure 4.12: Read from text file block diagram labelling

From the block diagram interface, there are six major parts to form the working operation of this “Read From Text File”. First, file dialog will be opened to select the file to read. The selected file will be read and displayed in string indicator. Then, the second part is used to convert the tab delimited string into string array and strip time information. Next, the string array of time stamp data will be loaded into the list box.

A while loop is used to convert the 2D string array of data to numeric array and pass into graph indicator. A list box is used to select the index of data to plot. A wait function is used for front panel activity to pause the while loop until it detects a front panel activity. After that, front panel controls of current data will be cleared. The last part of this block diagram is used for the errors checking.

The screenshot shows a Notepad window titled "test - Notepad" containing a text file with the following content:

```

L1 10:29:52 0 156 156 0 0 0 0 156 0 0 0
L2 10:29:52 0 156 0 156 0 0 0 0 156 0 0 0
L3 10:29:52 0 400 0 0 400 0 0 0 0 400 0 0
L4 10:29:52 0 394 0 0 0 394 0 0 0 0 0 3
L5 10:29:52 377 377 0 0 0 0 377 0 0 0 0 0
L1 10:29:52 0 156 156 0 0 0 0 156 0 0 0 0
L2 10:29:52 0 156 0 156 0 0 0 0 156 0 0 0
L3 10:29:52 0 400 0 0 400 0 0 0 0 400 0 0
L4 10:29:52 0 394 0 0 0 394 0 0 0 0 0 3
L5 10:29:52 377 377 0 0 0 0 377 0 0 0 0 0
L1 10:29:52 0 156 156 0 0 0 0 156 0 0 0 0
L2 10:29:52 0 156 0 156 0 0 0 0 156 0 0 0
L3 10:29:52 0 400 0 0 400 0 0 0 0 400 0 0
L4 10:29:52 0 394 0 0 0 394 0 0 0 0 0 3
L5 10:29:52 377 377 0 0 0 0 377 0 0 0 0 0
L1 10:29:52 0 156 156 0 0 0 0 156 0 0 0 0
L2 10:29:52 0 156 0 156 0 0 0 0 156 0 0 0
L3 10:29:52 0 400 0 0 400 0 0 0 0 400 0 0
L4 10:29:52 0 394 0 0 0 394 0 0 0 0 0 3
L5 10:29:52 377 377 0 0 0 0 377 0 0 0 0 0

```

Figure 4.13: Example of text file created

4.3 Gait Simulation

As mentioned earlier at the previous chapter, a few gait simulations are chosen to be discussed here besides the subject testing which involved in common human locomotion activities. A subject is asked to help in conducting the simulations and the gait simulation is completed around 30 minutes. The results of each type of simulation including the initial testing will be showed and explained further in the following sub-sections.

4.3.1 Initial Testing

The initial test is important in making sure that all the FSR sensors are working properly in a good condition by monitoring with LabVIEW. Eight FSR sensors are being tested separately and some output readings being generated as followed.

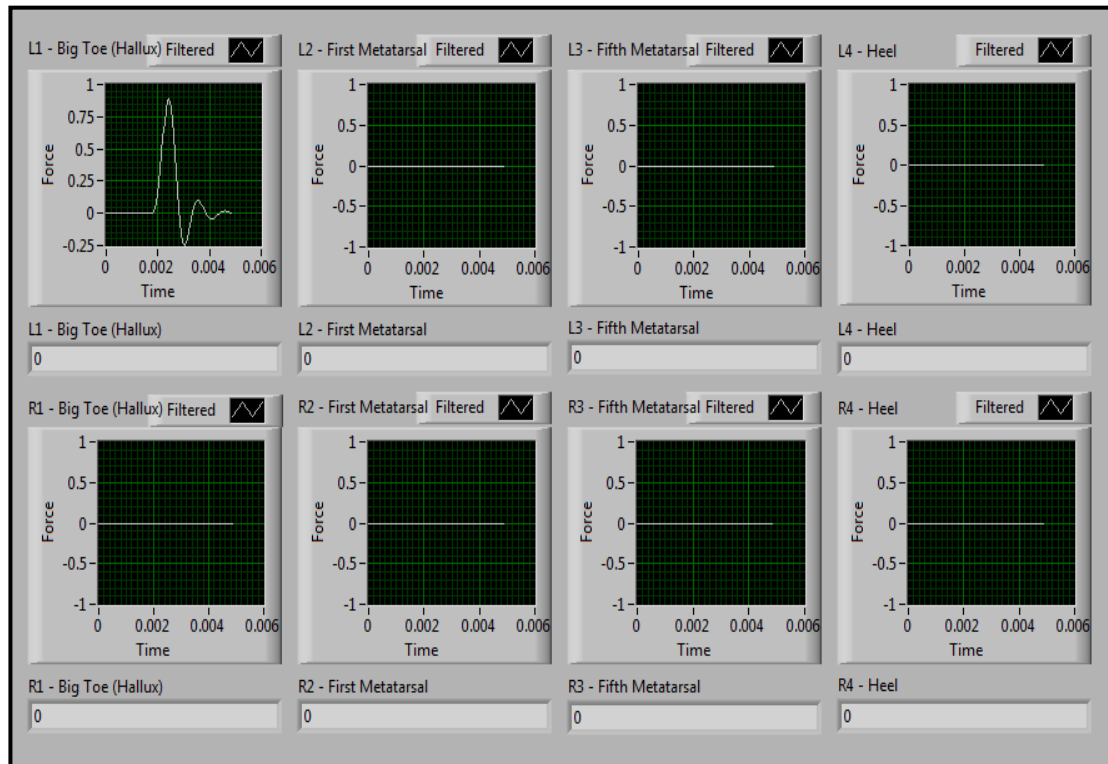


Figure 4.14: Initial testing of sensor L1

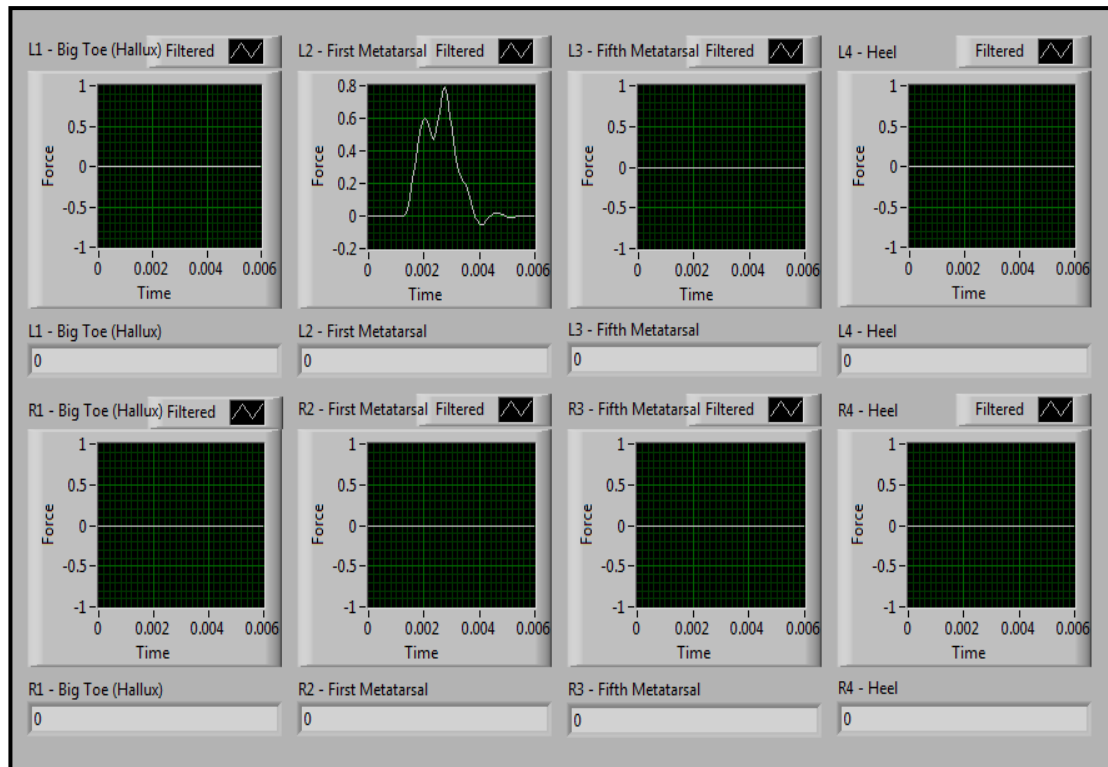


Figure 4.15: Initial testing of sensor L2

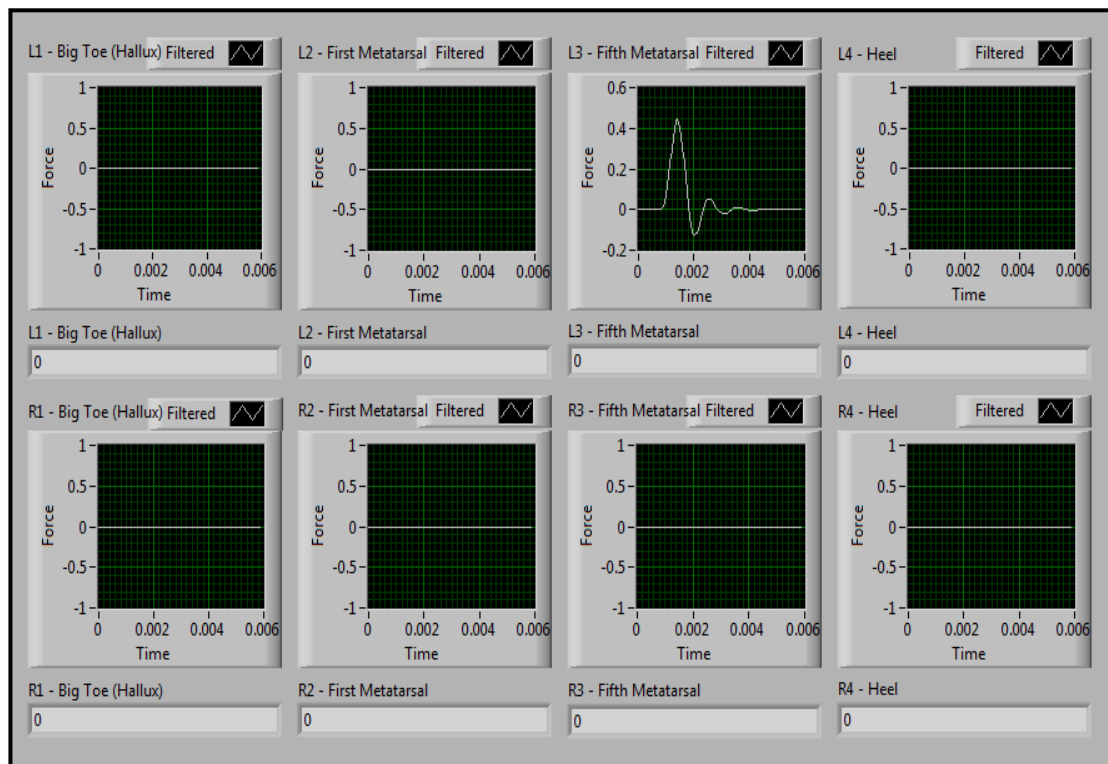


Figure 4.16: Initial testing of sensor L3

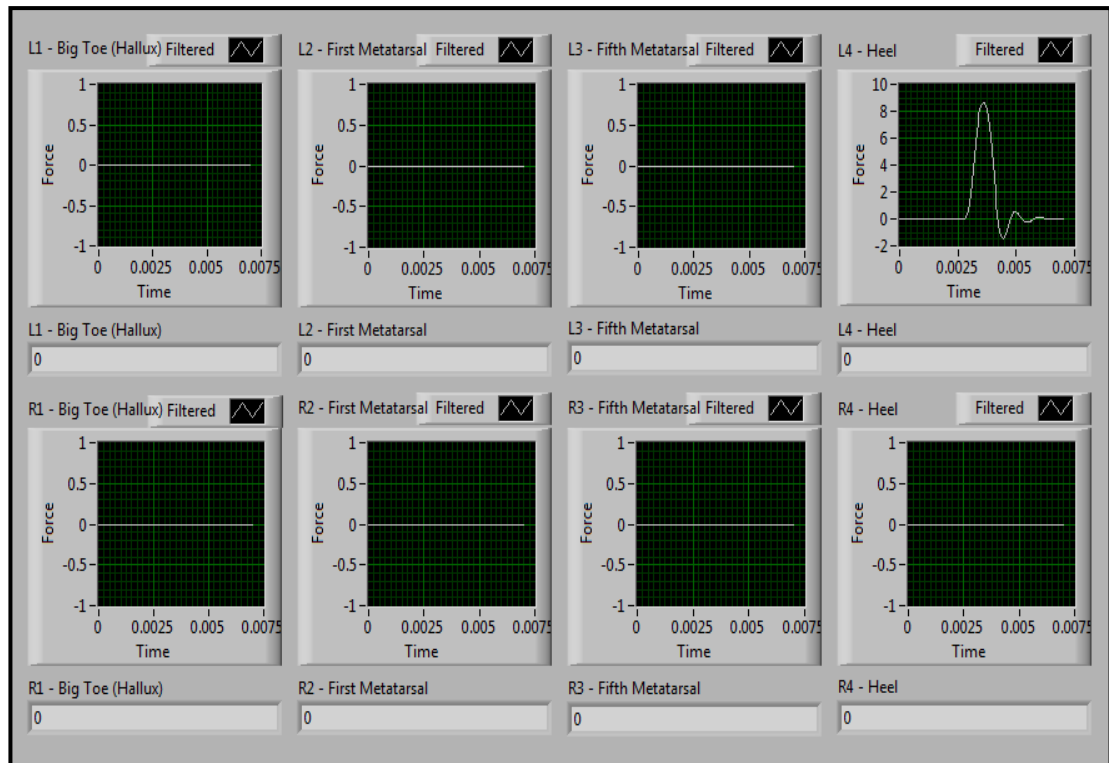


Figure 4.17: Initial testing of sensor L4

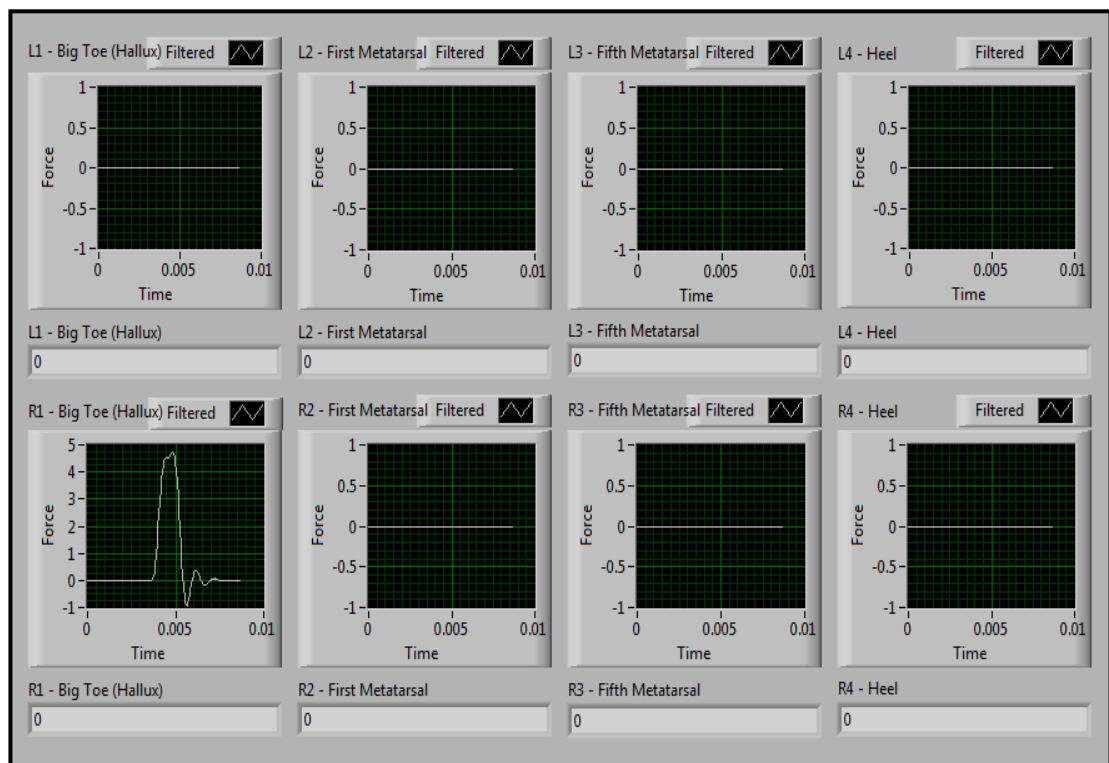


Figure 4.18: Initial testing of sensor R1

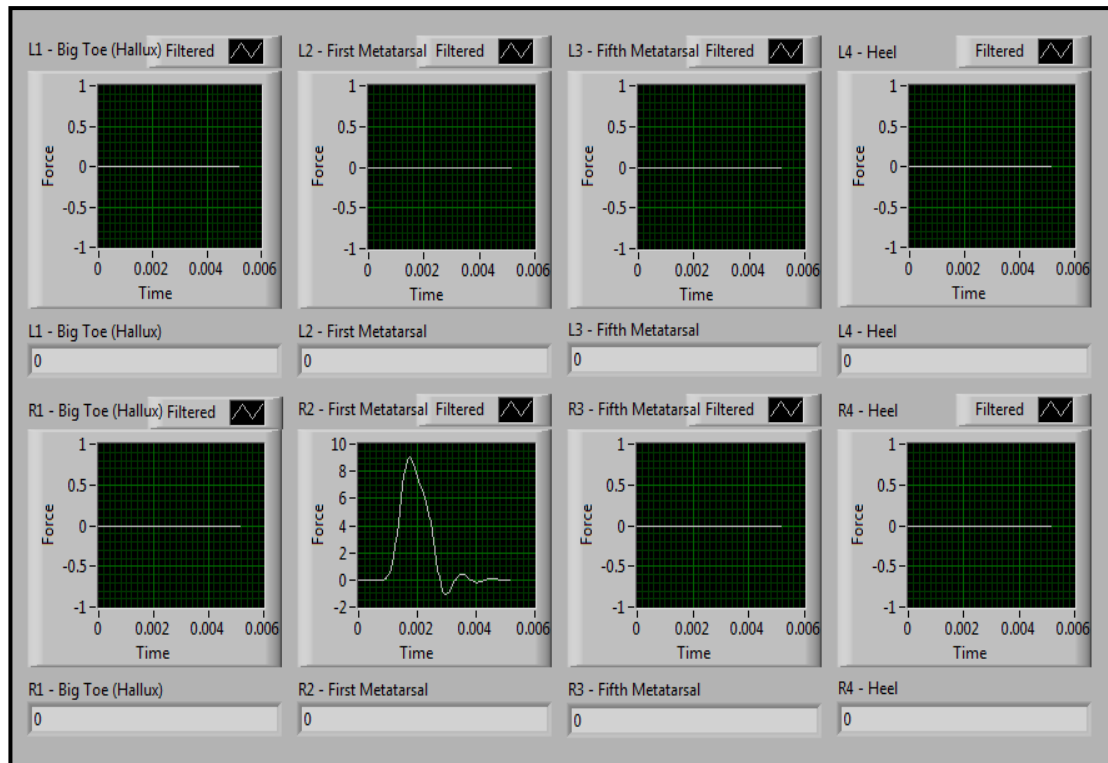


Figure 4.19: Initial testing of sensor R2

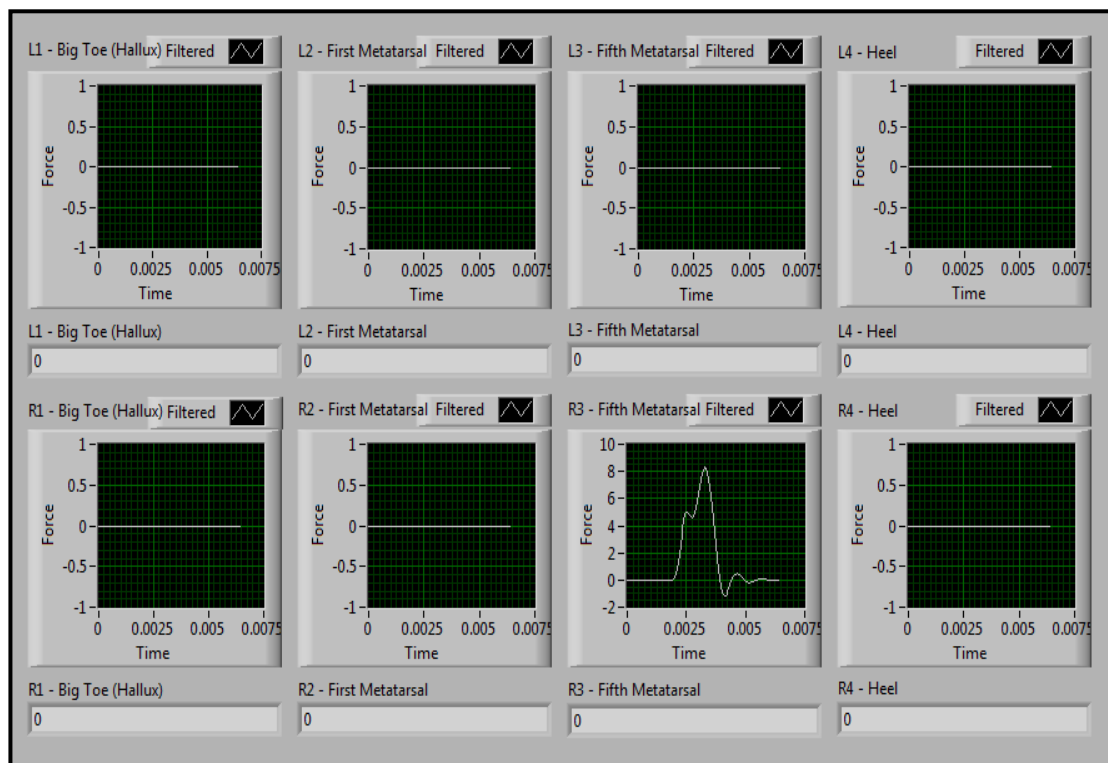


Figure 4.20: Initial testing of sensor R3

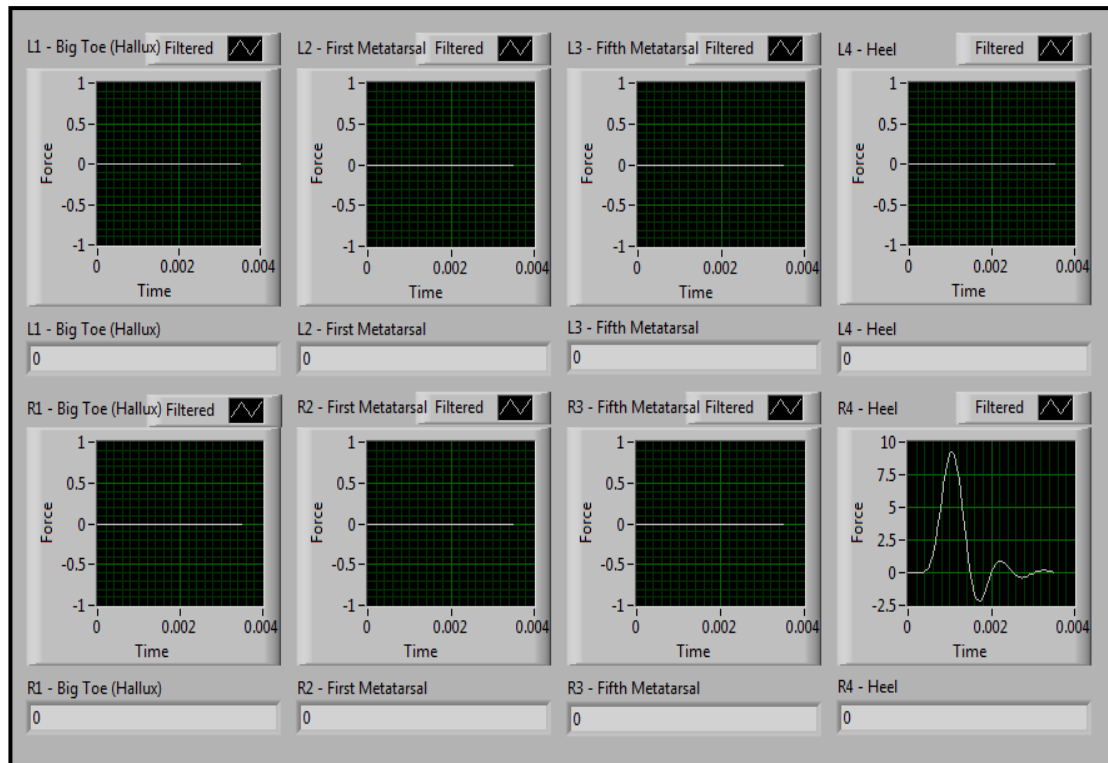


Figure 4.21: Initial testing of sensor R4

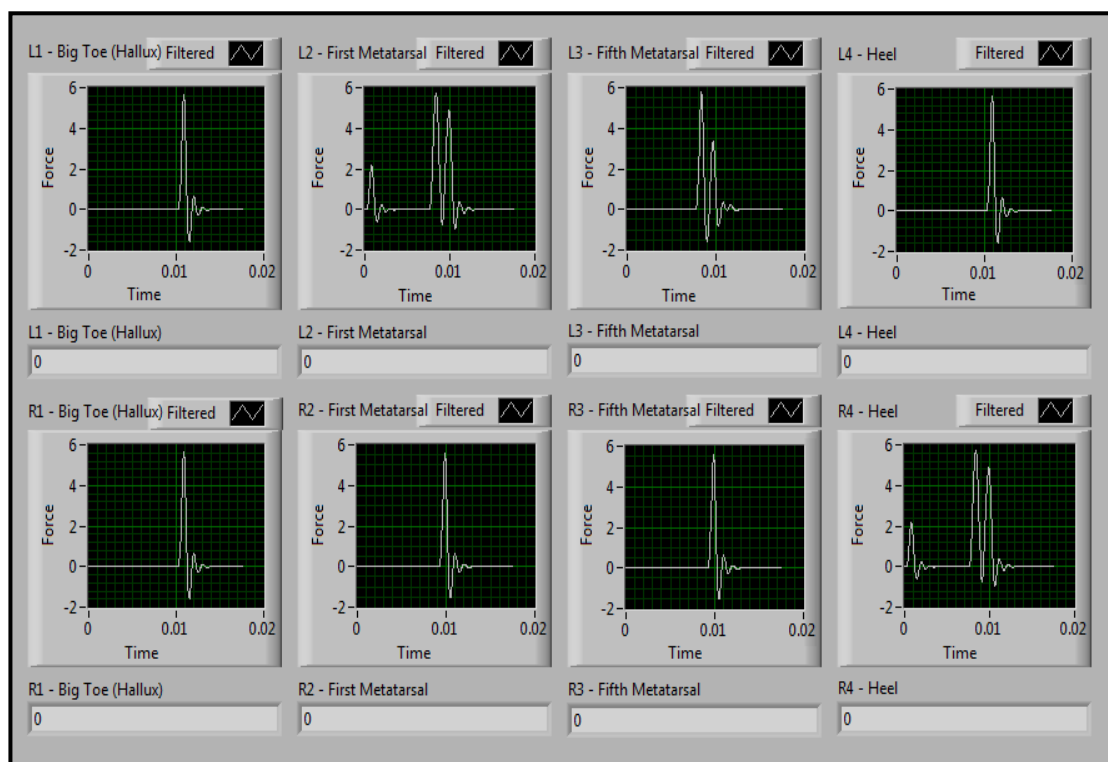


Figure 4.22: Combined readings for all sensors

By referring to the combined readings for all sensors, the measurable peak of forces is obtained at approximately 5.90 N. Hence, the maximum weight that can be distinguished by the system is around 0.60 kg. By converting this force to voltage, it is correlated to the maximum achievable voltage of 2.83 V.

4.3.2 Static Device with No Inputs

In this situation, static device with no inputs refers to the device when FSR sensors are not connected and the subject is not wearing the device. The purpose is to identify the noises created by the devices, like PIC18F4550 microcontroller, SK40C enhanced 40 pins PIC start-up kit, and XBee starter kit.

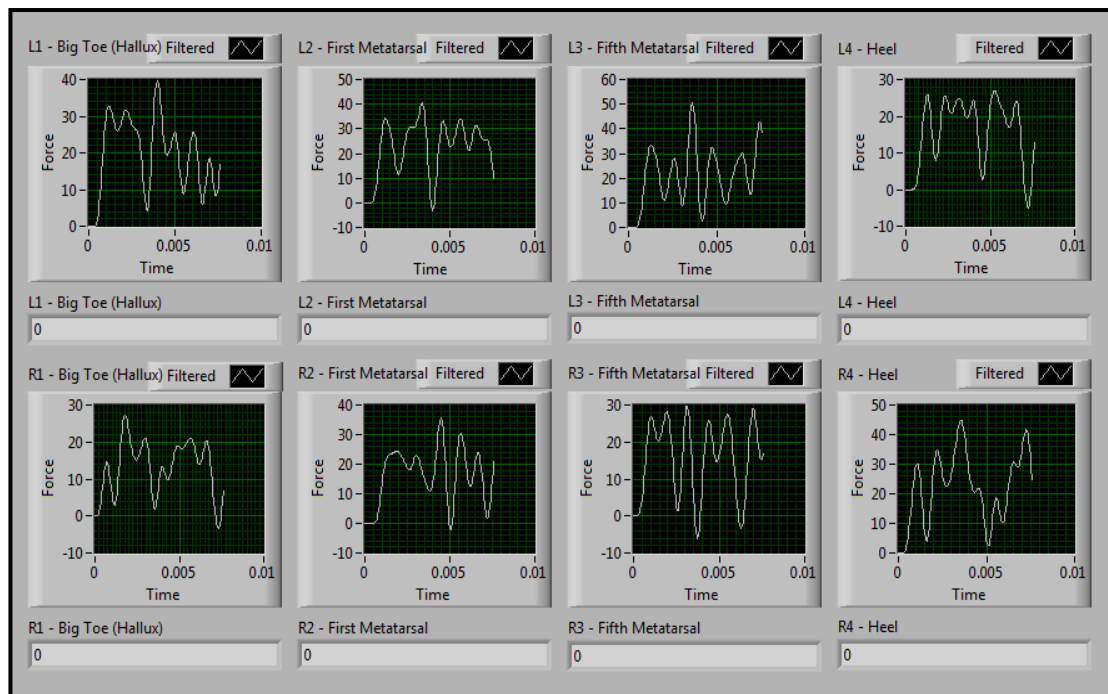


Figure 4.23: Static device with no inputs results by LabVIEW

From the results obtained, it can be observed that the values fluctuate at an average force between 20 N and 50 N for all graphs. By converting this force to voltage, it is correlated to the maximum achievable voltage of 23.99 V. These forces are referred as noises created by those devices.

There is unstable decrease and increase of the waveform in each graph probably because it is the combination of noises created by those devices. To reduce these noises, filter circuits can be used before the inputs and after the outputs. However, such filter is not taken into consideration in this project as the effect might not be that significant. The standard value when there are no readings from the FSR sensors will be assumed to be around 0 N to 1 N.

4.3.3 Static Device with Static Forces Inputs

Static device with static forces inputs refer to the devices which is connected with FSR inputs but not worn by subject. The purpose of this is to observe the effect of the FSR on the outputs, especially when the FSR sensors are not applied with any forces. It should not be worn and not being placed into a shoe during this simulation because different type of shoes consists of different patterns, shapes, and sizes of insole sheet.

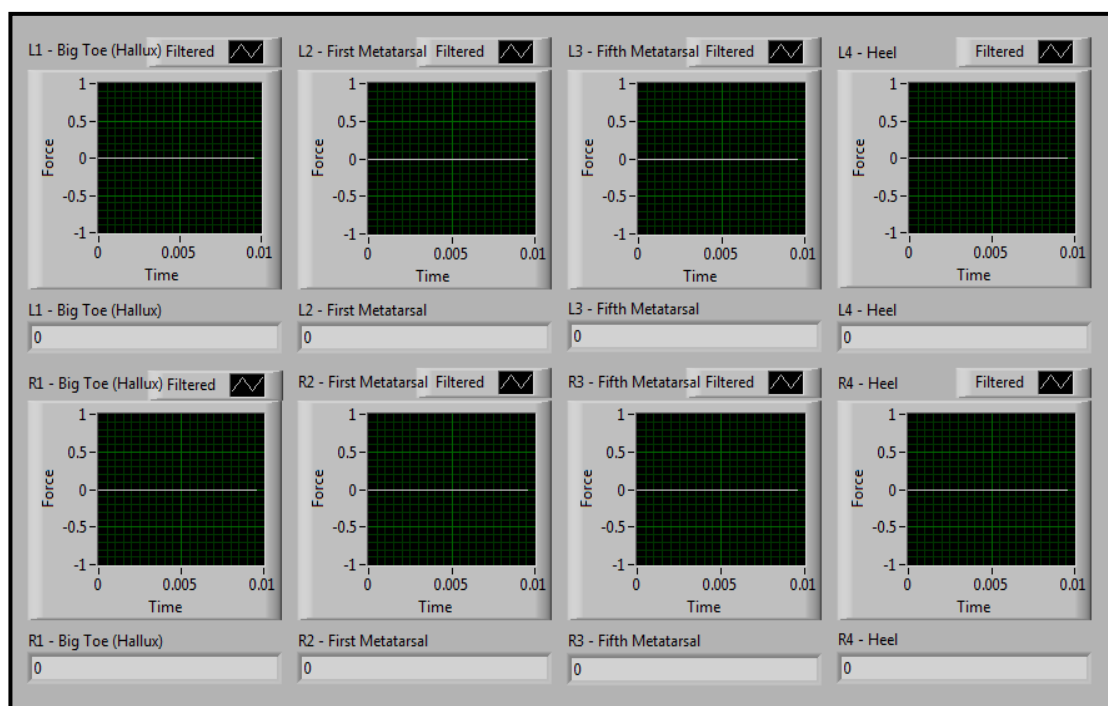


Figure 4.24: Static device with static forces inputs results by LabVIEW

From the results obtained, there are no waveforms displayed for all graphs after the FSR sensors are connected. This is reasonable as the sensors which being used in this system is the force sensors where they only generate outputs when there is any force applied to them. Hence, no waveforms should be detected by connecting the sensors in the condition where no any external forces have been applied to them.

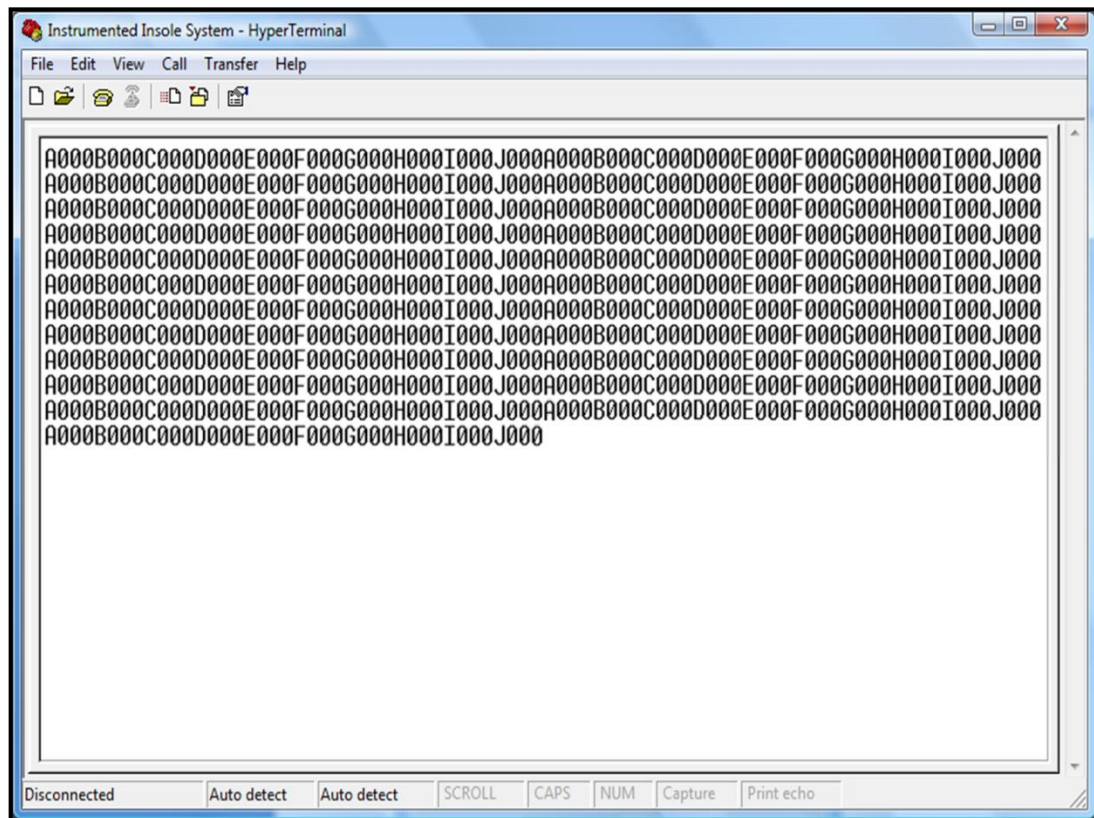


Figure 4.25: Static device with static forces inputs results by HyperTerminal

For the results generated by HyperTerminal testing, there is no any input from those devices. This is due to the reason that no forces changes are being detected by the FSR sensors, which is connected to the devices in this case. Hence, there is no input generated from the sensors into the microcontroller and send through XBee module to computer for recording.

4.3.4 Standing

A subject with weight approximately 45 kg is asked to follow the instructions and stand with the required position in order to conduct this simulation. The duration for this simulation is exactly 10 seconds. The results obtained are plotted in the graphs as followed.

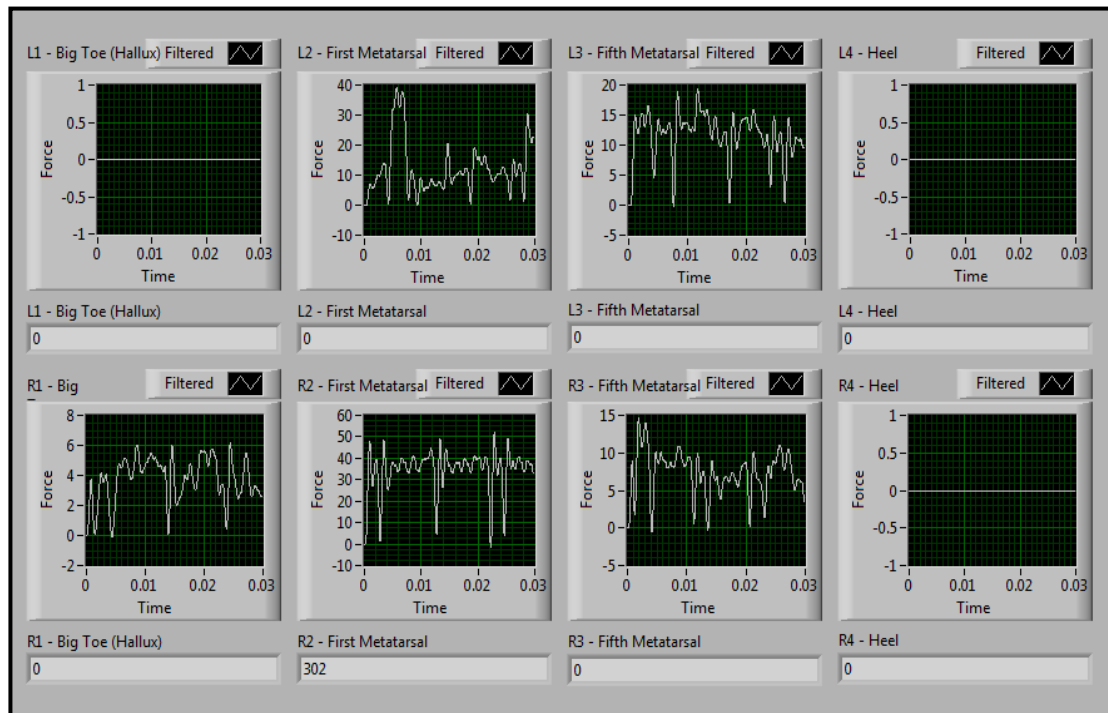


Figure 4.26: Standing results by LabVIEW

From the results obtained, the waveforms of forces fluctuated between values of above 0 N and below 50 N. Hence, the maximum weight that can be distinguished by the system is around 5.10 kg. By converting this force to voltage, it is correlated to the maximum achievable voltage of 23.99 V.

Comparing with static device with no static forces inputs, the range of forces generated in this case is slightly higher. However, the force distribution is quite consistent for some sensors and the no results have been generated for the other sensors. This is because there are always little movements of human body and the subject cannot stand completely still.

4.3.5 Sitting

In sitting simulation, a subject with weight approximately 45 kg is asked to follow the instructions, sit on a chair, and maintain the same position while the information is collected from the FSR sensors for exactly 10 seconds. The results obtained are plotted in the graphs as followed.

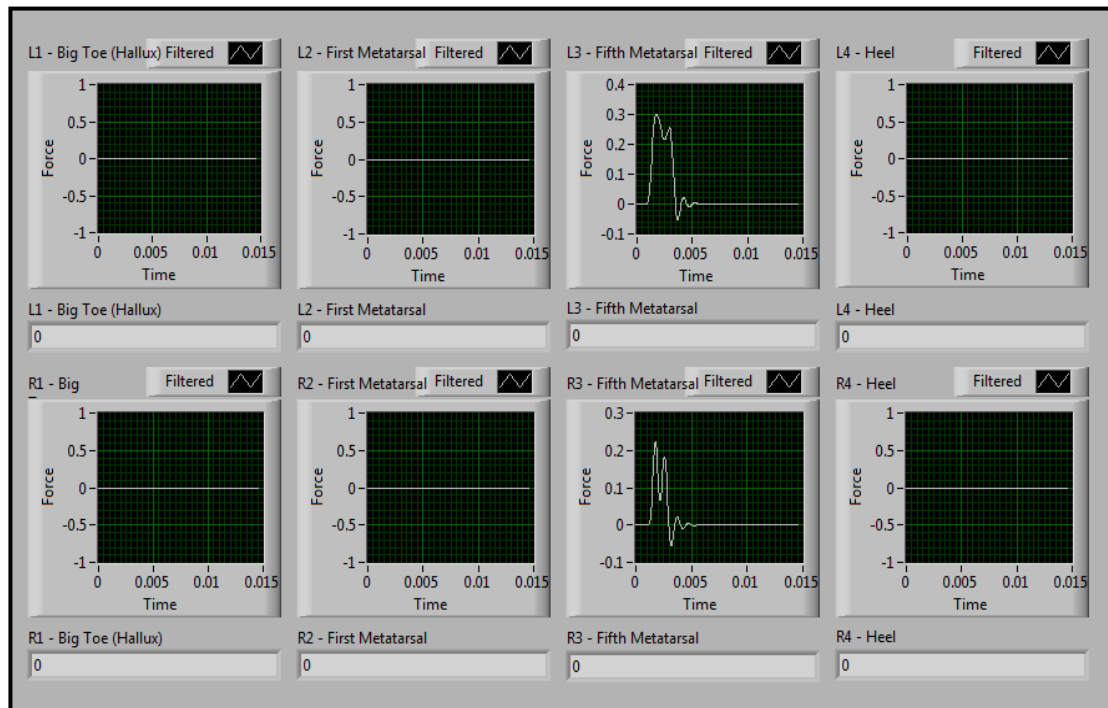


Figure 4.27: Sitting results by LabVIEW

From the observed results, it shows that the forces detected by sensors have the peak value of 0.30 N and below it. Hence, the maximum weight that can be distinguished by the system is around 0.03 kg. By converting this force to voltage, it is correlated to the maximum achievable voltage of 0.14 V.

The forces detected by the sensors are not high as expected where fewer sensors are generating results compared to standing position. This is because the subject is sitting while the foot is just in contact with the floor. Therefore, not much pressure pressing the foot towards the floor. Hence, light forces are applied to certain of the sensors only.

4.3.6 Walking

In this simulation, a subject with weight approximately 45 kg is asked to follow the instruction and walk at a normal and natural pace. The subject is asked to wear the instrumented insole and walk on the treadmill with 4 km/h (at least 30 steps) in this simulation for 60 seconds. The results are as followed.

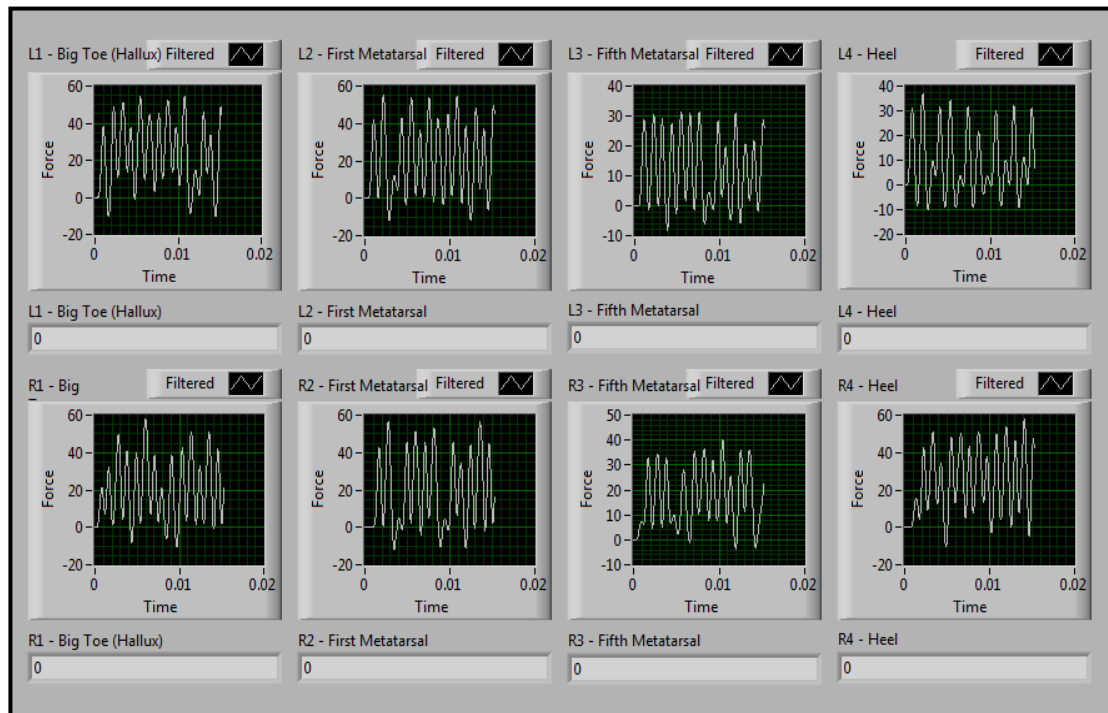


Figure 4.28: Walking results by LabVIEW

The sensors showed fluctuations in the waveform generated with between 40 N and 60 N. Hence, the maximum weight that can be distinguished by the system is around 6.12 kg. By converting this force to voltage, it is correlated to the maximum achievable voltage of 28.79 V.

By observing the results, eight sensors show comparable outcomes where stable peaks are formed. The graphs showed that the forces applied beneath each side of the foot changes continuously when a person walking. The changes are considered random and quite consistent for each step that has taken.

4.3.7 Running

In running simulation, a subject with weight approximately 45 kg is asked to follow the instruction and run at a faster than normal pace. The subject is asked to wear the instrumented insole and walk on the treadmill with 6 km/h (at least 30 steps) in this simulation for 60 seconds. The results obtained are plotted in the graphs as followed.

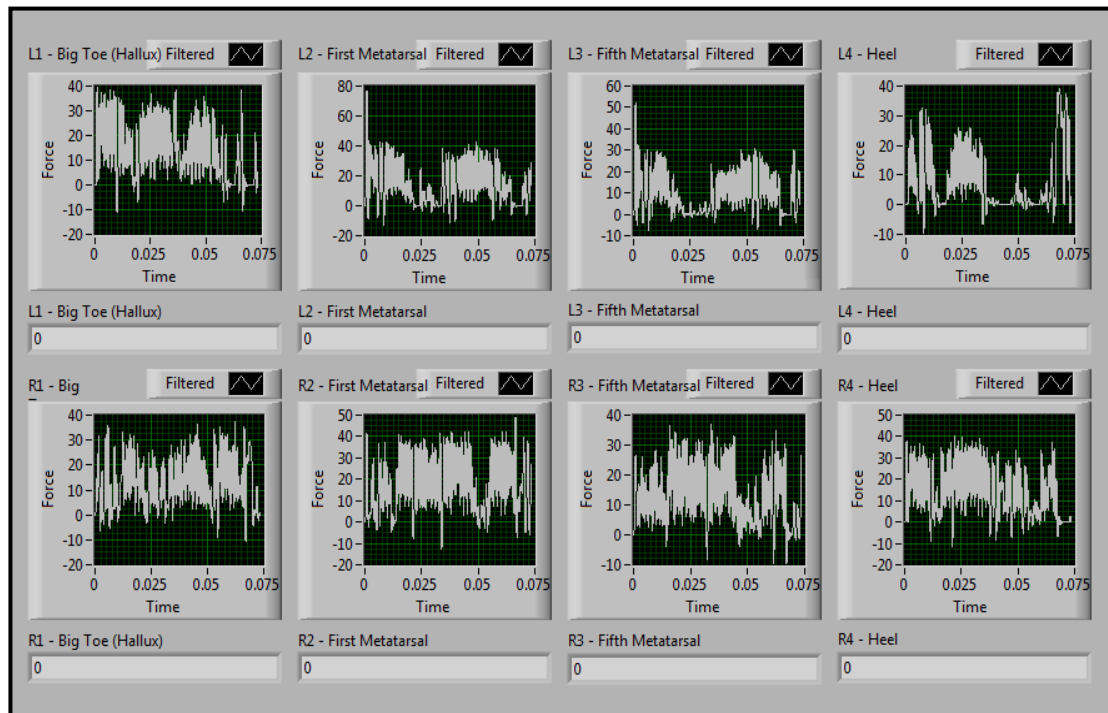


Figure 4.29: Running results by LabVIEW

From the results, the sensors detected forces within a wider range than in walking simulation, which is between 25 N and 80 N. Hence, the maximum weight that can be distinguished by the system is around 8.15 kg. By converting this force to voltage, it is correlated to the maximum achievable voltage of 38.39 V.

These results matched the simulation carried out because when the subject is running. More peaks are formed in an unstable condition with a big fluctuation. The force applied beneath the foot changed in a rapid sequence from time to time continuously and the waveforms are more packs or being repeated rapidly compared to the normal walking.

4.3.8 Summary of Results and Discussion

Each type of simulation has its characteristics and peak value which is different from others. From the results collected throughout the simulation, results are within the range of force values from 0 N to 80 N. This is quite a big range which might be due to the different simulation characteristics will produce different patterns of waveform graphs.

By referring to static device with no inputs and static device with static force inputs simulation, there are some noises generated by the devices. This is a normal phenomenon as most of the electronic devices will generate noises. However, these noises can be reduced as mentioned before but cannot be removed. This simulation is essential to let user figure out the standard value when there are no readings from FSR sensors so that assumption can be made for other simulations.

For the standing simulation, the forces applied are different on each sensor. Obviously, the sensor L4 and R4 (heel) exerted the most forces as they spike from the graphs and stay constantly higher than the rest of the sensors. On the other side, the forces exerted by L1, L2, L3, R1, R2, and R3 (big toe, first, and fifth metatarsals) are relatively same with not much differences as they are located near to each other.

In sitting simulation, the forces applied here are not as high as in standing simulation. In this case, the sensor L1, L2, L4, R1, R2, and R4 (big toe, first metatarsals, and heel) exerted no forces as the body is not supported by the foot. The forces exerted for supporting the body weight is being separated and shared by the chair. For other sensors like L3 and R3 (third metatarsals) are relatively same with not much differences in this simulation.

For the walking simulation, the pressure distribution is different compared to the results obtained from standing and sitting. By observing the waveform graphs, sensor L4 (heel) in left foot gave the first spike in the graph where the stance phase is started with the heel strike. The waveforms are then followed by the sensor L3 (fifth metatarsals), and L2 (first metatarsals). This showed that there is a transition of pressure from the back to the front of the foot.

At the end, sensor L1 (big toe) gave the last spike in the graph which indicates the ending of stance phase. This pressure is exerted by the big toe which indicates the action of toe off where the toe is pushing off to propel the body forward. After that, there is a short pause where no spikes are seen on the graph before another heel strike recorded. Swing phase is represented by this short pause where no pressure is exerted to the floor as the foot is lifted off. There will be the same actions occurred for the right foot.

In running simulation, the pressure distribution is likely the same as in walking simulation but with a rapid sequence. The first spike starts at the sensor R4 (heel) in the right foot which indicates the starting of stance phase. The waveforms are then followed by the sensor R3 (fifth metatarsals), and R2 (first metatarsals). This showed that there is a transition of pressure from the back to the front of the foot in a faster sequence.

At the end, sensor R1 (big toe) gave the last spike in the graph which indicates the ending of stance phase. The action of toe off occurred is bigger compared to walking simulation where the toe needs more forces is to push off to propel the body forward. After that, swing phase is occurred and represented by the short pause where the foot is lifted off. Again, this swing phase is shorter by roughly 33% than the swing phase in the walking simulation. There will be the same actions occurred for the left foot.

From the results obtained, the force distribution trends are studied to distinguish common locomotion activities of human being, such as standing, sitting, walking, and running. However, the results are only applicable to particular test subject and more results are required to prove these initial readings. Therefore, there is subject testing being conducted for future researching and data analyzing.

4.4 Subject Testing

The subject testing will be conducted for roughly for less than one week (four days), from March 28, 2011 until March 31, 2011. The results of the body segment and circumferences measurement (anthropometric dimensions), and each type of locomotion activity in the subject testing will be discussed in the following subsection regards the subject information and results from the gait simulation after processing and analysing.

4.4.1 Subject Information

The recruitment of this subject testing is carried out for one week (seven days), which started from March 21, 2011 until March 27, 2011. Total of 30 subjects are recruited for the validation of the instrumented insole system and nine groups are formed. A complete schedule for this subject testing is attached at Appendix F.

There are 50% (15) of male volunteers and 50% (15) of female volunteers with the ages between 20 to 28 years old where the development of gait is completed and no degenerative changes related to aging are present. Besides, all of them are from biomedical engineering where one if from year one trimester one, three of them are from year three trimester one, ten of them are from year three trimester three, one of them is from year four trimester one, and 15 of them are from year four trimester three. Statistically, the range for height is from 152 cm to 182 cm, whereas the weight is falls between 40 kg to 93 kg.

They are provided with identification number consecutively from 1 to 15 for both female and male subjects and dividing into nine different groups. As the results collected will be analyzed and grouped according to subject's gender. Thus, there will be an alphabet identification of "M" for male and "F" for female in front of their identification number. Therefore, there will be total of two set of results will be processed and analyzed.

For the size of shoes, one of them is between size 3.1 to 4.0, three of them are between size 4.1 to 5.0, and five of them are between size 5.1 to 6.0, seven of them are between size 6.1 to 7.0, four of them are between size 7.1 to 8.0, five of them are between size 8.1 to 9.0, four of them are between size 9.1 to 10.0, and one of them is between size 10.1 to 11.0. All the subjects' information regarding the identification number and alphabet, gender, age, height, weight, size of shoe, brand of shoe, and group for conducting the gait simulation are listed in detail at the Appendix G.

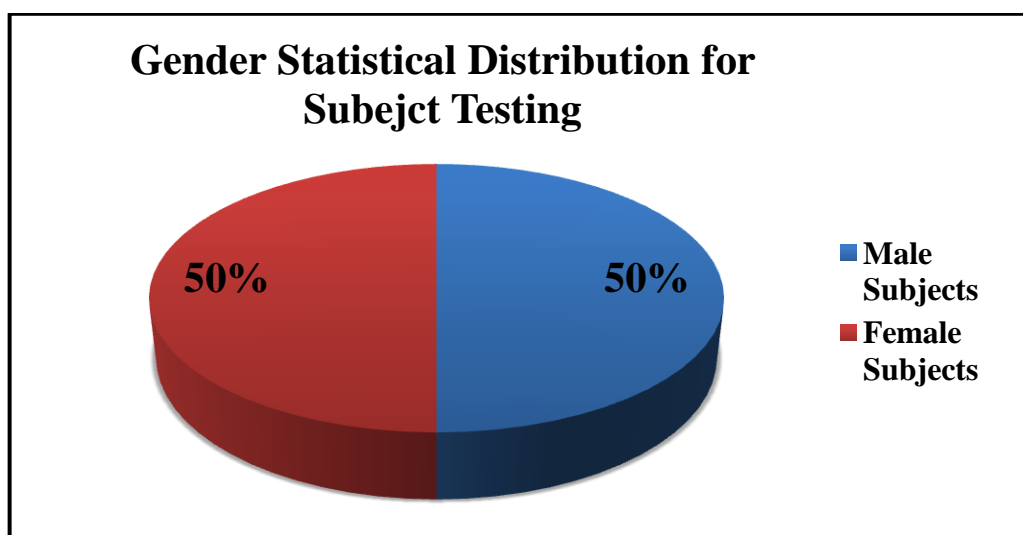


Figure 4.30: Pie chart of gender statistical distribution for subject testing

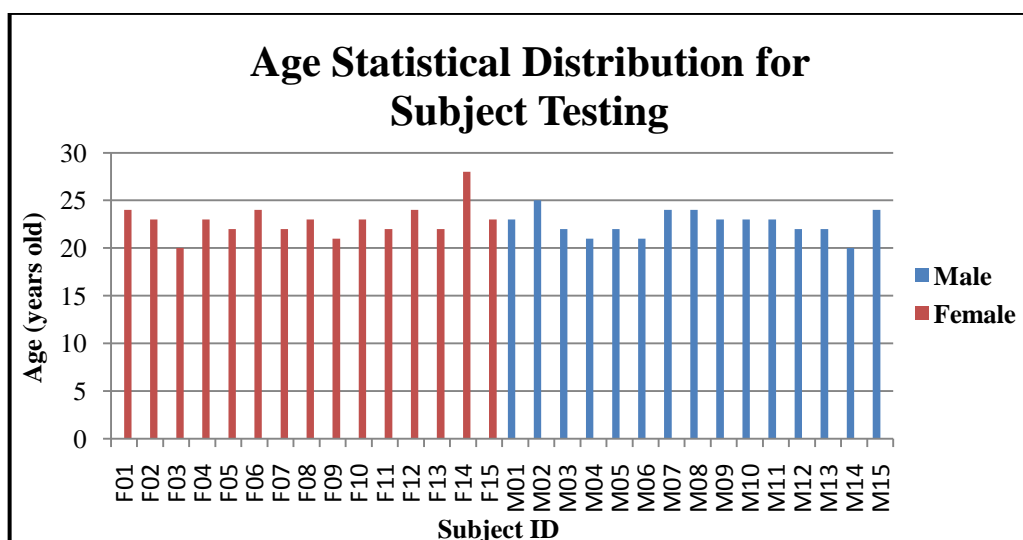


Figure 4.31: Bar chart of age statistical distribution for subject testing

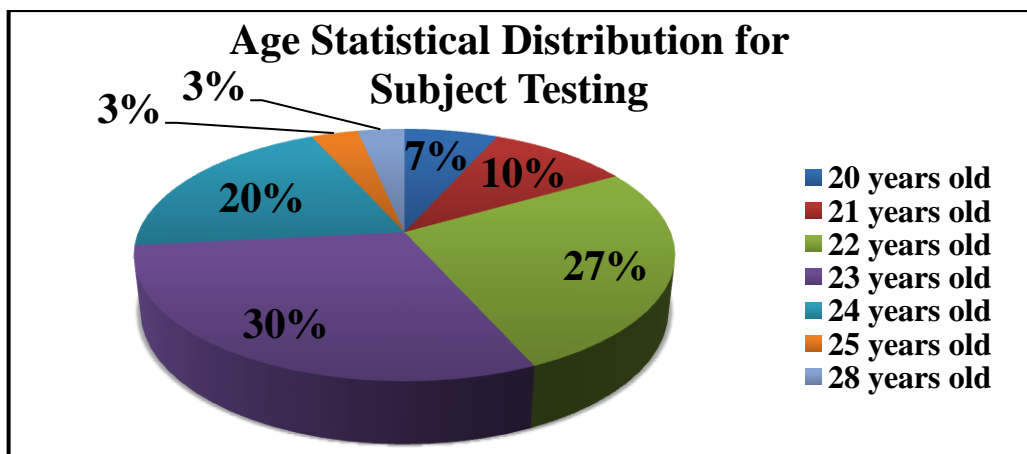


Figure 4.32: Pie chart of age statistical distribution for subject testing

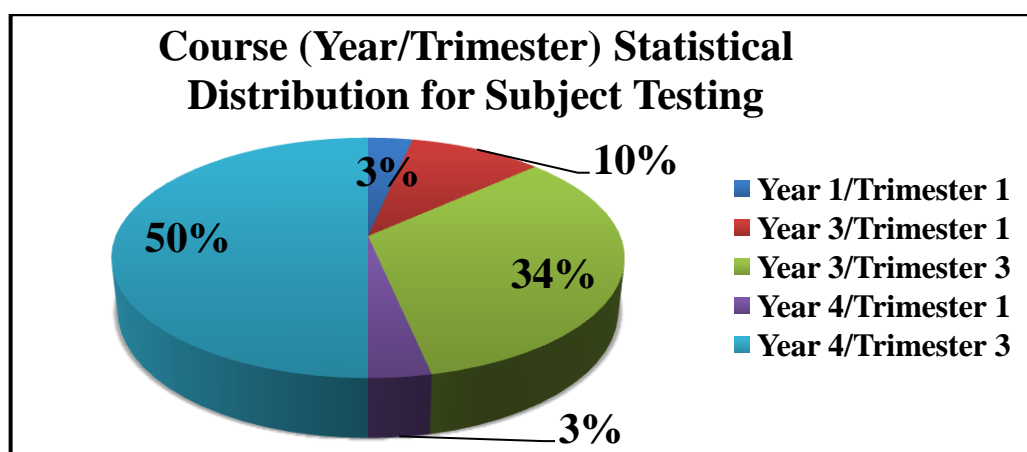


Figure 4.33: Pie chart of course (year/trimester) statistical distribution for subject testing

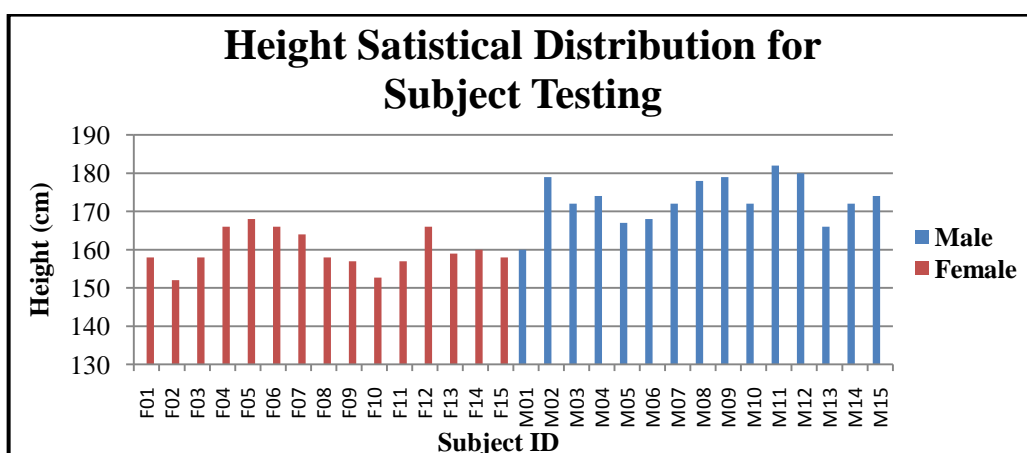


Figure 4.34: Bar chart of height statistical distribution for subject testing

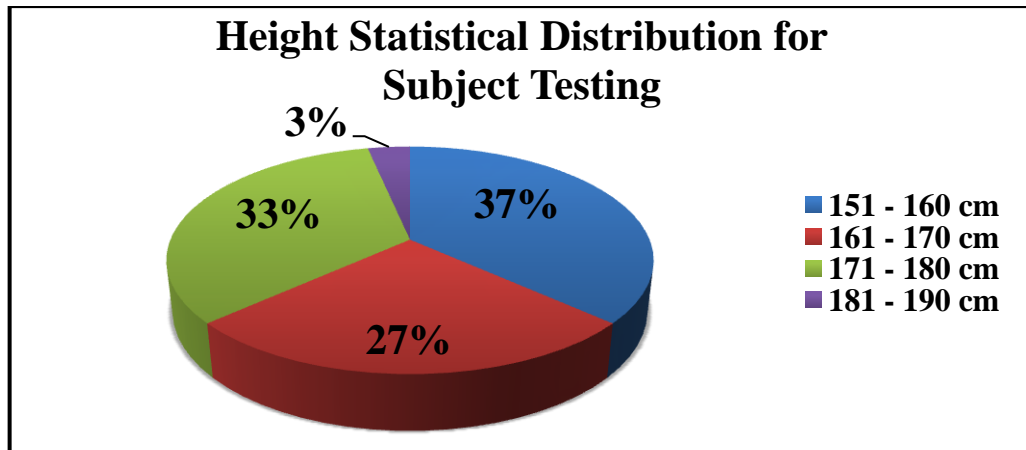


Figure 4.35: Pie chart of height statistical distribution for subject testing

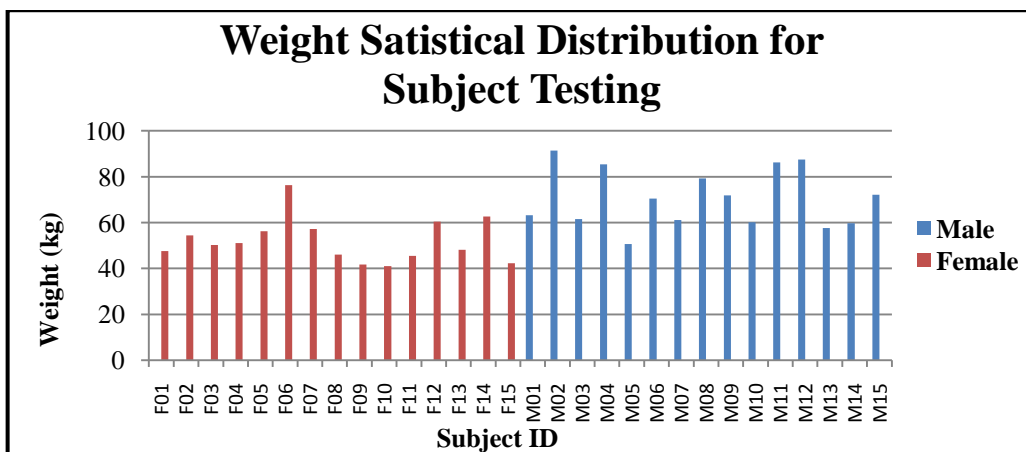


Figure 4.36: Bar chart of weight statistical distribution for subject testing

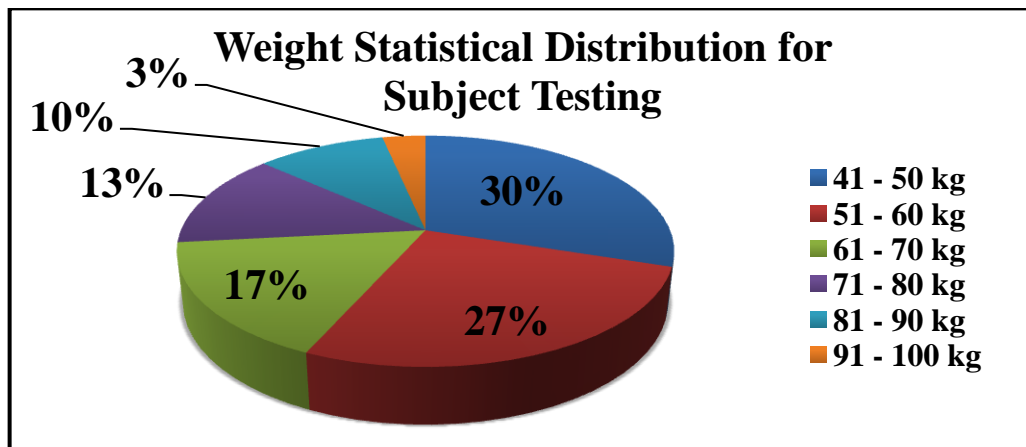


Figure 4.37: Pie chart of weight statistical distribution for subject testing

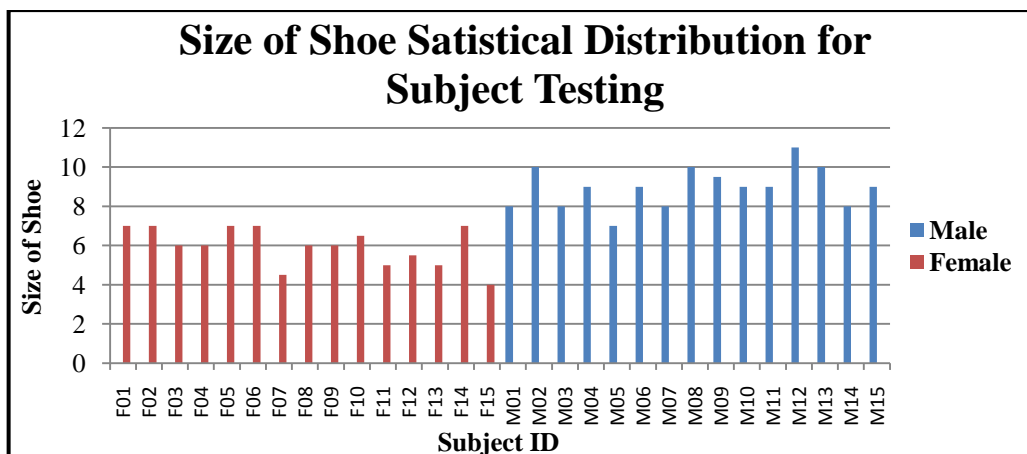


Figure 4.38: Bar chart of size of shoe statistical distribution for subject testing

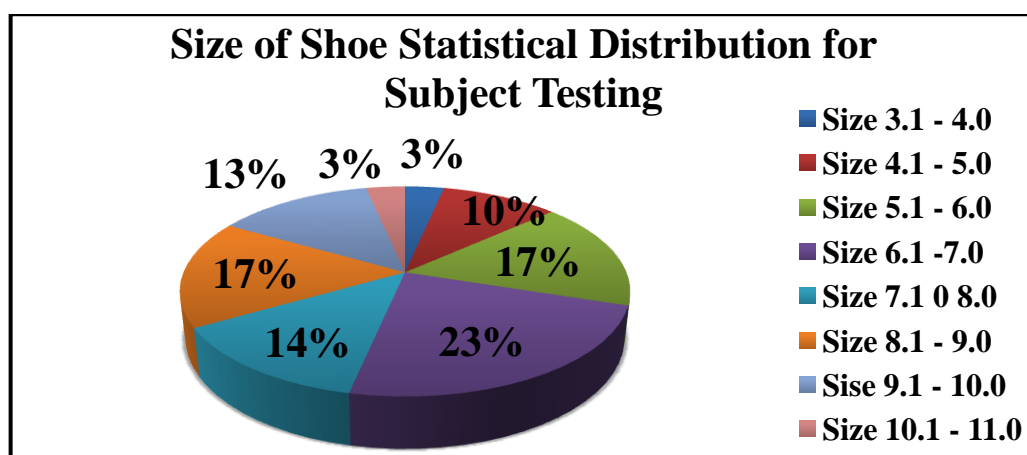


Figure 4.39: Pie chart of size of shoe statistical distribution for subject testing

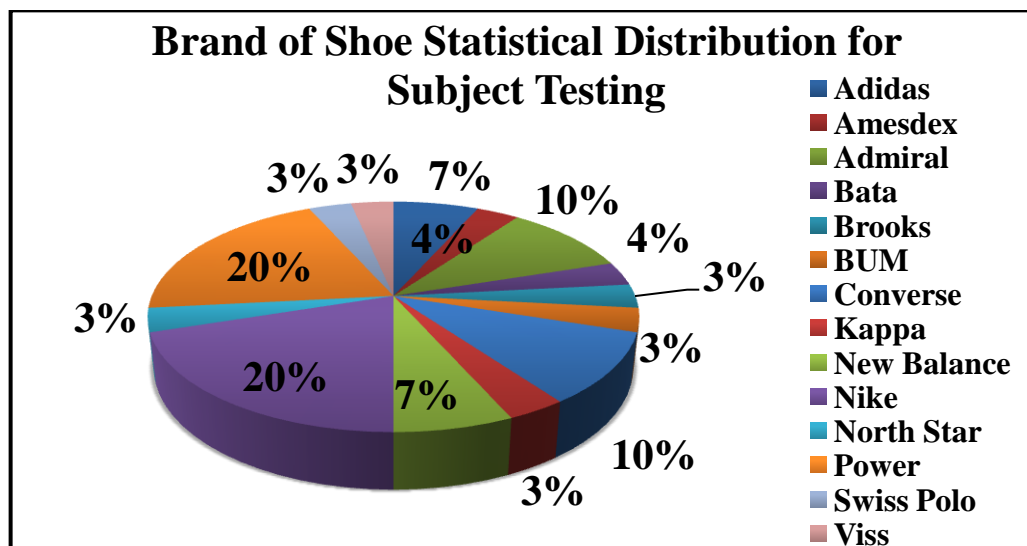


Figure 4.40: Pie chart of brand of shoe statistical distribution for subject testing

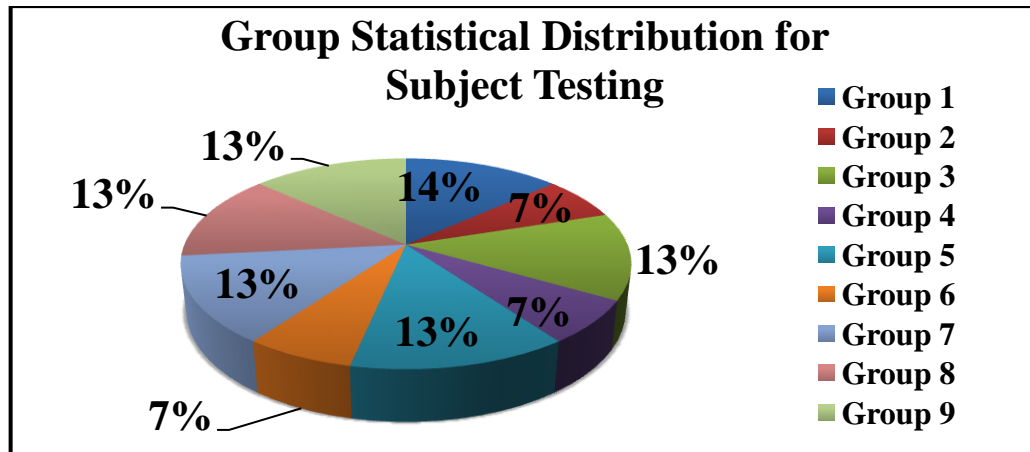


Figure 4.41: Pie chart of group statistical distribution for subject testing

4.4.2 Summary of Results

For the overall results collected from the subject testing, each type of locomotion activity consists of different characteristics and peak value along the period of subject testing. The collected results are within a big range, from 2 N to 429N which might due to the different simulation characteristics, patterns of walking by different subjects, and even the different brand and structure of subjects' shoes.

All the data collected are being summarized into tables and charts at Appendix H. The results and parameters of different locomotion activities are grouped according to genders and being summarized into the tables respectively, like walking speed, step length, step time, cadence, max applied force, force weight ratio and so on to make better use of numerical data relating to walking and running locomotion activities of the subject testing only.

The statistical data included the mean, median, standard deviation, and the variance of the subject testing is being added as part of the results. It cannot be denied that those data are useful for doing comparison with other researches and also wit own simulation results. Furthermore, bar charts are showed to represent all the statistical distribution of collected results in graphical form.

The mean values are calculated for the walking speed, step length, step time, stride length, stride time, cadence, and so forth. Mean is the sum of the data collected divided by the number of data collected. For example, the mean of the height of the male subjects is the sum of the height of all male subjects divided by the number of male subjects in the testing. It describes the central location of the data collected.

Next, median is described as the numeric value separating the higher half of the testing from the lower half. The median of the data is found by arranging all the observations from the lowest value to the highest value where the middle one will be picked. The data of subjects which are less than and greater than the median can be differentiated through this numerical method.

For the standard deviation, it is widely used to measure the variability or dispersion of data. It shows how much variation there is from the mean generated. A low standard deviation indicates that the data points tend to be very close to the mean, whereas high standard deviation indicates that the data is spread out over a large range of values.

The square root of the standard deviation is the variance. The amount of variation within the values of the variable can be measured by taking account of all possible values and their probabilities or weightings. The standard deviation and the expected deviation can both be used as an indicator of the “spread” of the testing distribution.

At the last part of the summary of results, a comparison of mean values for all parameters is made and analyzed between the genders. The purpose to do so is to find out the difference of the mean of all the parameters between male and female participants in the testing. This can be done by subtracting the parameters from two genders as the formula below.

$$\text{Difference} = \text{Mean}_M - \text{Mean}_F \quad (4.1)$$

where Mean_M = Mean for male subjects

Mean_F = Mean for female subjects

However, the difference formula is not sufficient to show the differences between the genders clearly. The range is not showed numerically and this will make the data to be analyzed difficultly especially when the data involved in large decimal points or digits, such as max applied force. Thus, the percentage of error is needed to further confirm the range of difference of mean values in each parameter between male and female subjects. The formula is as followed.

$$\%Error = \frac{\text{Difference}}{\text{Mean (Male)}} \times 100\% \quad (4.2)$$

For the parameters in the walking and running simulation, there are negative and positive values existed in the difference and percentage of error. For the negative values, it means that the parameters results from female subjects are larger than the male subjects and vice versa for the positive values. Overall, the male values are more than the female values for both walking and running simulations as expected.

The difference and percentage of error for walking speed, cadence, max applied force, and force weight ratio are existed in negative values which mean that those parameters are being monopolized and controlled by female subjects. Meanwhile, the anthropometric data, except the age, the height, weight, foot, ankle-to-knee, and ankle-to-thigh length of male subjects are larger than female subjects.

There are statistical difference between the subject testing of male subjects and female subjects in different locomotion activities. In general, male subjects have a longer stride and step length, but take fewer steps per minute in walking locomotion activities, as compared to female subjects. In overall results, male subjects have longer stride length as expected with fewer steps and these two factors combine to give male subjects a slightly faster velocity than female subjects.

In healthy subjects with normal gait, age does not have a measurable effect on gait unless the population includes older subjects. In this subject testing, the range of subjects' ages involved is less than 10 years, and thus not much comparison can be made between the ages. For a group of subjects aged from 20 to 28 years in this subject testing, the walking speed is maintained within in each locomotion activity.

For the statistical differences in subjects' height, the range is from 152 m to 168 m for female subjects and 160 m to 182 m for male subjects. There is a weak correlation between step and stride lengths with height during running locomotion activity, but a stronger correlation exists during walking locomotion activity. The group of male and female subjects (leg length generally corresponds to height) found only 7.53% different of the height distribution between male and female subjects.

On the other sides, the weight range for female subjects is from 41.06 kg to 71.32 kg and 50.72 kg to 91.45 kg for male subjects. In this statistical difference, there is a weak correlation between force weight ratios with weight during running locomotion activity, but a stronger correlation exists during walking locomotion activity. Total of 26.22% different between the weights distribution between two genders.

Size and brand of shoe is not considered as one of the factor that can affect the gait simulation in subject testing. There are nine different size and 14 brands of shoes used by subjects in this testing. From the mean values showed in tables and bar charts, there is not much different for each size of shoe. This can be explained by the equal forces distribution from different size of shoes in this testing.

So, the hypothesis of both simulations is made where the larger values of the anthropometric data might influence the step length, step time, stride length, stride time, walking speed, cadence, and force weight ratio. Another hypothesis is that a few parameters might be affected by the anthropometric data inversely, which means the larger the difference and percentage of error for the anthropometric data, the more the negative values the few parameters will be.

The force distribution trends are being studied well through the subject testing where the common locomotion activities of human being are distinguished with different gait parameters. Valuable data and results are being collected from this subject testing for further data processing and analyzing. The overall results generated are quite satisfied and matched with the readings from gait simulation reasonably. Hypothesis is made for the testing but further research has to be carried out in order to prove the accuracy and consistency of the hypothesis.

4.4.3 Benchmarking of Results

After processing and analysing the results collected, it is essential to benchmark the present results with other studies to understand the differences between the anthropometric details, parameters, and gait patterns of subject testing and experiment from other countries. There are four kind of benchmarking will be done, which are between genders, between devices, normal, and abnormal gait.

4.4.3.1 Benchmarking between Genders

First, a benchmarking between genders is made to study the differences of forces applied for female and male subjects during the standing, sitting, walking, and running locomotion. The average, maximum and minimum peak forces for female and male subjects during all kind of locomotion have been tabulated and represented graphically at Appendix I.

For the standing locomotion, most of the average and maximum peak forces for female subjects are higher than male subjects with more negative values of difference and percentage. But, the minimum peak force for male subjects is comparatively higher than female subjects. Overall, the range of average peak forces by both subjects are from 1.02 N to 13.03 N, the highest value for maximum peak force is 400 N by female subject, and the lowest value for minimum peak force is 2 N by most of the subjects.

By comparing the graphs of overall peak forces for female subjects, more forces have been applied at the left foot, especially at the heel region (L4). For the right foot, more forces are concentrated at the first metatarsal region (R2). The range of the forces from left foot is wider than the right foot where the maximum peak forces are around 1100 N from left foot and 1000 N from right foot. Therefore, by analyzing the forces distribution during standing locomotion, female subjects tend to shift their left foot to heel region and shift inner around the metatarsal region for their right foot.

Same for the male subjects, more forces have been applied at the left foot around the heel region (L4). For the right foot, more forces are distributed at the first metatarsal region (R2) which is slightly same with the female subjects. The maximum peak forces from left foot are around 1200 N and about 850 N from right foot. After analyzing the overall peak forces for male subjects, it can be concluded that male subjects tend to shift their left foot to heel region and shift inner around the metatarsal region for their right foot during standing locomotion.

By observing the overall peak forces from both foot for female and male subjects during standing locomotion, the graphs showed that more forces have been used by female subjects than male subjects. Most peak forces are below 2000 N for female subjects and below 1500 N for male subjects which are about 500 N different between both subjects. However, the results for male subjects are more reasonable compare with the female subjects. The inaccuracy of results might be caused by some factors, like the standing position, body angle while standing either forward or backward by referring to the vertical direction of standing posture.

Like standing locomotion, most of the average and maximum peak forces for female subjects are higher than male subjects with negative values of difference and percentage for the sitting locomotion. In addition, minimum peak force for female subjects is higher than male subjects as well. Overall, the range of average peak forces by both subjects are from 0.05 N to 11.69 N, the highest value for maximum peak force is 386 N by female subject, and the lowest value for minimum peak force is 2 N by most of the subjects.

By comparing the graphs of overall peak forces for female subjects, more forces have been applied at the left foot, especially at the heel region (L4) which is same as the standing locomotion. For the right foot, more forces are concentrated at the first metatarsal region (R2). The range of forces from left foot is wider than right foot where the maximum peak forces are around 1300 N from left foot and 500 N from right foot. Therefore, by analyzing the forces distribution during sitting locomotion, female subjects tend to shift their left foot to heel region and shift inner around the metatarsal region for their right foot.

Same for the male subjects, more forces have been applied at the left foot around the heel region (L4). For the right foot, more forces are distributed at the first metatarsal region (R2) which is slightly same with the female subjects. The maximum peak forces from left foot are around 600 N and below 250 N from right foot. After observing the overall peak forces for male subjects, it can be concluded that male subjects tend to shift their left foot to heel region and shift inner around the metatarsal region for their right foot during sitting locomotion.

By monitoring the overall peak forces from both foot for female and male subjects during the sitting locomotion, the graphs showed that more forces have been used by female subjects than male subjects. Most peak forces are around 1200 N for female subjects and below 800 N for male subjects which are about 400 N different between both subjects. Less force has been applied in this locomotion as expected because not much force will be used to support the body while sitting. But, the results showed for female subjects are less reasonable as the values should be lower than male subjects according to their ranges of body weight.

In the walking locomotion, most of the average peak forces and maximum peak forces for female subjects are higher than male subjects by getting more negative values of difference and percentage. However, the minimum peak force for male subjects is comparatively higher than female subjects. Overall, the range of average peak forces by both subjects are within 1.68 N to 12.79 N, the highest value for maximum peak forces is 417 N by female subjects, and the lowest value for minimum peak force is 2 N by most of the subjects.

By observing the graphs of overall peak forces for female subjects, overall forces are distributed equally at both foot and all the foot regions. The range of forces applied is similar for both foot, which are below 2000 N. Compare to previous locomotion, the forces generated in this locomotion are more pack, concentrated, and saturated. The peak forces generated during each step taken by the subjects can be monitored clearly along the walking locomotion. Therefore, the results showed that the pattern and forces applied by female subjects are distributed equally beneath the foot region during walking locomotion.

Same for the male subjects, overall forces are generated and distributed equally at both foot. The range of forces applied is slightly lower than female subjects, which are below 1600 N. Unlike female subjects, forces applied at the heel region (L4 and R4) from both foot for male subjects are comparatively lower than other regions. Compare to previous locomotion, the forces generated in this locomotion are more pack, concentrated, and saturated as well. By referring to the results, it can be concluded that male subjects tend to use the front part of the foot region rather than heel region during walking locomotion.

From the graphs of overall peak forces from both foot for female and male subjects, more forces have been generated by female subjects than male subjects. Most peak forces of female subjects are around 2500 N and 2000 N for male subjects which are about 500 N different between both subjects. Obviously, the range of forces applied is bigger for female and comparatively more steps have been taken than male subjects. The results for walking locomotion are quite reasonable and acceptable as the forces generated during walking locomotion are normally one to one and half times more than the body weight.

Like previous locomotion, most of the average and maximum peak forces for female subjects are higher than male subjects with more negative values of difference and percentage for the running locomotion. Besides, most of the minimum peak forces for male subjects are higher than female subjects. Overall, the ranges of average peak forces by both subjects are from 0.90 N to 15.54 N, the highest value for maximum peak forces is 429 N by female subjects, and the lowest value for minimum peak force is 2 N by most of the subjects.

The overall peak forces generated by female subjects from left foot is slightly lower than the right foot. However, the forces have been applied at both foot are equally distributed like in the walking locomotion. During running locomotion, forces are generated more at the big toe (L1) and first metatarsal (L2 and R2) regions. The range of forces from right foot is wider than right foot at this locomotion where most peak forces are around 1000 N from left foot and around 1500 N from right foot. By analyzing the forces distribution in this locomotion, female subjects tend to apply more forces and use the front part of foot while running.

Same for the male subjects, more forces have been applied at the right foot than left foot. Most of the forces have been applied around the big toe (L1) and first metatarsal (L2 and R2) regions which is slightly same with the female subjects. Like in the walking locomotion, fewer forces have been generated at the heel (L4 and R4) regions for both feet. Most peak forces from left foot are around 800 N and below 1000 N from right foot. After observing the overall peak forces for male subjects, it can be concluded that male subjects tend to shift their body much more to the front where more forces will be concentrated at the front part of the foot and there are only a little or light movement for the heel regions during running locomotion.

By monitoring the overall peak forces from both foot for female and male subjects during the running locomotion, the graphs showed that more forces have been used by female subjects than male subjects as usual. Most peak forces are below 3000 N for female subjects and below 2500 N for male subjects which are about 500 N different between both subjects. Obviously, the range of forces applied is bigger for both subjects and comparatively more steps have been taken than during the walking locomotion. Results showed that more force has been applied in this locomotion as expected because the forces used during running locomotion are normally two to three times more than the body weight.

After observing and analyzing all of the locomotion, the force distribution trends are being studied well through this subject testing where the common locomotion activities of human are being distinguished by monitoring the pattern, concentration, and saturation of peak forces generated. The average, maximum and minimum peak forces have been calculated and tabulated accordingly. The overall results generated by each sensors of the insole system are quite satisfied and matched with the theory from gait simulation reasonably. However, some of them are not close to the ideal values which might be affected by certain internal or external factors.

4.4.3.2 Benchmarking between Devices

Apart from the benchmarking between genders, an additional benchmarking between devices is performed as well for the instrumented insole system and treadmill system. The data like average, maximum and minimum peak forces are being calculated and tabulated for a clear understanding. Furthermore, graphs are plotted to show a clearer picture of the overall peak forces generated from both foot for both subjects.

The range of average peak forces for running locomotion is wider than the walking locomotion, where the values are around 310.46 N between female and male subjects in running locomotion from 565.42 N to 875.88 N. For walking locomotion, there is about 136.41 N different between female and male subjects which is from 395.44 N to 531.85 N. Overall, the average peak forces for running locomotion is higher than walking locomotion, which are 720.65 N and 463.65 N respectively.

The maximum peak forces achieved for walking locomotion is lower than in the running locomotion as expected where an overall peak forces of 1342.60 N for walking locomotion and 1766.49 N for running locomotion. For minimum peak forces, forces generated in the walking locomotion are lower than the running locomotion, which are 345.66 N and 427.86 N for running locomotion.

For walking locomotion, the overall peak forces recorded by insole system are within 500 N to 4500 N. At the other side, the overall peak forces recorded by treadmill system are lower than the insole system, where all the peak forces generated are below 3500 N. Next, the overall peak forces recorded during the running locomotion are higher than the walking locomotion, where the peak forces recorded by the treadmill system is around 4000 N and 4500 N by the insole system.

Obviously, there is a wide range of forces recorded by the insole system which is around 4000 N but there is a small range of forces detected by the treadmill system for both locomotion. Moreover, steps that taken by the subjects can be observed clearly in the results recorded by insole system. For results recorded by the treadmill system, not much change of peak forces can be monitored where the trend line is less fluctuated as compare to results recorded by insole system.

Furthermore, the big fluctuation of trend line showed at the graphs recorded by insole system provides the maximum and minimum peak forces for each step that have been taken by subjects from time to time in both locomotion which cannot be showed at the graphs recorded by treadmill system. The graphs showed for this comparison which are recorded by the insole system are the results from combination of all sensors for both foot. As mentioned in previous comparison, peak forces generated at different regions beneath the foot can be detected by different located sensors. Thus, insole system can provide both separated and combined peak forces according to different type of analysis and requirements.

Through this benchmarking, the advantages of using insole system in detecting the peak forces generated by subjects during each locomotion are being discovered and identified. It can be concluded that treadmill system is used particularly to provide a general peak forces generated beneath the foot but not as advance as insole system which is able to detect the peak forces at different regions beneath foot, the steps taken by the subjects, and even displaying out the maximum and minimum peak forces applied by the subjects at all of the locomotion either separately or combined together in a graphical form.

4.4.3.3 Benchmarking for Normal Gait

Some data from several researches and studies from other countries regarding the normal gait analysis are used in this benchmarking with the present results. The comparison tables between the present subject testing and other studies are showed at Appendix I. The lists of data from other researches and studies which used in the benchmarking are showed at the table below.

The earliest gait analysis which found for the benchmarking is by Oberg and his colleagues at 1993 which is about the basic gait parameters for normal subjects. For the study done by Auvinet and his colleagues involved in a big population which is around 200 subjects. But there are four times lesser for study of Titianova and his colleagues with quite a big range, from 21 to 61 years old.

For the studies done by Korea and Netherland researchers are the few studies from the table above which has the group of subjects whose age is nearer to the present subject testing. Studies from Canada (McKean, Landry, Hubley-Kozey, Dunbar, Stanish, and Deluzio, 2007) and Japan (Yu, Riskowski, Brower, and Sarkodie-Gyan, 2009) showed quite a big range of age for the subjects involved in their testing, which is roughly from 18 to 65 years old.

Table 4.1: Demographic Information and analysed parameters of previous gait analysis for normal gait

Study (Year)	Nationality of Population	Number of Subjects (Male, Female)	Age of Subjects
Oberg et al. (1993)	Sweden	30 (M: 15, F: 15)	20 – 29
Auvinet et al. (2002)	France	282 (M: 138, F: 144)	Over 20
Titianova et al. (2004)	Finland	62 (M: 21, F: 41)	21 – 61
Cho et al. (2004)	Korea	98 (M: 51, F: 47)	20 – 29
Ryu et al. (2006)	Korea	32 (M: 20, F: 12)	20 – 29
McKean et al. (2007)	Canada	42 (M: 18, F: 24)	35 – 65
Senden et al (2009)	Netherlands	20 (M: 10, F: 10)	20 – 29
Yu et al. (2009)	Japan	10 (M: 5, F: 5)	18 – 49

Two tables are formed to tabulate the data for comparison between present results and eight of other studies for both male and female subjects from a few countries. There are certain parameters are not stated or listed in some of the studies and thus some of the parameters are not available for the comparison. In the comparison, almost all the subjects from those studies are around twenties years old, which is the same as the present subject testing. This is important as the walking speed and step length might be affected by the age of subjects.

For female subjects, there are a few differences can be noticed from the comparison of normal gait parameters for female subjects. First, there is a different between the height of subjects from Asia and Western. The height for Asia female subjects are around 1.58 to 1.60 m and 1.65 to 1.70 m for Western female subjects.

Obviously, female subjects from Malaysia, Japan, and Korea share the similar heights due to the smaller physical condition of body of Asia countries.

In the weight aspects, it is common for Western female subjects to be higher because they are taller than Asia female subjects, and yet, in this case, the Malaysia female subjects have the mean of weight which is much lighter than the female subjects from Japan. This might be caused by the difference of nationality and the lifestyle that affect the physical condition of body indirectly in different countries. However, this might not affect much to other parameters in the studies and testing.

By comparing to other population, the walking speed of Malaysia female subjects is not comparable as a constant speed is set for the present testing. However, Asian country showed a slower walking speed than the other countries for the female subjects, such as Korea and Japan, which is more or less having the similar walking speed. For female subjects from Japan and Korea, the walking speed is around 0.88 to 1.12 m/s, where the other countries vary from 1.24 to 1.54 m/s.

The step length of female subjects from Malaysia is higher than other countries including the Asian countries, which is 0.94 m. The mean of the step length in the studies for female subjects from Korea, and Sweden are around 0.59 to 0.61 m, whereas for the France, Finland, and Netherlands are having the step length around 0.74 to 0.75 m. This may due to the differences of leg length, height, and walking speed between the countries. Thus, stride length is larger than the Asian and Western countries too.

The cadence of the female subjects from France, Finland, Netherlands, and Sweden are higher than female subjects from Korea and Malaysia. The cadence for the Western countries is around 120.24 to 124.80 step/min which is higher than male subjects as well. For Asia country, around 107.30 to 112.50 step/min of cadence is achieved. This might caused by the culture of different countries which the rhythm of living is slower than other countries.

On the other hands, the mean of height and weight for male subjects from the present testing is close to the studies from the Asia country. This may be one of the

factors that affect the walking speed for Asia subjects, including the present results, which is slower for the male subjects from Asian compare to Western countries. This might due to the same ratio of height and leg length of the population. However, a constant speed is set for the male subjects in the testing and hence, not much comparison can be done for this walking speed parameter.

In this benchmarking, the step and stride length of present results is slightly larger with the studies from other countries, which are 1.06 m and 1.92 m. The mean of the step length in the studies for male subjects from Sweden, Finland, Japan, and Korea are around 0.62 to 0.74 m, whereas for the France and Netherlands are having the step length about 0.83 m. For the stride length, the male subjects from Finland are having much longer stride than the male subjects from Korea and Japan but lower than the male subjects from Malaysia.

The male subjects from Finland produced the highest cadence, which is 120.80 step/min and the lowest is achieved by the male subjects from Malaysia with 89.68 step/min. This showed that more steps are taken by male subjects from Finland in a minute which approximately 0.50 seconds to step for a distance of 0.74 m. For the other countries, like Korea, France, Netherland, and Sweden, the male subjects scored around 107.24 to 118.80 step/min.

In conclusion, a few differences between the subjects from Asia and Western are being determined, like in the aspects of height, walking speed, step length, cadence, and so on. This might due to certain uncontrolled or controlled reasons and factors, such as physical condition of body, lifestyle, and nationality. It can be concluded that most of the parameters affect or change proportionally to each others. However, there are still a lot of parameters not included in this benchmarking which can be improved by considering more factors from every aspect, like races or ages in future.

4.4.3.4 Benchmarking for Abnormal Gait

Except for the normal gait comparison, some data for abnormal gait are being compared with the present testing results as well. Most of the abnormal gaits are taken from subjects with disabilities or diseases, such as multiple sclerosis and Parkinson's disease. The comparison table is showed at Appendix I. The lists of data from other researches and studies which used in the abnormal gait benchmarking are as followed.

Table 4.2: Demographic Information and analysed parameters of previous gait analysis for abnormal gait

Study (Year)	Nationality of Population	Number of Subjects (Male, Female)	Age of Subjects
Bogataj et al. (1997)	Austria	20 (M: 20, F: 0)	40 – 49
McKean et al. (2007)	Canada	39 (M: 24, F: 15)	35 – 65
Morris et al. (2008)	USA	5 (M: 2, F: 3)	54 – 77
Chen et al. (2009)	China	24 (M: 19, F: 5)	4 – 12
Givon et al. (2009)	Israel	81 (M: 28, F: 53)	22 – 41
Vergheze et al. (2010)	USA	40 (M:0, F: 40)	Over 70
Tanaka et al. (2010)	Japan	43 (M: 0, F: 43)	50 – 60
Allet et al. (2010)	Switzerland	71 (M: 35, F: 36)	55 – 71
Gaudreault et al. (2010)	Canada	11 (M: 5, F: 6)	7 – 15

By referring to the table above, the earliest study is by Bogataj and his colleagues at 1997 for 20 stroke subjects. After that, a study on osteoarthritis subjects from Canada is studied by McKean and her colleagues. Another latest study from Canada is by Gaudreault and his colleagues. Next, Morris and her colleagues have carried out a research at year of 2008, where the research is mainly focused about the subjects with Parkinson's disease.

Another study of the abnormal gait parameters found for the benchmarking is by Chen and his colleagues for cerebral palsy young subjects from China. For the

studies done from USA (Verghese and Xue, 2010) and Japan (Tanaka, Shigematsu, Motooka, Mawatari, and Hotokebuchi, 2010) are mainly focused for the subjects with arthroplasty and predisability problems.

Furthermore, Givon and his colleagues work on the gait impairment in multiple sclerosis. In addition, a big group of diabetic subjects are being recruited for the study by Allet and his colleagues from Switzerland. Huge amount of subjects and quite a wide range of ages of subjects are recruited in these studies where the information provided serves as a good reference for present testing.

Obviously, the walking speeds of stroke subjects are three to four times slower than healthy subjects. This might due to the reason that the excursions in the knee and hip are decreased and their weight bearing on the affected leg is not stable. Their independent during gait is comparatively lower than healthy subjects as external support is needed. They faced difficult in accomplishing the distance per session where bad gait symmetry is happened that the subjects lacked the push-off on the affected side.

According to Bogataj and his colleagues, knee flexion is performed instead of ankle plantar flexion at the beginning of the swing phase. More time is needed to make a small step, same as the stride. This might due to the slow weight shifting to the impaired side and small excursions in hip, knee, and ankle joints on both sides. Most of the subjects walked rigidly where the flexion of the knee for shortening the leg during the swing phase on the affected side is compensated by inclining the trunk on the non-affected side while leaning on the something, like crutch.

Osteoarthritis is a dynamic, progressive disease causing significant disability and loss of function (McKean, Landry, Hubley-Kozey, Dunbar, Stanish, and Deluzio, 2007). Knee osteoarthritis is two to three times more prevalent in females than males and females have two times the risk of developing bilateral knee osteoarthritis. This might affect the biomechanical environment of the lower limb. However, the gait parameters of these subjects having the values which is much closer to the readings of healthy subjects.

From the study, it mentioned that female subjects walked with less hip internal rotation, a smaller flexion moment, and a larger adduction moment than male subjects. Male subjects have greater hamstring and quadriceps strength than females. Like healthy subjects, their stride lengths are quite similar with the normal gait readings. As a summary, the osteoarthritis subjects are having higher weight, slower walking speed, and shorter stride length of the population relative to the healthy subjects.

Parkinson's disease is one of the most common degenerative diseases in the general population. The results showed that the stride length of Parkinson's disease subjects is smaller but more stride time is needed compare to healthy subjects. Like other abnormal gait studies, Parkinson's disease subjects have a tendency to be smaller in most of the parameters. Thus, those parameters, like step length, step time, walking speed, and so on can be extracted as features to evaluate gait disorder.

The walking speed of cerebral palsy children is selected as one of the better indicators of walking ability, speed decreases with injury pain, and increases with recovery. Walking speed different in the study probably resulted in the different age range of subjects. No difference in duration, which indicated that duration could not be an evaluation standard for children with cerebral palsy. Their step lengths are shorter as they faced difficult in stable walking and the requirement of the coordination ability of neuromuscular system is higher than the stable walking.

This might be caused by high muscle tension, weak control and balance ability of limbs, low speed and accuracy of posture change for children in cerebral palsy. During normal walking, they have to turn to compensatory mechanism, which is to decrease single support period and increase double support period to keep the balance of body to decrease the risk of fall and coordinate next motion. Thus, the results for the gait parameters are the lowest values among other studies.

Multiple sclerosis is a significant gait impairment leading to decreased activity and limitations in function. These parameters are consistent with spasticity and motor weakness, found in most of multiple sclerosis subjects from the study done by Givon and his colleagues. Overall estimation of gait parameters is

significantly lower in multiple sclerosis compare to healthy subjects, and highly correlated with neurological disability.

The gait parameters are found to be associated with decreased gait walking speed, decreased step length, and shortened single support with prolonged double support compared to healthy subjects. Thus, it can be concluded that the multiple sclerosis subjects experienced more replaced overtime their neurological impairment increased in severity and their walking ability is decreased.

Predisability is a common symptom that will be faced when a person gets older. From the study, the findings showed that elderly individuals with predisability have slower walking speed and stride length during normal pace walking compared to the nondisabled subjects. Thus, execution of customary motor tasks is said to require a substantially greater effort in older adults compared with young adults, and even normal older adults perform activities of daily living, such as walking close to their maximal capabilities.

Total hip arthroplasty is a well-accepted treatment modality for severe hip osteoarthritis, and it is considered as one of the most successful orthopaedic procedures. Gait analysis has been widely acknowledged as an objective method for evaluating the gait function after total hip arthroplasty. Thus, this study is being selected and added into the benchmarking. In comparison with subjects in other studies, the subjects in this study showed lower walking speed, stride length, and cadence although the mean age of subjects is not lower than the mean ages of those in other studies.

By referring to the study, these parameters have been reported to normalize within one year, one to three years, two to four years, and eight to ten years after total hip arthroplasty. These differences might be attributed to the fact that the subjects faced more severe hip pain, and tried to reduce the load-bearing ability of the involved hip. It is believed that the values of the mean stride length, single support duration of the involved legs, cadence, and walking speed increased after the operation.

Type two diabetes mellitus and its common complication peripheral neuropathy, affect a large population. Peripheral neuropathy leads to sensory and motor deficits, which often result in mobility-related dysfunction, alterations in gait characteristics and balance impairments. As expected, diabetic subjects with peripheral neuropathy have lower gait walking speed, shorter stride length, and decreased cadence compared to the normal gait from healthy subjects.

Foot ulceration is the most common cause of amputation in diabetic subjects. Neuropathic plantar ulcerations result from repetitive stress over areas of high pressure associated with deformity or joint limitation. Although the readings of parameters can be considered and categorized into normal gait but extra foot care and shoe gear education are needed essentially to prevent the increased of dynamic foot pressure. It is one of the identified risk factors in the formation of diabetic foot ulcer.

Locomotor system impairments such as progressive muscle weakness, muscle fatigue, and the development of joint contractures alter the gait abilities of children with Duchenne muscular dystrophy (Gaudreault, Gravel, Nadeau, Houde, and Gagnon, 2010). Natural walking speed is reduced in comparison with healthy subjects due to the decreased step length. Their short step length is a consequence of decreased hip extension angles seen during the locomotion activities.

The cadence observed is quite high for these subjects which might be a way to preserve their walking speed considering their reduced step length. As regards kinematics and kinetics, subjects with this disability modify their trunk and lower limb position so that the flexor muscles sustain the effort rather than the extensors during the locomotion activities. It can be concluded that the subjects can effectively use their quadriceps to sustain an external moment.

In a conclusion, the analysis on temporal and spatial gait parameter of normal and abnormal groups demonstrated some necessary parameters which can be used to assess the walking ability. This benchmarking successfully demonstrates a difference in gait characteristics between normal and abnormal gait. It is important for better understand the mechanism underlying the improvement in gait analysis and characteristics, further calculated the respective contributions of parameters.

4.5 Readings from Multimeter

The multimeter is used to test and measure the maximum voltage obtained when a force is exerted on the FSR sensors when the changes in force applied occurred during human locomotion activities.

A circular shape FSR sensor, FSR-402 is placed under the big toe (hallux) region and a square shape FSR sensor, FSR-406 is placed under the heel region of a subject with the body weight of approximately 45 kg. From the unit conversion, 1 kg of body mass is equivalent to 9.81 Newton. By converting the unit, 47 kg is equivalent to 461.07 Newton. An output resistance of 4.32 k Ω and 4.71 k Ω is recorded respectively from the multimeter.



Figure 4.42: Output resistance of FSR-402 (big toe region) by multimeter



Figure 4.43: Output resistance of FSR-406 (heel region) by multimeter

4.6 Problems and Difficulties

There are some problems and difficulties encountered during the whole process of developing this instrumented insole system. Most of these problems occurred due to the lack of basic knowledge especially in software and programming. Along the developing process, trial and error is carried out from time to time to gain more understanding on how the system works and fix those problems one by one. Some of these problems also affect the outcome of the results causing deviation and inaccuracy in the gait simulation. These problems and difficulties are mentioned and discussed in the following sections.

4.6.1 Force Sensing Resistors Interface

The Interlink Force Sensing Resistor (FSR) is the only sensor and the most important component that used in this design. However, this component is quite expensive and is not available in the local market. Therefore, some survey is done to look for a better quality and reasonable prices among companies from overseas. Finally, total of eight sensors purchased from a Singapore company (the nearest overseas company) through internet.

FSR sensor is a very sensitive component, but there are some disadvantages as well. First of all, the noises produced by the sensors are rather high. From the result collected, most of the results are affected by the noises (both from the devices and sensors) where the displayed results is not exactly the results that generated by the sensor. It affects the gait simulation due to the deviated and inaccurate results collected.

Moreover, the sensor is a very thin component with thickness at approximately 0.46 mm. Heat is generated when it is powered up. In the simulation, this sensor will be encapsulated beneath insole sheet and placed into subject's shoe. Thus, the heat generates faster (due to self-heat and environment temperature). There is a possibility that the heat will damage the sensor and causing it to malfunction.

4.6.2 XBee Module Interface

The efficiency and accuracy of XBee module will reduce when something is blocked by wall between the transmitter and receiver. Transmitted data to computer is found to be not same as the data generated by the sensors where some readings might be missing at the intermediate. Therefore, a wide space with no wall blocking between is needed for the gait simulation and subject testing to prevent such incident happened.

Another common transmission problem is the XBee module will not able to transmit the data properly when the battery gets weak. The XBee module will start sending looping results, which signifies that the power is low. Compare to Bluetooth module, XBee module in wireless transmission has a less power consumption.

The typical power consumption of XBee module transmitting data at default baud rate 9600 Kbps using UART is 45mA. A normal 9 V battery supply will usually last for three hours. However, it still used up quite a number of 9 V battery in this project during the subject testing. Total of six 9 V batteries and two rechargeable 9 V batteries are used for conducting 30 subjects of the subject testing.

Table 4.3: Specifications of XBee module

Specifications	Average	Unit
Transmit Current	45	mA
Receive Current	50	mA
Power-down Current	<10	μA
Sleep Time	3600	s
Wake Time	5000	ms
Time Transmitting	50	%
Average Current	0.9141	mA
Cyclic Sleep Current	0.045	mA
RF Data Rate	250	kbps

Source: XBee/XBee-PRO OEM RF Module, 2006

4.6.3 PIC Coding and Programming

PIC programming is one of the important softwares that being used in this project to collect the analogue signals and converts them into digital signals. PIC programming can be written either in Assembly language C, C language or a mixture of both. Because of this, there is some confusion in using both languages at the same time as there is lack of experience to program in assembly language. Finally, assembly language mixture with C language is used.

Besides, the UART or USART function used in ADC module in PIC is not written in any examples or books clearly. Different reference books explained different type of examples and style of writing this UART function. During the writing process, trial and errors have to be carried out in exploring the function of *Usart_write* in mikroC compiler, including the initial function to set the baud rate, reading function to collect input signals from sensors, and writing function to write and send the converted signals.

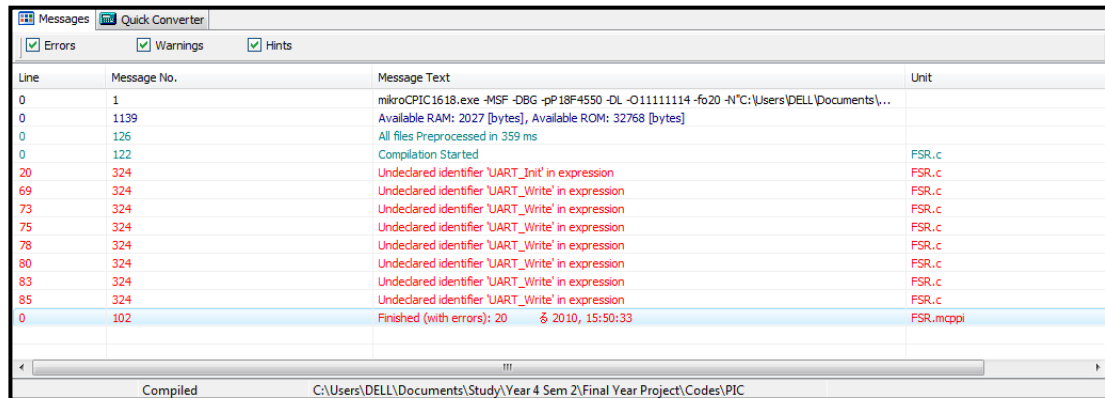


Figure 4.44: Error message during compiling UART function

Furthermore, there is also unclear information of what is the format of the output for the analogue to digital conversion. Some reference books mentioned that the output is a 10-bit binary data separated into lower bit and higher bit, but some of them wrote the output is the decimal voltage translated from the inputs (Mazidi, 2008). Therefore, there is no any idea about following which reference books due to the lack of understanding in judging and selecting the correct option to be taken.

4.6.4 LabVIEW Discovery

LabVIEW is another software that used in this project, which responsible for collecting data from microcontroller, processing them into a displayable graphical form, and analyzing those data using extra features, such as filters, conversion factor, and data storage functions.

This software is totally new and not included in the course structure. So, a lot of time is allocated to learn up this software and to practically implement it on this project. Due to the lack of references related to this software, limited and basic knowledge is acquired only. For sure, reading is done and examples are being referred from time to time in completing this task.

First, there are several times that LabVIEW is failed to read the data from the COM port even though the communication has been connected successfully through XBee module with microcontroller. Next, while loop and case structure are used in some parts of the system. Some troubles are faced in selecting the loop and structure condition (TRUE or FALSE) so that those parts can be operated well.

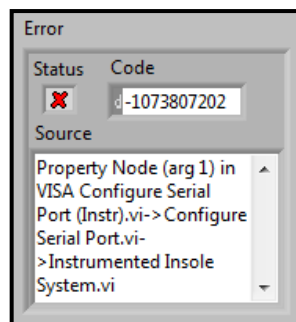


Figure 4.45: Error message during configuring serial port

Other problems are like in converting the string input to array format or converting the decimal string to number, using the match pattern function, formula node for conversion factor, build array and waveform for results displayed purpose. Besides, times are used to learn and build sub-VI like Configure Serial Port, Error Handler, Adjustment Filter, and Read File From Text File in order to carried out the required task and work the system perfectly.

4.6.5 Hardware Assembly

Some of the electronic components are fragile in this project. Mostly, the problems occurred during or after soldering process. One common recurring problem is the loose connection of wires and components on the donut board after soldering. In some cases, the fragile single core copper wires are snapped and detached from the solder points which might cause the circuit malfunction or even short circuit.

In additional, the pins of LM324 operational amplifier, PIC18F4550 microcontroller, SK40C enhanced 40 pins PIC start-up kit, and XBee starter kit can be bent or broken down easily. Sometimes, the pins might be loose and pops up from the donut board easily. Therefore, extra attention is needed in placing such components onto donut board, especially for LM324 operational amplifier as the pins are tiny and smaller compared to others.

Next, the connection of wires between components are quite complicated in this project as it involves ten FSR sensors, where each sensor are connected with two different output wires to the electronic circuit. Furthermore, each sensor outputs are connected to resistor and operational amplifier correspondingly. Hence, there are quite a number of electronic components needed to be connected together where an arrangement is needed to before placing all of them inside a donut board.

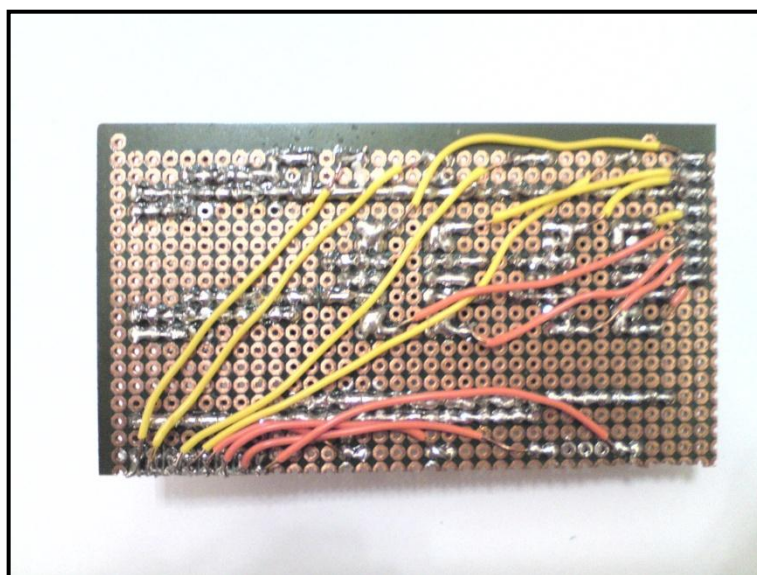


Figure 4.46: Wires connections of electronic components

4.6.6 Noise Disturbance

From the results obtained, there are noises existed without FSR sensors connected and even not wearing by user as well. The sources of these noises are still unknown and not mentioned in any data sheet. But, the guess would be that they origin from the sensors, PIC16F877A microcontroller, and SK40C enhanced 40 pins PIC start-up kit board outputs.

It is not denied that those noises affect the gait simulation results in terms of consistency and accuracy. The results displayed in the graphs are fluctuated and not stable along the period of gait simulation which makes the collected data difficult to be processed and analyzed.

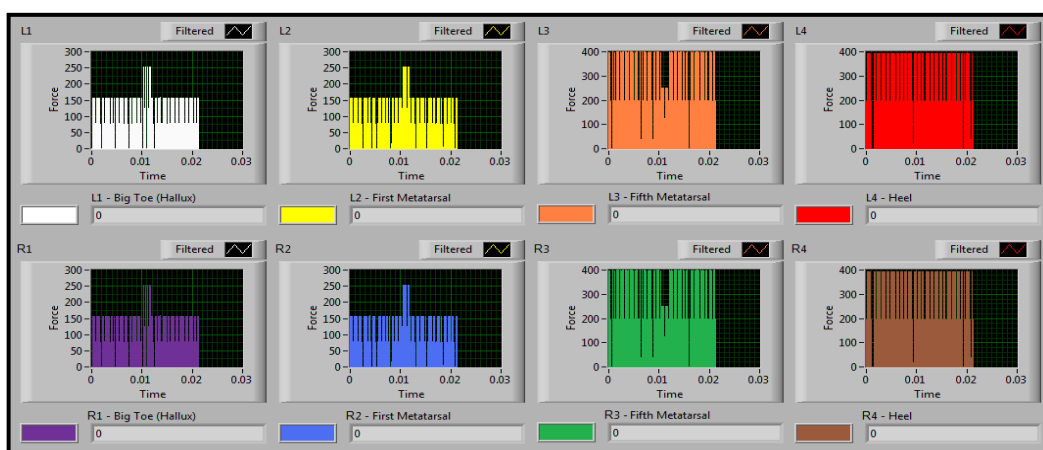


Figure 4.47: Noises generated by the devices (without filter)

As discussed earlier, there is a formula used as the voltage to force conversion factor. The input signals (output voltage) from the sensors will be converted by using this formula so that the output signal (force) can be displayed out as results. If there is the present of noises, this formula is not able to be performed in order to distinguish and record the correct and accurate readings from the sensors.

$$L1 = (L1 * 5 / 255) / 0.6 * 63.765;$$

Figure 4.48: Formula used for conversion factor

4.6.7 Time Delay

During the testing and trial of this project, LabVIEW will somehow has delay in displaying the readings and graphs after the system has been switched on and connected for a long time. When this happens, LabVIEW shows the results of the sensors after a few seconds. The possibility to this is that the delay time for each result sent from XBee module does not match with the result deliver to LabVIEW for data processing and displaying.

The total of eight sensors is sending signals out to the LabVIEW through XBee. This might used up a few milliseconds for collecting the data in the microcontroller. Therefore, there is a delay wrote in the PIC coding with the purpose to wait for the data collecting process from sensors and buffering the collected data before sending out to the LabVIEW. Besides, a few milliseconds might be used as well for the data transmission through XBee module.

Inside the LabVIEW, delay functions are used for this incident. Delays of 50 milliseconds are used in the VISA read and write for incoming data from the sensors, matching alphabet of each sensor, and storage of data in text file. The accumulation of a few milliseconds of delay for each result from the sensors outputs to the LabVIEW system eventually will stack up to a few seconds of delay after a long run.

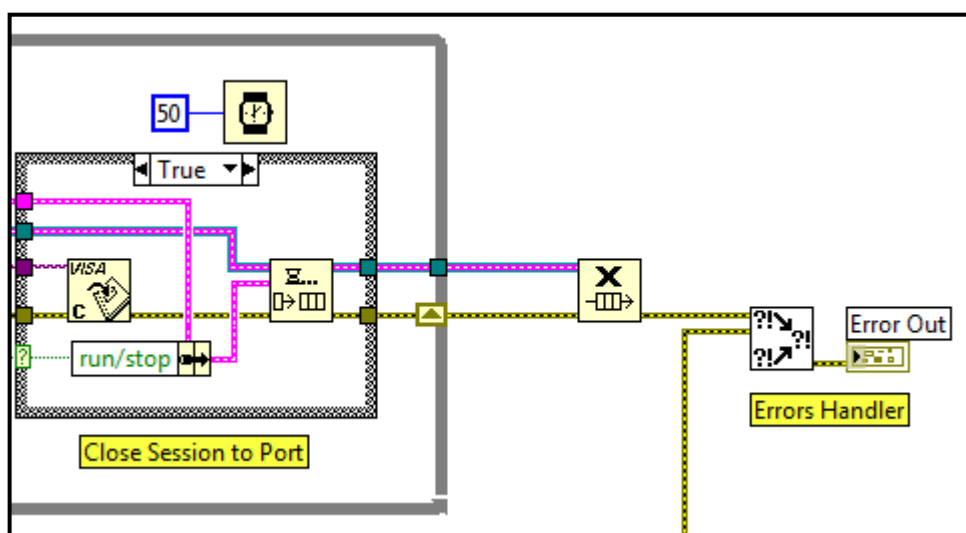


Figure 4.49: Delay function in LabVIEW

4.6.8 Text File Saving

In the LabVIEW graphical programming system created, sensors from each side of foot are saved to an individual text file. Since there are ten sensors from two side of foot, there are two individual text files. If the number of input increased, there will be more text file created.

LabVIEW is capable of saving the inputs in a spreadsheet format by using the “Write To Spreadsheet File”. However, this function is not being carried out due to the insufficient of knowledge and examples of such function. So, “Write To Text File” function is used instead of the “Write To Spreadsheet File” as it might carry the same function in saving the files. For this, “Read From Text File” VI is created to read and display the results that being recorded through “Write To Text File” function.

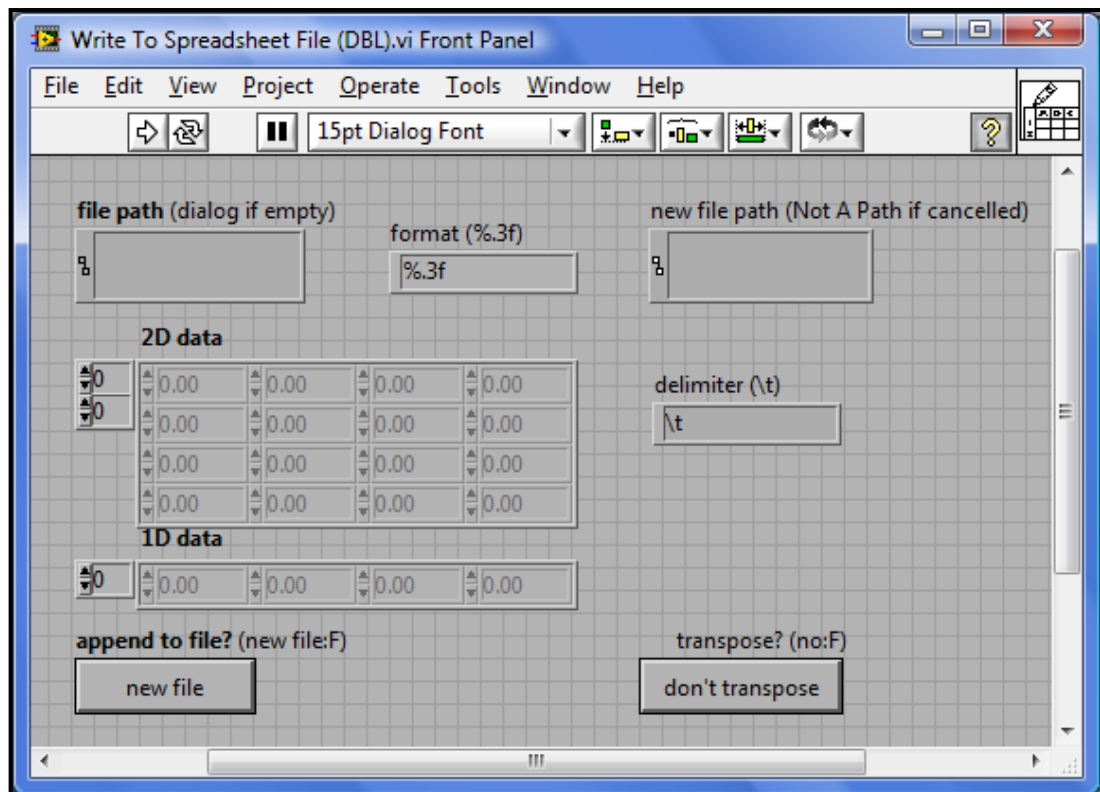


Figure 4.50: Write to spreadsheet file front panel interface

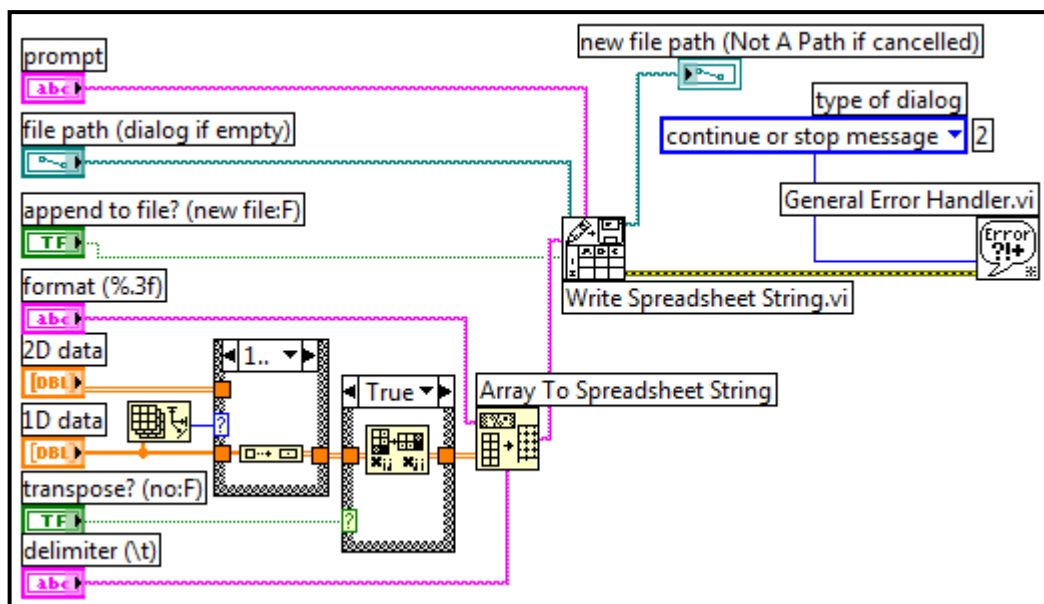


Figure 4.51: Write to spreadsheet file block diagram interface

Although there are only two individual text files being created for each time of gait simulation, they might eat up quite a number of memory and space in the computer. For 10 minutes, the text file size might go up to 700 KB for one individual text file, so total of two individual text file will be around 1.40 MB. This might be inconvenient to the gait simulation for long period of time.

4.6.9 Data Analysis Format

Only a basic data analysis and summary of results are done due to the insufficient of time and pack schedule for the subject testing. In this project, basic and general techniques are used to summarize the data collected from subject testing through a few types of software, like Microsoft Office Word and Microsoft Office Excel.

The data collected from the subject testing is being analyzed by summarizing all of the results in terms of step length, stride length, cadence, walking speed, and so on for each locomotion activity. After that, tables and bar charts are formed. Other advanced methods are not being used in this project for the data analysis purposes.

4.7 Further Improvements and Optimizations

After identifying the problems and difficulty, efforts and precautionary steps should be taken to minimize or overcome the problems and difficulty highlighted previously. The following sub-section will discuss about the improvements and optimizations that has need to be carried out in order to perform the system perfectly.

4.7.1 Force Sensing Resistors Interface

Due to the budget constraints, FSR is the only sensors that used in this project. In order to get a more accurate or informative results, a few bend sensors, accelerometers or gyroscopes can be added into this instrumented insole system. This might improve the results generated with more information about the bending of the foot, the velocity, acceleration, and the angle of the foot positions.

During the gait cycle especially the mid stance phase, the foot is bent because the body weight is being transferred to the front part of the feet before pushing off with a toe off. Therefore, flexible bend sensor which is around RM 85.00 can be added to the arch of each foot to measure the forces exerted, dorsi-flexion and plantar-flexion of foot.

On the other hands, triple axis accelerometer which costs around RM 150.00 can be attached on the ankle, knee, and waist level to measure the angle of rotation and linear acceleration during gait simulation. Gyroscope with RM 125.00 can be considered as well to be attached together with the accelerometers to measure the angular velocity.

By using such extra sensors, the gait simulation is not restricted to two dimensional measurements, but three dimensional measurements. In this case, the parameters that being focused is no longer the forces only, but the linear and angular acceleration, linear and angular velocity, and the angle of rotation. This made the system becomes more professional and specific in monitoring the gait simulation.

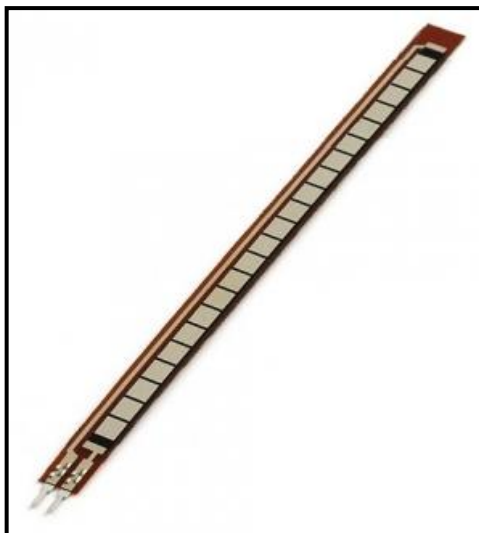


Figure 4.52: An example of flexible bend sensor (Flexible Bend Sensor, 2010)

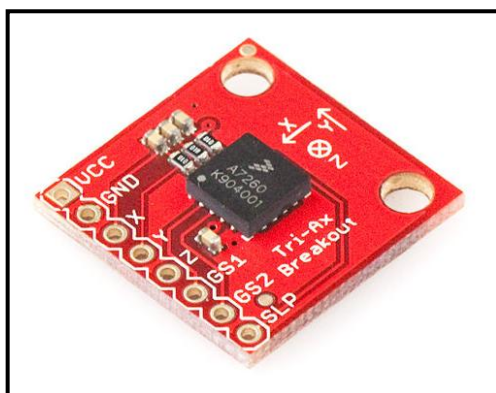


Figure 4.53: An example of triple axis accelerometer (Triple Axis Accelerometer Breakout – MMA7260Q, 2010)

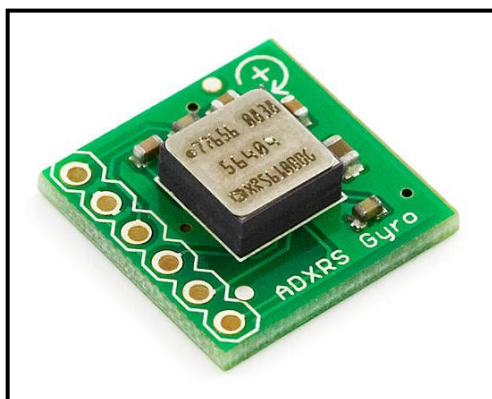


Figure 4.54: An example of gyroscope (Gyro Breakout Board – ADXRS610 300 degree/sec, 2010)

4.7.2 XBee Module Interface

In this project, the instrumented insole system works wirelessly through XBee module. However, the transmission will be disturbed sometimes due to certain reasons, like environmental factors. This might be enhanced by replacing it with XBee-PRO module, which is the upgraded version of XBee module.

XBee-PRO starter kit which costs RM 225.00 has a better communication range than XBee module. Like XBee module, XBee-PRO module is soldered on SKXBee-PRO. This XBee-PRO module supports the unique needs of low-cost, low power wireless sensor networks. The module requires minimal power and provides reliable delivery of data between devices.

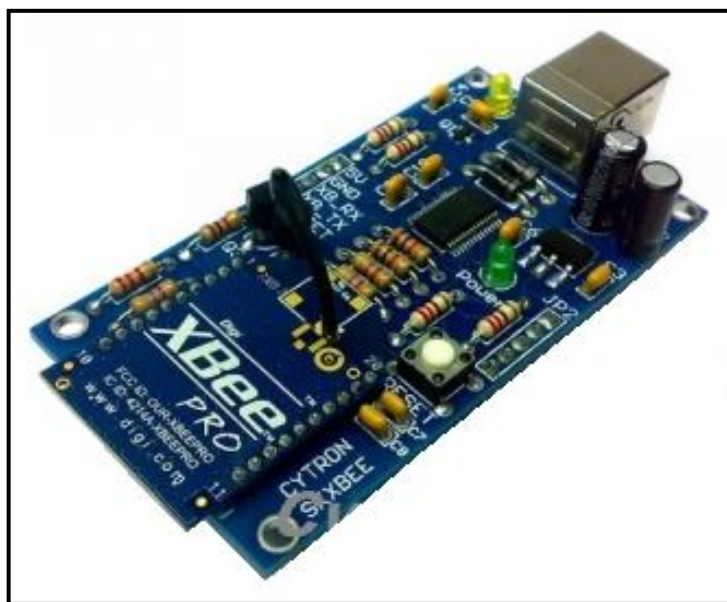


Figure 4.55: An example of XBee-PRO starter kit (XBee Starter Kit SKXBee User's Manual V1.0, 2008)

The module operates within the industrial, scientific, and medical (ISM) 2.4 GHz frequency band and is pin-for-pin compatible with each other. It offers higher transmitter power which will cover up to 1.5 km of wireless communication range. Long range data integrity, point-to-point, point-to-multipoint, and peer-to-peer topologies are supported in this enhanced module.

Table 4.4: Comparison between XBee module and XBee-PRO module

Specifications	XBee	XBee-PRO
Transmit Current	45 mA	215 mA
Receive Current	50 mA	55 mA
Power-down Current	<10 μ A	<10 μ A
Indoor/Urban	30 m	100 m
Outdoor Line-of-sight	100 m	1500 m
Transmit Power	1 mW	100 mW
Receiver Sensitivity	-92 dBm	-100 dBm

Source: XBee/XBee-PRO OEM RF Module, 2006

4.7.3 PIC Coding and Programming Enhancement

The main problems of PIC programming in this project are related to a few main functions, such as USART and ADC conversion. It cannot be denied that these functions are important for the PIC programming as they functioned to get the output signals from sensors, collect the data generated, convert them into digital signals, and then send to computer for processing and analyzing. Without such functions, the system cannot function and thus the gait simulation cannot be carried out.

In completing this project, the process of learning PIC programming is done in a very short time and only fundamentals are being used to compile the program. To enhance the understanding and writing skill in this PIC programming, a lot of readings have to be done by exploring more information, examples, and suggestions which can be found from reference books and forums.

There are a lot of styles in writing the codes, extra time is needed in researching different style and format of writing to figure out which style and format is the best suit for this system. Besides, trial and errors cannot be avoided and must be carried on from time to time by checking the compiled codes. This is essential in figuring out the problems and solving them with better solutions.

4.7.4 LabVIEW Enhancement

As mentioned before, LabVIEW has a “Write To Spreadsheet File” function which can be used to reduce the chances of mixing up the text files of each sensor. The entire text file can be merged together into a single spreadsheet file. A proper format of data inputs can be preset to suit the user’s need.

This function converts 2D or 1D array of string, signed integers, or double-precision numbers to a text string and writes the string to a new byte stream file or appends the string to an existing file. As for reducing the size of the files, results can be selectively chosen before it is written into the text file.

There are some inputs that can be wired to configure the format of data, such as format of string, file path, 2D data, 1D data, append to file, transpose, and new file path. Through this function, the user can make modifications by setting a specific period of time or in what threshold amplitudes that the software should start recording the data.

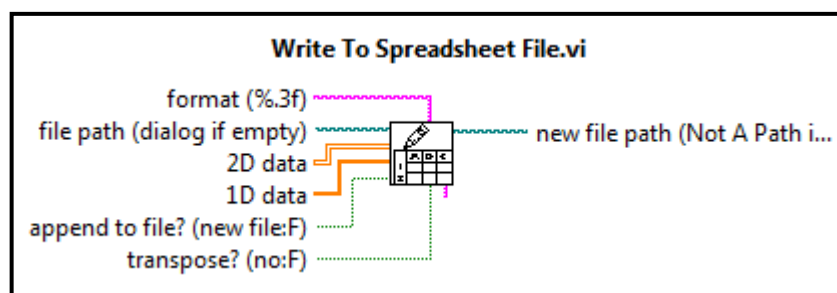


Figure 4.56: Write to spreadsheet file VI

Nowadays, LabVIEW has a new function that offer the convenient way of acquiring the data from COM port, like “Bluetooth Discovery”. Same as this function, a “SKXBee Discovery” is believed to be developed as well in future by eliminating the use of third party software in establishing a XBee module connection between the devices and the computer. Without third party software, lesser procedures can be carried out providing a more user friendly interface to the user.

4.7.5 Advanced Hardware Assembly

Several precautionary steps are being carried out in the hardware assembly process to reduce the time taken for troubleshooting and hastened the progress of the project. First of all, a suitable and flexible protective plastic casing is added to house the circuit board from external harm. The plastic casing is being worn by subjects together with a belt during gait simulation.

The tail of FSR sensor is secured with a layer of building tape and the sensing layer is protected with a layer of masking tape. This can prevent the sensors from slipping out of position or dislocation of the wires. Moreover, the wires are carefully arranged and sorted out to maximise their length going out from the sensors to the circuit board. In this case, rainbow cables are used instead of red and black wires to pair sensors according to each side to avoid unnecessary criss-crossing and tangling.

As mentioned before regarding the messy soldering on the donut board, the tip of the solder gun is cleaned and sharpened using sand papers. The copper wire leads should not be bent too much or rotated before inserting into the donut board as this might cause the wires to snap off easily. For those messy wires, cellophane tape is used to tie them together.

After the soldering process, the connectivity of all the components is checked using multimeter. Furthermore, a lot of patience and time are invested in the process of troubleshooting these hardware components. Apart from that, printed circuit board (PCB) is recommended to reduce the complexity of wires and the inconvenient that faced during soldering process.

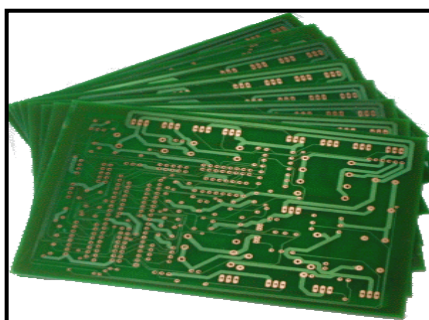


Figure 4.57: An example of PCB (PCB Fabrication, 2010)

4.7.6 Noise Reduction

One of the most important steps to improve the design system in this project is to reduce the source of noises. With less noise generated and constant outputs from the FSR sensors and devices, a more accurate results can be collected, processed, displayed, and analyzed. In addition, the actual forces applied beneath foot can be determined if less noise is produced by the design.

One of the common ways to reduce the noises from the sensors is to place an RC (resistor and capacitor) filter on each sensors before the input signals go into the microcontroller as showed below. The resistor will be connected in series with the input from the voltage divider and sensors; the capacitor will be connected to the ground, and the output of this RC filter will be connected to the input of microcontroller.

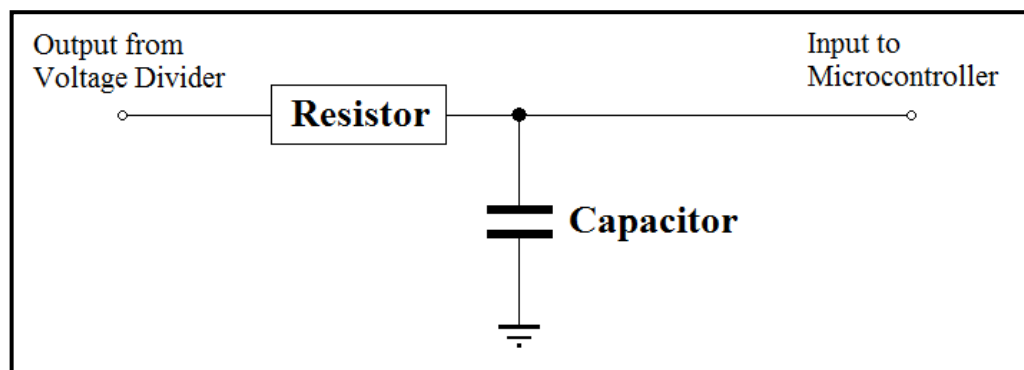


Figure 4.58: An example of RC filter

Besides, another suggestion is by changing the values of the pull-down resistor used in the voltage divider configuration to lower than $1.0\text{ k}\Omega$ in order to improve the measurement range of the applied force. This pull-down resistor is chosen to maximum the desired force sensitivity range and to limit current. The current through the FSR should be limited to less than 1 mA/cm^2 of applied force. These low bias currents from the operational amplifier reduce the error due to the source impedance of the voltage divider.

4.7.7 Rechargeable Power Supply

As mentioned before, power supply is one of the problems that faced during gait simulation. The first idea intended is using rechargeable lithium-ion battery as power supply to the design system. In this project, 9 V rechargeable batteries are used instead of rechargeable lithium-ion battery due to the budget constraints.

The market price for a 7.4 V (1300 mAh) and 11.1 V (2200 mAh) lithium-ion battery cost around RM105.00 and RM180.00. Plus, they need a specific lithium-ion battery charger which would cost around RM 50.00. By comparing the price with a normal 9 V rechargeable battery, they are far more expensive than expected. However, lithium-ion batteries consist of more voltage and current supply where they are able to be recharged and last for more than six hours.



Figure 4.59: An example of lithium-ion battery (ThunderPower Lithium Polymer Battery – 480mAh 11.1V with JST Connector, 2010)

In this project, rechargeable 9 V batteries are being considered, but it is not as useful as lithium-ion battery because it can only last up to three hours for the XBee module. In this project, batteries that can last for at least half a day are recommended to avoid the frequent time of charging and changing the batteries. Thus, lithium-ion battery is still the best optimization.

4.7.8 Amounts and Positions of Sensors

Increasing the number of FSR sensors is always a good way in improving this instrumented insole system. With more sensors, more force distribution can be observed and determined during gait simulation. By adding more sensors, it is believed that the effectiveness and accuracy of this system can be greatly improved.

In this case, two to six sensors can be added into this system. Those sensors can be placed beneath the second and fourth metatarsals for a better force distribution monitoring. Then, the total of seven sensors can be placed beneath the foot to form a better instrumented insole system as shown in the figure below. But if the cost is within the budget limit, more sensors can be attached at the lesser toes.

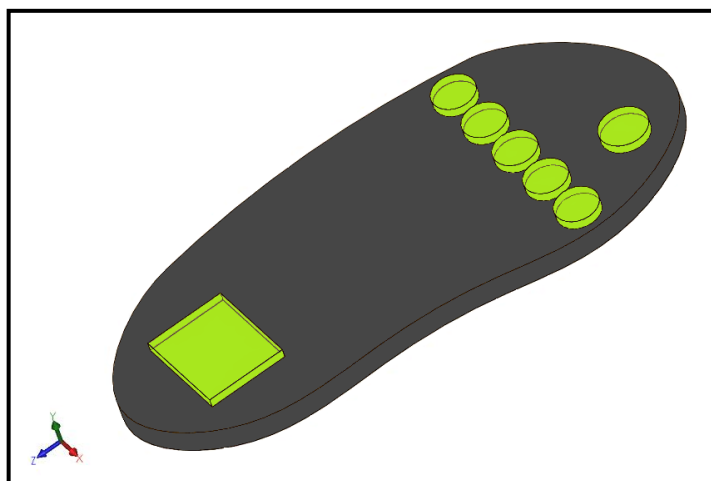


Figure 4.60: Possible of FSR sensors' arrangements

This will increase the ability of system to detect toe off timing more accurately than the force plate. Besides, the four coarsely spaced sensors provide reasonable approximation to the force distribution measured by the force plate, and are capable of providing information about shifting weight patterns from stride to stride which is not available from a force plate.

As mentioned before at the FSR interface, other types of sensors can be added as well to work together in getting the readings in term of different parameters. Bend sensors can be added at the arch of foot. On the other side, the accelerometers

and gyroscopes can be attached at the ankle, knee, and waist level. For the main circuit board, it can be worn together with the belt by the subject at waist level.

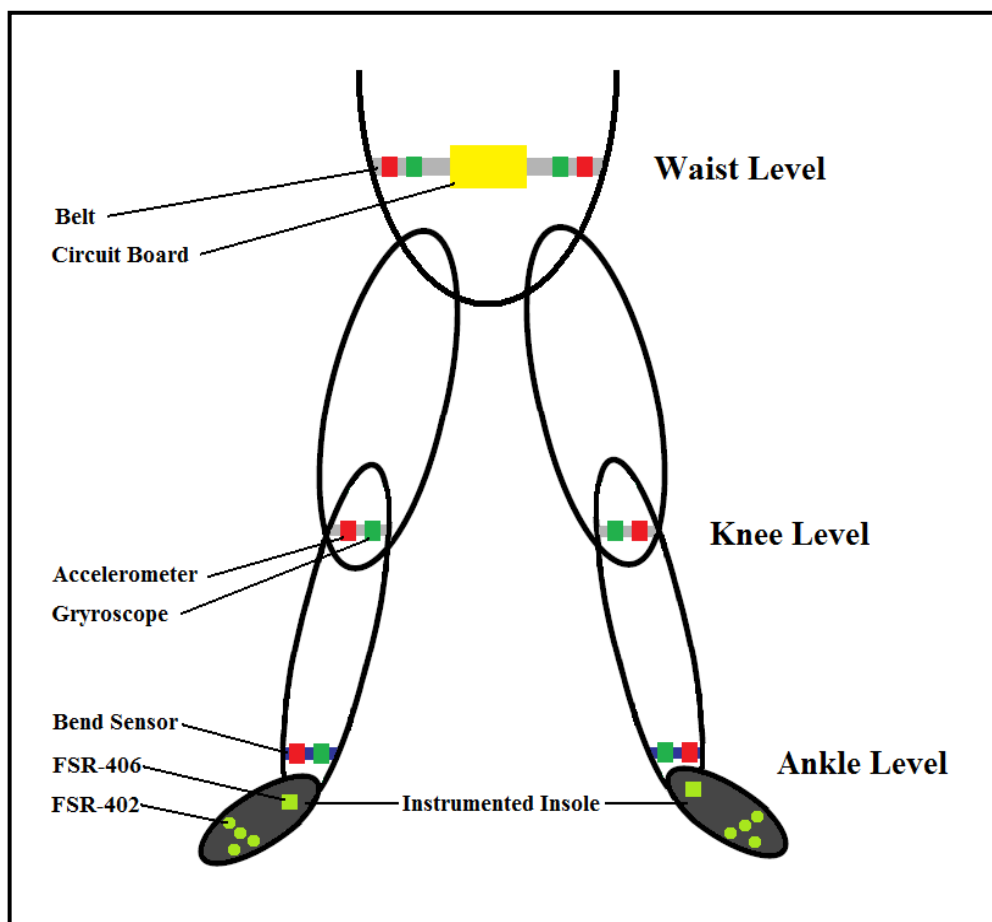


Figure 4.61: Possible of sensors' arrangements

The inclusion of other sensing parameters could further improve the accuracy and effectiveness of the instrumented insole system. The measurements from these individual parameters should complement each other in order to accurately detect the force distribution of a human locomotion activity with more information and details can be processed and analyzed.

With such advanced system, the overall lower extremity movements can then be observed, as well as the outcomes from the gait simulation can be enhanced. At that time, this instrumented insole system is no longer restricted for the gait analysis, but it can be used with other medical purposes, like fall detection system, athlete training system, podiatric laboratory, and so on.

4.7.9 Data Analysis Enhancement

There are varieties of methods that can be used for the data analysis in this project. Some common methods that can be used are like Classification and Regression Trees (CART), Bayes Decision Theory, Naïve Bayes, Support Vector Machines (SVM), Neural Network, and so on.

CART is a decision tree tool which is distributed by Salford Systems software. It uses binary recursive partitioning; each node is split into exactly two nodes, and the process is repeated with each child node. This software analyzes the data through a set of rules which determine the following node splitting (to create the tree), tree completion, tree pruning, and terminal node classification. One of the great benefits of CART is that the tree provides information about the most useful parameters in the feature set, as the splits at each of the nodes represent the features which best classify the data.

Bayes decision theory is a classification method based on probabilities. It assumes that the classification problem can be described in probabilistic terms, and that all the underlying probability values are known or can be reasonably approximated. Use of Bayesian approach is usually to update the prior probabilities as new information becomes known. However, Naïve Bayes assumptions are unlikely to apply to the gait feature data, which are certainly not independent and this is not expected to provide the best classification. But, it is included to see how well a simple technique could perform.

$$\begin{aligned}
 P(\omega_j|x) &= \frac{p(x|\omega_j)P(\omega_j)}{p(x)} \\
 p(x) &= \sum_{j=1}^n p(x|\omega_j)P(\omega_j) \\
 p(\omega_j|x) &\propto \prod_{i=1}^d p(x_i|\omega_j)
 \end{aligned}$$

Figure 4.62: Example formulas of Bayes rules (Morris, 2004)

SVMs are a classification method based on a linear learning machine (a learning algorithm that uses linear combinations of the input variables). This method uses linear discriminant functions, which means that the form of the underlying function is known or assumed), and the testing data are used to estimate the values of the parameters of the classifier. Unlike Bayes methods, SVMs require no knowledge or assumptions of the underlying probability distribution of the samples.

$$\Phi(w, \xi) = \frac{1}{2} \|w\|^2 + C \cdot \sum_i \xi_i$$

$$L(\alpha) = \sum_i \alpha_i - \frac{1}{2} \sum_{k,j} \alpha_j \alpha_k z_j z_k K(x_1, x_2)$$

$$\sum_{k=1}^N z_k \alpha_k = 0 \quad \alpha_k \geq 0, k = 1, \dots, n,$$

Figure 4.63: Example formulas of Support Vector Machines (Morris, 2004)

An artificial neural network is an adaptive learning method that represents the data through the use of a parallel network of nodes (“neurons”) arranged in layers and connected by weighted links. The link weights are determined by the testing data. The neural network is built by composing layers consisting of multiple neurons, where the input is usually a vector of multiple features. Neural networks are not limited to a single layer; multiple layers can be added serially, by using the outputs of the first layer as inputs to the next layer.

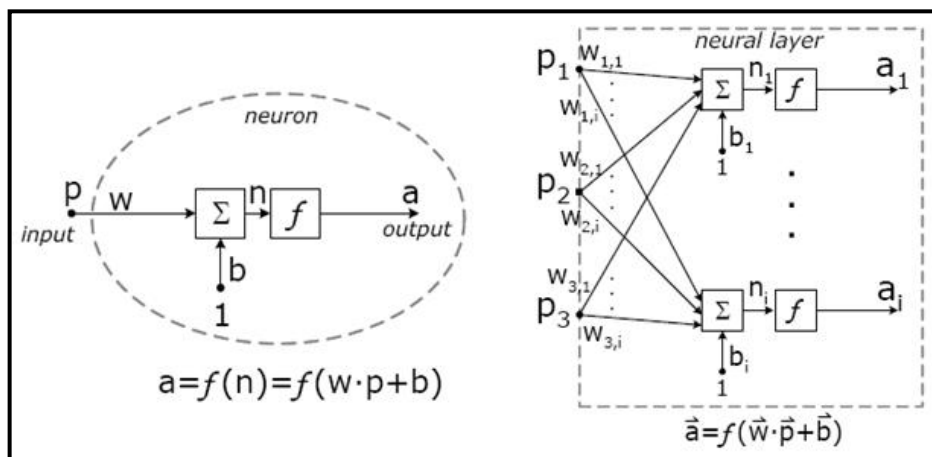


Figure 4.64: Example formulas of neural network (Morris, 2004)

CHAPTER 5

CONCLUSION AND RECOMMENDATIONS

5.1 Conclusion and Future Work

As a conclusion, a Force Sensing Resistor (FSR) based instrumented insole system for gait analysis has been successfully developed. Basically, the design of this project can be classified into two categories which are hardware and software setups. A circuit diagram is drawn and the setup is planned for the construction of hardware components. The hardware setup includes the fabrication of the instrumented insole and the configuration of electronic circuitry using FSR sensors.

For software part, mikroC Compiler is used to write the codes for the microcontroller behaviours in getting the output signals from sensors, collecting them, and send to processing unit. Besides, PICkit 2 Programmer is executed to program the corresponding language code into the microcontroller. And lastly, LabVIEW graphical programming interface is used to create a system that can collect, filter, and display input readings from all the sensing components used in this design. Furthermore, HyperTerminal is used to test for the connection between SKXBee between microcontroller and computer.

Subject testing has been carried out in getting more valuable information and data regarding the gait simulation. The results have been processed and analyzed where the walking pattern and gait analysis have been monitored and studied. Overall, the results collected are satisfied and matched with the description of a gait analysis as expected.

Comparison and benchmarking are done for the collected results between genders, devices, and other studies from other countries for normal and abnormal gait. However, only a group of subjects with a small range of ages involved in this subject testing. It is believe that the changes of the basic gait parameters most frequently seen with advancing age are a reduction of gait speed and step length. Therefore, gait of different groups of subjects with different ages should be studied in order to complete a perfect gait database for a wider range of age's population.

In this project, real time gait simulation using sensors is proven to have the capability of providing sufficient information. With the successfully integrated wireless communication of XBee module, real time gait simulation can be carried out in a radius up to 20 meters distance. This range provides a large space for the subject to move around during the gait simulation. The software LabVIEW is also having more than 80.65% success rate in identifying the data coming from the XBee module.

The gait parameters analysis indicated that the system can be further developed into a better force distribution system like wearable podiatric laboratory, which can be great use in evaluating gait over longer periods of time than are available in motion laboratories. These enhancements also allow the evaluation to be carried out in a neutral environment, such as subject's home. It would allow the evaluation of subjects without access to a motion laboratory.

The design of the instrumented insole for gait analysis can be further enhanced by incorporating other sensing components coupled with a critically programmed force detection algorithm. Other improvements on the design like using lithium ion battery to prolong the usage time and RC filter to reduce the noises can be done as well for a better performance. Therefore, the whole system could set a new milestone for future researches in areas related to gait analysis.

In a nutshell, valuable experiences and plenty of knowledge are gained in completing this project by constructing the hardware and utilizing the programming language. This project serves as a great opportunity to apply the knowledge and theory practically which has been studied throughout the four years and be prepared before going to the industry.

5.2 Cost and Expenses

For a student, budget of RM 500 will be given to carry out a project. Since this is a group project of two students, total of RM 1000 is given to purchase the required electronic components in completing this project. The total amounts spend achieving this project is RM 981.83, where the shipping fees, travelling expenses, and paper photocopy are not included. The expenditure of this project is within the given budget, as shown at Appendix J.

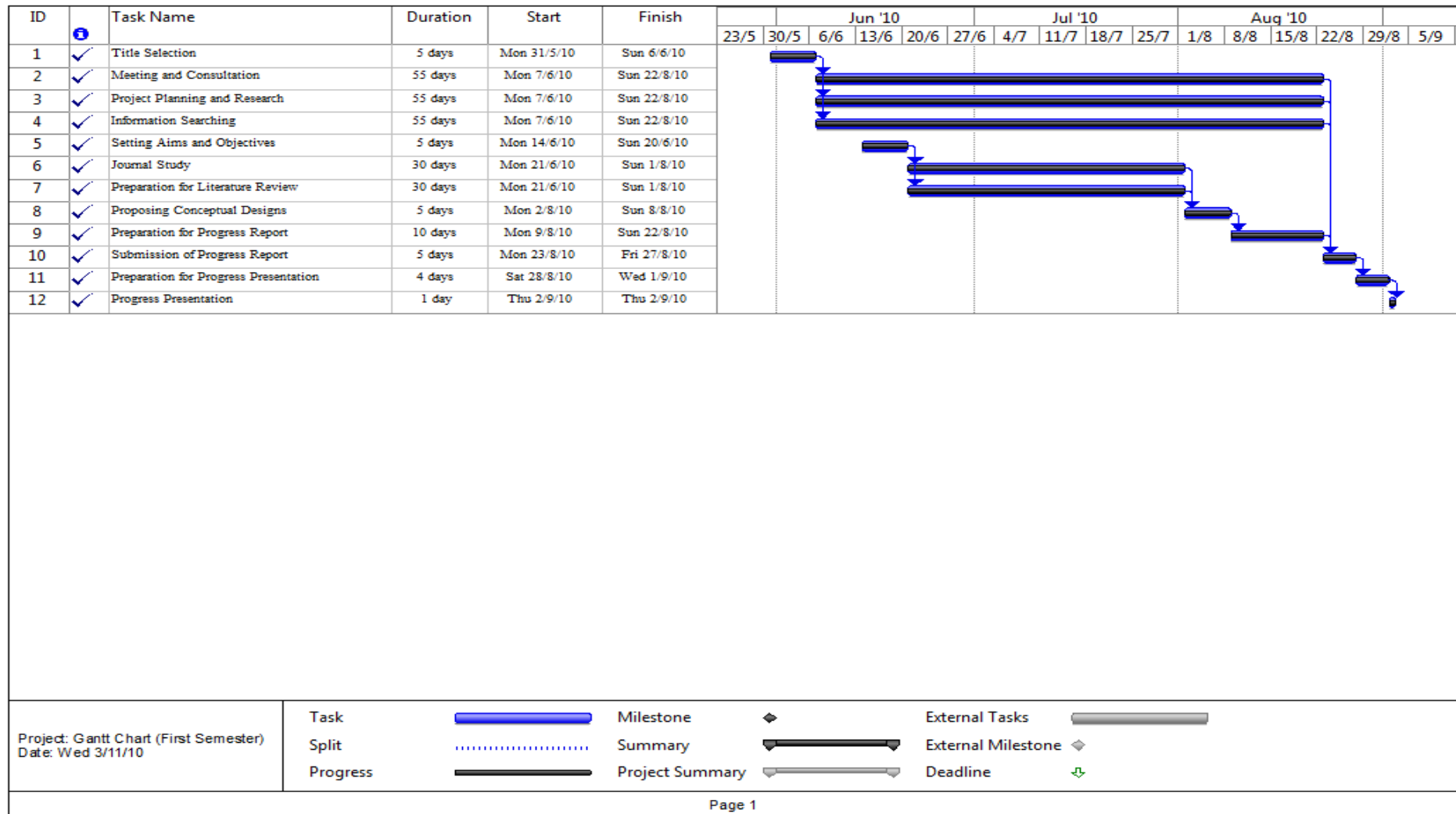
5.3 Gantt Chart

This project started from the title selection and subsequent tasks like setting aims and objectives in order to come out with conceptual designs, and journal study for the preparation of literature review. Project planning and research are needed throughout the timeframe of this project to update the latest information and technology. Along the way to complete the project, meeting and consultation with supervisor weekly is set for reporting the status and progression. At the end of the semester, a progress report and presentation are presented to show the work done for the whole semester.

For the following semester, work continued from last semester, where preferred design is selected from the proposed conceptual design or combination of them. Then, a list of electronic components is prepared for building the prototype. After a thorough market research and survey, electronic components and parts will be purchased with a reasonable price within the budget limit. Construction and building of prototype will be started in line with the programming codes are written.

Next, the prototype is being debugged and tested to ensure if it meets the requirement of this project. In addition, troubleshooting and improvement is needed to enhance the performance of prototype. Data is collected from subjects and being analyzed. Finally, thesis report submission and presentation is done in order to draw a conclusion for the project. Gantt charts are shown at next page for details about the progress of work being carried out during these two semesters.

First Semester

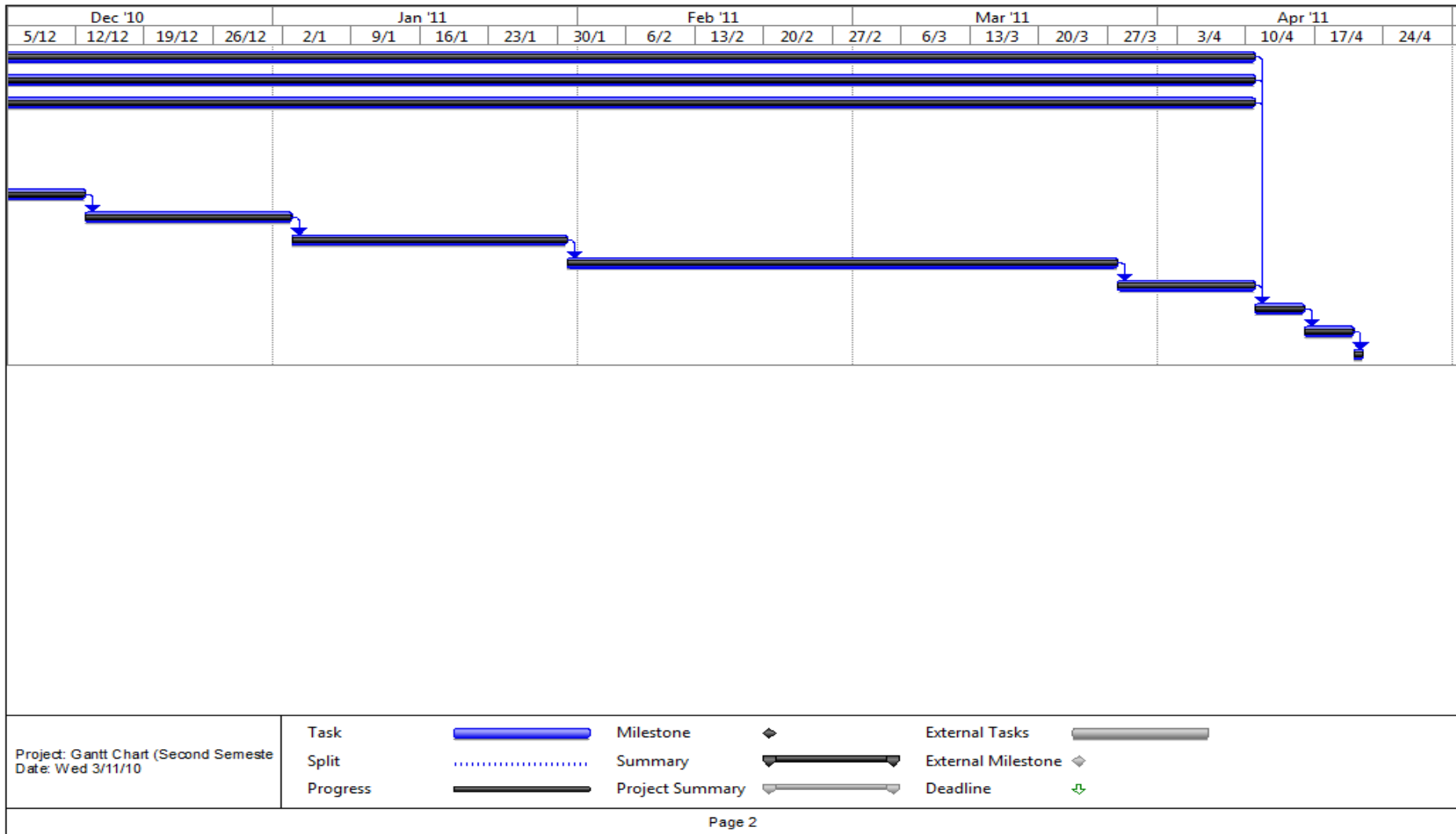


Second Semester

ID	Task Name	Duration	Start	Finish	19/9		Oct '10				Nov '10				5/
						26/9	3/10	10/10	17/10	24/10	31/10	7/11	14/11	21/11	
1	Meeting and Consultation	135 days	Mon 4/10/10	Sun 10/4/11											
2	Project Planning and Research	135 days	Mon 4/10/10	Sun 10/4/11											
3	Information Searching	135 days	Mon 4/10/10	Sun 10/4/11											
4	Selection of Preferred Design	10 days	Mon 4/10/10	Sun 17/10/10											
5	Market Research for Parts	10 days	Mon 18/10/10	Sun 31/10/10											
6	Parts and Components Purchase	10 days	Mon 1/11/10	Sun 14/11/10											
7	Prototype Construction	20 days	Mon 15/11/10	Sun 12/12/10											
8	Programming and Debugging	15 days	Mon 13/12/10	Sun 2/1/11											
9	Troubleshooting and Testing	20 days	Mon 3/1/11	Sun 30/1/11											
10	Data Collection and Analysis	40 days	Mon 31/1/11	Sun 27/3/11											
11	Preparation for Thesis	10 days	Mon 28/3/11	Sun 10/4/11											
12	Submission of Thesis	5 days	Mon 11/4/11	Fri 15/4/11											
13	Preparation for Thesis Presentation	4 days	Sat 16/4/11	Wed 20/4/11											
14	Thesis Presentation	1 day	Thu 21/4/11	Thu 21/4/11											



Project: Gantt Chart (Second Semeste Date: Wed 3/11/10)	Task		Milestone		External Tasks	
	Split		Summary		External Milestone	
	Progress		Project Summary		Deadline	



REFERENCES

- 9V Battery Snap Connector.* (2010). Retrieved October 23, 2010, from Solarbotics Ltd: <http://www.solarbotics.com/products/bhold9v/>.
- 9V Sealed Battery Holder with Wires.* (2010). Retrieved October 23, 2010, from Addison Electronics: http://www.addison-electronique.com/catalog/product_info.php?products_id=202006.
- 10 μ F Electrolytic Capacitor.* (2010). Retrieved October 23, 2010, from C-Stamp Product Line: <http://www.c-stamp.com/CS532000.htm>.
- 100 μ F Electrolytic Capacitor.* (2010). Retrieved October 23, 2010, from C-Stamp Product Line: <http://www.c-stamp.com/CS538000.htm>.
- Abraham, J.K., Whitchurch, A.K., Varadan, V.K. & Sarukesi, K. (2003). Wireless patient monitoring on shoe for the assessment of foot dysfunction: An overview. *Proceedings of SPIE, 5119*, 160-164.
- Abu-Faraj, Z.U., Harris, G.F., Abler, J.H., Wertsch, J.J. & Smith, P.A. (1996). A holter-type microprocessor-based rehabilitation instrument for acquisition and storage of plantar pressure data in children with cerebral palsy. *Proceedings of IEEE Transactions on Rehabilitation Engineering, Milwaukee, WI, 4* (1), 33-38.
- Abu-Faraj, Z.U., Harris, G.F., Wertsch, J.J., Abler, J.H. & Vengsarkar, A.S. (1994). Holter system development for recording plantar pressures: Design and instrumentation. *Proceedings of IEEE International Conference, Baltimore, MD, 934-935*.
- Allet, L., Armand, S., Aminian, K., Pataky, Z., Golay, A., de Bie, R.A., et al. (2010). An exercise intervention to improve diabetic patients' gait in a real-life environment. *Gait & Posture, 32*, 185-190.
- Aluminium Box (130x71x45mm) Silver.* (2010). Retrieved October 23, 2010, from Cytron Technologies: <http://www.cytron.com.my/viewProduct.php?pid=Dh8RBBcCJT05Og8rIgwOEsuIfno7em6N89!!!!GG/4xthk=>.

- AL-Tayyar, S.S. (1997). *The importance of plantar pressure measurements and appropriate footwear for diabetic patients*. College of Medicine and King Khalid University Hospital, King Saud University.
- Arnaud, F., Marc, D., Bernard, P. & Guy, M. (2005). *Instrumented shoes for ground reaction forces assessment of pathological gait*. Besancon, France.
- Auvinet, B., Berrut, G., Touzard, C., Moutel, L., Collet, N., Chaleil, D., et al. (2002). Reference data for normal subjects obtained with an accelerometric device. *Gait & Posture*, 16, 124-134.
- Bachschtmidt, R.A., Harris, G.F. & Simoneau, G.G. (1995). Development of a force sensing walker for rehabilitation. Proceedings of IEEE-EMBC and CMBEC Theme 5: Neuromuscular System/Biomechanics, Montreal, Que, 2, 1267-1268.
- Bae, J., Kong, K., Byl, N. & Tomizuka, M. (2009). A mobile gait monitoring system for gait analysis. Proceedings of IEEE 11th International Conference on Rehabilitation Robotics Kyoto International Conference Center, Japan, 73-79.
- Baker, R. (2007). The history of gait analysis before the advent of modern computers. *Gait & Posture Review*, 26, 331-342.
- Battery Super Heavy Duty 9 Volt*. (2010). Retrieved October 23, 2010, from Digi-Key Corporation: <http://uk.digikey.com/1/1/4457055-battery-super-heavy-duty-9-volt-1222.html>.
- Beauchet, O., Herrmann, F.R., Grandjean, R., Dubost, V. & Allali, G. (2008). Concurrent validity of SMTEC footswitches system for the measurement of temporal gait parameters. *Gait & Posture*, 27, 156-159.
- Benbasat, A.Y. & Paradiso, J.A. (2005). A compact modular wireless sensor platform. Proceedings of IEEE International Conference in Information Processing in Sensor Networks (IPSN), Cambridge, MA, USA, 410-415.
- Benbasat, A.Y., Morris, S.J. & Paradiso, J.A. (2003). A wireless modular sensor architecture and its application in on-shoe gait analysis. Proceedings of IEEE Transaction of Information Technology in Biomedicine, Cambridge, MA, USA, 2, 1086-1091.
- Bilas, V., Santic, A., Lackovic, I. & Ambrus, D. (2001). A low-power wireless interface for human gait assessment. Proceedings of IEEE Instrumentation and Measurement Technology Conference, Budapest, Hungary, 614-618.
- Billing, D. & Hayes, J. (2005). *In-shoe measurement for biomechanical monitoring*. Australian Institute of Sport.

- Bisiaux, M. & Moretto, P. (2008). The effects of fatigue on plantar pressure distribution in walking. *Gait & Posture*, 28, 693-698.
- Body Measurement (Anthrometry). *National Health and Nutrition Examination Survey III*. Westat, Inc, 1650 Research Boulevard Rockville, October 1988.
- Bogataj, U., Gros, N., Kljajic, M. & Acimovic-Janezic, R. (1997). Enhanced rehabilitation of gait after stroke: A case report of a therapeutic approach using multichannel functional electrical stimulation. *Proceeding of IEEE transactions on Rehabilitation Engineering*, 5 (2), 221-232.
- Cable Belt*. (2010). Retrieved October 23, 2010, from Keetsa: <http://keetsa.com/blog/recycle/the-cable-belt/>.
- Catalfamo, P., Moser, D., Ghoussayni, S. & Ewins, D. (2008). Detection of gait events using F-Scan in-shoe pressure measurement system. *Gait & Posture*, 28, 420-426.
- Che, D.W., Kwon, O.H., Shim, J. & Park, J.H. (2006). Design of multipurpose sensing system for human gait analysis. *Proceedings of SICE-ICASE International Joint Conference*, Bexco, Busan, Korea, 1168-1171.
- Chen, L.W., Wang, J., Li, S.W., Gao, L., Li, H.X., Wang, Z.M., et al. (2009). Analysis of temporal and spatial gait parameters in children with spastic cerebral palsy. *Proceedings of 2nd International Conference on Biomedical Engineering and Informatics*, Tianjin, China, 1-4.
- Chen, M., Huang, B.F. & Xu, Y.S. (2008). Intelligent shoes for abnormal gait detection. *Proceedings of IEEE International Conference on Robotics and Automation*, Pasadena, CA, USA, 2019-2024.
- Chen, M., Huang, B.F., Lee, K.K. & Xu, Y.S. (2006). An intelligent shoe-integrated system for plantar pressure measurement. *Proceedings of IEEE International Conference on Robotics and Biomimetics*, Kuming, China, 416-412.
- Chen, W.P., Ju, C.W. & Tang, F.T. (2003). Effects of total contact insoles on the plantar stress redistribution: A finite element analysis. *Clinical Biomechanics*, 18, 17-24.
- Chen, Y.C., Su, F.C. & Huang, C.Y. (2007). Effects of the shoes and insoles on gait patterns in the flatfoot. *Proceedings of XXI ISB Congress, Podium Sessions*, Dubai, 40, 472.
- Chevalier, T.L., Hodgins, H. & Chockalingam, N. (2010). Plantar pressure measurements using an in-shoe system and a pressure platform: A comparison. *Gait & Posture*, 31, 397-399.

- Cho, S.H., Park, J.M. & Kwon, O.Y. (2004). Gender differences in three dimensional gait analysis data from 98 healthy Korean adults. *Clinical Biomechanics*, 19, 145-152.
- Choi, I. & Ricci, C. (1997). Foot-mounted gesture detection and its application in virtual environments. *Proceedings of IEEE Transaction on Biomedical Engineering*, Orlando, FL, 5, 4248-4253.
- Chong, Y.Z. (2009). Full body wearable instrumented motion analysis system. *Proceedings of 3rd IEEE International Conference in Bioinformatics and Biomedical Engineering (ICBBE)*, Beijing, 1-4.
- Chuckpaiwong, B., Numley, J.A., Mall, N.A. & Queen, R.M. (2008). The effect of foot type on in-shoe plantar pressure during walking and running. *Gait & Posture*, 28, 405-411.
- Cytron USB to UART Converter UC00A User's Manual V1.1*. (2009). Cytron Technologies.
- Deleu, P. S., Leemrijse, T., Vandeleene, B., Maldague, P. & Bevernage, B.D. (2009). Plantar pressure relief using a forefoot offloading shoe. *Foot and ankle surgery*, 5-10.
- Donut Board*. (2010). Retrieved October 23, 2010, from Cytron Technologies: <http://www.cytron.com.my/listProductGroup.php?pid=FDwsDx4kIA0TJggyGilFke63f0ulBdbtDo8MXHokSM=>.
- Drerup, B., Szczepanial, A. & Wetz, H.H. (2008). Plantar pressure reduction in step-to gait: A biomechanical investigation and clinical feasibility. *Clinical Biomechanics*, 23, 1073-1079.
- Electrical & Electronic Connectors*. (2010). Retrieved October 23, 2010, from Indiamart: <http://www.indiamart.com/guptaenterprises.products.html>.
- Energizer Ni-Mh Rechargeable 9V Square Batteries*. (2010). Retrieved October 23, 2010, from Battery Hut: http://www.batteryhut.co.uk/acatalog/9_Volt_Square_Rechargeable_Batteries_Energizer_Uniross.asp
- Faivre, A., Dahan, M., Parratte, B. & Monnier, G. (2003). *Instrumented shoes for pathological gait assessment*. Laboratory, Bichat, CHU, Besancon, France.
- Female connector*. (2010). Retrieved October 23, 2010, from Wikimedia Commons: http://commons.wikimedia.org/wiki/File:Molex_female_connector.jpg.
- Flexible Bend Sensor*. (2010). Retrieved November 24, 2010, from Cytron Technologies:

<http://cytron.com.my/viewProduct.php?pid=IBcMKwUTIRYiOhs1GRkREHx5sY6F8obZfyXivxRXoaY=>

Fong, D.T.P, Chan, Y.Y., Hong, Y.L., Yung, P.S.H., Fung, K.Y. & Chan, K.M. (2008). Estimating the complete ground reaction forces with pressure insoles in walking. *Short Communication*, 41, 2597-2601.

Force Sensing Resistor. (2010). Interlink Electronics.

Force Sensitive Resistor 0.5". (2010). Retrieved October 23, 2010, from sgbotic: http://www.sgbotic.com/index.php?dispatch=products.view&product_id=471

Force Sensitive Resistor – Square. (2010). Retrieved October 23, 2010, from sgbotic: http://www.sgbotic.com/index.php?dispatch=products.view&product_id=492

Formica, M., Tabernig, C. & Escobar, S. (2003). A multichannel telemetry system for monitoring physiological information from the human gait: Preliminary results. Proceedings of the 25th Annual International Conference of the IEEE EMBS Cancun, Mexico, 1799-1802.

Forner-Cordero, A., Koopman, H.J.F.M. & Helm, F.C.T. (2004). Use of pressure insoles to calculate the complete ground reaction forces. *Short Communication*, 37, 1427-1432.

Forner-Cordero, A., Koopman, H.J.F.M. & Helm, F.C.T. (2006). Inverse dynamics calculations during gait with restricted ground reaction force information from pressure insoles. *Gait & Posture*, 23, 189-199.

FSR Force Sensing Resistor Integration Guide and Evaluation Parts Catalog. (2010). Interlink Electronics.

Gaudreault, N., Gravel, D., Nadeau, S., Houde, S. & Gagnon, D. (2010). Gait patterns comparison of children with Duchenne muscular dystrophy to those of control subjects considering the effect of gait velocity. *Gait & Posture*, 32, 342-347.

Giansanti, D., Tiberi, Y. & Maccioni, G. (2008). New wearable system for the step counting based on the codivilla-spring for daily activity monitoring in stroke rehabilitation. Proceedings of 30th Annual International IEEE Conference Vancouver, British Columbia, Canada, 4720-4723.

Givon, U., Zeilig, G., Achiron, A. (2009). Gait analysis in multiple sclerosis: Characterization of temporal-spatial parameters using GAITRite functional ambulation system. *Gait & Posture*, 29, 138-142.

Goulermas, J.Y., Findlow, A.H., Nester, C.J., Liatsis, P., Zeng, X.J., Kenney, L.P.J., et al. (2008). An instance-based algorithm with auxiliary similarity information

for the estimation of gait kinematics from wearable sensors. *Proceedings of IEEE Transactions on Neural Network*, Liverpool, 19 (9), 1574-1582.

Gouwanda, D., Senanayake, S.M.N.A., Marasinghe, M.M.D.R., Chandrapal, M., Kumar, J.M., Tung, M.H., et al. (2008). Real time force sensing mat for human gait analysis. *Proceedings of World Academy of Science, Engineering, and Technology*, Cambridge, USA, 39, 26-31.

Grandez, K., Bustamante, P., Solas, G., Gurutzeaga, I. & Garcia-Alonso, A. (2009). Wearable wireless sensor for the gait monitorization parkinsonian patients. *Proceedings of IEEE International Conference in Electronics, Circuits, and Systems*, San Sebastian, Spain, 215-218.

Guldmond, N.A., Leffers, P., Schaper, N.C., Sanders, A.P., Nieman, F., Willems, P., et al. (2007). The effects of insole configurations on forefoot plantar pressure and walking convenience in diabetic patients with neuropathic feet. *Clinical Biomechanics*, 22, 81-87.

Gyro Breakout Board – ADXRS610 300 degree/sec. (2010). Retrieved November 24, 2010, from sgbotic: http://www.sgbotic.com/index.php?dispatch=products.view&product_id=355

Hall, R.S., Desmoulin, G.T. & Milner, T.E. (2008). A technique for conditioning and calibrating force-sensing resistors for repeatable and reliable measurement of compressive force. *Short Communication*, 41, 3492-3495.

Hanlon, M. & Anderson, R. (2009). Real-time gait even detection using wearable sensors. *Gait & Posture*, 30, 523-527.

Hannula, M., Sakkinen, A. & Kylmanen, A. (2007). Development of EMFI-sensor based pressure sensitive insole for gait analysis. *Proceedings of International Workshop on Medical Measurement and Application, MeMeA Warsaw, Poland*, 1-3.

Heever, D.J., Schreve, K. & Scheffer, C. (2009). Tactile sensing using force sensing resistors and a super-resolution algorithm. *Sensors*, 9 (1), 29-35.

Hollinger, A. & Wanderley, M.M. (2007). *Evaluation of commercial force-sensing resistors*. Schulich School of Music McGill University, Montreal, QC, Canada.

How to Solder. (2010). Retrieved October 23, 2010, from PC in Control: <http://www.pc-control.co.uk/soldering.htm>.

Huang, B.F., Chen, M., Shi, X. & Xu, Y.S. (2007). Gait event detection with intelligent shoes. *Proceedings of IEEE International Conference on Information Acquisition*, Jeju City, Korea, 579-584.

- Hurkmans, H.L.P., Bussmann, J.B.J., Benda, E., Verhaar, J.A.N. & Stam, H.J. (2006). Accuracy and repeatability of the pedar mobile system in long-term vertical force measurements. *Gait & Posture*, 23, 118-125.
- Jagos, H., Oberzaucher, J., Reichel, M., Zagler, W.L. & Hlauschek, W. (2010). A multimodal approach for insole motion measurement and analysis. Proceedings of the 8th Conference of the International Sports Engineering Association (ISEA). *Procedia Engineering*, 2, 3103-3108.
- Karkokli, R. (2006). Design and development of a cost effective plantar pressure distribution analysis system for the dynamically moving feet. Proceedings of the 28th IEEE EMBS Annual International Conference, New York City, USA, 6008-6011.
- Kavanagh, J.K., Morrison, S., James, D.A. & Barrett, R. (2006). Reliability of segmental accelerations measured using a new wireless gait analysis system. *Sensors*, 39, 2863-2872.
- Kirtley, C. (2001). An instrumented insole for kinematic and kinetic gait measurements. Proceedings of the 5th Symp. on Footwear Biomechanics, Zuerich/Switzerland, 52-53.
- Kirtley, C. (2003). *An instrumented insole for measurement of foot motion*. Catholic University of America, Washington DC, USA.
- Kiss, R.M. (2010). Comparison between kinematic and ground reaction force techniques for determining gait events during treadmill walking at different walking speeds. *Medical Engineering & Physics*, 6-12.
- Kong, K. & Tomizuka, M. (2008). Estimation of abnormalities in a human gait using sensor-embedded shoes. Proceedings of IEEE/ASME International Conference on Advanced Intelligent Mechatronics, Xi'an, China, 1331-1336.
- Kong, K. & Tomizuka, M. (2008). Smooth and continuous human gait phase detection based on foot pressure patterns. Proceedings of IEEE International Conference on Robotics and Automation Pasadena, CA, USA, 3678-3683.
- Kong, P.W. & Heer, H.D. (2009). Wearing the F-Scan mobile in-shoe pressure measurement system alters gait characteristics during running. *Gait & Posture*, 29, 143-145.
- Kyriazis, V., Rigas, C. & Xenakis, T. (2001). A portable system for the measurement of the temporal parameters of gait. Proceedings of International Conference on Prosthetics and Orthotics, Chicago, IL, 25, 96-101.
- L7800 Series Positive Voltage Regulators*. (2004). ST Microelectronics.

- Lawrence, T.L. & Schmidt, R.N. (1997). Wireless in-shoe force system. Proceedings of the 19th International Conference IEEE/EMBS, Chicago, IL. USA, 2238-2241.
- Lemaire, E.D., Biswas, A. & Kofman, J. (2006). Plantar pressure parameters for dynamic gait stability analysis. Proceedings of the 28th IEEE EMBS Annual International Conference New York City, USA, 4465-4468.
- Liedtke, C., Fokkenrood, S.A.W., Menger, J.T., Kooij, H. & Veltink, P.H. (2007). Evaluation of instrumented shoes for ambulatory assessment of ground reaction forces. *Gait & Posture*, 26, 39-47.
- Liu, T., Inoue, Y. & Shibata, K. (2008). New method for assessment of gait variability based on wearable ground reaction force sensor. Proceedings of 30th Annual International IEE EMBS Conference, Vancouver, British Columbia, Canada, 2341-2344.
- Liu, T., Inoue, Y. & Shibata, K. (2009). Development of a wearable sensor system for quantitative gait analysis. *Measurement*, 42, 978-988.
- Liu, T., Inoue, Y., Shibata, K. & Morioka, H. (2006). Development of wearable sensor combinations for human lower extremity motion analysis. Proceedings of the IEEE International Conference on Robotics and Automation Orlando, Florida, 1655-1660.
- Liu, Y.Y., Yu, P., Wang, Y.C., Dong, Z.L. & Xi, N. (2007). Design and development of a micro-force sensing device. Proceedings of IEEE International Conference on Robotics and Biometrics, Sanya, China, 77-81.
- LM341/LM78MXX Series 3 – Terminal Positive Voltage Regulators.* (2005). National Semiconductor.
- LM7805 5V Regulator.* (2010). Retrieved October 23, 2010, from Loja LusoRobotica: <http://loja.lusorobotica.com/lang-en/circuitos-integrados/27-lm7805-5v-regulator.html>.
- LM78XX/LM78XXA 3 – Terminal 1A Positive Voltage Regulator.* (2010). Fairchild Semiconductor.
- Low Power Quad Operational Amplifiers.* (1999). ST Microelectronics.
- Lyon, R. & Liu, X.C. (2000). Dynamic plantar pressure measurements in children with teasel coalition. Proceedings of IEEE International Conference in Pediatric Gait, Chicago, IL, 189-193.
- Male Connector.* (2010). Retrieved October 23, 2010, from Wikimedia Commons: http://commons.wikimedia.org/wiki/File:Molex_male_connector.jpg.

- Martinez-Nova, A., Cuevas-Garcia, J.C., Pascual-Huerta, J. & Sanchez-Rodriguez, R. (2007). Biofoot in-shoe system: Normal values and assessment of the reliability and repeatability. *The Foot*, 17, 190-196.
- Martinez-Nova, A., Cuevas-Garcia, J.C., Sanchez-Rodriguez, R., Pascual-Huerta, J. & Sanchez-Barradoc, E. (2008). Study of plantar pressure patterns by means of instrumented insoles in subjects with hallux valgus, 94-98.
- McKean, K.A., Landry, S.C., Hubley-Kozey, C.L., Dunbar, M.J., Stanish, W.D. & Deluzio, K.J. (2007). Gender differences exist in osteoarthritic gait. *Clinical Biomechanics*, 22, 400-409.
- Morley, R.E., Richter, E.J., Klaesner, J.W., Maluf, K.S. & Mueller, M.J. (2001). In-shoe multisensory data acquisition system. Proceedings of IEEE Transactions on Biomedical Engineering St. Louis, MO, USA, 48 (7), 815-820.
- Morris, S.J. (2004). *A shoe-integrated sensor system for wireless gait analysis and real-time therapeutic feedback*. Sc.D. dissertation, Harvard/MIT Division Health Sci. Technol., Cambridge, MA.
- Morris, S.J. (2008). Gait analysis using a shoe-integrated wireless sensor system. Proceedings of IEEE Transaction of Information Technology in Biomedicine, Salt Lake City, UT, 12 (4), 413-423.
- Morris, S.J. & Paradiso, J.A. (2002). Shoe-integrated sensor system for wireless gait analysis and real-time feedback. Proceedings of the Second Joint EMBS/BMES Conference, Houston, TX, USA, 2468-2469.
- Morris, S.J., LaStayo, P. & Dibble, L. (2006). Development of a quantitative in-shoe measurement system for assessing balance: Sixteen-sensor insoles. Proceedings of the 28th IEEE EMBS Annual International Conference, New York City, USA, 6641-6644.
- Muhammad Ali Mazidi, R.D. (2008). *PIC microcontroller and embedded systems*. New Jersey: Pearson Prentice Hall.
- Muller, I., Brito, R.M., Pereira, C.E. & Brusamarello, V. (2009). *Load cells in force sensing analysis – Theory and a novel application*. IEEE Instrumentation & Measurement Magazine, 15-19.
- Multimeter*. (2010). Retrieved October 23, 2010, from TopBits.com Tech Community: <http://www.tech-faq.com/multimeter.html>.
- Nambu, M. (2007). Body surface mounted biomedical monitoring system. Proceedings of the 29th Annual International Conference of the IEEE EMBS Cite Internationale, Lyon, France, 1824-1825.

- Nicolopoulos, C. & Barnett, S. (1999). *Plantar pressure review using the FSCAN system*. Gartnavel General Hospital, Glasgow, U.K. and University of West England, Bristol, U.K.
- Nicolopoulos, C.S., Solomonidis, S., Anderson, E.G. & Black, J.A. (2001). *In-shoe plantar pressure measurements for the diagnosis of different foot pathologies using FSR technology*. University of Strathclyde, Glasgow, U.K.
- Nikolopoulos, C.S. (2001). *Normal motion and normal foot*. Foot laboratory, Gartnavel General Hospital, Glasgow, Scotland.
- Nikolopoulos, C.S. (2001). *Normative pressure measurements studies*. Foot laboratory, Gartnavel General Hospital, Glasgow, Scotland.
- Nikolopoulos, C.S. (2001). *Normative study using plantar pressure measurements*. Foot laboratory, Gartnavel General Hospital, Glasgow, Scotland.
- Oberg, T.M.P., Karsznia, A.P.P & Oberg, K.P. (1993). Basic gait parameters: Reference data for normal subjects, 10-79 years of age. *Journal of Rehabilitation Research and Development*, 30 (2), 210-223.
- Okuno, R., Fujimoto, S., Akazawa, J., Yokoe, M., Sakoda, S. & Akazawa, K. (2008). Analysis of spatial temporal plantar pressure pattern during gait in parkinson's disease. Proceedings of 30th Annual International IEEE EMBS Conference Vancouver, British Columbia, Canada, 1765-1768.
- Pappas, I.P.I., Keller, T. & Mangold, S. (2002). A reliable, gyroscope based gait phase detection sensor embedded in a shoe insole. Proceedings of IEEE International Conference, Zurich, Switzerland, 2, 1085-1088.
- Pappas, I.P.I., Keller, T., Mangold, S., Popovic, M., Dietz, V. & Morari, M. (2003). A reliable, insole-embedded gait phase detection sensor for FES-assisted walking. University of Toronto, Canada, 300-312.
- Pappas, I.P.I., Keller, T., Mangold, S., Popovic, M., Dietz, V. & Morari, M. (2004). A reliable gyroscope-based gait-phase detection sensor embedded in a shoe insole. *Sensors*, 4 (2), 268-274.
- Pappas, I.P.I., Popovic, M.R., Keller, T., Dietz, V. & Morari, M. (2001). A reliable gait phase detection system. Proceedings of IEEE Transactions on Neural Systems and Rehabilitation Engineering, Zurich, Switzerland, 9 (2), 113-125.
- PCB Fabrication*. (2010). Retrieved November 24, 2010, from H-Tek Circuit Company LTD:
http://www.hitekircuit.com/article/view.php?ps_db=prod&pnid=2&ps_aid=6

- Perino, V.V., Kawcak, C.E., Frisbie, D.D., Reiser, R.F. & McIlwraith, C.W. (2007). The accuracy and precision of an equine in-shoe pressure measurement system as a tool for gait analysis. *Gait Analysis*, 27 (4) 161-166.
- PIC16F877A. (2010). Retrieved October 23, 2010, from Micros: http://www.micros.com.ve/tienda/product_info.php?products_id=39
- PIC16F87XA Data Sheet. (2003). Microchip.
- Polchaninoff, M. (1983). Gait analysis using a portable, microprocessor-based segmental foot measuring system. Proceedings of IEEE International Conference in Computer Applications in Medical Care, Deer Park, NY, 897-899.
- Pons, J.L., Rocon, E., Forner-Cordero, A. & Moreno, J. (2007). Biomedical instrumentation based on piezoelectric ceramics. *Journal of the European Ceramic Society*, 27, 4191-4194.
- Putti, A.B., Arnold, G.P., Cochrane, L. & Abboud, R.J. (2007). The Pedar in-shoe system: Repeatability and normal pressure values. *Gait & Posture*, 25, 401-405.
- Quad Operational Amplifier. (2010). Retrieved October 23, 2010, from Solarbotics Ltd: <http://www.solarbotics.com/products/lm324>.
- Queen, R.M., Abbey, A.N., Wiegerinck, J.I., Yoder, J.C. & Nunley, J.A. (2010). Effect of shoe type on plantar pressure: A gender comparison. *Gait & Posture*, 31, 18-22.
- Racic, V., Pavic, A. & Brownjohn, J.M.W. (2009). Experimental identification and analytical modelling of human walking forces: Literature review. *Sound and Vibration*, 326, 1-49.
- Ramanathan, A.K., Kiran, P., Arnold, G.P., Wang, W. & Abboud, R.J. (2010). Repeatability of the Pedar-X in-shoe pressure measuring system. *Foot and ankle surgery*, 16, 70-73.
- Rana, N.K. (2009). Application of force sensing resistors (FSR) in design of pressure scanning system for plantar pressure measurement. Proceedings of the Second International Conference on Computer and Electrical Engineering, Dubai, 2, 678-685.
- Ranu, H.S. (1995). Gait analysis of diabetic foot. Proceedings of IEEE International Conference, Shreveport, LA, 197-200.
- Razian, M.A. & Pepper, M.G. (2003). Design, development, and characteristics of an in-shoe triaxial pressure measurement transducer utilizing a single element of piezoelectric copolymer film. Proceedings of IEEE Transactions on Neural Systems and Rehabilitation Engineering, Canterbury, UK, 11 (3), 288-293.

- Resistor 1K Ohm ¼ Watt.* (2010). Retrieved October 23, 2010, from Basic Micro Technology At Work: http://www.basicmicro.com/Resistor-1K-Ohm-14-Watt_p_118.html.
- Richter, E., Morley, R., Pickard, W., Maluf, K., Klaesner, J. & Mueller, M. (1999). In-shoe multisensory data acquisition. Proceedings of the First Joint BMES/EMBS Conference Serving Humanity, Advancing Technology, Atlanta, GA, USA, 618.
- Rodriguez-Silva, D. A., Gil-Castineira, F., Gonzalez-castano, F. J., Duro, R. J., Lopez-Pena, F. & Vales-Alonso, J. (2008). Human motion tracking and gait analysis: A brief review of current sensing systems and integration with intelligent environments. Proceedings of IEEE International Conference on Virtual Environments, Human-Computer Interfaces, and Measurement Systems, Istanbul, Turkey, 166-171.
- Roetenberg, D., Slycke, P.J. & Veltink, P.H. (2007). Ambulatory position and orientation tracking fusing magnetic and inertial sensing. Proceedings of IEEE Transactions on Biomedical Engineering in Biomedical Engineering, Enschede, 54 (5), 883-890.
- Rueterbories, J., Spaich, E.G., Larsen, B. & Andersen, O.K. (2010). Methods for gait event detection and analysis in ambulatory systems. *Medical Engineering & Physics*, 8-16.
- Ryu, T., Choi, H.S., Choi, H.W. & Chung, M.K. (2006). A comparison of gait characteristics between Korean and Western people for establishing Korean gait reference data. *International Journal of Industrial Ergonomics*, 36, 1023-1030.
- Salpavaara, T., Verho, J., Lekkala, J. & Halttunen, J. (2009). Wireless insole sensor system for plantar force measurements during sport events. Proceedings of the XIX IMEKO World Congress, Fundamental and Applied Metrology, Lisbon, Portugal, 2118-2123.
- Sean, Yip, W. & Prieto, T.E. (1996). A system for force distribution measurement beneath the feet. Proceedings of IEEE International Conference in Biomedical Engineering, Dayton, OH, 32-34.
- Senanayake, S.M.N.A., Chong, Y.Z., Chong, Y.S., Chong, J. & Sirisinghe, R.G. (2006). Instrumented orthopaedics analysis system. Proceedings of IEEE International Conference on Automation Science and Engineering, Shanghai, China, 194-197.
- Senanayke, C. & Senanayake, S.M.N.A. (2009). Human assisted tools for gait analysis and intelligent gait phase detection. Proceedings of Conference on Innovative Technologies in Intelligent Systems and Industrial Applications, Monash University, Sunway Campus, Malaysia, 230-235.

- Senden, R., Grimm, B., Heyligers, I.C., Savelberg, H.H.C.M. & Meijer, K. (2009). Acceleration-based gait test for healthy subjects: Reliability and reference data. *Gait & Posture*, 30, 192-196.
- Shock Absorbing Sheet*. (2010). Retrieved October 23, 2010, from Inventables: <http://www.inventables.com/technologies/shock-absorbing-sheet>.
- Shu, L., Hua, T., Wang, Y.Y., Li, Q., Feng, D.D.G. & Tao, X.M. (2010). In-shoe plantar pressure measurement and analysis system based on fabric pressure sensing array. Proceedings of IEEE Transactions on Information Technology in Biomedicine, Kowloon, China, 14 (3), 767-775.
- Simon, S.R. (2004). Quantification of human motion: gait analysis-benefits and limitations to its application to clinical problems. *Gait & Posture*, 37, 1869-1880.
- SK40C Enhanced 40 Pins PIC Start-Up Kit User's Manual V1.1*. (2010). Cytron Technologies.
- Smith, B.T., Coiro, D.J., Finson, R., Betz, R.R. & McCarthy, J. (2002). Evaluation of force-sensing resistors for gait event detection to trigger electrical stimulation to improve walking in the child with cerebral palsy. Proceedings of IEEE Transaction on Neural System and Rehabilitation Engineering, Paris, France, 10 (1), 22-29.
- Solberg, J., Sutton, S. & Yung, S.J. (1999). *Conductive polymer sensor in-shoe discrete plantar pressure measurement system*. ECE 314 Final Project.
- Svensson, W. & Holmberg, U. (2005). Foot and ground measurement using portable sensors. Proceedings of IEEE 9th International Conference on Rehabilitation Robotics, Chicago, IL, USA, 448-450.
- Tanaka, R., Shigematsu, M., Motooka, T., Mawatari, M. & Hotokebuchi, T. (2010). Factors influencing the improvement of gait ability after total hip arthroplasty. *Journal of Arthroplasty*, 25 (6), 982-985.
- ThunderPower Lithium Polymer Battery – 480 mAh 11.1V with JST Connector*. (2010). Retrieved November 24, 2010, from sgbotic: http://www.sgbotic.com/index.php?dispatch=products.view&product_id=390
- Titianova, E.B., Mateev, P.S. & Tarkka, I.M. (2004). Footprint analysis of gait using a pressure sensor system. *Journal of Electromyography and Kinesiology*, 14, 275-281.
- Triple Axis Accelerometer Breakout – MMA7260Q*. (2010). Retrieved November 24, 2010, from sgbotic: http://www.sgbotic.com/index.php?dispatch=products.view&product_id=107

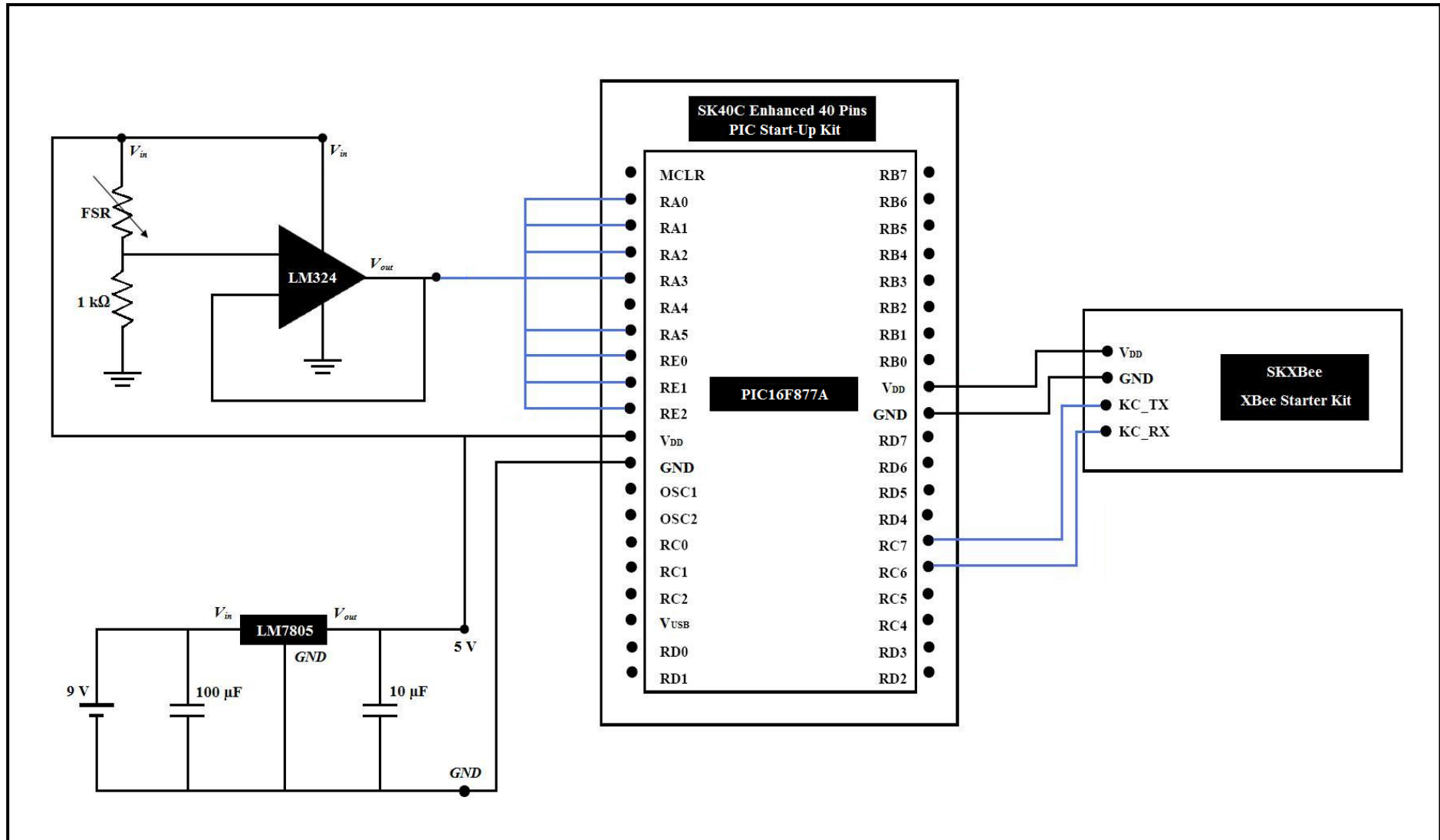
- UIC00B USB ICSP PIC Programmer User's Manual V1.0.* (2010). Cytron Technologies.
- Veltink, P.H., Liedtke, C. & Droog, E. (2004). Ambulatory measurement of ground reaction forces. *Proceedings of IEEE International Conference on Systems, Man and Cybernetics, Enschede, Netherlands, 13*, 701-703.
- Vengsarkar, A.S., Abler, J.H., Abu-Faraj, Z.U., Harris, G.F. & Wertsch, J.J. (1994). Holter system development for recording plantar pressures: Software development. *Proceedings of 16th IEEE Annual International Conference, Baltimore, MD 2*, 936-937.
- Venugopal, G., Parmar, B.J., Rajanna, K. & Nayak, M.M. (2007). Multi-point sensing system for plantar pressure measurement. *Proceedings of IEEE International Conference, Atlanta, GA*, 978-981.
- Verghese, J. & Xue, X.N. (2010). Predisability and gait patterns in older adults. *Gait & Posture, 3*, 24-27.
- Voth, D. (2003). You can tell me by the way I walk. *In The News*, 4-6.
- Wahab, Y., Zayegh, A., Veljanovski, R. & Begg, R.K. (2008). Design of MEMS biomedical pressure sensor for gait analysis. *Proceedings of ICSE, Johor Bahru, Malaysia*, 166-169.
- Wahab, Y., Zayegh, A., Veljanovski, R. & Begg, R.K. (2008). Sensitivity optimization of a foot plantar pressure micro-sensor. *Proceedings of IEEE International Conference on Microelectronics, Sharjah*, 131-134.
- Wahab, Y., Zayegh, A., Veljanovski, R. & Begg, R.K. (2009). Micro-sensor for foot pressure measurement. *Proceedings of IEEE International Conference, Hyderabad*, 1-5.
- Wang, H.J., Liu, J.Y. & Chen, S.F. (2009). An intelligent 3D platform for plantar pressure distribution measurement. *Proceedings of the IEEE International Conference on Mechatronics and Automation, Changchun, China*, 4479-4483.
- Wertsch, J.J., Webster, J.G. & Tompkins, W.J. (1992). A portable insole plantar pressure measurement. *Journal of Rehabilitation Research and Development, 29* (1), 13-18.
- Wervey, R.A., Abler, J.H., Abu-Faraj, Z.U., Harris, G.F. & Wertsch, J.J. (1995). Data preview software for interactive review of holter type plantar pressure data. Wheeler, J., Rohrer, B., Kolwadwala, D., Buerger, S., Gilver, R., Neely, J., et al. (2009). In-shoe MEMS pressure sensing for a lower-extremity exoskeleton. *Proceedings of the 1st IEEE/RAS-EMBS International Conference in Biomedical Robotics and Biomechanics, Pisa*, 31-34.

- Wires*. (2010). Retrieved October 23, 2010, from Cytron Technologies: <http://cytron.com.my/viewProduct.php?pid=GxE3DjQfBxwgIwgMDwEsBQZ6xQRcK/z0NM0VBIOjd8Q=>
- Wong, W.Y., Wong, M.S. & Lo, K.H. (2007). Clinical applications of sensors for human posture and movement analysis: A review. *Proceedings of International Conference on Prosthetics and Orthotics, Cambridge, USA, 31* (1), 62-75.
- XBee/XBee-PRO OEM RF Modules*. (2006). MaxStream.
- XBee Starter Kit SKXBee User's Manual V1.0*. (2008). Cytron Technologies.
- Yang, C.M., Chou, C.M., Hu, J.S., Hung, S.H., Yang, C.H., Wu, C.C., et al. (2009). A wireless gait analysis system by digital textile sensors. *Proceedings of 31st Annual International Conference of the IEEE EMBS Minneapolis, Minnesota, USA, 7256-7260*.
- Yaniger, S.J. (1991). Force sensing resistors: A review of the technology. *Electronics*, 666-668.
- Ye, W.Z., Xu, Y.S. & Lee, K.K. (2005). Shoe-mouse: An integrated intelligent shoe. *Proceedings of IEEE/RSJ International Conference in Intelligent Robots and Systems (IROS), Hong Kong, China, 1163-1167*.
- Yu, H.Y., Riskowski, J., Brower, R. & Sarkodie-Gyan, T. (2009). Gait variability while walking with three different speeds. *Proceedings of IEEE 11th International Conference in Rehabilitation Robotics, Kyoto International Conference Center, Japan, 4, 823-827*.
- Zehr, E.P., Stein, R.B., Komiyama, T. & Kenwell, Z. (1995). Linearization of force sensing resistors (FSR's) for force measurement during gait. *Proceedings of IEEE-EMBC and CMBEC Theme 7: Instrumentation, Montreal, Que, 2, 1571-1572*.
- Zequera, M.L, Stephan, S. & Paul, J. (2007). Effectiveness of modulated insoles in reducing plantar pressure in diabetic patients. *Proceedings of the 29th Annual International Conference of the IEEE EMBS Cite Internationale, Lyon, France, 4671-4674*.
- Zequera, M.L., Solomonidis, S.E., Vega, F. & Rondon, L.M. (2003). Study of the plantar pressure distribution on the sole of the foot of normal and diabetic subjects in the early stages by using a hydrocell pressure sensor. *Proceedings of the 25th Annual International Conference of the IEEE EMBS Cancun, Mexico, 1874-1877*.
- Zhang, K., Sun, M., Lester, D.K., Pi-Sunyer, F.X., Boozer, C.N. & Longman, R.W. (2005). Assessment of human locomotion by using an insole measurement system and artificial neural networks. *Journal of Biomechanics, 38, 2276-2287*.

- Zhu, H.S., Harris, G.F., Wertsch, J.J., Tompkins, W.J. & Webster, J.G. (1991). A microprocessor-based data-acquisition system for measuring plantar pressures from ambulatory subjects. *Proceedings of IEEE Transactions on Biomedical Engineering*, Milwaukee, WI, USA, 38 (7), 710-714.
- Zhu, H.S., Maalej, N., Webster, J.G., Tompkins, W.J., Bach-Y-Rita, P. & Wertsch, J.J. (1990). An umbilical data-acquisition system for measuring pressures between the foot and shoe. *Proceedings of IEEE Transaction on Biomedical Engineering*, Madison, WI, USA, 37 (9), 908-911.
- Zhu, H.S., Wertsch, J.J., Harris, G.F., Price, M.B. & Alba, H.M. (1989). Pressure distribution beneath sensate and insensate feet. *Proceedings of IEEE Engineering in Medicine and Biology Society 11th Annual International Conference*, Seattle, WA, 822-823.

APPENDICES

APPENDIX A: Circuit Diagram of Instrumented Insole System



APPENDIX B: PIC Microcontroller Coding

```

char force_L1, force_L2, force_L3,
    force_L4;           //Defining FSR variables from left foot.
char force_R1, force_R2, force_R3,
    force_R4;           //Defining FSR variables from right foot.
char txt[6];           //Defining an array or string.

void tx_data(char, char); //Defining a sub-function.

void main(void)         //Starting of main function.
{
ADCON1 = 0x80;          //Setting result format, conversion clock and
                        //activating ADC function.

TRISA = 0x2F;           //Setting Port A as input.
TRISE = 0x07;           //Setting Port E as input.
TRISC = 0x80;           //Setting Port C as input and output.

PORTA = 0x00;           //Clearing up Port A.
PORTE = 0x00;           //Clearing up Port E.
PORTC = 0x00;           //Clearing up Port C.

Usart_init(9600);      //Setting up baud rate.

do
{
force_L1 = adc_read(0)/4; //Read forces of left foot FSR 1.
Delay_ms(5);              //Delay for 5 milliseconds.
tx_data('A', force_L1);  //Transfer information to sub-function.

force_L2 = adc_read(1)/4; //Read forces of left foot FSR 2.
Delay_ms(5);              //Delay for 5 milliseconds.
tx_data('B', force_L2);  //Transfer information to sub-function.
}

```

```

force_L3 = adc_read(2)/4;           //Read forces of left foot FSR 3.
Delay_ms(5);                       //Delay for 5 milliseconds.
tx_data('C', force_L3);           //Transfer information to sub-function.

force_L4 = adc_read(3)/4;           //Read forces of left foot FSR 4.
Delay_ms(5);                       //Delay for 5 milliseconds.
tx_data('D', force_L4);           //Transfer information to sub-function.

force_R1 = adc_read(5)/4;           //Read forces of right foot FSR 1.
Delay_ms(5);                       //Delay for 5 milliseconds.
tx_data('E', force_R1);           //Transfer information to sub-function.

force_R2 = adc_read(6)/4;           //Read forces of right foot FSR 2.
Delay_ms(5);                       //Delay for 5 milliseconds.
tx_data('F', force_R2);           //Transfer information to sub-function.

force_R3 = adc_read(7)/4;           //Read forces of right foot FSR 3.
Delay_ms(5);                       //Delay for 5 milliseconds.
tx_data('G', force_R3);           //Transfer information to sub-function.

force_R4 = adc_read(8)/4;           //Read forces of right foot FSR 4.
Delay_ms(5);                       //Delay for 5 milliseconds.
tx_data('H', force_R4);           //Transfer information to sub-function.

}while(1);                          //Always loop.
}

void tx_data(char a, char b)         //Start of sub-function.
{
  Usart_write(a);                  //UART write character (a).
  bytetostr(b,txt);                //Converts (b) into string and store in txt
                                   //array.
}

```

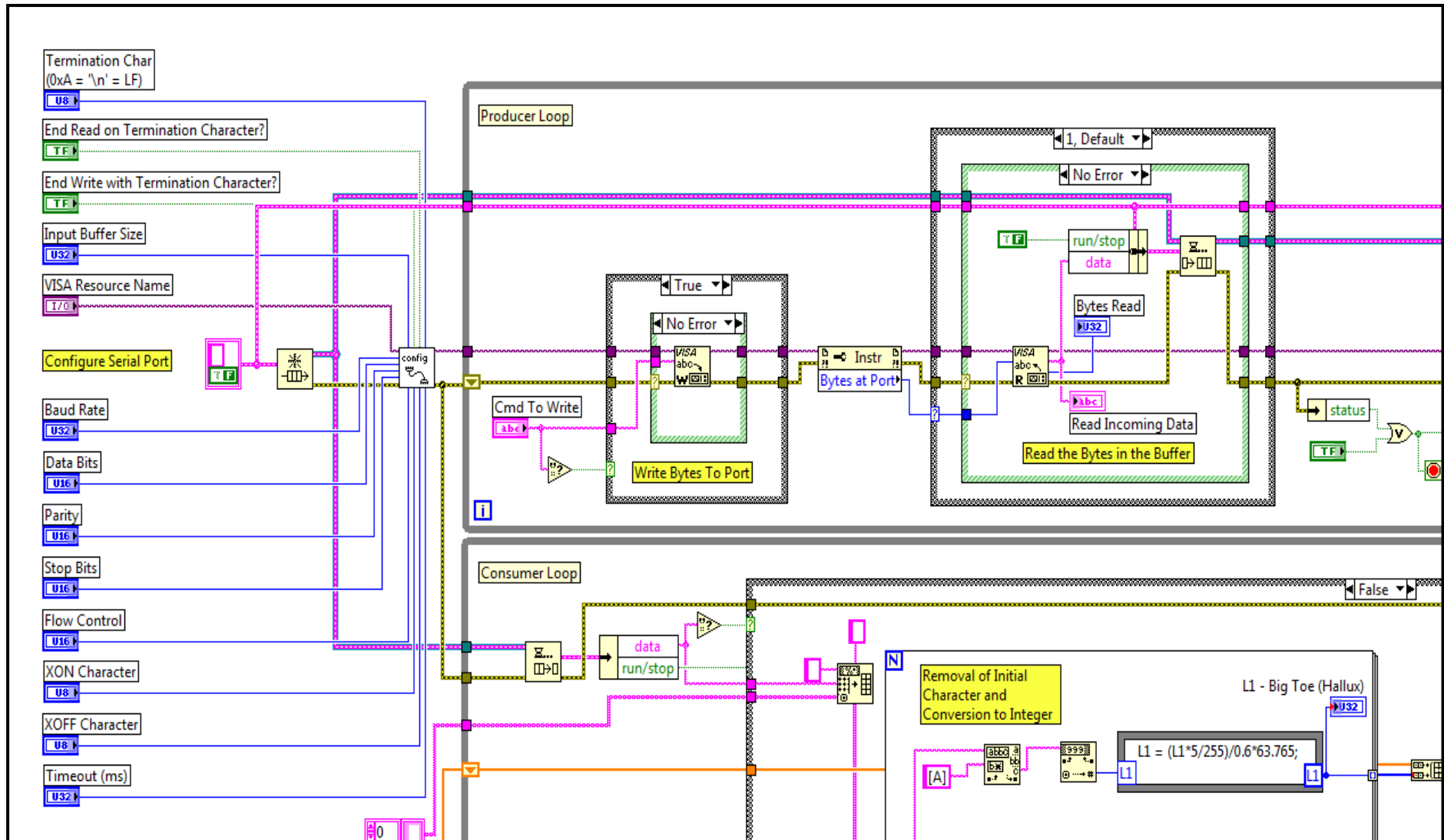
```
if(txt[0] == ' ')
Usart_write('0');           //If txt[0] stores nothing, UART writes 0.
else
Usart_write(txt[0]);       //Otherwise, UART writes the value.

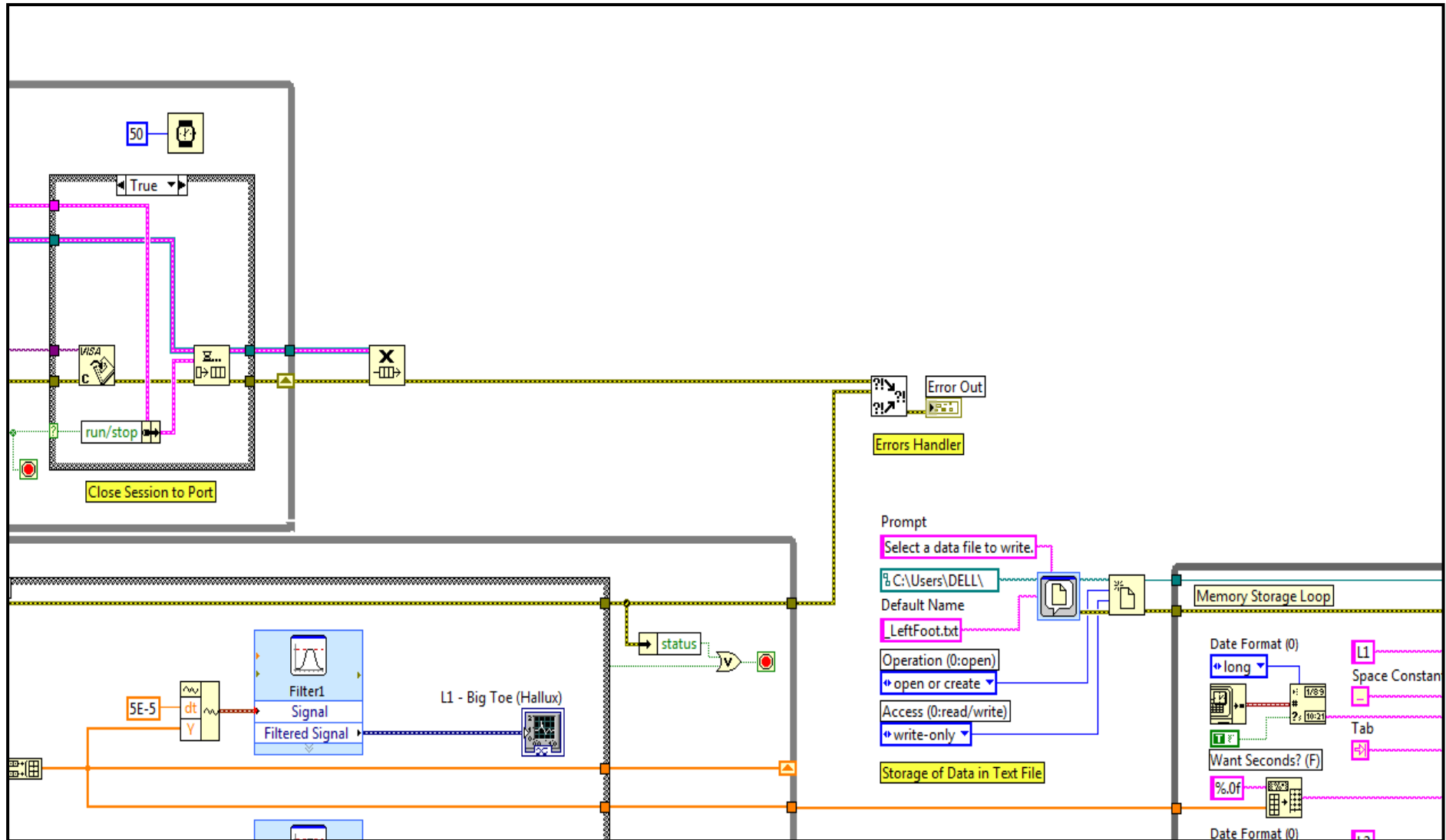
if(txt[1] == ' ')
Usart_write('0');           //If txt[1] stores nothing, UART writes 0.
else
Usart_write(txt[1]);       //Otherwise, UART writes the value.

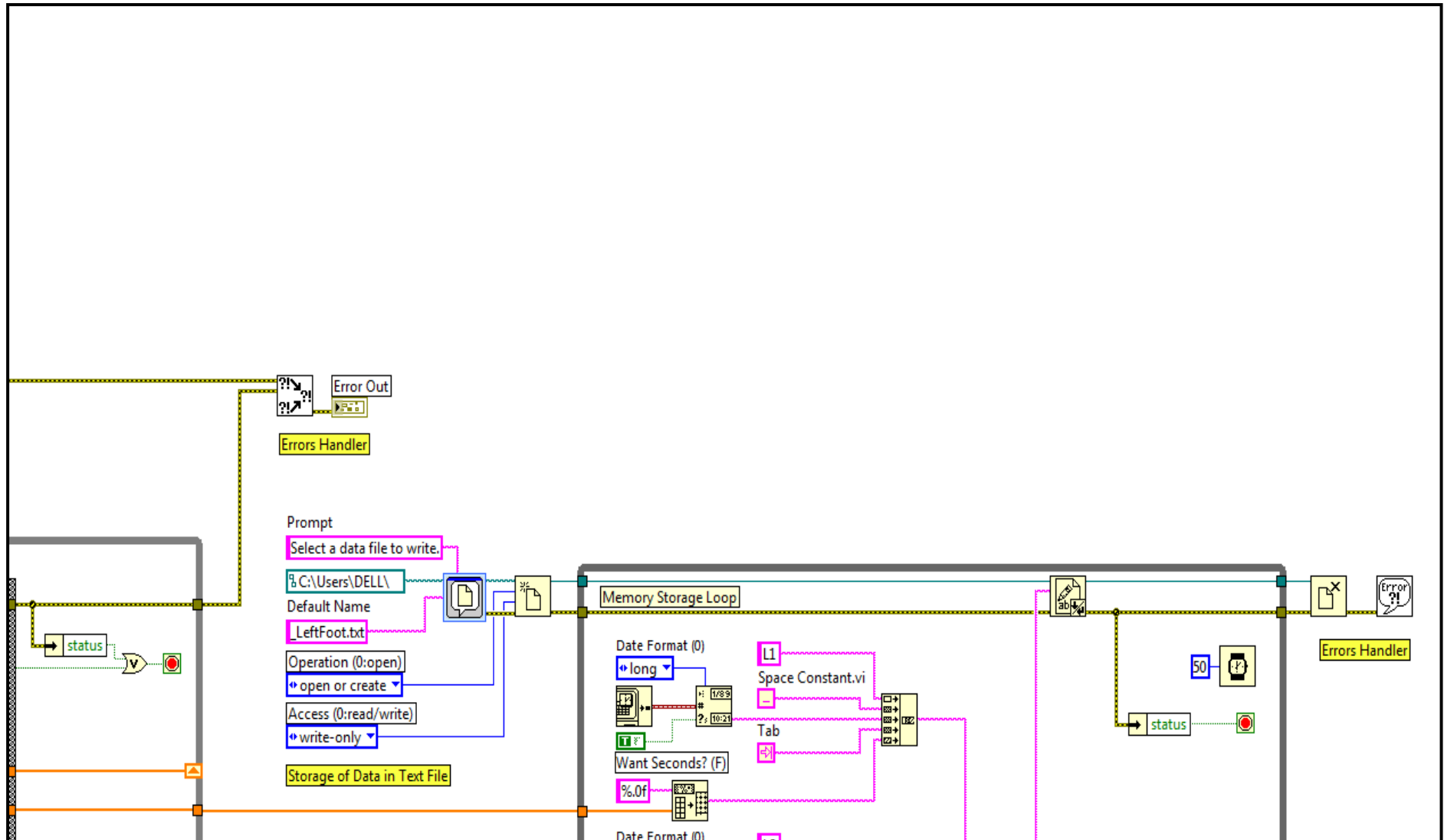
if(txt[2] == ' ')
Usart_write('0');           //If txt[2] stores nothing, UART writes 0.
else
Usart_write(txt[2]);       //Otherwise, UART writes the value.

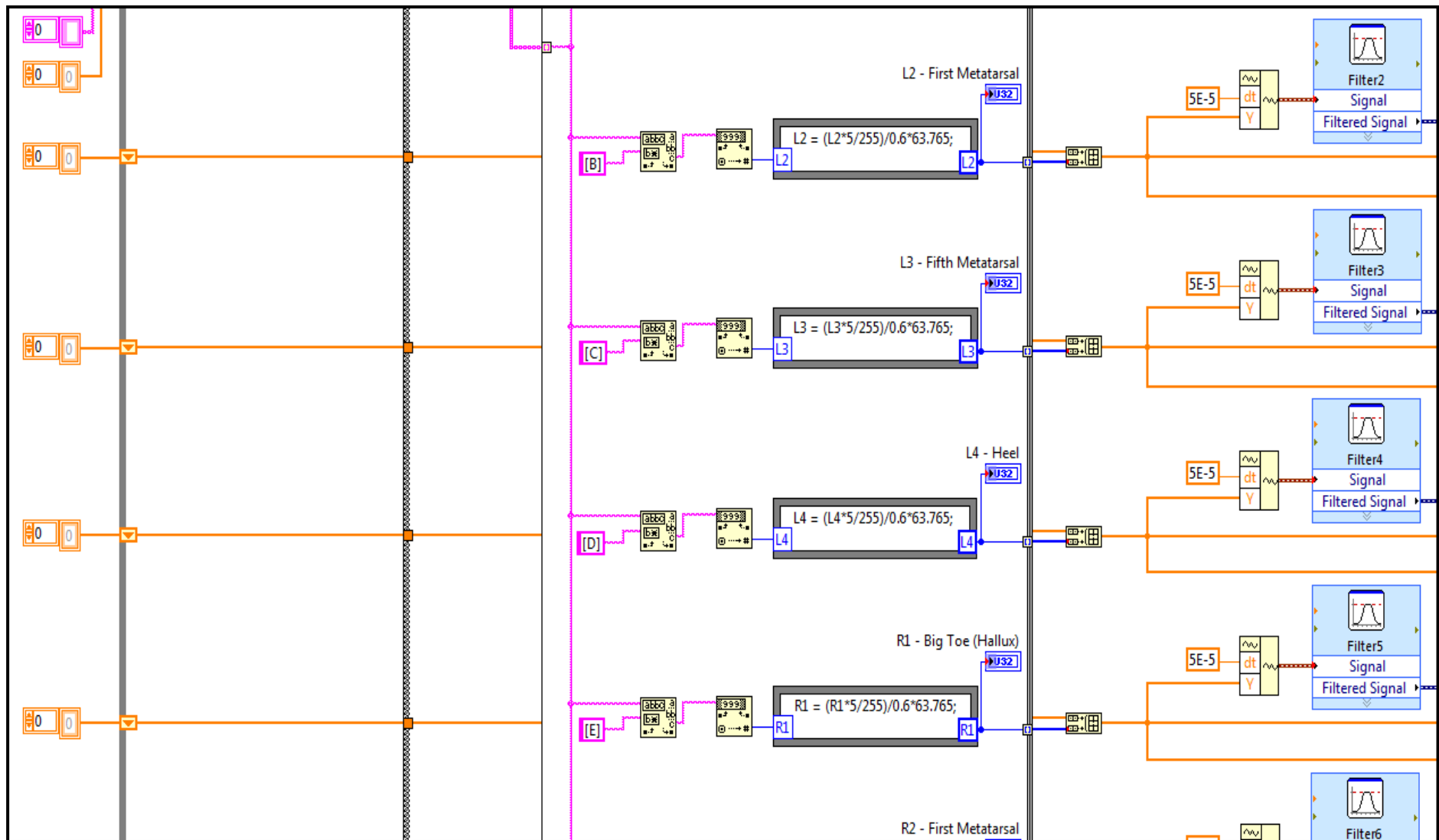
Delay_ms(50);              //Delay for 50 milliseconds.
}
```

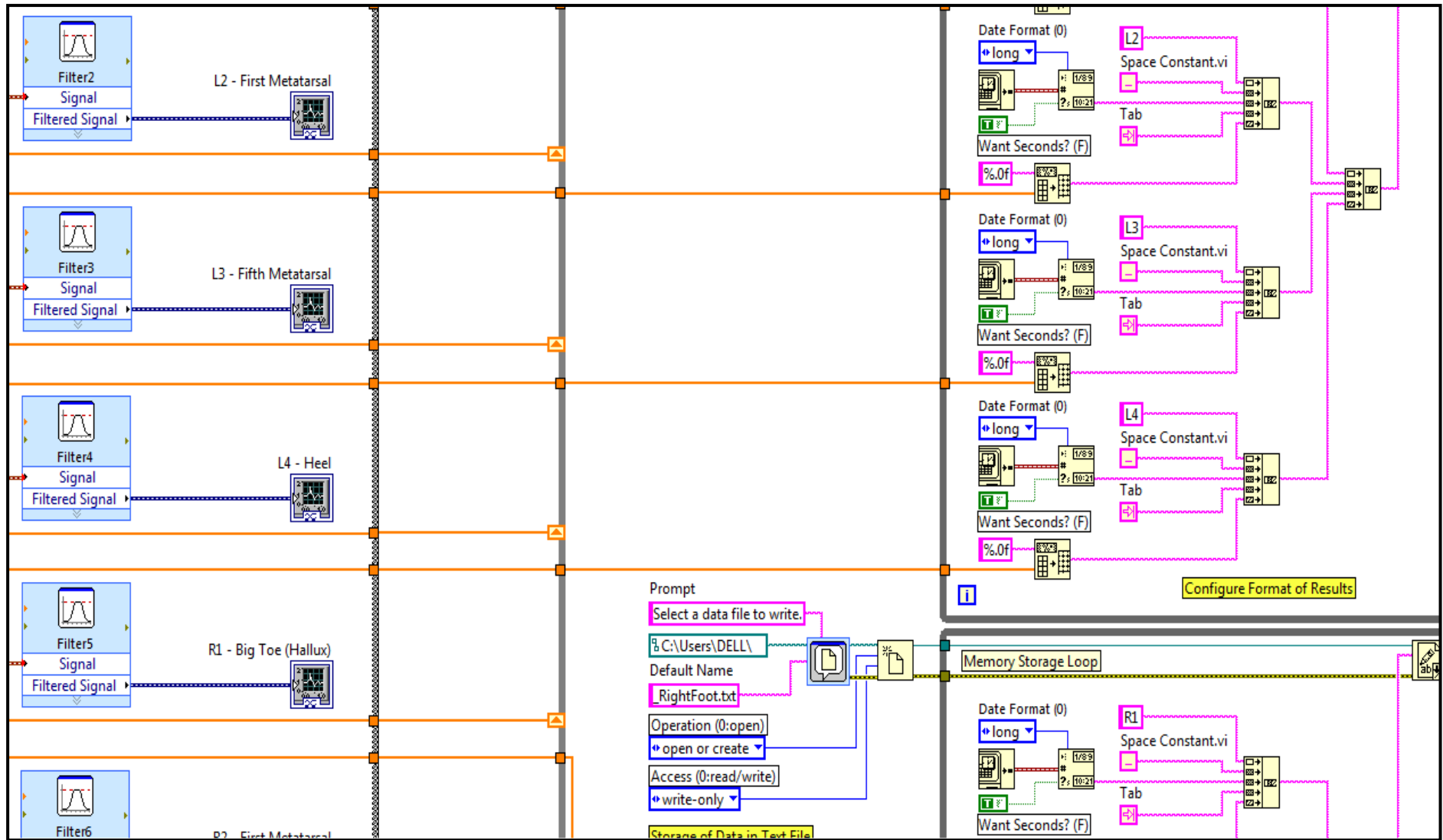
APPENDIX C: LabVIEW Block Diagram

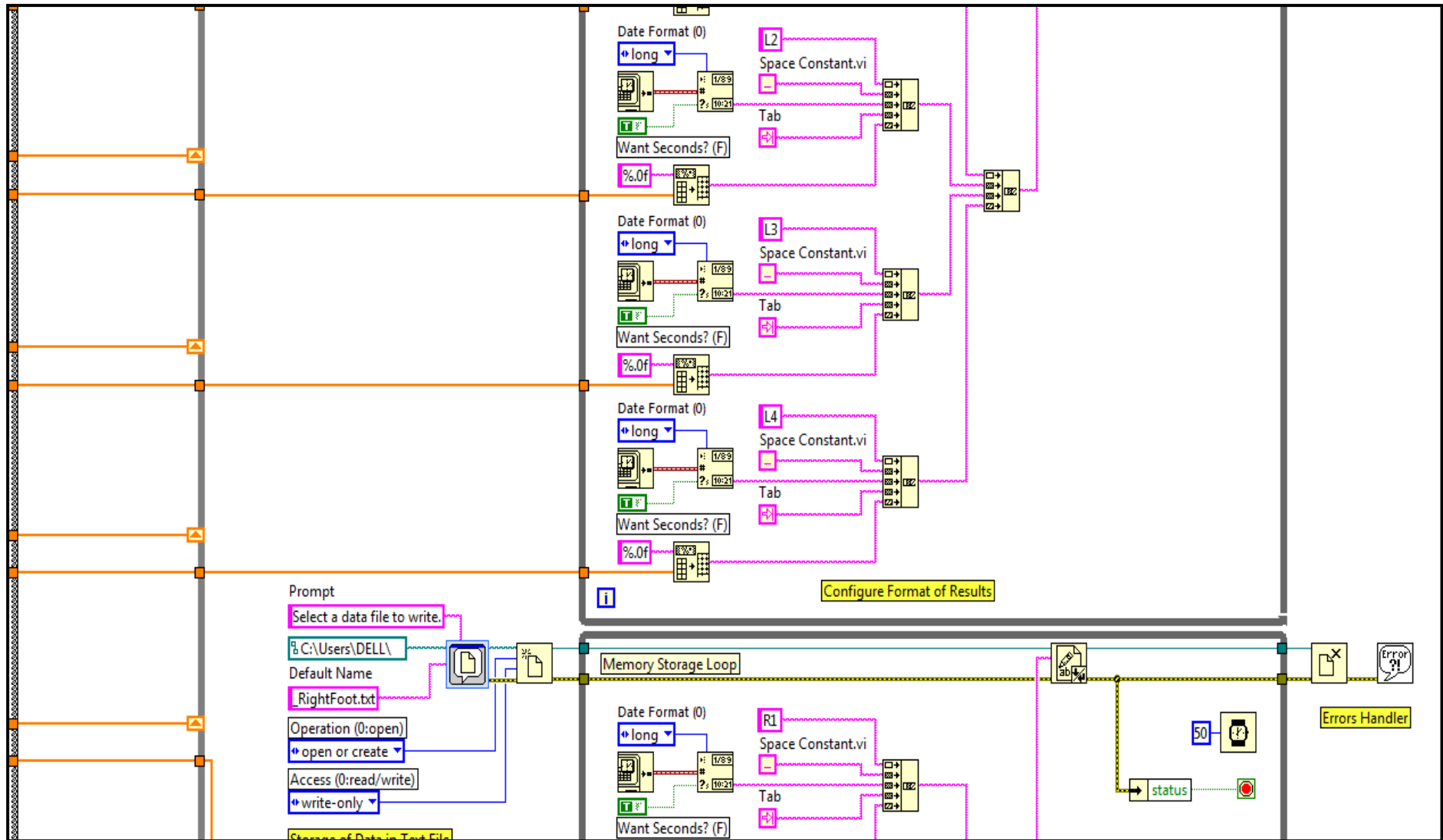


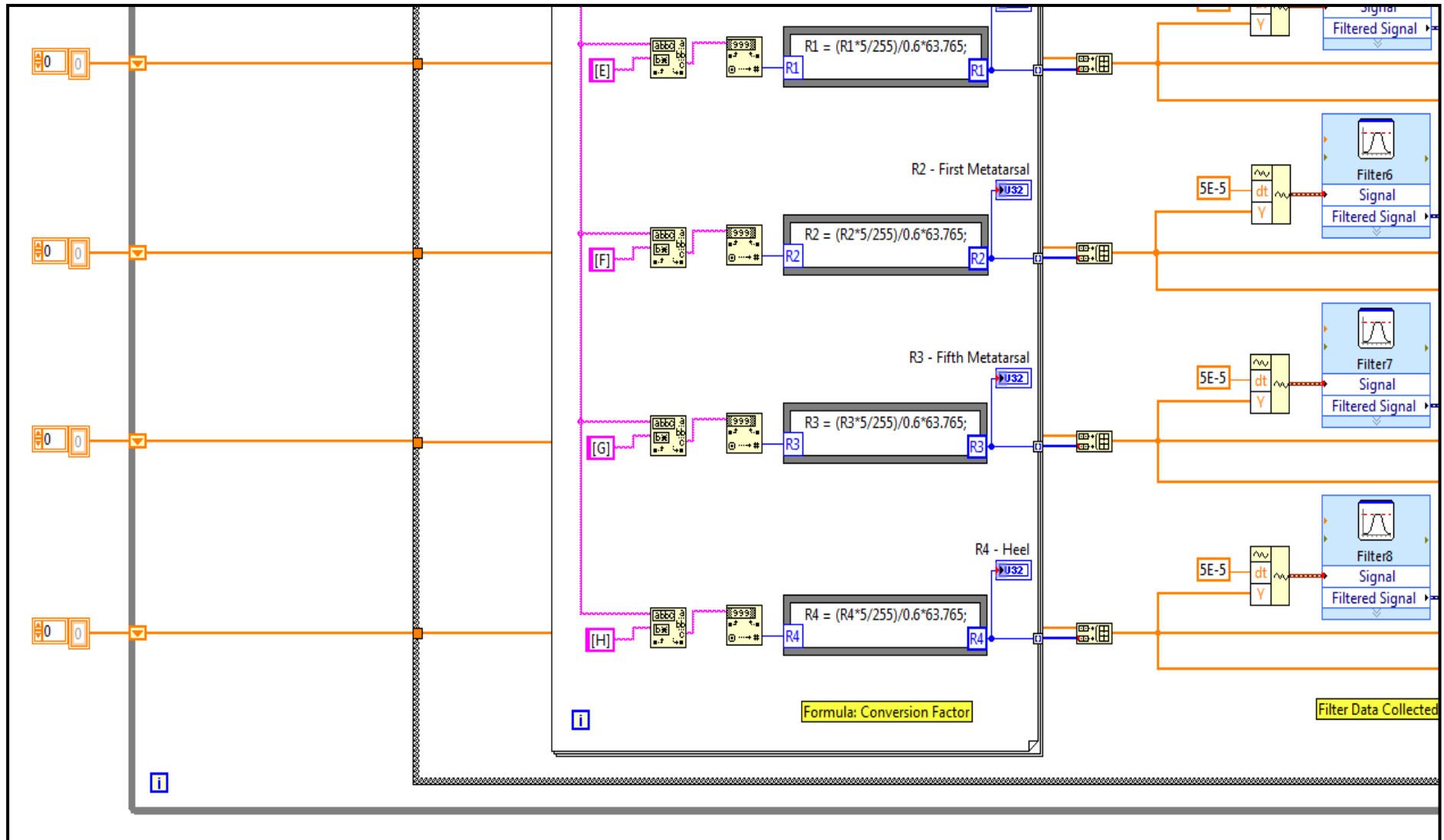


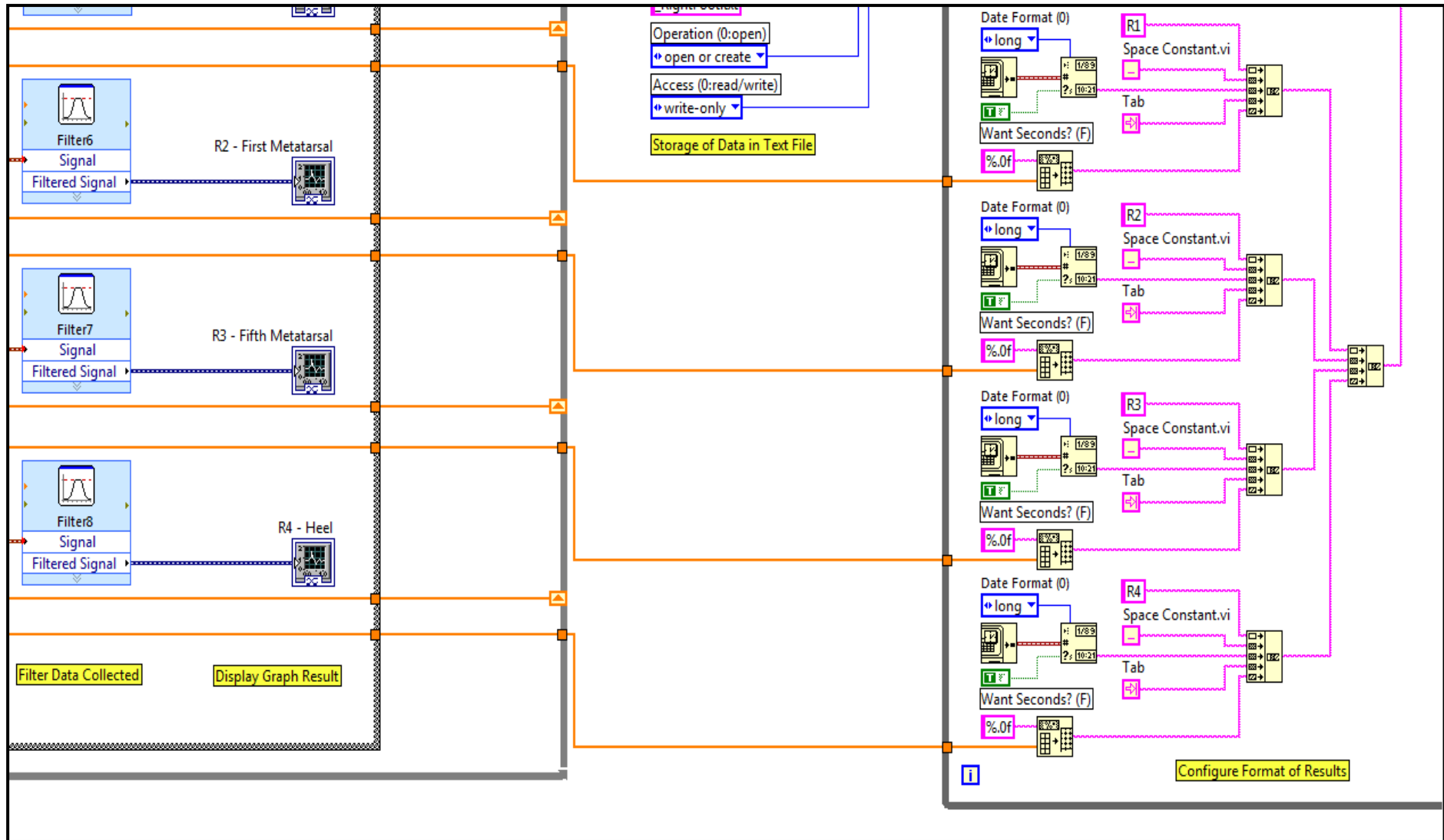


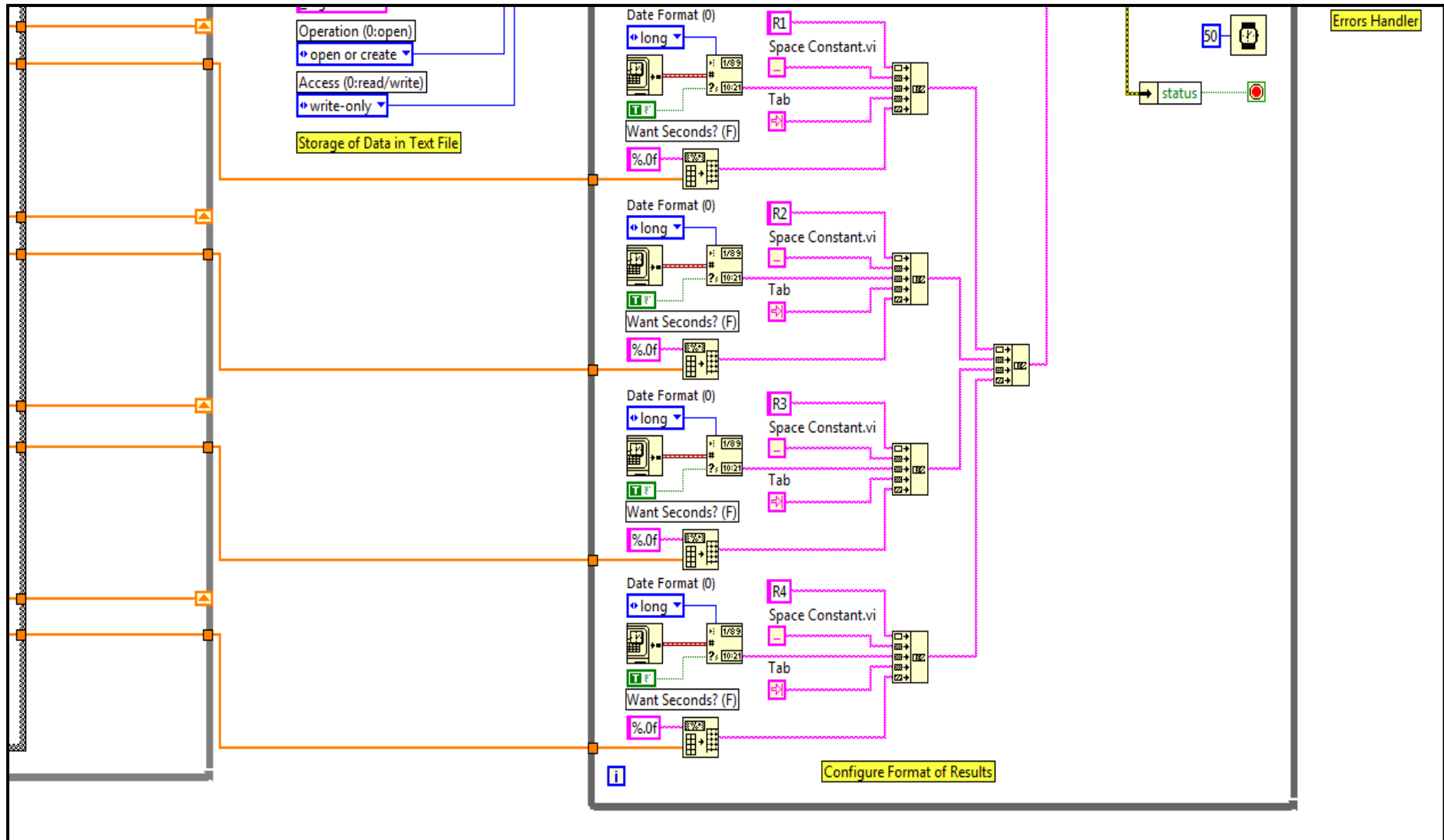












APPENDIX D: Subject Testing Consent Form



SUBJECT TESTING CONSENT FORM

Healthy and Pathological Gait Subjects Instrumented Insole Evaluator Testing

We are students from Universiti Tunku Abdul Rahman, who are currently studying year four trimester two in Biomedical Engineering. The purpose of this consent form is to find out your interest in joining our research as a voluntary participant. It will be grateful if you would like to assist us in completing this research.

PART A – INTRODUCTION

Gait analysis is the study and investigation of the human locomotion pattern, which can be carried out by using visual observation, sensor technology, video or optical cameras or integration of these technologies. Gait analysis is used in many applications namely, sports performance analysis, product design, gait rehabilitation, post injury assessments, and improvement of human walking orientation.

Therefore, the motivation of our project is to design and develop a low cost, reliable, and portable instrumented insole system. An insole system is investigated which is capable of real-time pressure analysis at decided locations of sensor beneath each foot. In addition, it is designed to provide qualitative and quantitative information on how the ground reaction forces distributed on the human foot.

This instrumented insole system will provide instrumented gait analysis outside of traditional, expensive motion labs. Such a system has the potential to be highly informative by allowing data collection throughout the day in variety of environments, thus providing a vast quantity of long-term data not obtainable with current gait analysis system where this analysis cannot be done by using force platform in current technology.

This is why this subject testing is being proposed and conducted to collect more and more data in proving the functionality of the system. Through this subject testing, problems and difficulties of the system can be figured out. Further improvements and optimizations can be taken to prevent the same incident happened again in future.

This subject testing involved in placing the instrumented insole inside your shoes and the circuit board will be attached to your waist by using an adjustable belt. While you are walking, the sensors will detect the forces distribution beneath your foot. After that, the output signals from the sensors will be collected by microcontroller. The small antenna of XBee module on the circuit board will then transmit the output signals to the receiving transmitter at computer. All signals are saved on a laptop computer set.

PART B – INSTRUCTION

Before the test is being carried out, initial test will be conducted to let you familiar with the instrumented insole inside your shoe. This initial test is important in making sure the system can work properly in a good condition in order to prevent any unwanted errors occurred during the subject testing. Besides, a photo of eight-segment representation will be captured where the body segment lengths and circumferences (anthropometric dimensions) are being measured at the same time.

A series of tasks will then be conducted for each subject approximately 30 minutes, which is divided into different locomotion activities; they are standing, sitting, walking, and running. The idea schedule to conduct such subject testing will be on week 11. The details of these tasks are as followed:

a) Standing

- Look straight ahead; stand as still as possible with two hands lower down on the sides, and the knees should not bend. Place your feet so they point forward (and parallel to X-Axis).
- Maintain the standing position at least for 10 seconds.
- Two trials are needed.

b) Sitting

- Look straight ahead, sit 90° vertical position on a chair with two hands lowered down on the sides, the legs facing down, and slight contact with the floor.
- Maintain the sitting position at least for 10 seconds.
- Two trials are needed.

c) Walking

- Look straight ahead, move forward in as straight a line as possible, and walking at your normal pace, as if you are taking a brisk walk in the park.
- Walking for at least 30 steps within 60 seconds.
- Two trials are needed.

d) Running

- Look straight ahead, move forward without leaning any sides, and run faster than your normal pace, as if you are chasing a bus.
- Running for at least 30 steps within 60 seconds.
- Two trials are needed.

***** ATTENTION *****

If you are interested and willing to join our testing, please fill in the consent form at next page and send back to us (with your academic timetable as well). We will confirm you with the date, time, and venue for the testing as soon as possible.

PART C – PERSONAL INFORMATION

Name : **Compulsory Digital Photo**

Gender :

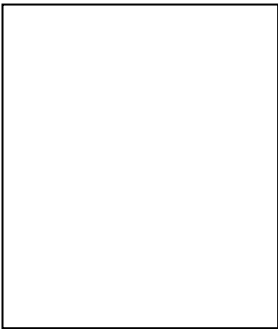
Age :

Date of Birth :

Address :

Telephone :

Email :



Student ID :

Course :

Year/Trimester :

Height (in cm) :

Weight (in kg) :

Size of Shoe :

Brand of Shoe :

History of Falls* : _____ (in the past year) _____ (in the past month)

***Fall = Inadvertently coming to ground**

Other Medical Records (Related to lower extremities):

PART D – TERMINOLOGY

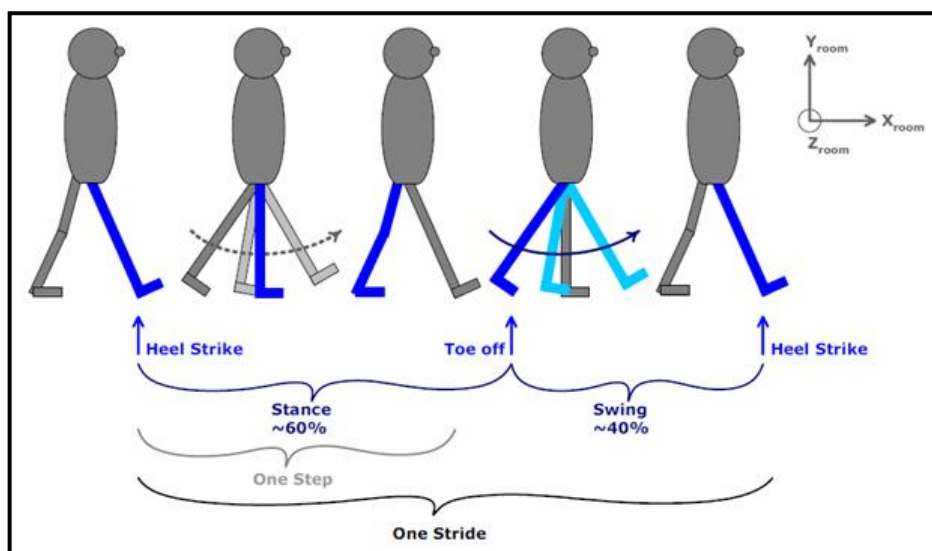


Figure D.1: The gait cycle (Morris, 2004)

<i>Gait</i>	Manner of walking.
<i>Heel strike</i>	Time at which the heel first makes contact with the floor; indicates end of swing and start of stance.
<i>Stance</i>	Period in which the foot is in contact with the floor; this generally takes up about 60% of the stride cycle.
<i>Step</i>	Interval between two successive heel strikes for opposite feet.
<i>Stride</i>	Interval between two successive heel strikes of the same foot.
<i>Swing</i>	Period during which the foot is not in contact with the floor; this generally takes up about 40% of the stride cycle.
<i>Toe off</i>	Time at which the great toe is first no longer in contact with the floor; indicates end of stance and start of swing.

Contact us if you have any doubt:

Chan Meng Nen 017-6180923 cmengnen@gmail.com

Leng Yen Ran 016-8119232 yenran_87@hotmail.com

APPENDIX E: Subject Testing Protocol



SUBJECT TESTING PROTOCOL

Healthy and Pathological Gait Subjects

Instrumented Insole Evaluator Testing

PART A – PERSONAL INFORMATION

Name : _____

Student ID : _____

Course : _____

Year/Trimester : _____

Size of Shoe : _____

Brand of Shoe : _____

Group : _____

Date of Test : _____

Time of Test : _____

Subject ID

PART B – AGREEMENT

Attention: The information and results of this subject testing are private and confidential in order to protect the right and privacy of volunteers. These data and results obtained will be used for project and research purpose only.

My participation in this study is voluntary. Refusal to participate or dropping out of the subject testing at any time will involve no penalty or loss of benefits. I confirm that the purpose of the research, the study procedures, the possible risks, discomfort, and potential benefits that I may experience have been explained to me. Alternatives to my participation in this research study also have been discussed. All my questions have been answered. I have read this agreement. My signature below indicates my willingness to participate in this research study.

Subject's Signature (Date/Time)

PART C – TASKS

No.	Tasks to be Completed	Remarks
1	Photo of eight-segment representation ➤ <u>Right side</u> of the subject. ➤ Standing straight and the face look straight ahead.	
2	Anthropometric data measurement ➤ Foot length (m) ➤ Ankle-to-knee length (m) ➤ Ankle-to-thigh length (m)	_____m _____m _____m
3	Standing e) Look straight ahead; stand as still as possible with two hands lower down on the sides, and the knees should not bend. Place your feet so they point forward (and parallel to X-Axis). f) Maintain the standing position at least for 10 seconds.	
4	Sitting g) Look straight ahead, sit 90 °vertical position on a chair with two hands lowered down on the sides, the legs facing down, and slight contact with the floor. h) Maintain the sitting position at least for 10 seconds.	
5	Walking i) Look straight ahead, move forward in as straight a line as possible, and walking at your normal pace, as if you are taking a brisk walk in the park. j) Walking for at least 30 steps within 60 seconds.	
6	Running k) Look straight ahead, move forward without leaning any sides, and run faster than your normal pace, as if you are chasing a bus. l) Running for at least 30 steps within 60 seconds.	

PART D – RECOMMENDATION AND IMPROVEMENT

Comments:

Contact us if you have any doubt:

Chan Meng Nen 017-6180923 cmengnen@gmail.com

Leng Yen Ran 016-8119232 yenran_87@hotmail.com

APPENDIX F: Subject Testing Schedule



SUBJECT TESTING SCHEDULE

Healthy and Pathological Gait Subjects

Instrumented Insole Evaluator Testing

INSTRUCTION

The schedule of subject testing is arranged according to the size of shoes. You may check your name, time, and location at each group. There are some requirements hope to be followed by you for the day of subject testing in order to collect and process a better results from the testing. The requirements are as followed:

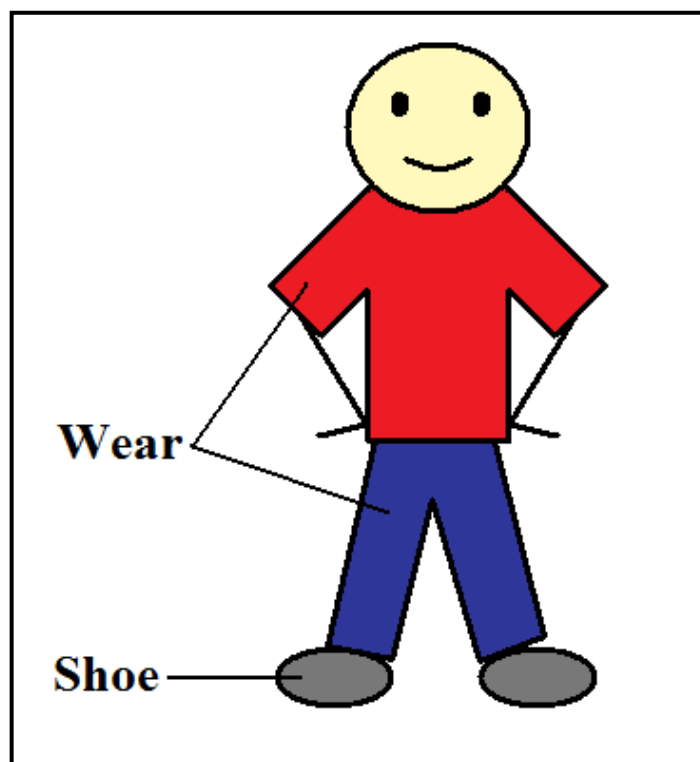


Figure F.1: Sample of wearing for subject testing

a) Wear

- A comfortable t-shirt and long pants will be good.
- Other extra accessories or decorations are not recommended.

b) Shoe

- Enclosed shoe with stocking, sport shoe is recommended.
- Slippers or sandals are not allowed for this subject testing.

c) Time

- Please be punctual, report yourself at the location of subject testing about 15 minutes earlier than your testing time.
- If possible, arrive at the time before we start the subject testing for each group.
- A short briefing will be given at the start of subject testing.

GROUP 1

Date : March 28, 2011 (Monday)
Location : SE Block, Biomechanics Lab
Time : 12.00 pm – 2.00 pm

No.	Name	Size of Shoe	Brand of Shoe	Contact No.
1	Chou Miew Fatt	6	Nike	016-7312108
2	Cheah Ee Ling	7	Power	016-6697425
3	Chew Kah Mun	7	Amesdex	016-2823802
4	Fong Suw Wei	7	Adidas	012-2762418

GROUP 2

Date : March 28, 2011 (Monday)
Location : SE Block, Biomechanics Lab
Time : 3.00 pm – 4.00 pm

No.	Name	Size of Shoe	Brand of Shoe	Contact No.
1	Leng Yen Ran	6	Power	016-8119232
2	Chan Meng Nen	8	Nike	017-6180923

GROUP 3

Date : March 28, 2011 (Monday)
Location : SE Block, Biomechanics Lab
Time : 4.00 pm – 6.00 pm

No.	Name	Size of Shoe	Brand of Shoe	Contact No.
1	Wong Wei Fong	4	BUM	016-7057702
2	Karen Ho Shin Jye	4.5	Converse	012-8774133
3	Loo Yi Shing	5	Converse	019-3999673
4	Fong Lai Imm	8	New Balance	019-5528836

GROUP 4

Date : March 29, 2011 (Tuesday)
Location : SE Block, Biomechanics Lab
Time : 9.00 am – 10.00 am

No.	Name	Size of Shoe	Brand of Shoe	Contact No.
1	Lim Yin Pei	4	Nike	019-3852203
2	Low Me Yin	5.5	Converse	016-2442301

GROUP 5

Date : March 29, 2011 (Tuesday)
Location : SE Block, Biomechanics Lab
Time : 3.00 pm – 5.00 pm

No.	Name	Size of Shoe	Brand of Shoe	Contact No.
1	Wong Zhen Yang	8	Power	017-3692038
3	Yap Kian Ming	9	Nike	016-2579417
4	Tung Ren Sin	10	Power	016-4533281
5	Cheah Soon Keong	10	Admiral	012-3166647

GROUP 6

Date : March 30, 2011 (Wednesday)
Location : SE Block, Biomechanics Lab
Time : 10.00 am – 11.00 am

No.	Name	Size of Shoe	Brand of Shoe	Contact No.
1	Kho Ching Leong	7	North Star	016-8652343
2	Dennis Tan Eng Beng	8	Kappa	016-7496118

GROUP 7

Date : March 30, 2011 (Wednesday)
Location : SE Block, Biomechanics Lab
Time : 3.00 pm – 5.00 pm

No.	Name	Size of Shoe	Brand of Shoe	Contact No.
1	Ng Eng Hui	8	Bata	017-6298606
2	Joseph Ting Shyue Horng	9	Nike	012-6278115
3	Ong Chin Horng	10	Admiral	016-7000520
4	Teoh Boon Yew	11	Adidas	016-6938726

GROUP 8

Date : March 31, 2011 (Thursday)
Location : SE Block, Biomechanics Lab
Time : 9.00 am – 11.00 am

No.	Name	Size of Shoe	Brand of Shoe	Contact No.
1	Lee Zhi Hong	9	Power	017-2889144
2	Teng Woon Sheng	9	Nike	012-6698115
3	Teh Chek Min	9	Power	016-4892480
4	Ooi Heap Guan	9.5	New Balance	016-4952414

GROUP 9

Date : March 31, 2011 (Thursday)
Location : SE Block, Biomechanics Lab
Time : 1.00 pm – 3.00 pm

No.	Name	Size of Shoe	Brand of Shoe	Contact No.
1	Mah Wai Lai	5	Swiss Polo	017-4343088
2	Chong Chau Ling	6	Viss	016-2209821
3	Loh Mey Chern	6.5	Brooks	014-6002785
4	Nurul Izwazi Mohd Nor	7	Admiral	013-3115460

Contact us if you have any doubt:

Chan Meng Nen 017-6180923 cmengnen@gmail.com

Leng Yen Ran 016-8119232 yenran_87@hotmail.com

APPENDIX G: Subjects' Information



SUBJECTS' INFORMATION

Healthy and Pathological Gait Subjects

Instrumented Insole Evaluator Testing

SUBJECT TESTING GROUPS

The subject testing is divided into nine groups, where each group is carried out with different date, time, location, and certain amount of subject involved. The details are as followed:

Group	Date	Time	Location	Total of Subjects
1	28.03.2011	12.00 – 14.00	Biomechanics Lab	4
2	28.03.2011	15.00 – 16.00	Biomechanics Lab	2
3	28.03.2011	16.00 – 18.00	Biomechanics Lab	4
4	29.03.2011	09.00 – 10.00	Biomechanics Lab	2
5	29.03.2011	15.00 – 17.00	Biomechanics Lab	4
6	30.03.2011	10.00 – 11.00	Biomechanics Lab	2
7	30.03.2011	15.00 – 17.00	Biomechanics Lab	4
8	31.03.2011	09.00 – 11.00	Biomechanics Lab	4
9	31.03.2011	13.00 – 15.00	Biomechanics Lab	4
Total No. of Subjects				30

SUBJECT TESTING INFORMATION

Attention: The information and of this subject testing are private and confidential in order to protect the right and privacy of volunteers. These data obtained will be used for project and research purpose only.

There are 30 volunteers (15 females and 15 males) are being invited to join this subject testing. All of them are being divided into nine groups as mentioned before according to their size of shoes. The basic information, like name, gender, age, course, height, weight, size of shoe, and brand of shoe are being listed into a table as below:

ID	Name	Gender	Age	Course	Height	Weight	Size of Shoe	Brand of Shoe	Group
F01	Cheah Ee Ling	F	24	BI Y4T3	158.0	45.0	7.0	Power	1
F02	Chew Kah Mun	F	23	BI Y4T3	152.0	53.0	7.0	Amesdex	1
F03	Chong Chau Ling	F	20	BI Y3T1	158.0	50.0	6.0	Viss	9
F04	Chou Miew Fatt	F	23	BI Y4T3	166.0	49.0	6.0	Nike	1
F05	Fong Lai Imm	F	22	BI Y3T3	168.0	56.0	7.0	New Balance	3
F06	Fong Suw Wei	F	24	BI Y4T3	166.0	75.0	7.0	Adidas	1
F07	Karen Ho Shin Jye	F	22	BI Y3T3	164.0	56.0	4.5	Converse	3
F08	Leng Yen Ran	F	23	BI Y4T3	158.0	45.0	6.0	Power	2
F09	Lim Yin Pei	F	21	BI Y3T3	157.0	45.0	6.0	Nike	4
F10	Loh Mey Chern	F	23	BI Y4T3	152.7	40.5	6.5	Brooks	9
F11	Loo Yi Shing	F	22	BI Y3T3	157.0	45.0	5.0	Converse	3
F12	Low Me Yin	F	24	BI Y4T3	166.0	60.0	5.5	Converse	4
F13	Mah Wai Lai	F	22	BI Y3T1	159.0	48.0	5.0	Swiss Polo	9
F14	Nurul Izwazi Mohd Nor	F	28	BI Y1T1	160.0	65.0	7.0	Admiral	9
F15	Wong Wei Fong	F	23	BI Y3T3	158.0	40.0	4.0	BUM	3
M01	Chan Meng Nen	M	23	BI Y4T3	160.0	63.0	8.0	Nike	2
M02	Cheah Soon Keong	M	25	BI Y4T3	179.0	93.0	10.0	Admiral	5
M03	Dennis Tan Eng Beng	M	22	BI Y3T3	172.0	60.0	8.0	Kappa	6
M04	Joseph Ting Shyue Horng	M	21	BI Y3T1	174.0	80.0	9.0	Nike	7
M05	Kho Ching Leong	M	22	BI Y3T3	167.0	50.0	7.0	North Star	6
M06	Lee Zhi Hong	M	21	BI Y4 T1	168.0	67.0	9.0	Power	8
M07	Ng Eng Hui	M	24	BI Y4T3	172.0	62.0	8.0	Bata	7
M08	Ong Chin Horng	M	24	BI Y4T3	178.0	79.0	10.0	Admiral	7
M09	Ooi Heap Guan	M	23	BI Y4T3	179.0	71.0	9.5	New Balance	8
M10	Teh Chek Min	M	23	BI Y4T3	172.0	61.0	9.0	Power	8
M11	Teng Woon Sheng	M	23	BI Y4T3	182.0	87.0	9.0	Nike	8
M12	Teoh Boon Yew	M	22	BI Y3T3	180.0	85.0	11.0	Adidas	7
M13	Tung Ren Sin	M	22	BI Y3T3	166.0	57.0	10.0	Power	5
M14	Wong Zhen Yang	M	20	BI Y3T3	172.0	63.0	8.0	Power	5
M15	Yap Kian Ming	M	24	BI Y4T3	174.0	72.0	9.0	Nike	5

APPENDIX H: Summary of Results

Total amount of female subjects (n) : 15
 Range of age (years) : 20 - 28
 Range of height (cm) : 152 - 168
 Range of weight (kg) : 41.06 – 71.32

Table H.1: Descriptive statistics for female subjects

	Parameters	Mean	Median	Standard Deviation	Variance
Anthropometric Information	Age (years)	22.9333	23.0000	1.7915	3.2095
	Height (cm)	159.9800	158.0000	4.9301	24.3060
	Weight (kg)	52.0560	50.2100	9.5097	90.4353
	Foot Length (m)	24.6000	25.0000	1.5024	2.2571
	Ankle-to-knee Length (m)	39.6667	40.0000	3.9219	15.3810
	Ankle-to-thigh Length (m)	46.2000	45.0000	3.4476	11.8857
Walking	Walking Speed (km/h)	4.0320	4.0300	0.0056	0.0000
	Cadence (steps/min)	107.2960	106.6200	11.9026	141.6715
	Avg. Step Length (cm)	94.2652	62.9595	111.8085	12501.1385
	Avg. Step Time (s)	0.7545	0.6391	0.2824	0.0798
	Avg. Stride Length (cm)	145.2347	125.2716	86.2999	7447.6681
	Avg. Stride Time (s)	1.1326	1.1254	0.1387	0.0192
	Contact Time (s)	0.7416	0.7078	0.1694	0.0387
	Max Applied Force (N)	558.9549	534.9138	107.2339	11499.1060
	Force Weight Ratio	10.7869	10.9041	1.0704	1.1457
Running	Running Speed (km/h)	5.9400	5.9400	0.0000	0.0000
	Cadence (steps/min)	134.8827	130.6100	25.7500	663.0638
	Avg. Step Length (cm)	115.9519	75.0466	175.7047	30872.1525
	Avg. Step Time (s)	0.5276	0.4615	0.2848	0.0811
	Avg. Stride Length (cm)	189.6623	149.2736	191.4172	36640.5299
	Avg. Stride Time (s)	0.9409	0.9188	0.3057	0.0935
	Contact Time (s)	0.5071	0.5507	0.0886	0.0079
	Max Applied Force (N)	1353.0350	766.4539	2364.2750	5589796.225
	Force Weight Ratio	25.2245	13.0424	41.6566	1735.2682

Total amount of male subjects (n) : 15
 Range of age (years) : 20 - 25
 Range of height (cm) : 160 - 182
 Range of weight (kg) : 50.72 – 91.45

Table H.2: Descriptive statistics for male subjects

	Parameters	Mean	Median	Standard Deviation	Variance
Anthropometric Information	Age (years)	22.6000	23.0000	1.3522	1.8286
	Height (cm)	173.0000	172.0000	6.0474	36.5714
	Weight (kg)	70.5520	70.5100	12.7652	162.9496
	Foot Length (m)	28.4667	28.0000	1.6847	2.8381
	Ankle-to-knee Length (m)	43.8000	43.0000	4.6629	21.7429
	Ankle-to-thigh Length (m)	50.4000	50.0000	3.3123	10.9714
Walking	Walking Speed (km/h)	4.0307	4.0300	0.0026	0.0000
	Cadence (steps/min)	89.6787	96.4800	27.3990	750.7043
	Avg. Step Length (cm)	105.6119	69.0911	114.2695	13057.5195
	Avg. Step Time (s)	0.9786	0.6615	0.8639	0.7462
	Avg. Stride Length (cm)	191.8486	132.4668	185.5299	34421.3257
	Avg. Stride Time (s)	1.7018	1.2437	1.3069	1.7081
	Contact Time (s)	0.9780	0.7698	0.8204	0.6731
	Max Applied Force (N)	795.8732	737.6018	178.9941	32038.8891
	Force Weight Ratio	11.2517	11.1740	0.9186	0.8438
Running	Running Speed (km/h)	5.9407	5.9400	0.0088	0.0001
	Cadence (steps/min)	130.3580	125.1200	15.7022	246.5582
	Avg. Step Length (cm)	81.0904	78.6935	16.7633	281.0076
	Avg. Step Time (s)	0.5068	0.5037	0.1196	0.0143
	Avg. Stride Length (cm)	144.6860	152.0150	23.4828	551.4418
	Avg. Stride Time (s)	0.9323	0.9591	0.1050	0.0110
	Contact Time (s)	0.5180	0.5522	0.1129	0.0128
	Max Applied Force (N)	1084.2188	1086.8190	302.7396	91651.2802
	Force Weight Ratio	15.3884	13.5814	3.6179	13.0893

Anthropometric Information

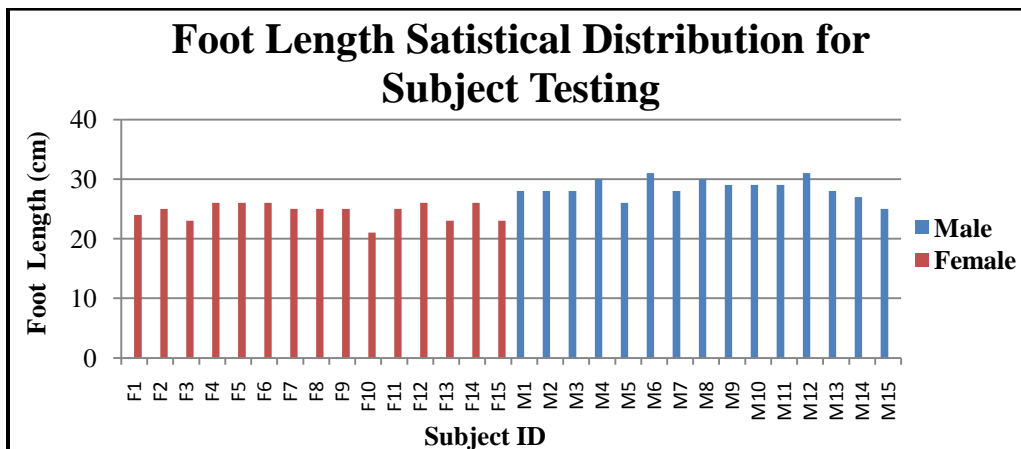


Figure H.2: Bar chart of foot length versus subject ID

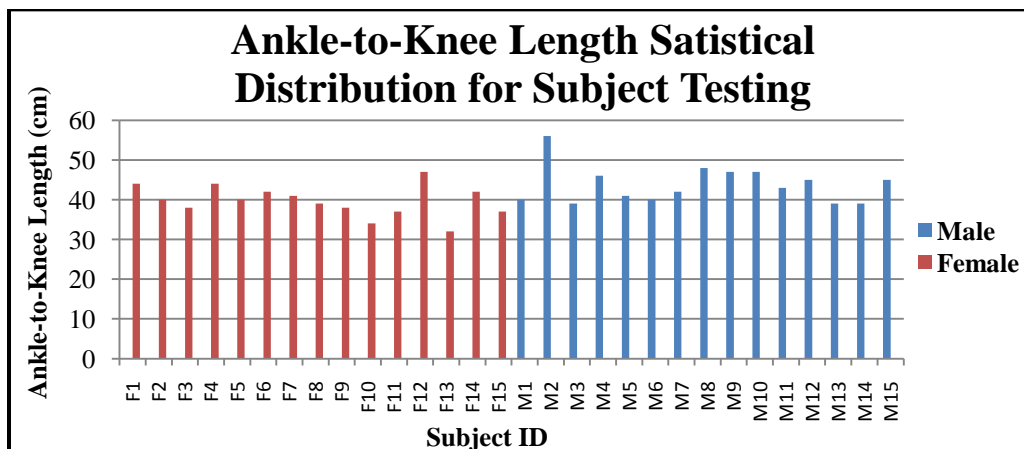


Figure H.3: Bar chart of ankle-to-knee length versus subject ID

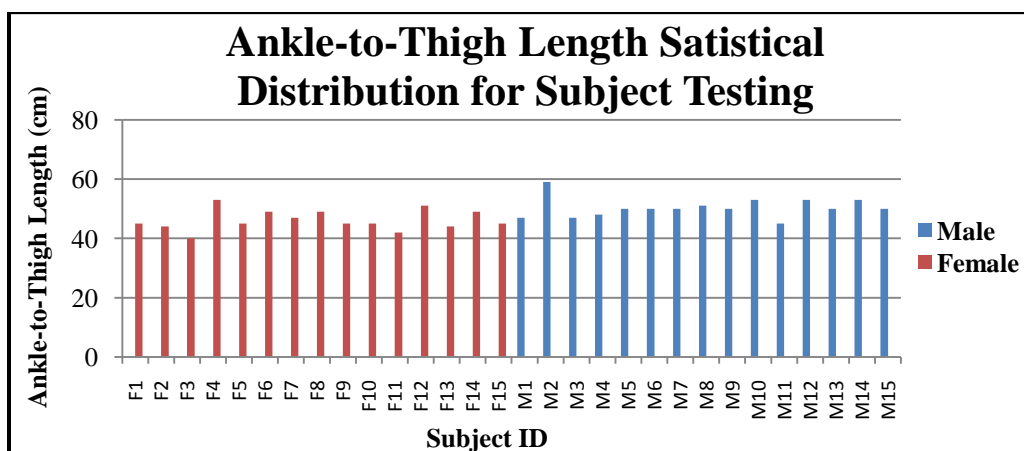


Figure H.4: Bar chart of ankle-to-thigh length versus subject ID

Subject Testing – Walking

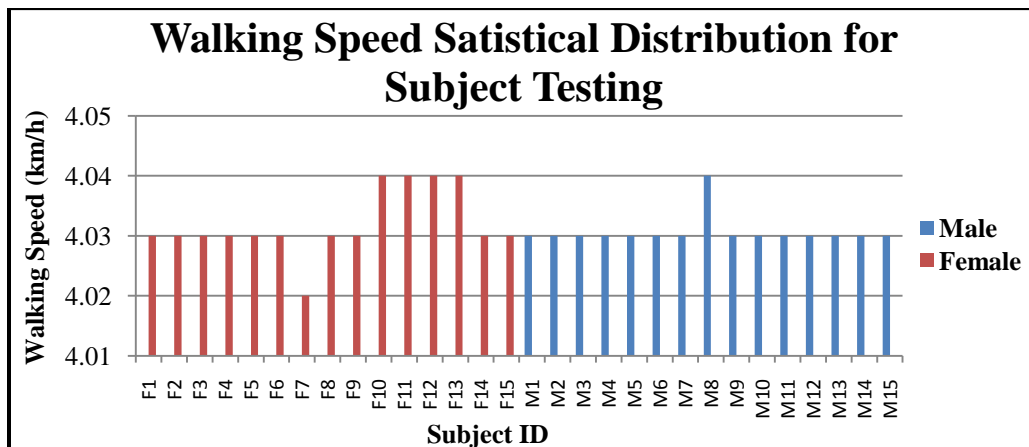


Figure H.5: Bar chart of walking speed versus subject ID

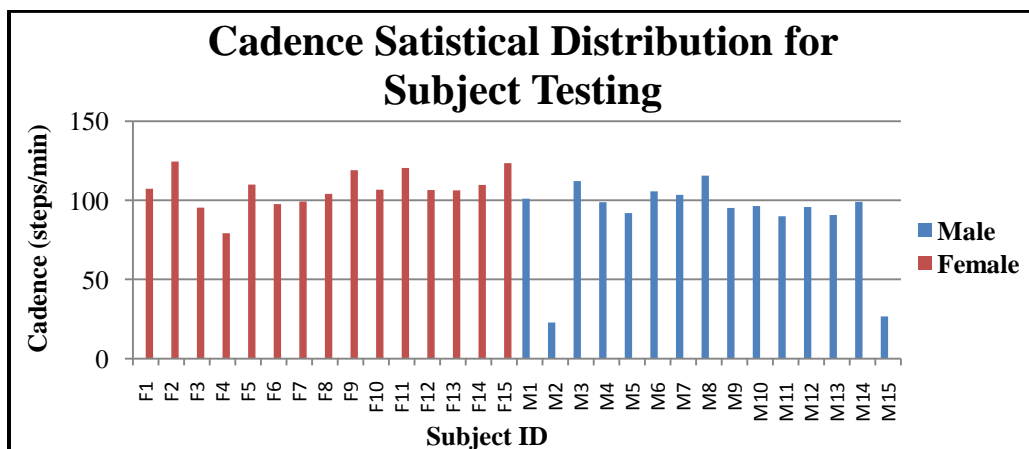


Figure H.6: Bar chart of cadence versus subject ID

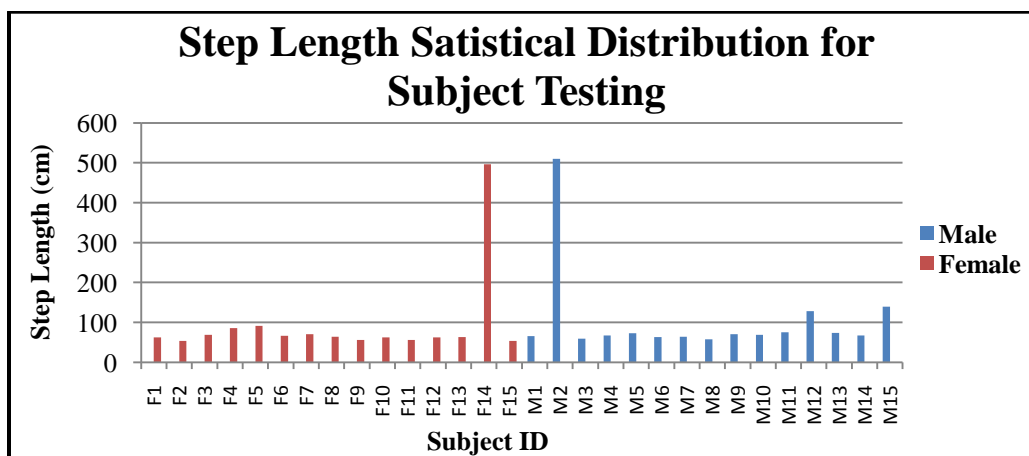


Figure H.7: Bar chart of step length versus subject ID

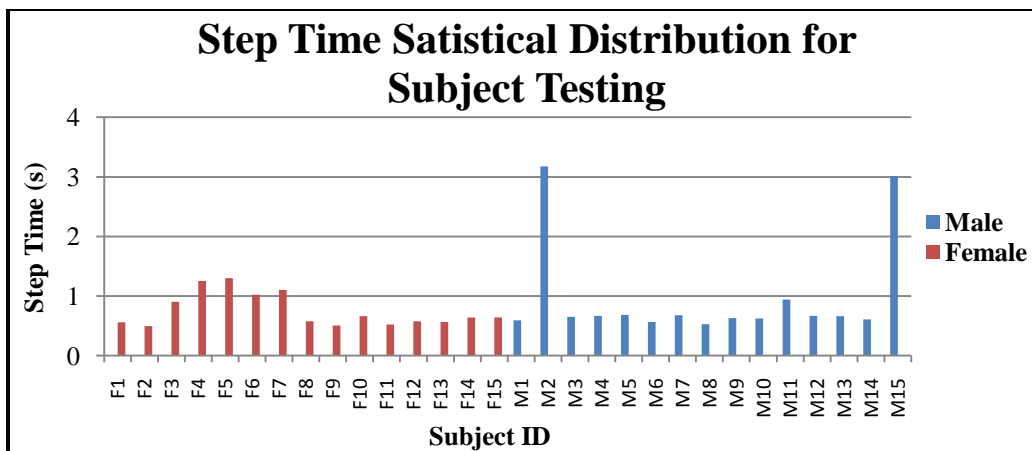


Figure H.8: Bar chart of step time versus subject ID

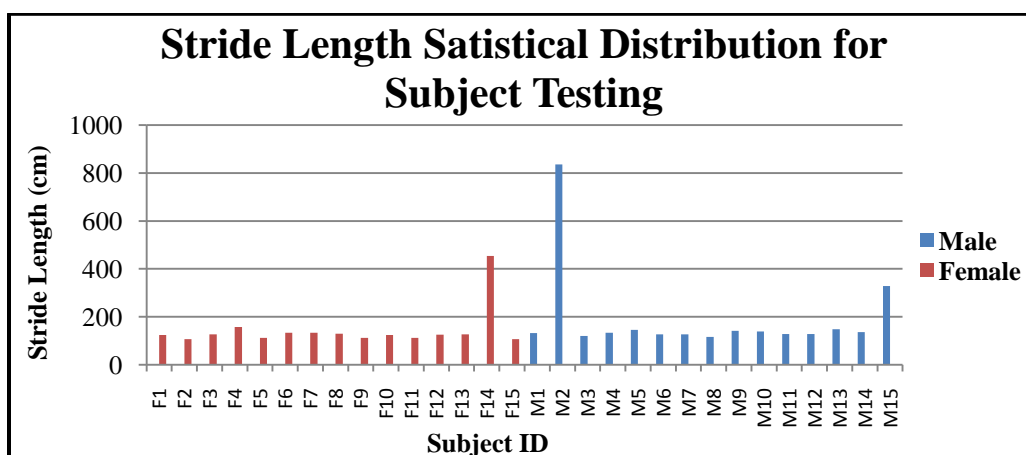


Figure H.9: Bar chart of stride length versus subject ID

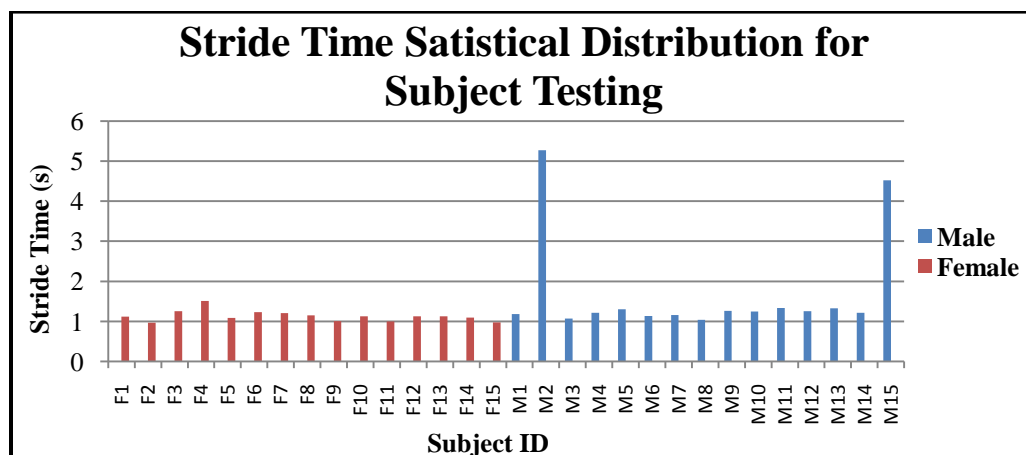


Figure H.10: Bar chart of stride time versus subject ID

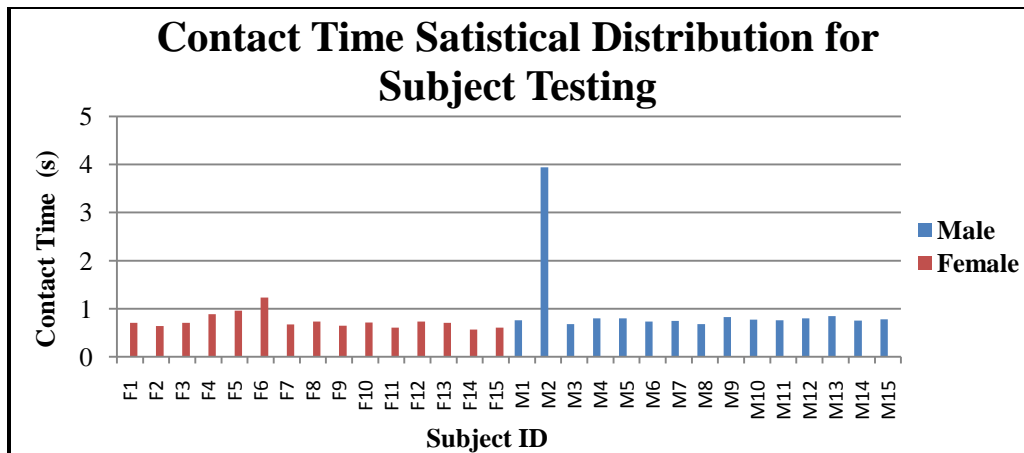


Figure H.11: Bar chart of contact time versus subject ID

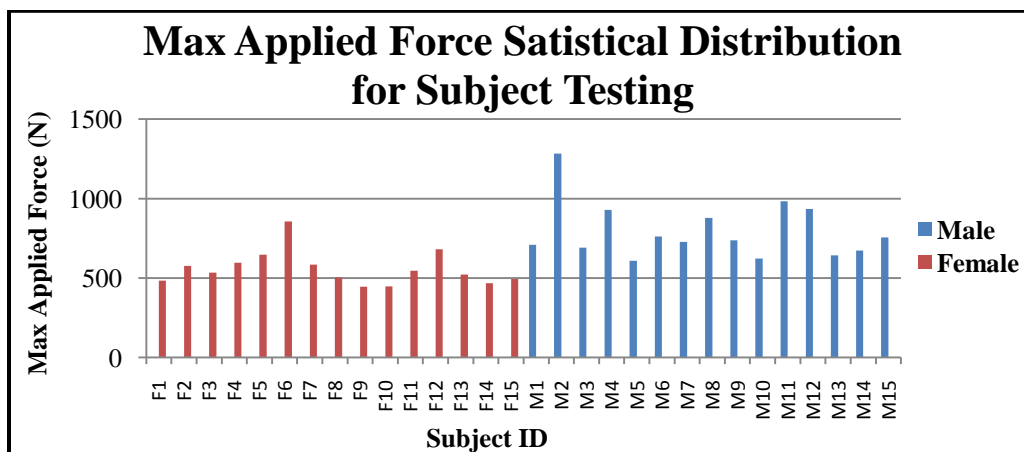


Figure H.12: Bar chart of max applied force versus subject ID

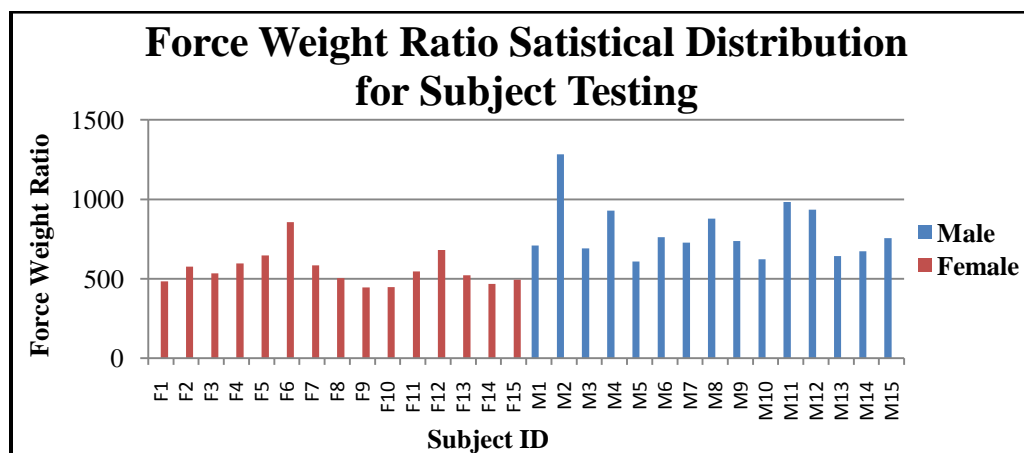


Figure H.13: Bar chart of force weight ratio versus subject ID

Subject Testing – Running

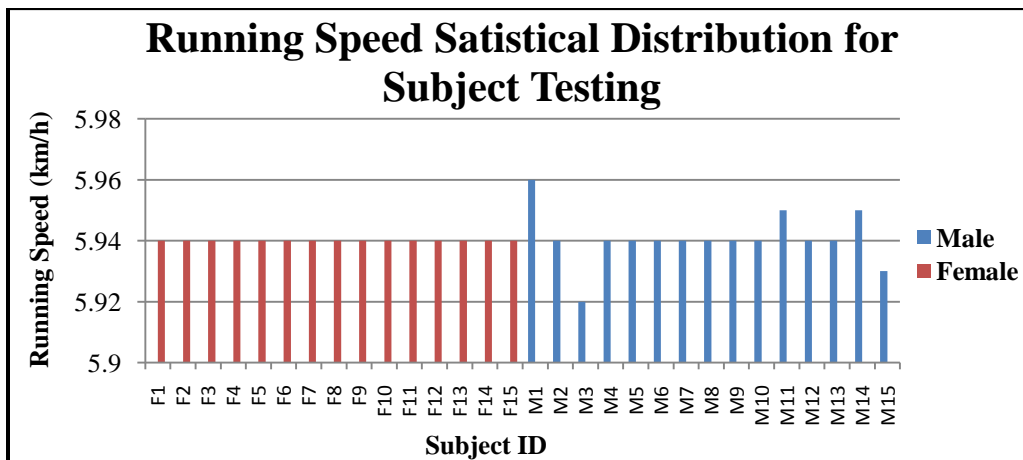


Figure H.14: Bar chart of running speed versus subject ID

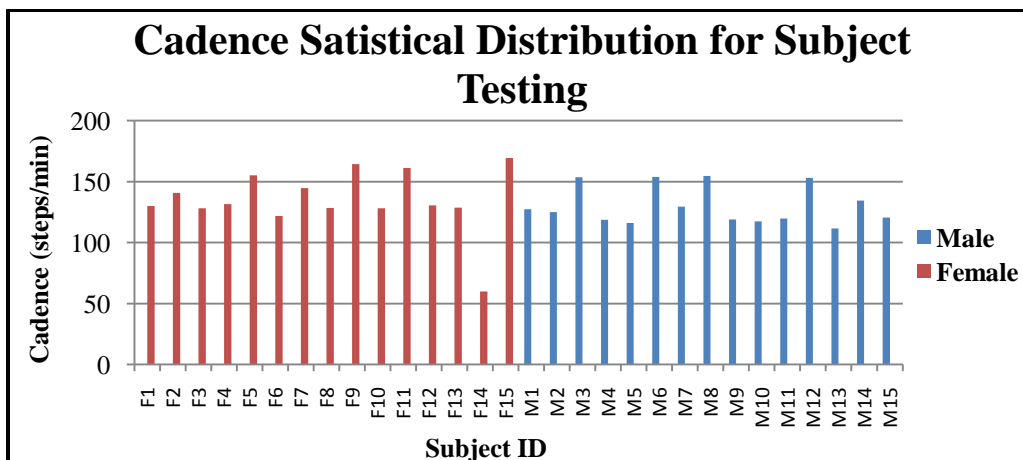


Figure H.15: Bar chart of cadence versus subject ID

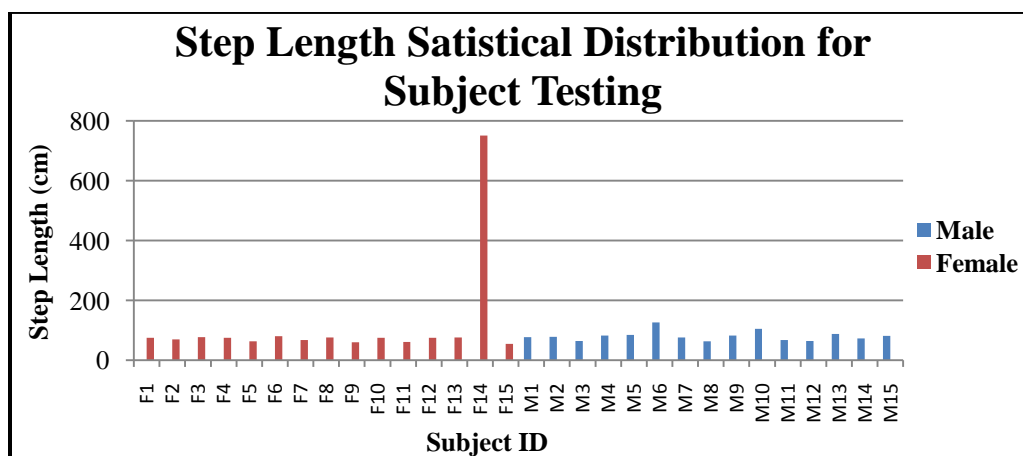


Figure H.16: Bar chart of step length versus subject ID

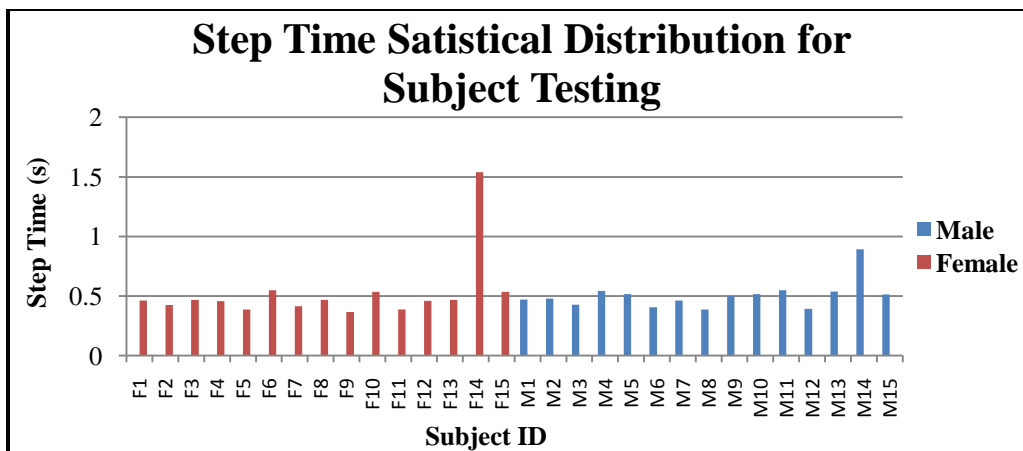


Figure H.17: Bar chart of step time versus subject ID

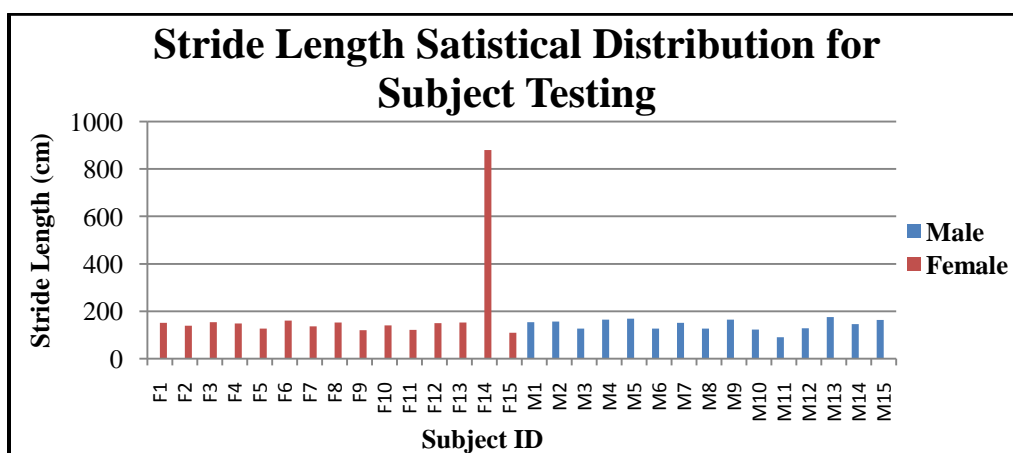


Figure H.18: Bar chart of stride length versus subject ID

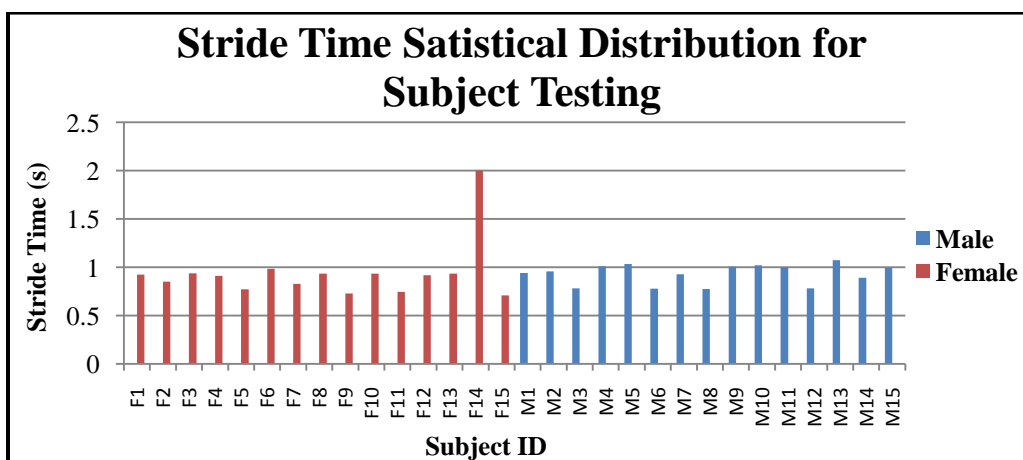


Figure H.19: Bar chart of stride time versus subject ID

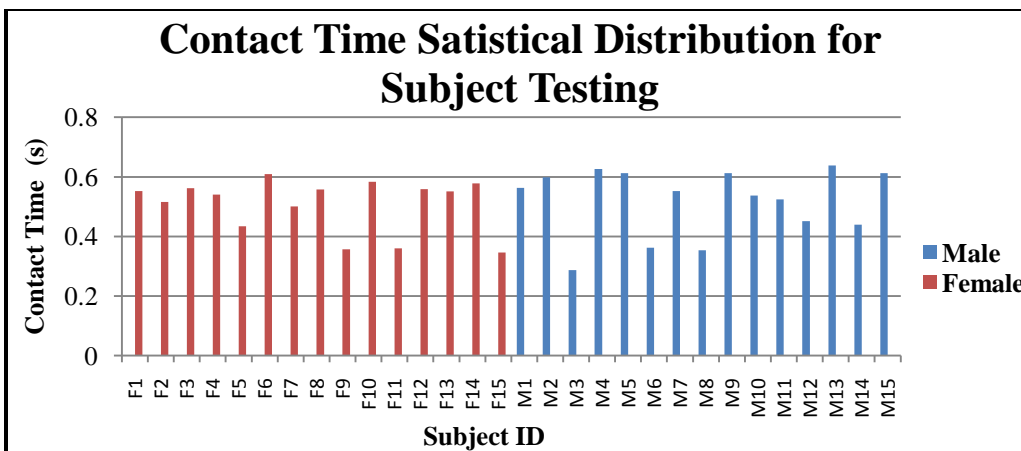


Figure H.20: Bar chart of contact time versus subject ID

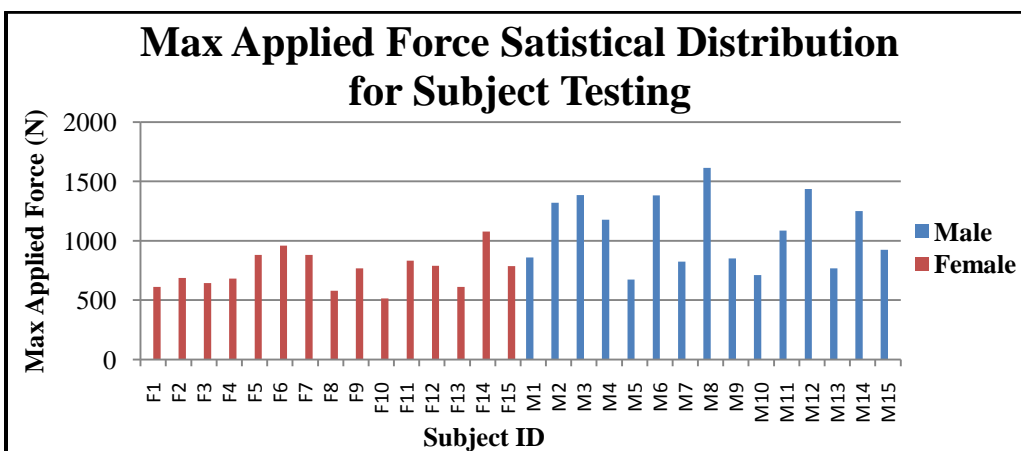


Figure H.21: Bar chart of max applied force versus subject ID

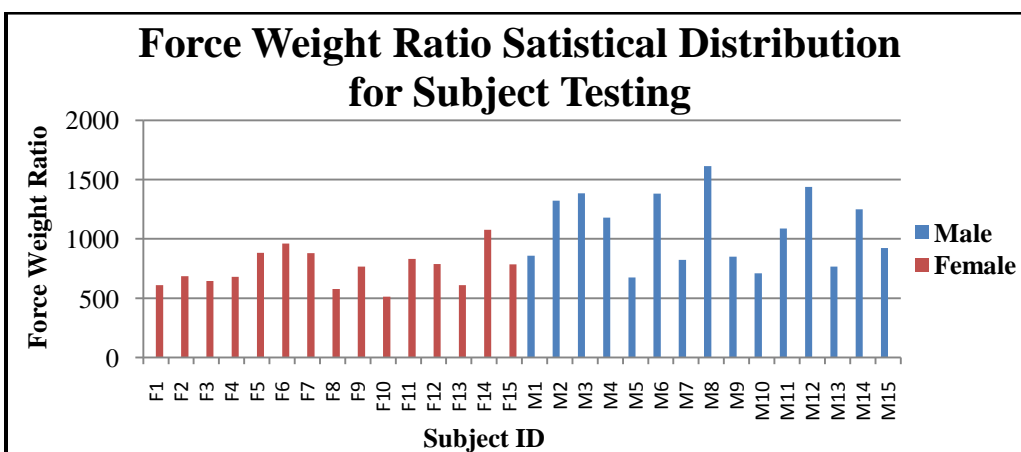


Figure H.22: Bar chart of force weight ratio versus subject ID

Table H.3: Comparison of mean between genders

	Parameters	Mean (Female)	Mean (Male)	Difference	%Error (%)
Anthropometric Information	Age (years)	22.9333	22.6000	0.3333	1.4748
	Height (cm)	159.9800	173.0000	13.0200	7.5260
	Weight (kg)	52.0560	70.5520	18.4960	26.2161
	Foot Length (m)	24.6000	28.4667	3.8667	13.5832
	Ankle-to-knee Length (m)	39.6667	43.8000	4.1333	9.4368
	Ankle-to-thigh Length (m)	46.2000	50.4000	4.200	8.3333
Walking	Walking Speed (km/h)	4.0320	4.0307	0.0013	0.0000
	Cadence (steps/min)	107.2960	89.6787	17.6173	19.6449
	Avg. Step Length (cm)	94.2652	105.6119	11.3467	0.0000
	Avg. Step Time (s)	0.7545	0.9786	0.2241	22.9001
	Avg. Stride Length (cm)	145.2347	191.8486	46.6139	0.0000
	Avg. Stride Time (s)	1.1326	1.7018	0.5692	33.4469
	Contact Time (s)	0.7416	0.9780	0.2364	0.0000
	Max Applied Force (N)	558.9549	795.8732	236.9183	29.7683
	Force Weight Ratio	10.7869	11.2517	0.4648	0.0000
Running	Running Speed (km/h)	5.9400	5.9407	0.0007	0.0118
	Cadence (steps/min)	134.8827	130.3580	4.5247	3.7410
	Avg. Step Length (cm)	115.9519	81.0904	34.8615	42.9909
	Avg. Step Time (s)	0.5276	0.5068	0.0208	4.1042
	Avg. Stride Length (cm)	189.6623	144.6860	44.9763	31.0855
	Avg. Stride Time (s)	0.9409	0.9323	0.0086	0.9224
	Contact Time (s)	0.5071	0.5180	0.0109	2.1042
	Max Applied Force (N)	1353.0350	1084.2188	268.8162	24.7935
	Force Weight Ratio	25.2245	15.3884	9.8361	63.9189

APPENDIX I: Benchmarking of Results

Comparison between Genders

Table I.1: Average peak forces for female and male subjects during standing locomotion by using instrumented insole system

	Female	Male	Difference	%Difference
L1	5.05	5.36	0.31	5.78
L2	5.42	7.43	2.01	27.05
L3	2.74	2.44	-0.30	-12.30
L4	13.03	7.38	-5.65	-76.56
R1	2.84	1.02	-1.82	-178.43
R2	8.36	5.25	-3.11	-59.24
R3	2.84	0.38	-2.46	-647.37
R4	5.03	5.33	0.30	5.63

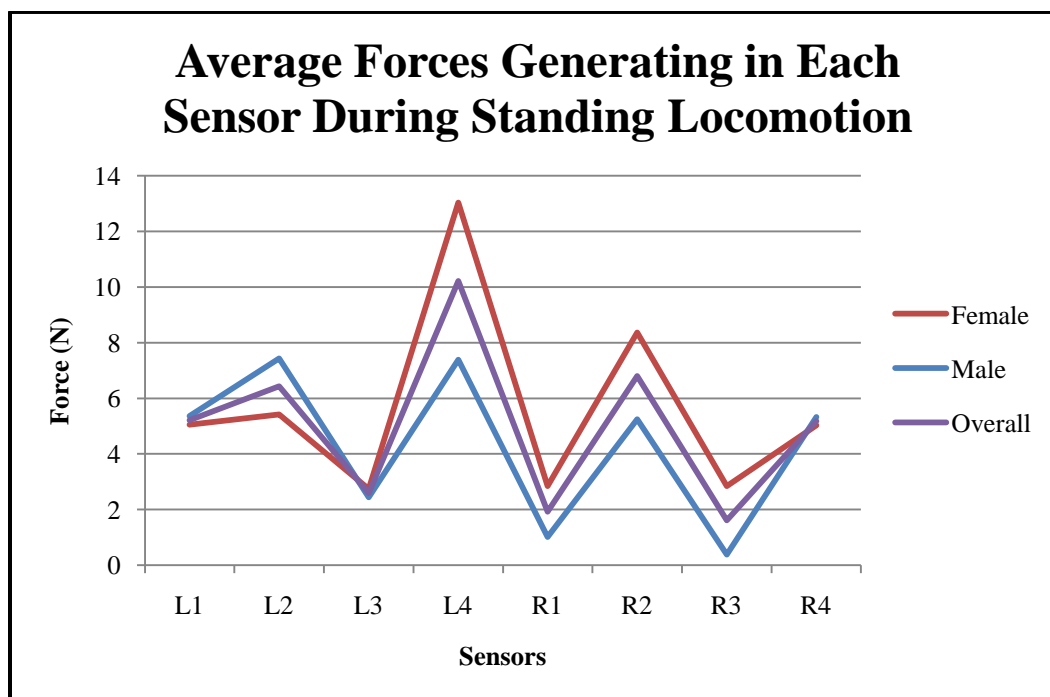


Figure I.1: Graph of average forces generating during standing locomotion versus sensors by using instrumented insole system

Table I.2: Maximum peak forces for female and male subjects during standing locomotion by using instrumented insole system

	Female	Male	Difference	%Difference
L1	338.00	215.00	-123.00	-57.21
L2	329.00	250.00	-79.00	-31.60
L3	138.00	231.00	93.00	40.26
L4	400.00	398.00	-2.00	-0.50
R1	304.00	206.00	-98.00	-47.57
R2	400.00	296.00	-104.00	-35.14
R3	217.00	83.00	-134.00	-161.45
R4	340.00	192.00	-148.00	-77.08

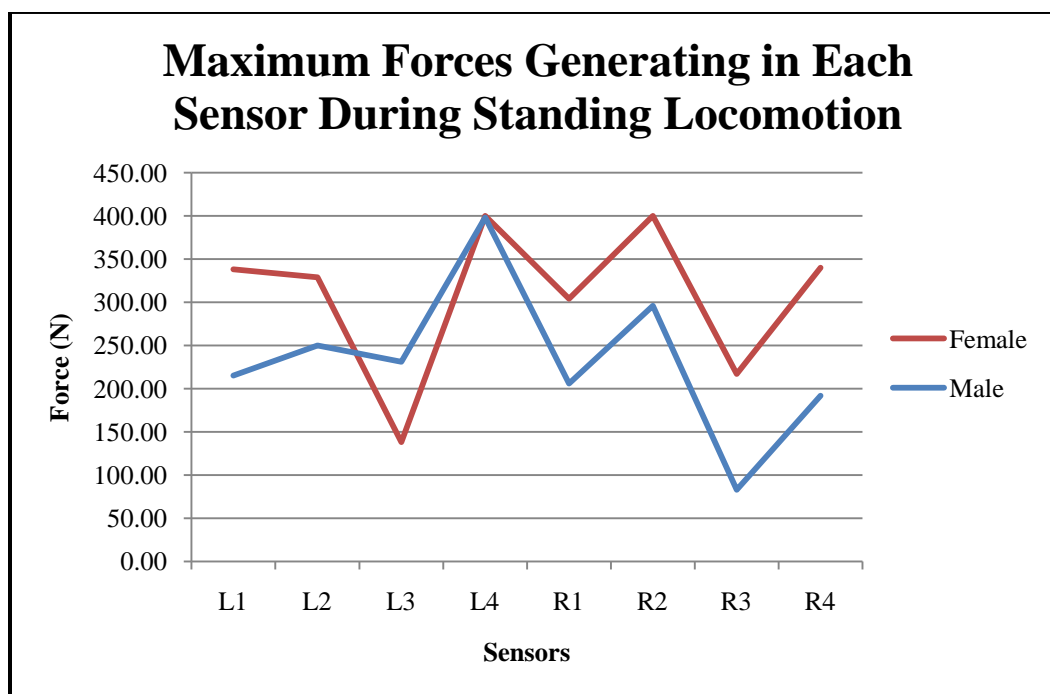


Figure I.2: Graph of maximum forces generating during standing locomotion versus sensors by using instrumented insole system

Table I.3: Minimum peak forces for female and male subjects during standing locomotion by using instrumented insole system

	Female	Male	Difference	%Difference
L1	2.00	4.00	2.00	50.00
L2	2.00	10.00	8.00	80.00
L3	2.00	4.00	2.00	50.00
L4	4.00	4.00	0.00	0.00
R1	2.00	4.00	2.00	50.00
R2	2.00	2.00	0.00	0.00
R3	2.00	2.00	0.00	0.00
R4	2.00	2.00	0.00	0.00

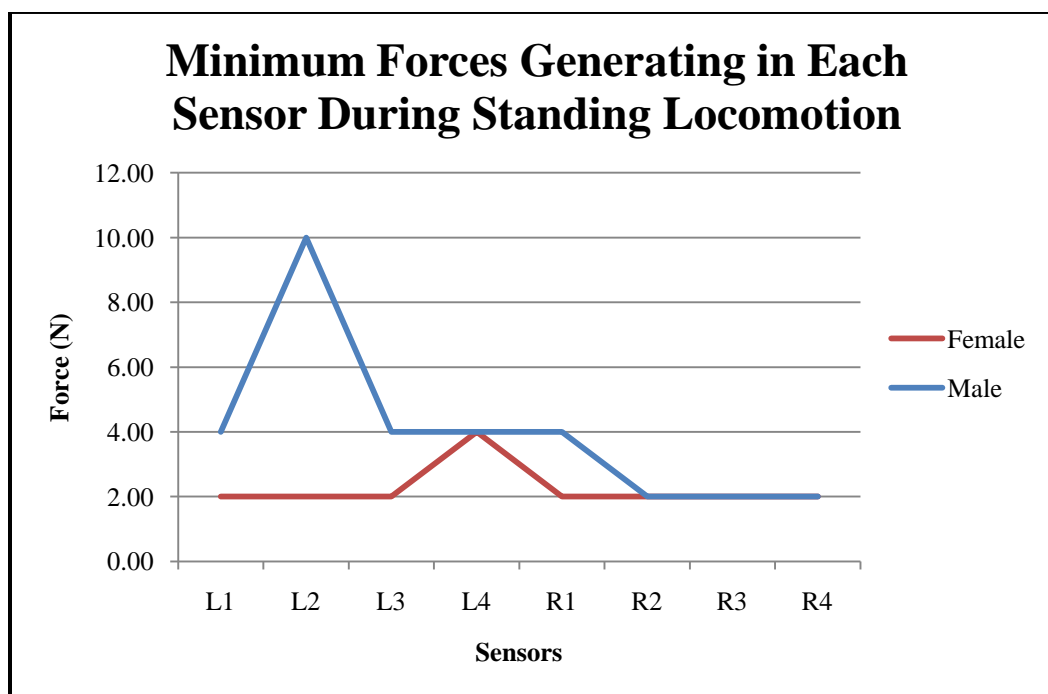


Figure I.3: Graph of minimum forces generating during standing locomotion versus sensors by using instrumented insole system

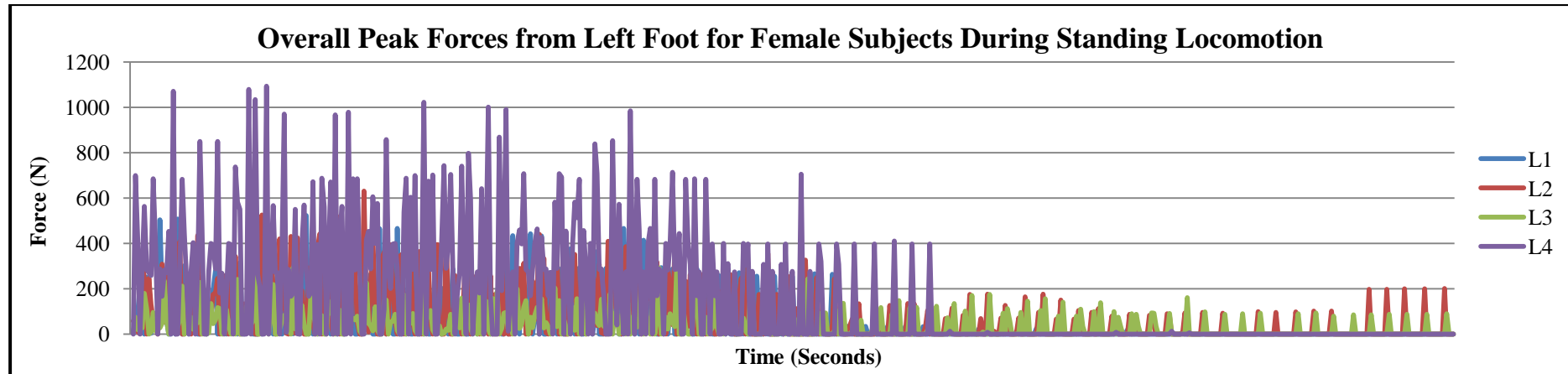


Figure I.4: Graph of overall peak forces from left foot for female subjects during standing locomotion versus time (Insole System)

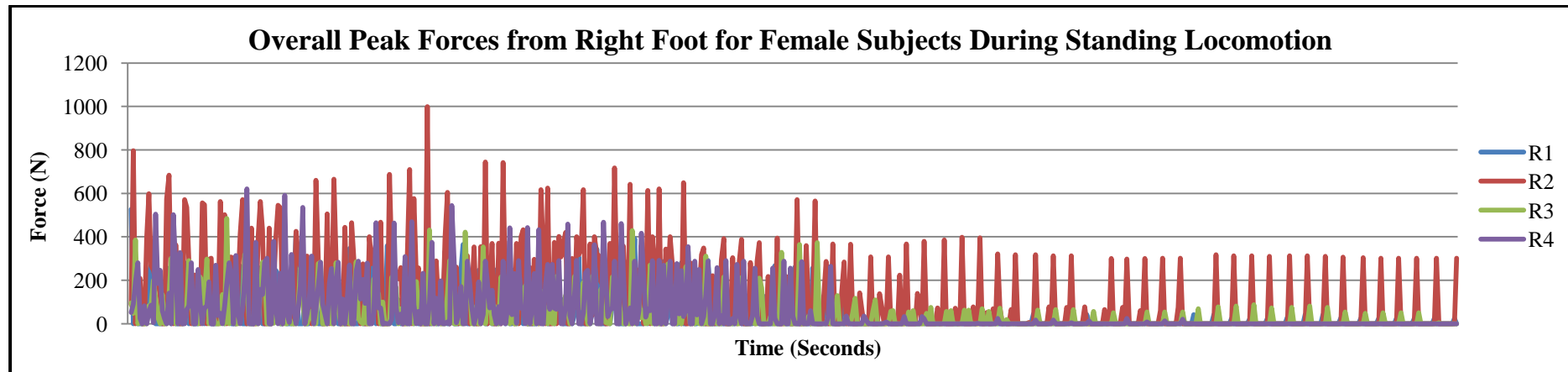


Figure I.5: Graph of overall peak forces from right foot for female subjects during standing locomotion versus time (Insole System)

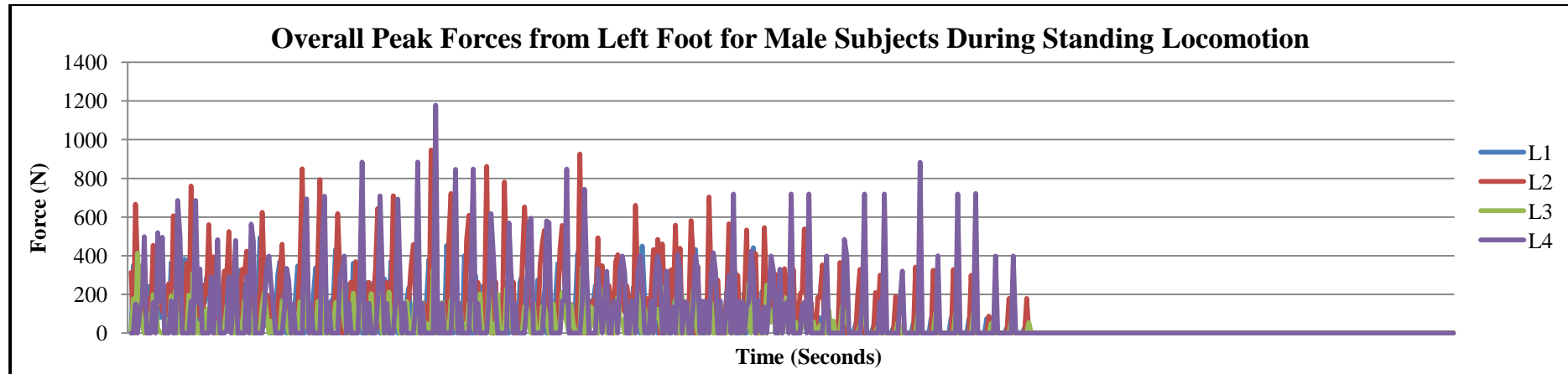


Figure I.6: Graph of overall peak forces from left foot for male subjects during standing locomotion versus time (Insole System)

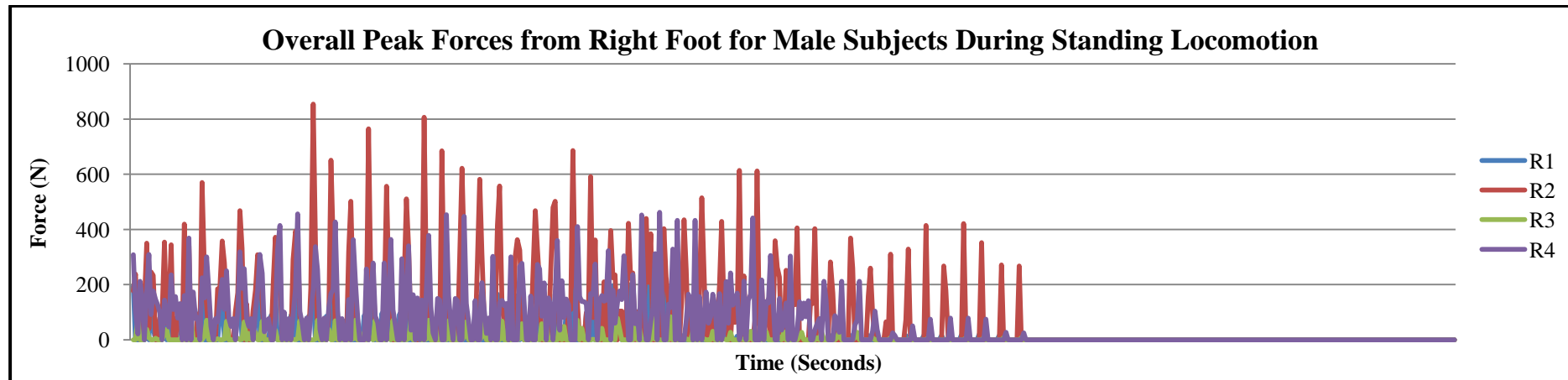


Figure I.7: Graph of overall peak forces from right foot for male subjects during standing locomotion versus time (Insole System)

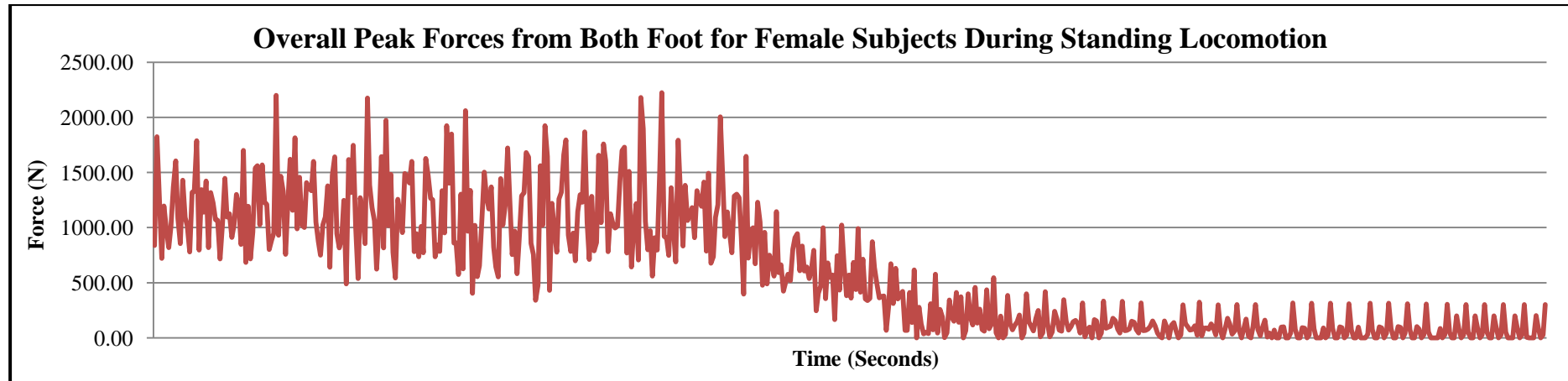


Figure I.8: Graph of overall peak forces from both foot for female subjects during standing locomotion versus time (Insole System)

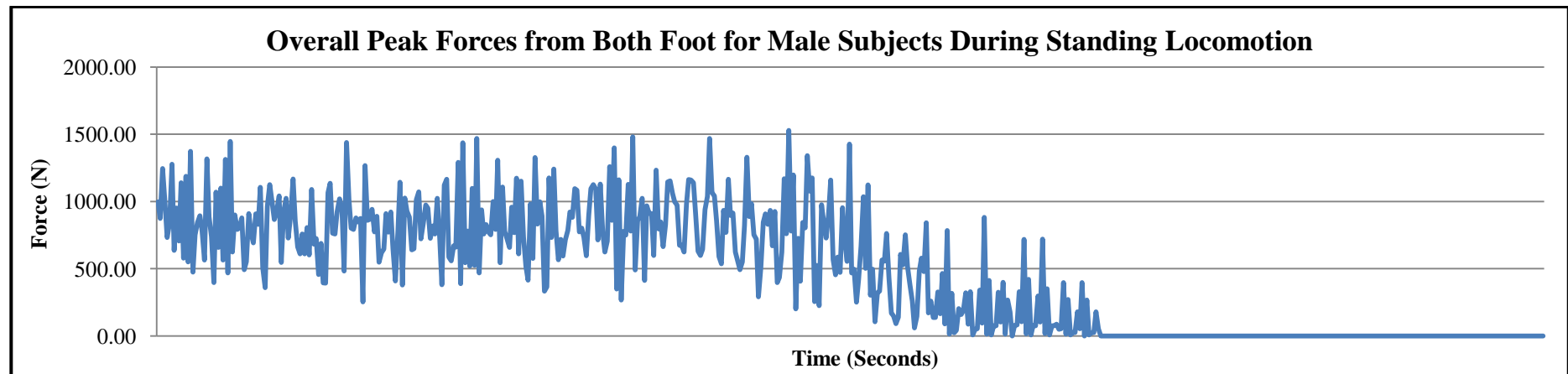


Figure I.9: Graph of overall peak forces from both foot for male subjects during standing locomotion versus time (Insole System)

Table I.4: Average peak forces for female and male subjects during sitting locomotion by using instrumented insole system

	Female	Male	Difference	%Difference
L1	2.31	0.43	-1.88	-437.21
L2	0.68	2.00	1.32	66.00
L3	0.59	0.39	-0.20	-51.28
L4	11.69	3.66	-8.03	-219.40
R1	0.83	0.48	-0.35	-72.92
R2	2.44	1.13	-1.31	-115.93
R3	1.76	0.05	-1.71	-3420.00
R4	2.28	0.43	-1.85	-430.23

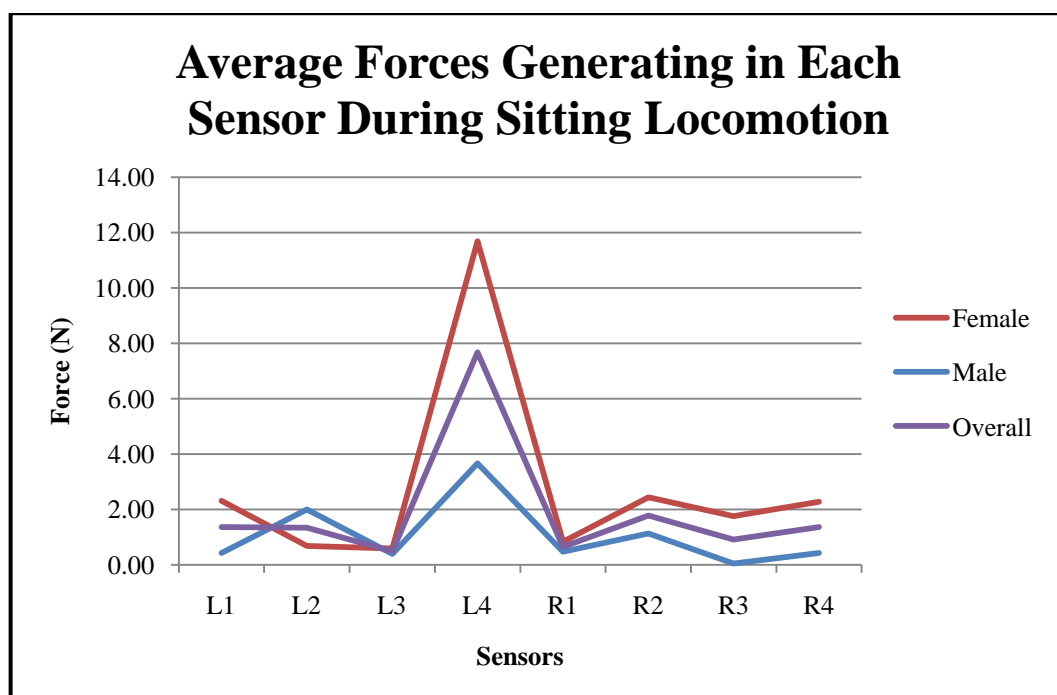


Figure I.10: Graph of average forces generating during sitting locomotion versus sensors by using instrumented insole system

Table I.5: Maximum peak forces for female and male subjects during sitting locomotion by using instrumented insole system

	Female	Male	Difference	%Difference
L1	160.00	38.00	-122.00	-321.05
L2	81.00	104.00	23.00	22.12
L3	46.00	85.00	39.00	45.88
L4	386.00	267.00	-119.00	-44.57
R1	77.00	117.00	40.00	34.19
R2	400.00	131.00	-269.00	-205.34
R3	190.00	21.00	-169.00	-804.76
R4	160.00	38.00	-122.00	-321.05

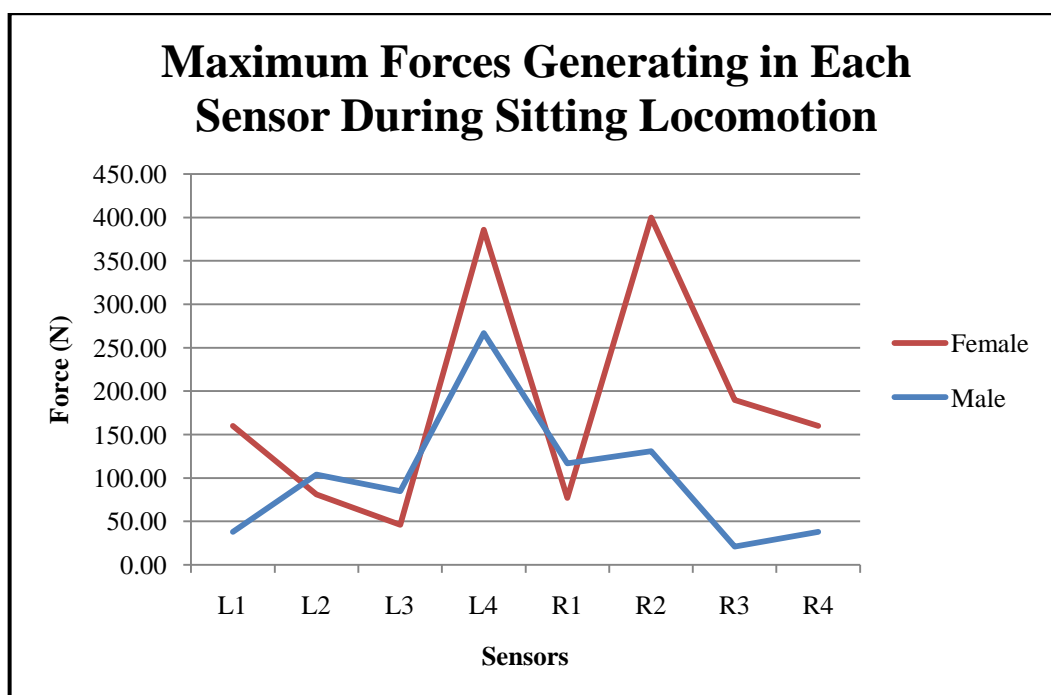


Figure I.11: Graph of maximum forces generating during sitting locomotion versus sensors by using instrumented insole system

Table I.6: Minimum peak forces for female and male subjects during sitting locomotion by using instrumented insole system

	Female	Male	Difference	%Difference
L1	21.00	2.00	-19.00	-950.00
L2	2.00	4.00	2.00	50.00
L3	2.00	2.00	0.00	0.00
L4	152.00	140.00	-12.00	-8.57
R1	4.00	85.00	81.00	95.29
R2	6.00	4.00	-2.00	-50.00
R3	2.00	2.00	0.00	0.00
R4	21.00	2.00	-19.00	-950.00

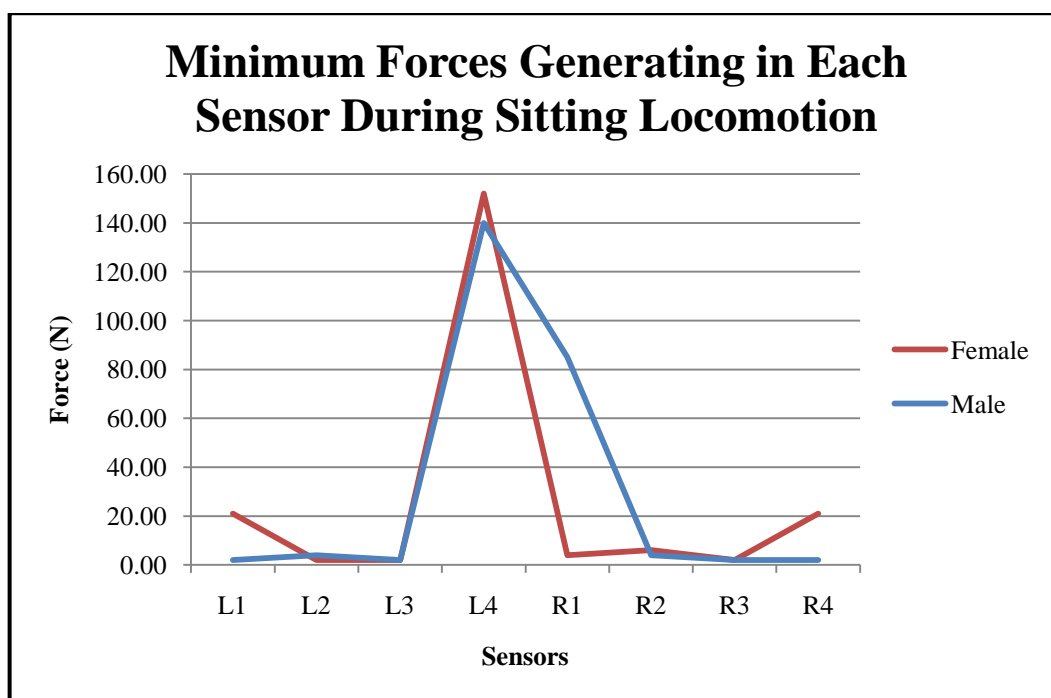


Figure I.12: Graph of minimum forces generating during sitting locomotion versus sensors by using instrumented insole system

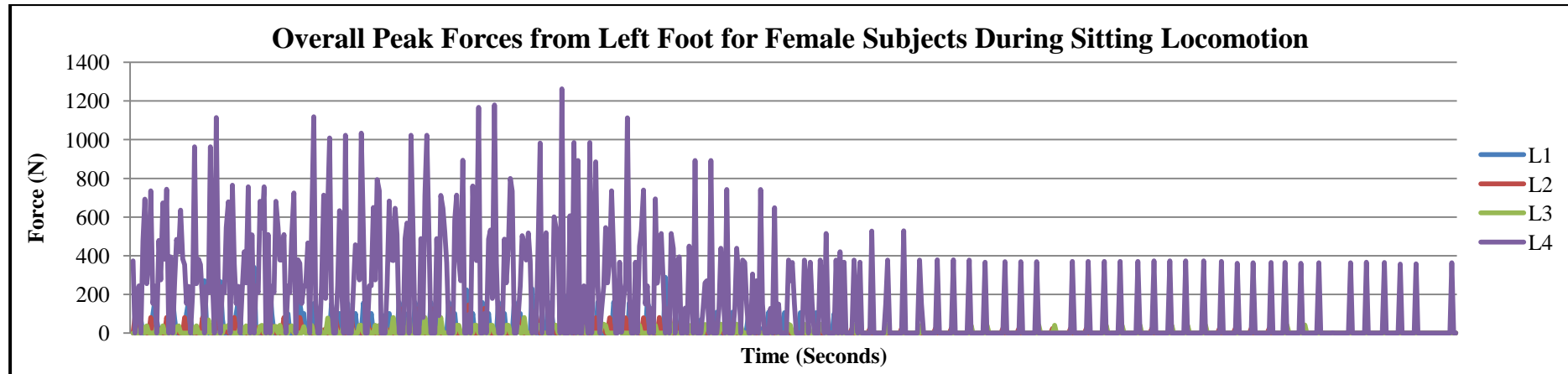


Figure I.13: Graph of overall peak forces from left foot for female subjects during sitting locomotion versus time (Insole System)

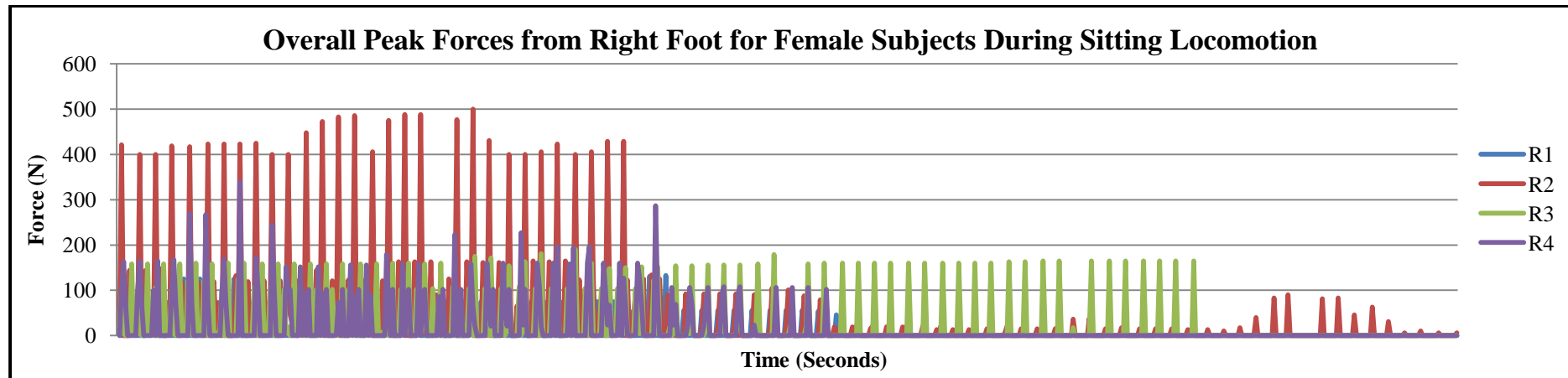


Figure I.14: Graph of overall peak forces from right foot for female subjects during sitting locomotion versus time (Insole System)

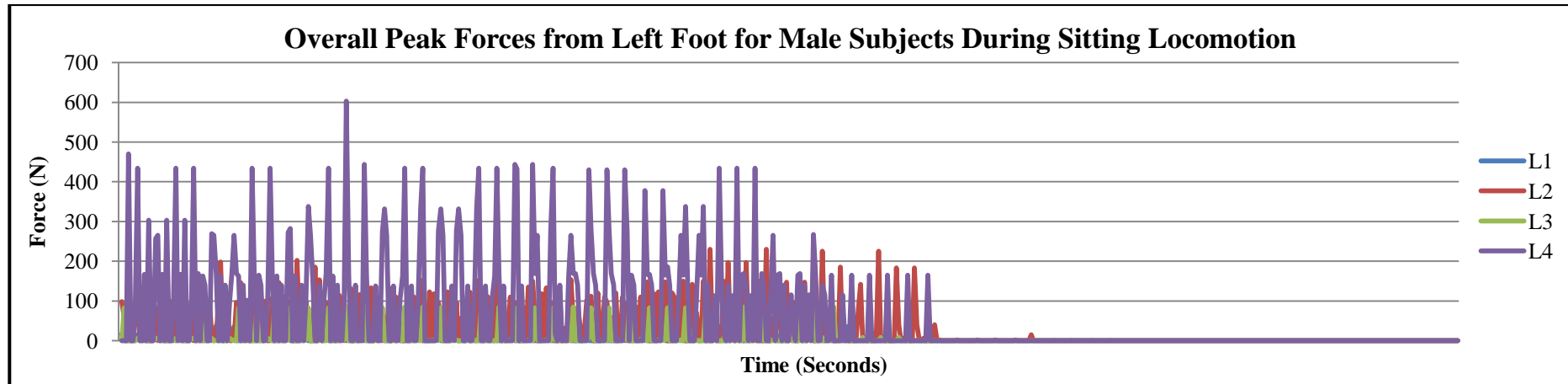


Figure I.15: Graph of overall peak forces from left foot for male subjects during sitting locomotion versus time (Insole System)

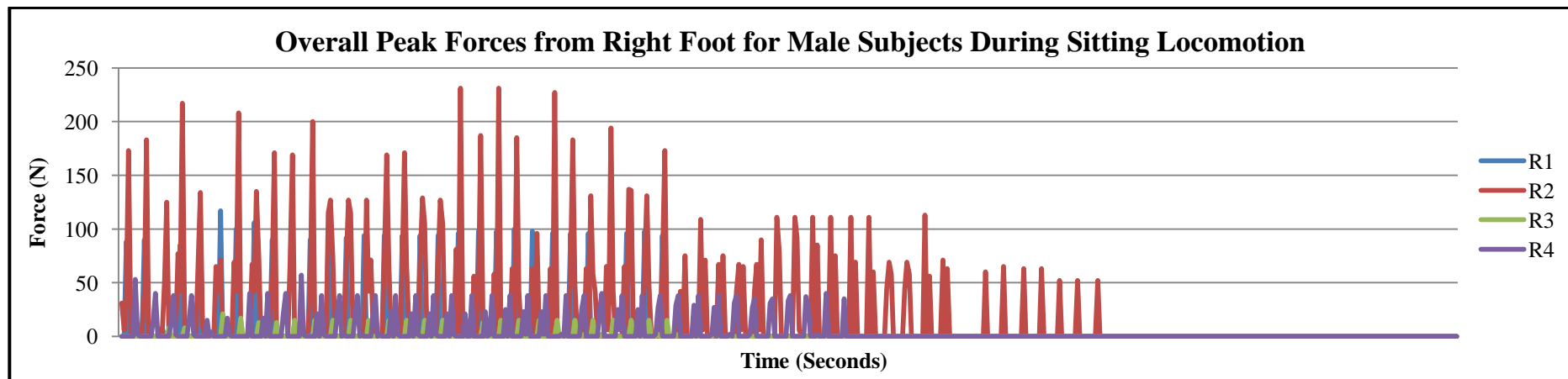


Figure I.16: Graph of overall peak forces from right foot for male subjects during sitting locomotion versus time (Insole System)

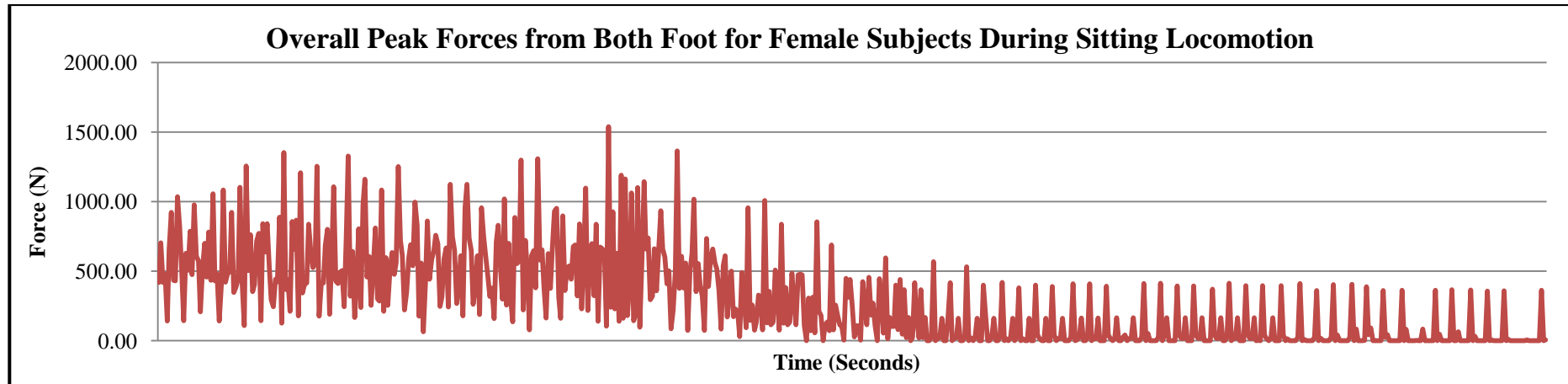


Figure I.17: Graph of overall peak forces from both foot for female subjects during sitting locomotion versus time (Insole System)

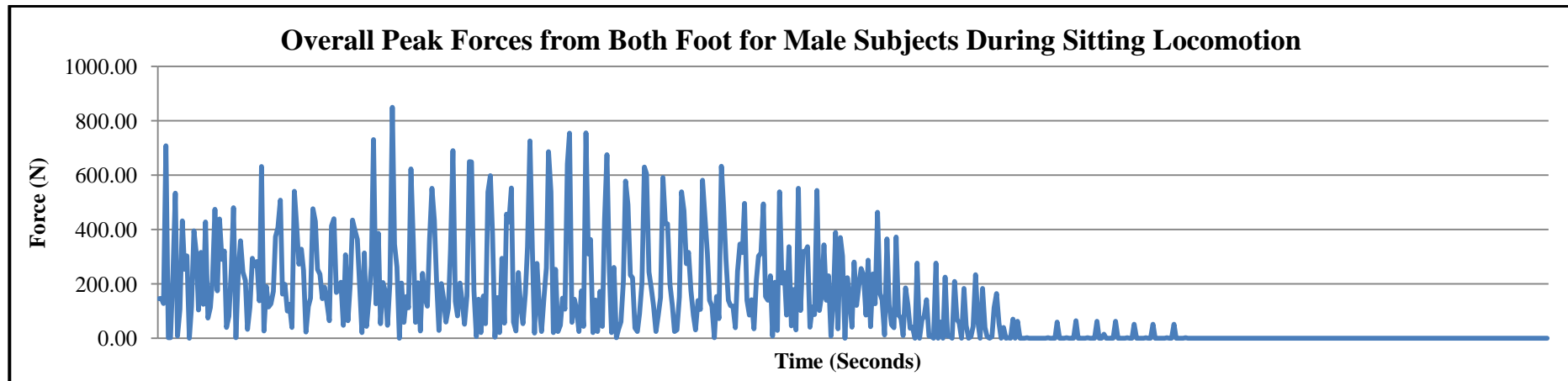


Figure I.18: Graph of overall peak forces from both foot for male subjects during sitting locomotion versus time (Insole System)

Table I.7: Average peak forces for female and male subjects during walking locomotion by using instrumented insole system

	Female	Male	Difference	%Difference
L1	10.87	8.66	-2.21	-25.52
L2	11.11	9.44	-1.67	-17.69
L3	5.48	3.30	-2.18	-66.06
L4	8.96	1.68	-7.28	-433.33
R1	9.07	3.56	-5.51	-154.78
R2	12.79	8.39	-4.40	-52.44
R3	7.45	1.90	-5.55	-292.11
R4	10.24	1.77	-8.47	-478.53

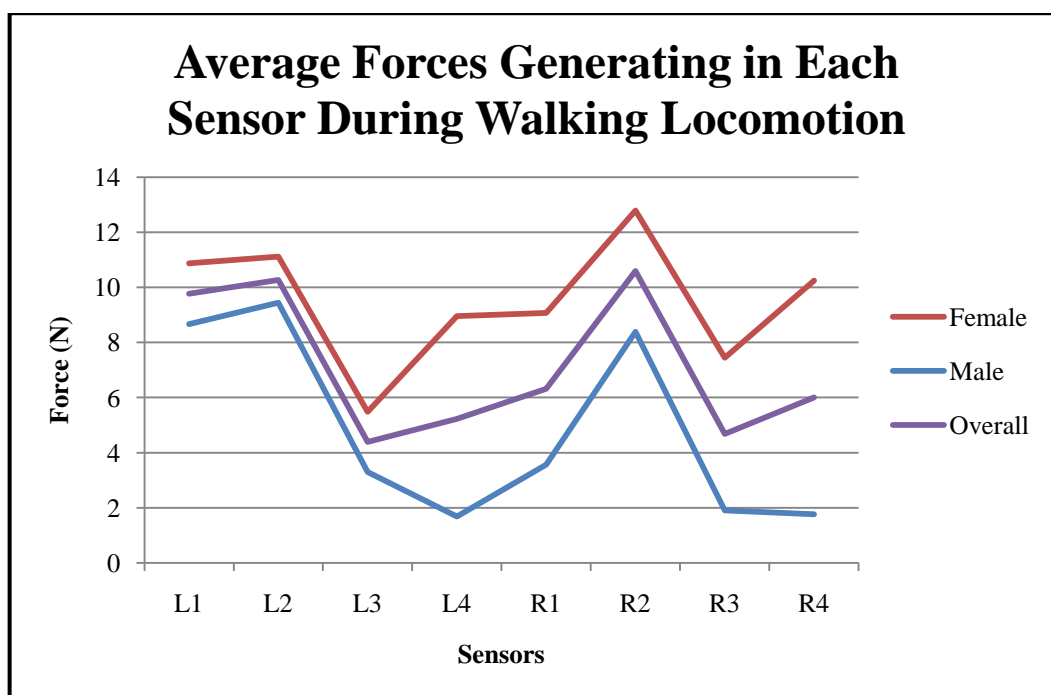


Figure I.19: Graph of average forces generating during walking locomotion versus sensors by using instrumented insole system

Table I.8: Maximum peak forces for female and male subjects during walking locomotion by using instrumented insole system

	Female	Male	Difference	%Difference
L1	402.00	402.00	0.00	0.00
L2	402.00	400.00	-2.00	-0.50
L3	327.00	333.00	6.00	1.80
L4	400.00	354.00	-46.00	-12.99
R1	338.00	379.00	41.00	10.82
R2	417.00	400.00	-17.00	-4.25
R3	392.00	323.00	-69.00	-21.36
R4	400.00	402.00	2.00	0.50

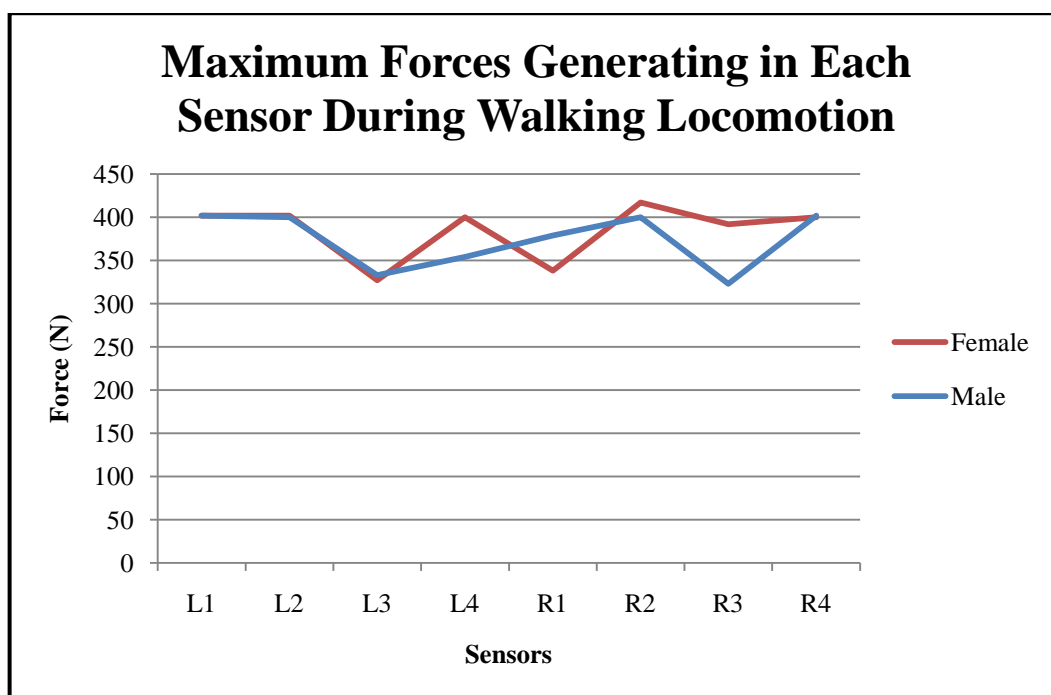


Figure I.20: Graph of maximum forces generating during walking locomotion versus sensors by using instrumented insole system

Table I.9: Minimum peak forces for female and male subjects during walking locomotion by using instrumented insole system

	Female	Male	Difference	%Difference
L1	2.00	13.00	11.00	84.62
L2	13.00	2.00	-11.00	-550.00
L3	10.00	4.00	-6.00	-150.00
L4	2.00	2.00	0.00	0.00
R1	2.00	10.00	8.00	80.00
R2	2.00	2.00	0.00	0.00
R3	4.00	13.00	9.00	69.23
R4	2.00	2.00	0.00	0.00

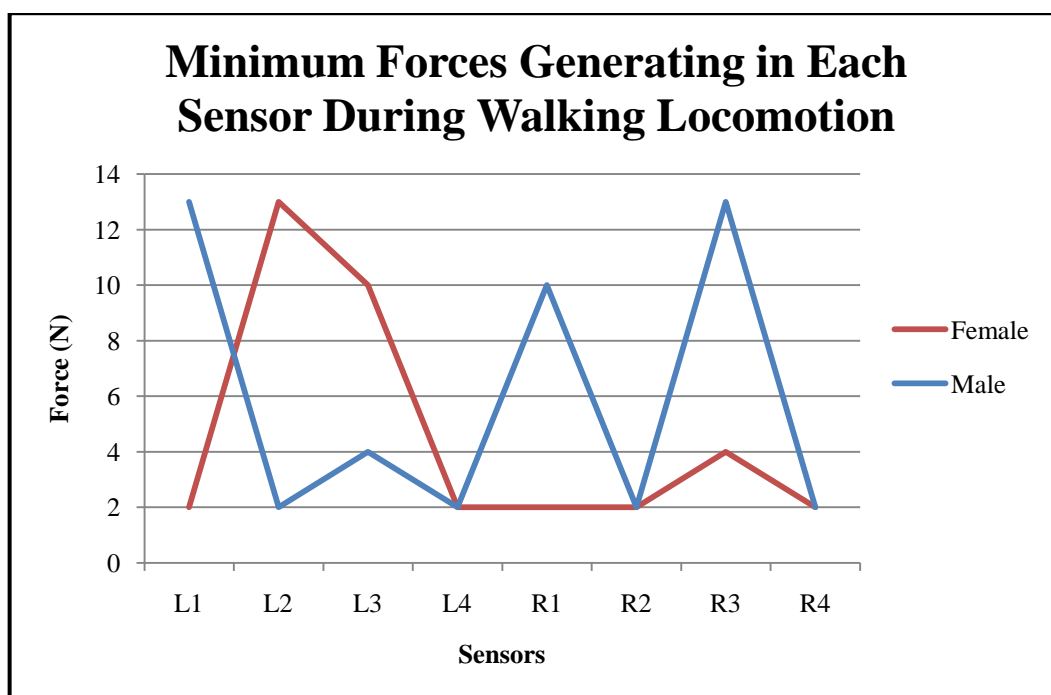


Figure I.21: Graph of minimum forces generating during walking locomotion versus sensors by using instrumented insole system

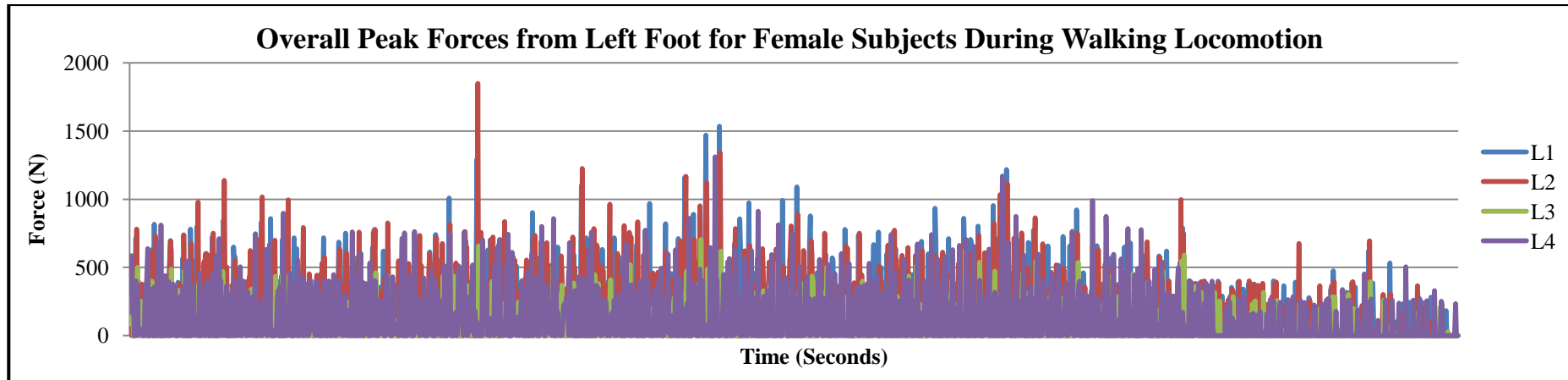


Figure I.22: Graph of overall peak forces from left foot for female subjects during walking locomotion versus time (Insole System)

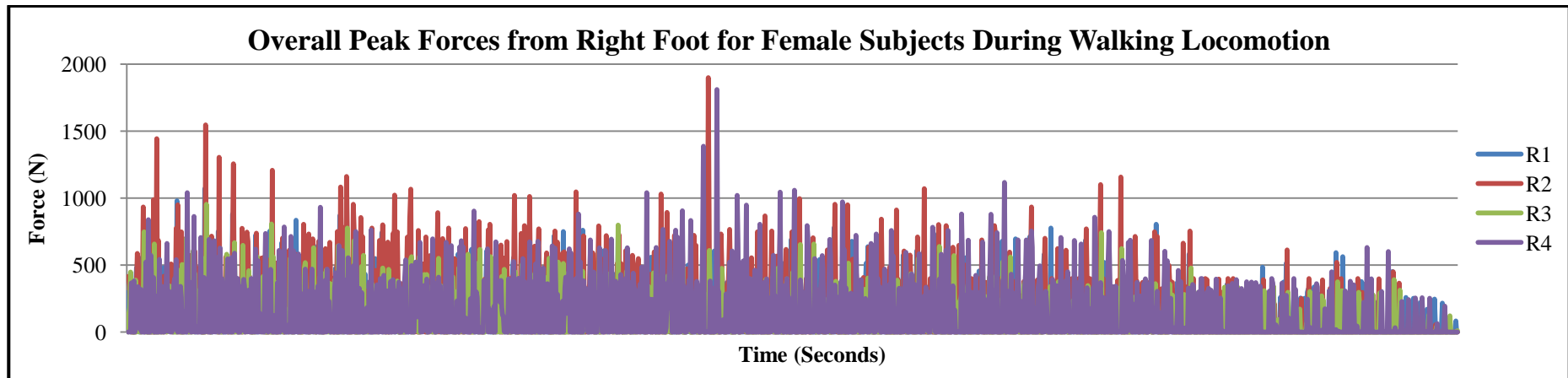


Figure I.23: Graph of overall peak forces from right foot for female subjects during walking locomotion versus time (Insole System)

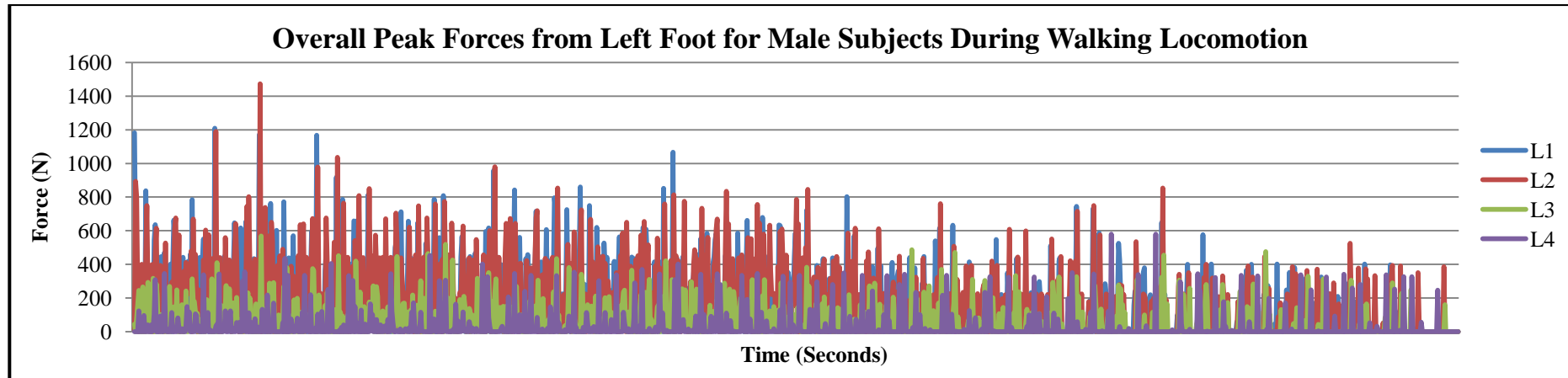


Figure I.24: Graph of overall peak forces from left foot for male subjects during walking locomotion versus time (Insole System)

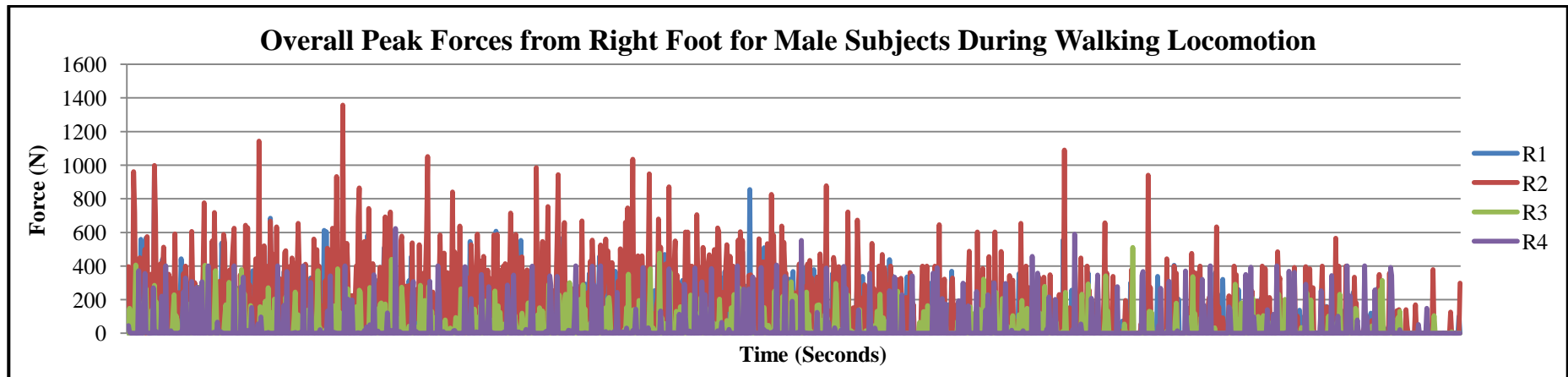


Figure I.25: Graph of overall peak forces from right foot for male subjects during walking locomotion versus time (Insole System)

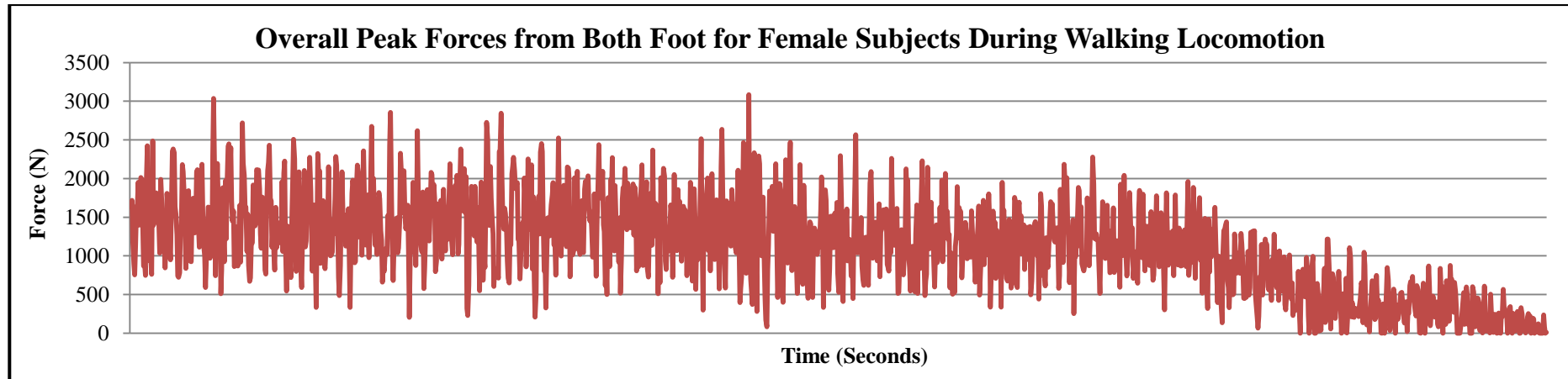


Figure I.26: Graph of overall peak forces from both foot for female subjects during walking locomotion versus time (Insole System)

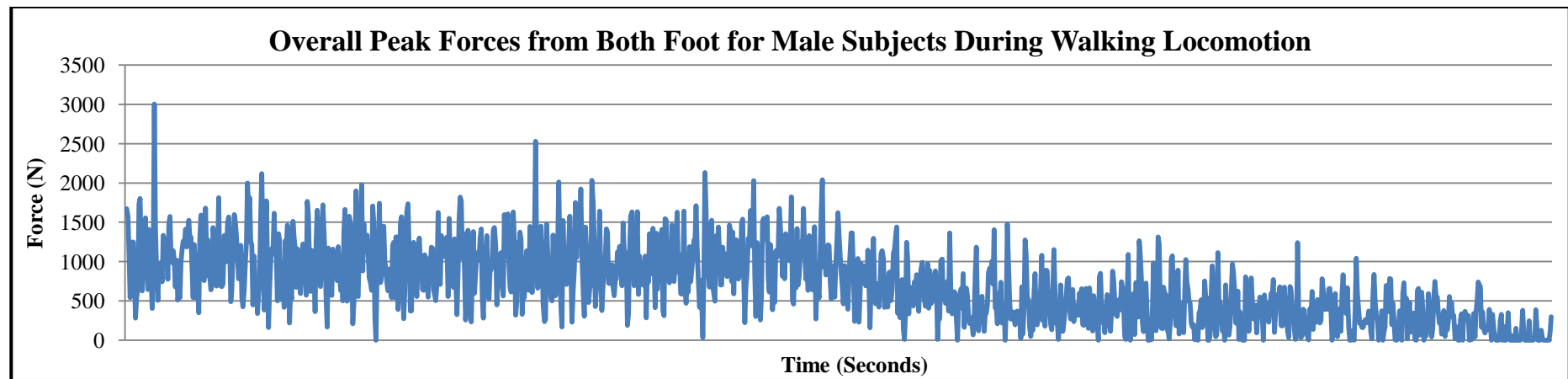


Figure I.27: Graph of overall peak forces from both foot for male subjects during walking locomotion versus time (Insole System)

Table I.10: Average peak forces for female and male subjects during running locomotion by using instrumented insole system

	Female	Male	Difference	%Difference
L1	10.73	8.66	-2.07	-23.90
L2	10.62	7.15	-3.47	-48.53
L3	5.41	1.83	-3.58	-195.63
L4	5.58	0.90	-4.68	-520.00
R1	9.69	4.71	-4.98	-105.73
R2	15.54	11.54	-4.00	-34.66
R3	7.32	3.09	-4.23	-136.89
R4	9.73	1.53	-8.20	-535.95

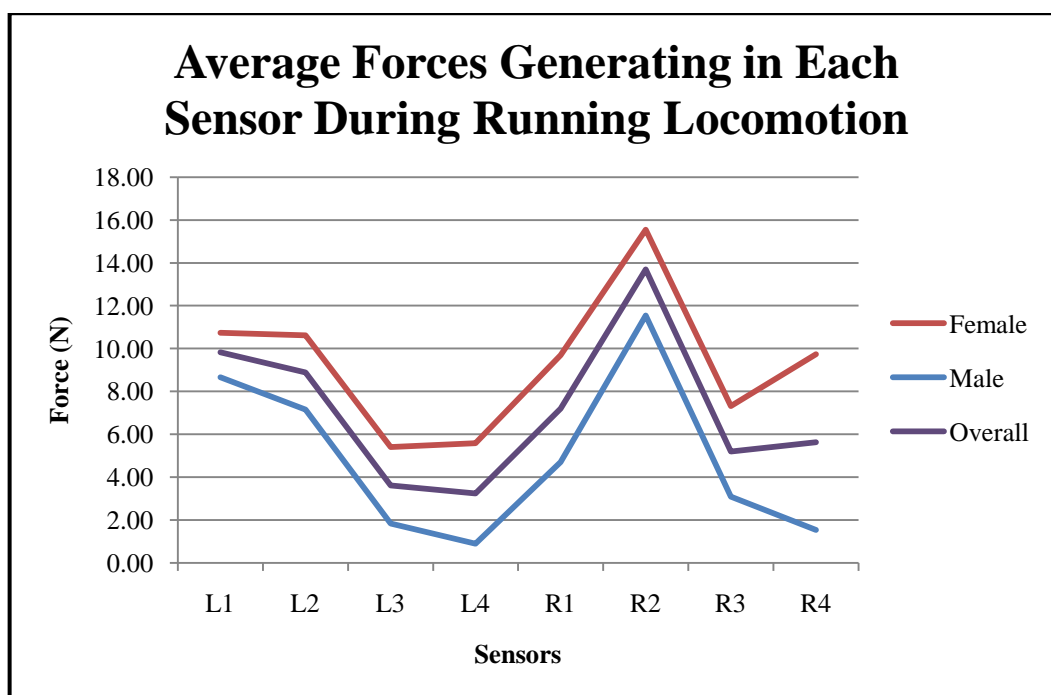


Figure I.28: Graph of average forces generating during running locomotion versus sensors by using instrumented insole system

Table I.11: Maximum peak forces for female and male subjects during running locomotion by using instrumented insole system

	Female	Male	Difference	%Difference
L1	402.00	402.00	0.00	0.00
L2	402.00	400.00	-2.00	-0.50
L3	338.00	346.00	8.00	2.31
L4	400.00	331.00	-69.00	-20.85
R1	398.00	396.00	-2.00	-0.51
R2	429.00	400.00	-29.00	-7.25
R3	404.00	325.00	-79.00	-24.31
R4	402.00	402.00	0.00	0.00

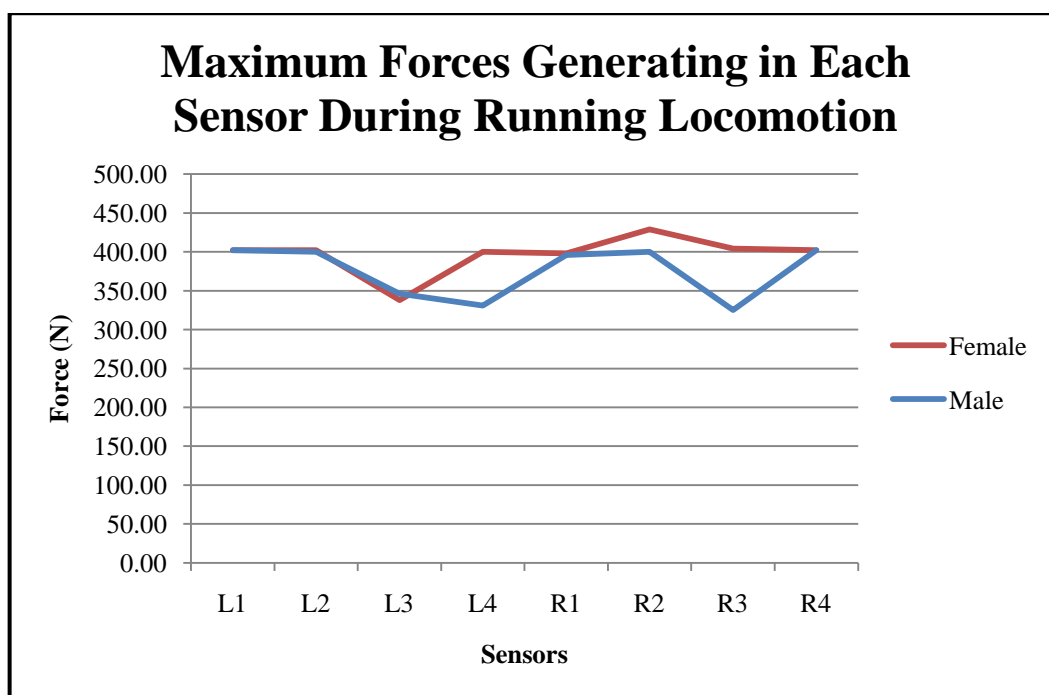


Figure I.29: Graph of maximum forces generating during running locomotion versus sensors by using instrumented insole system

Table I.12: Minimum peak forces for female and male subjects during running locomotion by using instrumented insole system

	Female	Male	Difference	%Difference
L1	2.00	13.00	11.00	84.62
L2	2.00	2.00	0.00	0.00
L3	2.00	13.00	11.00	84.62
L4	2.00	2.00	0.00	0.00
R1	17.00	10.00	-7.00	-70.00
R2	2.00	2.00	0.00	0.00
R3	2.00	4.00	2.00	50.00
R4	4.00	13.00	9.00	69.23

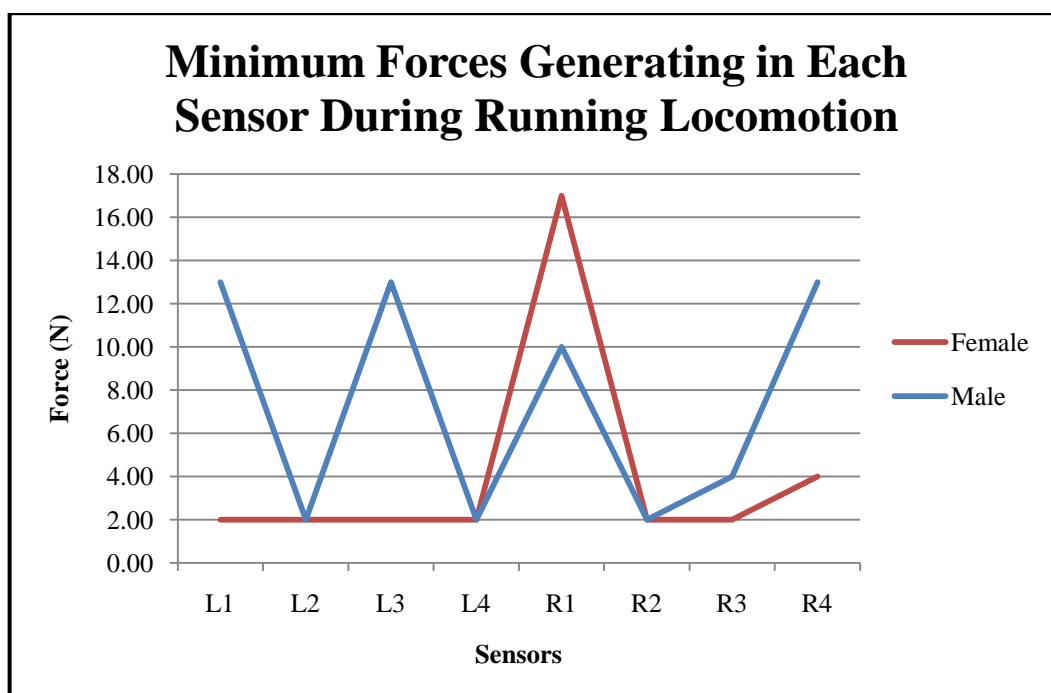


Figure I.30: Graph of minimum forces generating during running locomotion versus sensors by using instrumented insole system

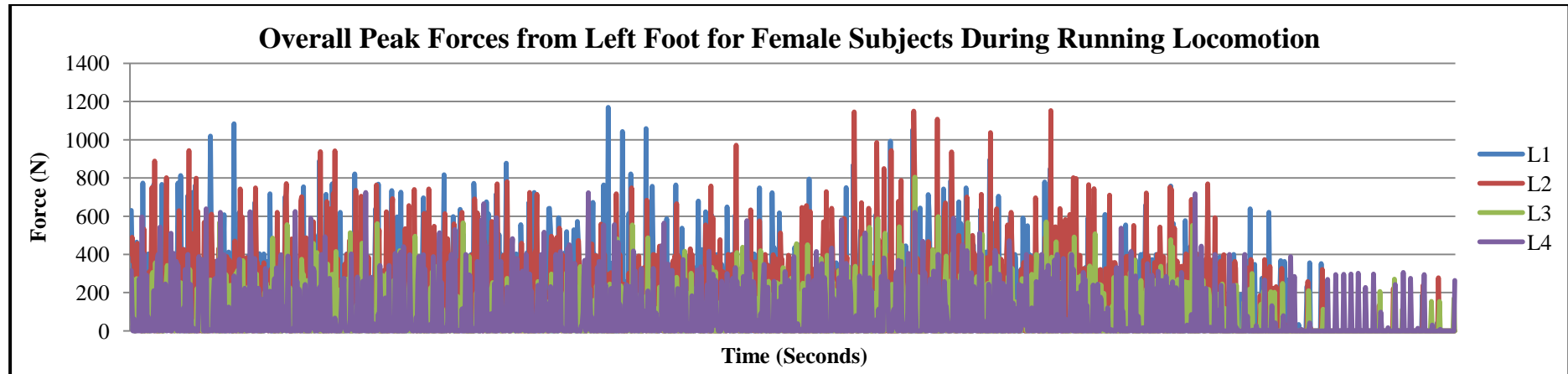


Figure I.31: Graph of overall peak forces from left foot for female subjects during running locomotion versus time (Insole System)

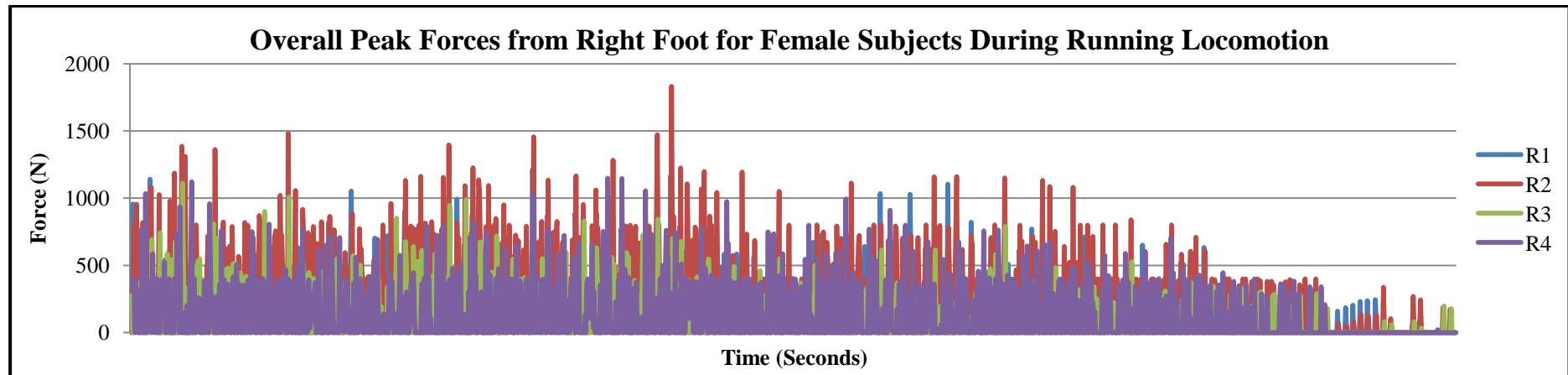


Figure I.32: Graph of overall peak forces from right foot for female subjects during running locomotion versus time (Insole System)

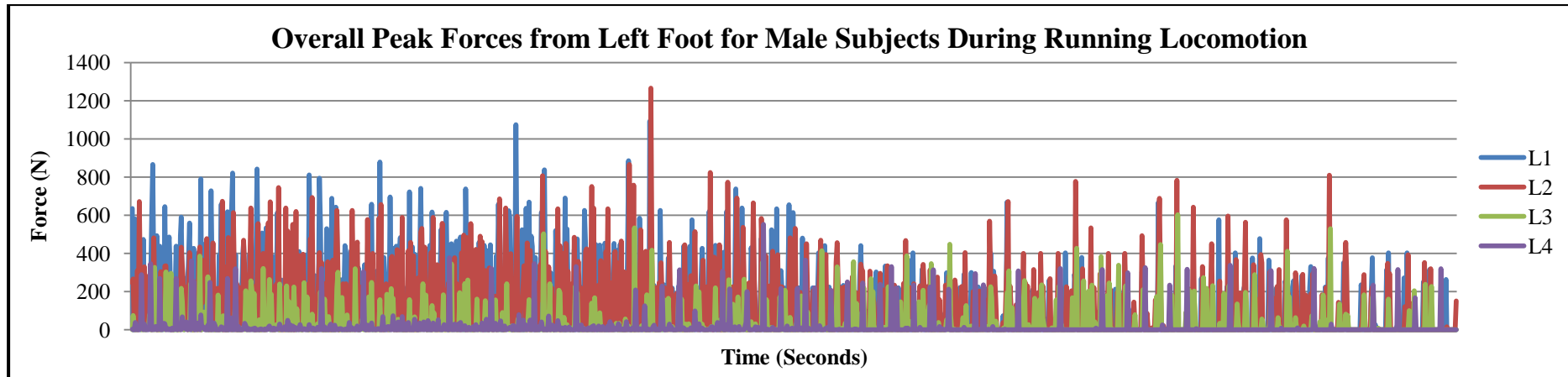


Figure I.33: Graph of overall peak forces from left foot for male subjects during running locomotion versus time (Insole System)

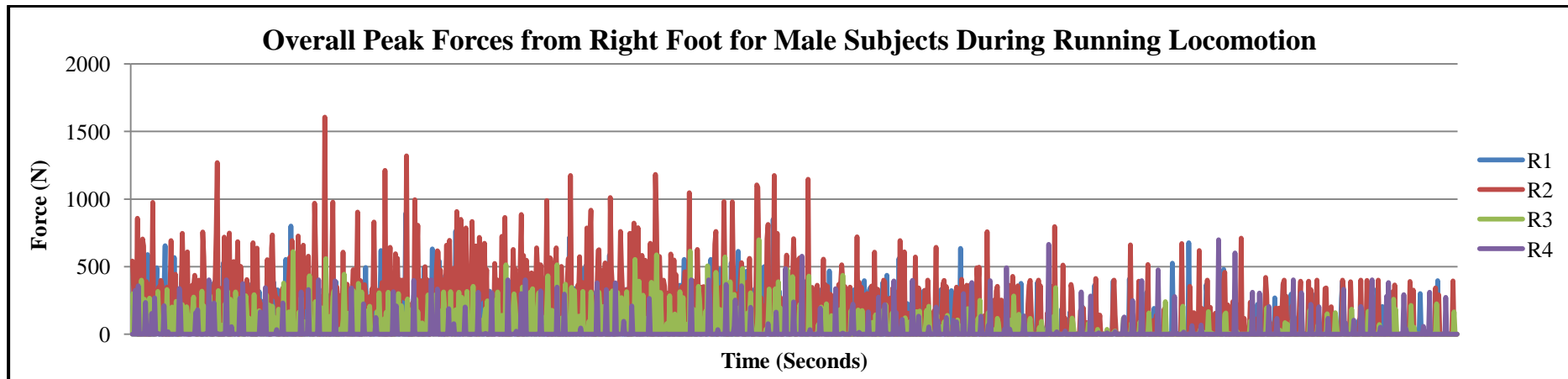


Figure I.34: Graph of overall peak forces from right foot for male subjects during running locomotion versus time (Insole System)

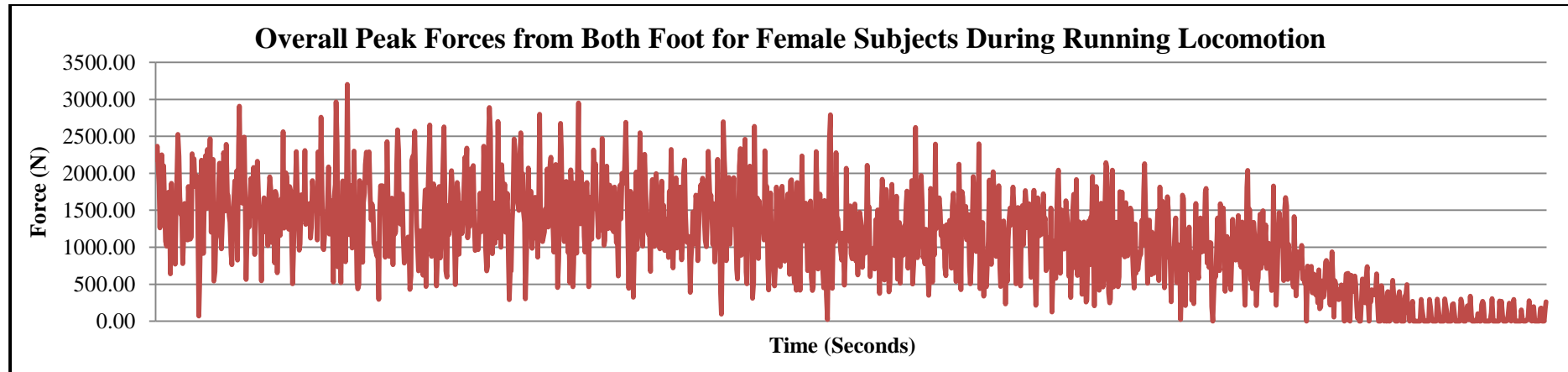


Figure I.35: Graph of overall peak forces from both foot for female subjects during running locomotion versus time (Insole System)

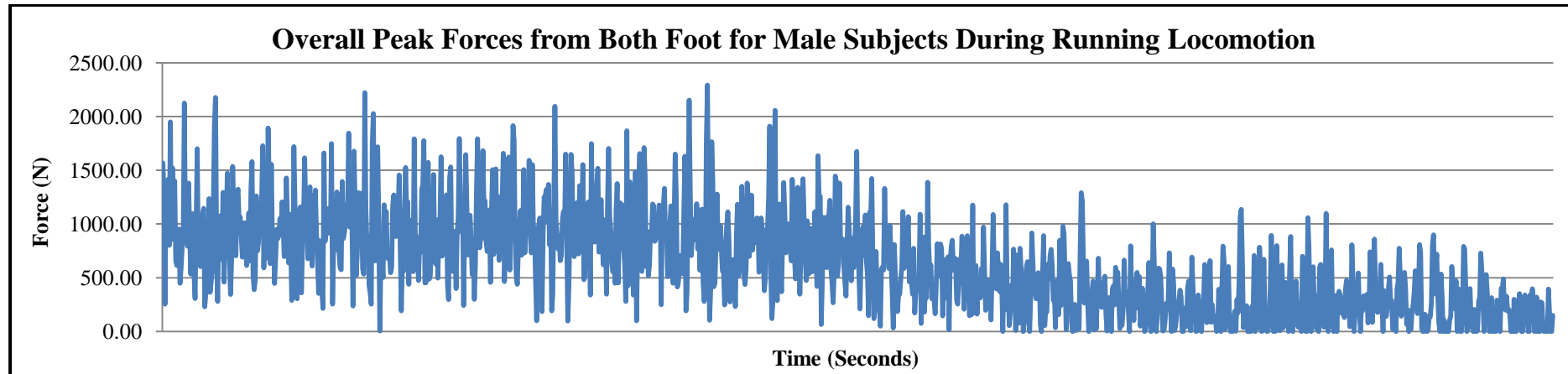


Figure I.36: Graph of overall peak forces from both foot for male subjects during running locomotion versus time (Insole System)

*Comparison between Devices***Table I.13: Average, maximum and minimum peak forces for female and male subjects during walking locomotion by using treadmill**

	Female	Male	Overall
Average	395.44	531.85	463.65
Maximum	1021.31	1342.60	1342.60
Minimum	345.66	570.41	345.66

Table I.14: Average, maximum and minimum peak forces for female and male subjects during running locomotion by using treadmill

	Female	Male	Overall
Average	565.42	875.88	720.65
Maximum	1342.21	1766.49	1766.49
Minimum	488.25	427.86	427.86

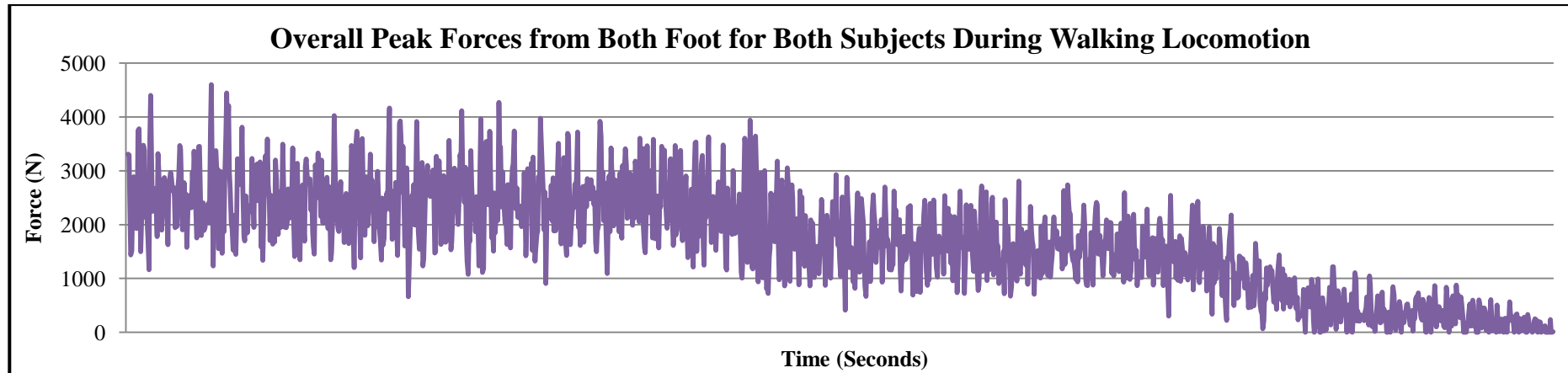


Figure I.37: Graph of overall peak forces from both foot for both subjects during walking locomotion versus time (Insole System)

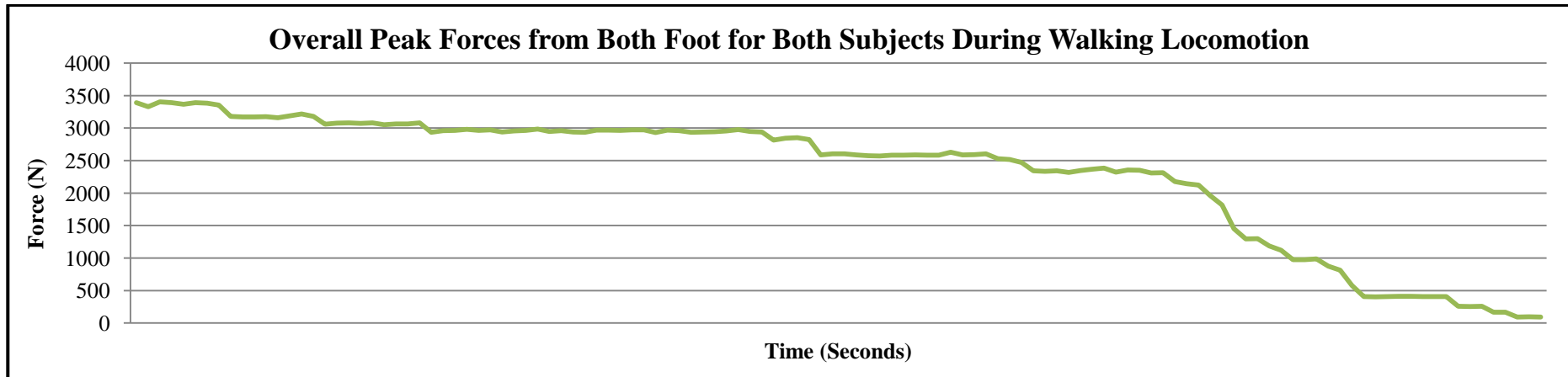


Figure I.38: Graph of overall peak forces from both foot for both subjects during walking locomotion versus time (Treadmill)

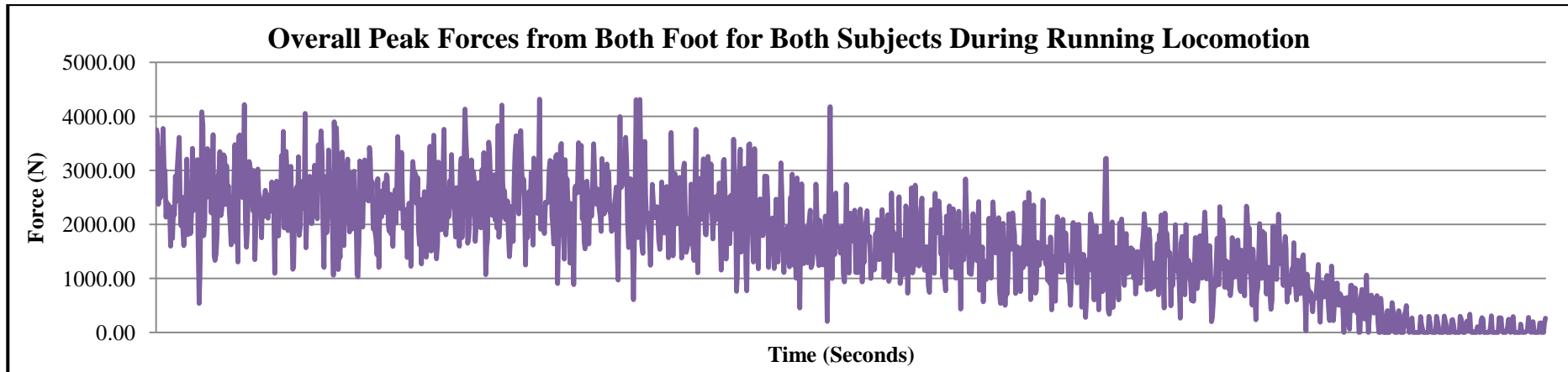


Figure I.39: Graph of overall peak forces from both foot for both subjects during running locomotion versus time (Insole System)

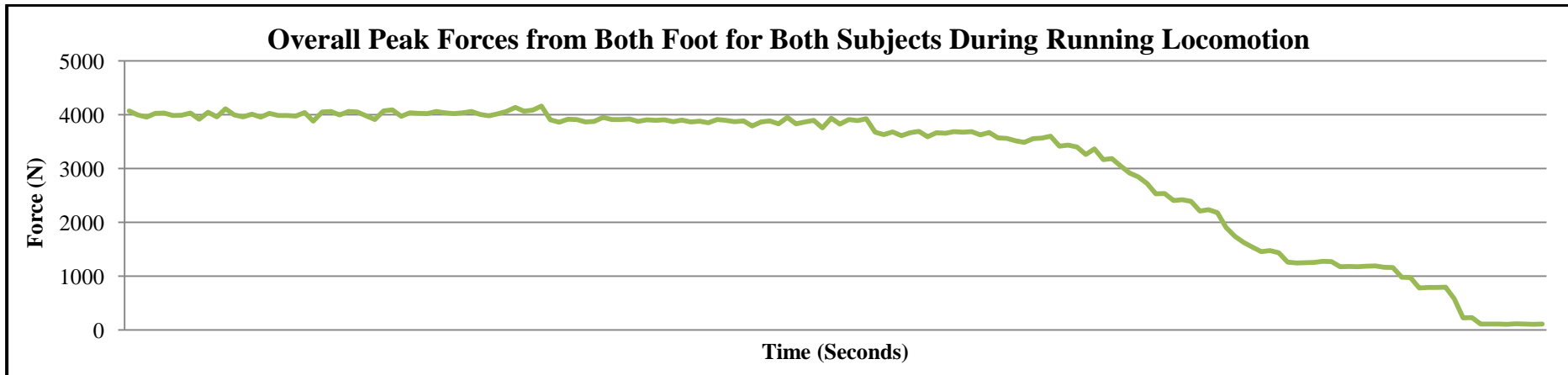


Figure I.40: Graph of overall peak forces from both foot for both subjects during running locomotion versus time (Treadmill)

Comparison of Parameters with Other Studies for Female Subjects (Normal Gait)

Table I.15: Comparison of parameters with other studies for female subjects

	Oberg et al. (1993)	Auvinet et al. (2002)	Titianova et al. (2004)	Cho et al. (2004)	Ryu (2006)
	Mean (SD) (n = 15)	Mean (SD) (n = 144)	Mean (SD) (n = 41)	Mean (SD) (n = 47)	Mean (SD) (n = 12)
Age (years)	N/A	N/A	41.20 (10.90)	22.90 (4.90)	24.10 (1.60)
Height (m)	N/A	N/A	1.65 (0.05)	1.59 (4.90)	1.58 (0.06)
Weight (kg)	N/A	N/A	66.70 (8.90)	52.30 (6.90)	50.70 (6.30)
Walking Speed (m/s)	1.24 (0.17)	1.54 (0.12)	1.49 (19.60)	1.12 (0.11)	1.08 (0.14)
Step Length (m)	0.59 (0.06)	0.75 (0.05)	0.74 (7.30)	N/A	0.61 (0.04)
Step Time (s)	N/A	N/A	0.50 (0.04)	N/A	N/A
Stride Length (m)	N/A	N/A	1.49 (14.40)	1.17 (12.50)	1.19 (0.09)
Stride Time (s)	N/A	N/A	N/A	N/A	N/A
Cadence (step/min)	124.80 (9.00)	123.60 (7.20)	120.80 (8.30)	112.50 (6.50)	109.26 (10.71)

Table I.16: Comparison of parameters with other studies for female subjects (Continue)

	McKean et al. (2007)	Senden et al. (2009)	Yu et al. (2009)	Present Testing (2010)
	Mean (SD) (n = 24)	Mean (SD) (n = 10)	Mean (SD) (n = 5)	Mean (SD) (n = 15)
Age (years)	48.70 (10.30)	24.50 (3.03)	29.40 (11.40)	22.93 (1.79)
Height (cm)	1.70 (0.10)	1.70 (0.06)	1.59 (6.70)	1.60 (4.93)
Weight (kg)	66.20 (9.70)	63.70 (7.30)	60.80 (15.60)	52.06 (9.51)
Walking Speed (m/s)	1.40 (0.20)	1.50 (0.15)	0.88 (0.10)	4.03 (0.01)
Step Length (m)	N/A	0.75 (0.06)	N/A	0.94 (111.81)
Step Time (s)	N/A	0.50 (0.03)	N/A	0.76 (0.28)
Stride Length (m)	1.40 (0.20)	N/A	1.25 (0.10)	1.45 (86.30)
Stride Time (s)	N/A	N/A	1.09 (0.10)	1.13 (0.14)
Cadence (step/min)	N/A	120.24 (6.96)	N/A	107.30 (11.90)

Comparison of Parameters with Other Studies for Male Subjects (Normal Gait)

Table I.37: Comparison of parameters with other studies for male subjects

	Oberg et al. (1993)	Auvinet et al. (2002)	Titianova (2004)	Cho et al. (2004)	Ryu et al. (2006)
	Mean (SD) (n = 15)	Mean (SD) (n = 138)	Mean (SD) (n = 21)	Mean (SD) (n = 51)	Mean (SD) (n = 20)
Age (years)	N/A	N/A	41.90 (11.60)	23.50 (2.70)	24.90 (2.00)
Height (m)	N/A	N/A	1.79 (0.06)	1.72 (5.00)	1.71 (0.04)
Weight (kg)	N/A	N/A	81.10 (10.30)	68.30 (9.70)	69.10 (7.90)
Walking Speed (m/s)	1.23 (0.11)	1.59 (0.13)	1.50 (19.60)	1.19 (0.11)	1.17 (0.11)
Step Length (m)	0.62 (0.04)	0.83 (0.06)	0.74 (7.40)	N/A	0.66 (0.04)
Step Time (s)	N/A	N/A	0.50 (0.04)	N/A	N/A
Stride Length (m)	N/A	N/A	1.49 (14.90)	1.27 (9.90)	1.32 (0.08)
Stride Time (s)	N/A	N/A	N/A	N/A	N/A
Cadence (step/min)	118.80 (7.80)	116.40 (7.20)	120.80 (8.30)	111.80 (6.40)	107.24 (7.78)

Table I.18: Comparison of parameters with other studies for male subjects (Continue)

	McKean et al. (2007)	Senden et al. (2009)	Yu et al. (2009)	Present Testing (2010)
	Mean (SD) (n = 18)	Mean (SD) (N = 10)	Mean (SD) (n = 5)	Mean (SD) (n = 15)
Age (years)	52.20 (10.10)	24.50 (2.76)	30.80 (12.90)	22.60 (1.35)
Height (m)	1.80 (0.10)	1.84 (0.05)	1.77 (7.40)	1.73 (6.05)
Weight (kg)	78.90 (13.50)	72.50 (8.89)	85.0 (19.60)	70.55 (12.77)
Walking Speed (m/s)	1.60 (0.20)	1.55 (0.18)	0.92 (0.10)	4.03 (0.00)
Step Length (m)	N/A	0.83 (0.07)	N/A	1.06 (114.27)
Step Time (s)	N/A	0.54 (0.03)	N/A	0.98 (0.86)
Stride Length (m)	1.50 (0.10)	N/A	1.26 (0.10)	1.92 (185.53)
Stride Time (s)	N/A	N/A	1.16 (0.10)	1.70 (1.31)
Cadence (step/min)	N/A	112.32 (5.79)	N/A	89.68 (27.40)

Comparison of Parameters with Other Studies for Abnormal Gait

Table I.19: Comparison of parameters with other studies for abnormal gait

	Bogataj et al.	McKean et al.	Morris et al.	Chen et al.	Givon et al.
	Stroke	Osteoarthritis	Parkinson	Cerebral Palsy	Multiple Sclerosis
	Mean (SD)	Mean (SD)	Mean (SD)	Mean (SD)	Mean (SD)
	(n = 20)	(n = 39)	(n = 5)	(n = 24)	(n = 81)
Age (years)	N/A	56.05 (12.50)	65.30 (N/A)	6.38 (1.67)	36.20 (0.50)
Height (cm)	N/A	1.75 (0.10)	1.70 (N/A)	1.12 (0.11)	N/A
Weight (kg)	N/A	89.90 (15.55)	71.30 (N/A)	18.63 (4.76)	N/A
Walking Speed (m/s)	0.46 (N/A)	1.30 (0.25)	N/A	0.44 (0.31)	0.86 (3.00)
Step Length (m)	0.22 (N/A)	N/A	N/A	0.13 (0.06)	0.45 (1.05)
Step Time (s)	2.10 (N/A)	N/A	N/A	0.17 (0.08)	0.66 (0.02)
Stride Length (m)	0.44 (N/A)	1.35 (0.15)	1.13 (0.26)	0.25 (0.11)	N/A
Stride Time (s)	4.15 (N/A)	N/A	1.22 (0.21)	N/A	N/A
Cadence (step/min)	N/A	N/A	N/A	N/A	94.40 (2.10)

Table I.20: Comparison of parameters with other studies for abnormal gait (Continue)

	Verghese et al.	Tanaka et al.	Allet et al.	Gaudreault et al.	Present Testing
	Predisability	Arthroplasty	Diabetic	Duchenne	Healthy
	Mean (SD)	Mean (SD)	Mean (SD)	Mean (SD)	Mean (SD)
	(n = 40)	(n = 43)	(n = 71)	(n = 11)	(n = 30)
Age (years)	79.70 (5.80)	59.70 (7.90)	63.00 (8.00)	9.30 (2.60)	22.77 (1.57)
Height (cm)	N/A	1.52 (5.20)	1.66 (8.50)	N/A	1.66 (8.56)
Weight (kg)	N/A	56.20 (7.60)	83.60 (16.60)	N/A	61.30 (14.52)
Walking Speed (m/s)	1.04 (0.12)	1.02 (0.25)	1.22 (0.17)	0.62 (0.12)	4.03 (0.00)
Step Length (m)	N/A	N/A	N/A	0.37 (0.07)	0.99 (111.23)
Step Time (s)	N/A	N/A	N/A	N/A	0.87 (0.64)
Stride Length (m)	1.18 (0.11)	0.71 (6.70)	1.32 (0.13)	N/A	1.69 (144.13)
Stride Time (s)	N/A	N/A	N/A	N/A	1.42 (0.96)
Cadence (step/min)	N/A	117.40 (12.00)	110.06 (10.82)	100.40 (8.40)	98.49 (22.61)

APPENDIX J: Expenditure of Project

No.	Product Code	Product Name	Qty	Retail Price (RM)	Amount (RM)
1	SK40C	Enhanced 40 Pins PIC Start-Up Kit.	1	19.95	19.95
2	SK40-C2	40 pins PIC Start-Up Kit Combo 2	1	65.90	65.90
3	SKXBee	XBee Starter Kit	2	97.50	195.00
4	UIC00B	USB ICSP PIC Programmer V2010	1	25.45	25.45
5	UIC-S	ICSP Programmer Socket	1	20.00	20.00
6	UC00A	USB to UART Converter	1	29.00	29.00
7	IC-PIC-18F4550	IC PIC18F4550	1	17.50	17.50
8	KC-USB	Bluetooth USB Dongle	1	20.00	20.00
9	CR-H49S-20M	Crystal H49S (Low Profile) 20MHz	2	2.00	4.00
10	CP-CC-1PF	Ceramic Capacitor 1pF	2	0.20	0.40
11	CP-MC-0.33U	Multilayer Capacitor 33 μ F	2	0.30	0.60
12	CP-EC-16-10	Electrolytic Capacitor 16V 10 μ F	3	0.20	0.60
13	CP-EC-16-100	Electrolytic Capacitor 16V 100 μ F	3	0.25	0.75
14	RS-025W-1K	Resistor 0.25W 5% 1K	15	0.05	0.75
15	RS-050W-1K	Resistor 0.5W 5% 1K	12	0.10	1.20
16	RS-1W-1K	Resistor 1W 5% 1K	10	0.20	2.00
17	VR-7805	Voltage Regulator +5V	5	1.00	5.00
18	IC-LM-324	IC LM324	3	1.50	4.50

19	IC-LM-324N	IC LM324N	3	1.10	3.30
20	IS-14PIN	IC Socket-14 Pin	6	0.20	1.20
21	CN-PH-M140S	Straight Pin Header (Male) 1x40 Ways	2	2.00	4.00
22	BD-DB-PP-1024	Donut Board (Big) 10x24cm	1	2.25	2.25
23	BD-DB-PP-0615	Donut Board (Small) 6x15cm	1	0.80	0.80
24	CN-02-2510	2510 PCB Connector 2 Ways	2	0.36	0.72
25	CN-04-2510	2510 PCB Connector 4 Ways	5	0.60	3.00
26	CN-05-2510	2510 PCB Connector 5 Ways	5	0.75	3.75
27	CN-08-2510	2510 PCB Connector 8 Ways	8	0.80	6.40
28	-	KC01-101 2 Pin R/Switch Black	4	0.80	3.20
29	-	Heat Sink TO-220 30x25x10mm	2	0.65	1.30
30	-	Heat Sink TO-220 (02-21)	2	0.55	1.10
31	-	Heat Sink TO-220 25x15x10mm	2	1.50	3.00
32	BC-3	Super Battery Charger	1	35.00	35.00
33	-	Energizer Rechargeable Battery	2	48.00	96.00
34	BA-9V	9V Battery (Maxell)	4	5.00	20.00
35	-	Power Heavy Duty 9V Battery	2	2.50	5.00
36	-	Panasonic 9V Battery	2	4.50	9.00
37	CN-BA-9S	9V Battery Snap	2	0.40	0.80

38	CN-BA-9H	9V Battery Holder	2	3.00	6.00
39	WR-RM10	Rainbow Cable 10 Ways (meter)	5	4.50	22.50
40	TO-PH-17150	Philips Test Pen	1	3.50	3.50
41	BO-130071045-SA	Aluminium Box (130x71x45mm) Silver	1	15.00	15.00
42	-	Single Core Wire 10.5 mm (meter)	16	0.30	4.80
43	FSR-402	Force Sensing Resistor (Circular)	8	24.40	195.20
44	FSR-406	Force Sensing Resistor (Square)	2	31.26	62.52
45	-	971-PC Adapter	1	5.00	5.00
46	-	Polymer Shoe Insole	6	3.90	23.40
47	-	Loop Hook (meter)	3	1.40	4.20
48	-	Shoe Belts	4	2.50	10.00
49	-	Waist Belt	1	5.90	5.90
50	-	Binding Tape	1	1.90	1.90
51	-	Black Tape CTP 24mm	1	1.70	1.70
52	-	Cellotape 24x30 3 IN 1	1	3.99	3.99
53	-	Modelling Clay	1	1.20	1.20
54	-	Foam Board	1	2.60	2.60
				Total (RM)	981.83